

H-Bond Stabilized Columnar Discotic Liquid Crystals

Promotor

Prof. dr. Ernst J. R. Sudhölter, hoogleraar in de organische chemie, Wageningen Universiteit

Co-promotoren

Dr. Antonius T. M. Marcelis, universitair hoofddocent, Laboratorium voor Organische Chemie, Wageningen Universiteit

Dr. Han Zuilhof, universitair hoofddocent, Laboratorium voor Organische Chemie, Wageningen Universiteit

Samenstelling promotiecommissie

Prof. dr. M. A. Cohen Stuart

Wageningen Universiteit

Dr. W. F. Jager

Technische Universiteit Delft

Dr. J. Lub

Philips Research B.V., Eindhoven

Prof. dr. S. J. Picken

Technische Universiteit Delft

Prof. dr. R. P. Sijbesma

Technische Universiteit Eindhoven

Dit onderzoek is uitgevoerd binnen de onderzoeksschool VLAG

Ioan Paraschiv

H-Bond Stabilized Columnar Discotic Liquid Crystals

Proefschrift

ter verkrijging van de graad van doctor

op gezag van de Rector Magnificus

van Wageningen Universiteit,

Prof. dr. M. J. Kropff,

in het openbaar te verdedigen

op vrijdag 19 januari 2007

des namiddags te vier uur in de Aula

Paraschiv, I.

H-Bond Stabilized Columnar Discotic Liquid Crystals

Ph.D. Thesis Wageningen University – with summaries in English, Dutch and Romanian

Cover: optical microphotographs of the liquid crystalline textures of several triphenylene derivatives described in this thesis (taken by the author).

ISBN 90 - 8504 - 558 - 4

“De câte ori te gândești la Dumnezeu,
e semn că Dumnezeu s-a gândit deja la tine!”
părintele Cleopa

Contents

Chapter 1	1
Columnar Discotic Triphenylene-Based Compounds: Synthesis and Mesomorphic Properties	
Chapter 2	21
Amide, Urea and Thiourea-Triphenylene Derivatives: Synthesis and Mesomorphic Properties	
Chapter 3	53
Asymmetry in Liquid Crystalline Hexaalkoxytriphenylene Discotics	
Chapter 4	73
A H-Bond Stabilized Hexagonal Plastic Columnar (Col _{hp}) Discotic Phase	
Chapter 5	91
High Charge Carrier Mobility in H-Bond Stabilized Columnar Discotic Triphenylene Derivatives	
Appendix: Polarized Optical Microphotographs	127
Summary, Samenvatting & Rezumat	
Curriculum Vitae	
List of Publications	
Dankwoord	

Chapter 1

Columnar Discotic Triphenylene-Based Compounds: Synthesis and Mesomorphic Properties

Abstract – *This chapter presents a preface to the thesis. A short introduction into the field of liquid crystals is given, with focus on columnar discotic mesophases. Subsequently, several pathways for the synthesis of 2,3,6,7,10,11-hexakis(hexyloxy)triphenylene (HAT6)* derivatives are described. The advantages of columnar discotic mesophases stabilization for their use in organic-based electronic devices are outlined. Finally, the contents of this thesis are given.*

* **HATn** = **H**exaalkoxytriphenylene, where **n** is the number of C atoms in the alkoxy substituent at the triphenylene core.

1.1 Introduction

The daily implications of science and technology are nowadays very large, *via* new electronic devices present on the current market, i.e. flat LCD and plasma TV screens, mobile phones, PDA's (*personal digital assistants*), GPS (*global positioning system*), new solar cells devices, *etc.* Furthermore, a constant demand exists for better performing electronic devices, due to the very rapid technological developments.

The progress in organic optoelectronically active materials allows a strong competition between currently used *metals* or *inorganic materials* and novel *organic* materials. Specifically their easy processibility and endless tenability make organic materials attractive. Given their potential use in a high diversity of electronic devices, *liquid-crystalline* (LC) materials are especially attractive. Especially discotic columnar liquid crystals have been investigated over the last 30 years, for their potential use as electron and hole conductive properties in electronic devices such as organic light-emitting diodes (OLEDs),¹ organic photovoltaic cells,² and field-effect transistors (FET's).³

Just to have a general idea about the amount of research that has been performed, an up-to-date overview of published scientific articles, regarding discotic liquid crystal molecules, is plotted in Figure 1. From the 2284 published articles in this category, at least 433 deal with triphenylene derivatives.

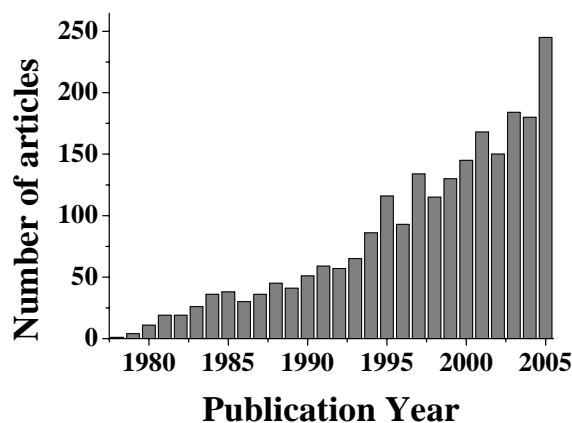


Figure 1. Number of published articles, per year, about “*discotic*” molecules.

1.2 Discotic liquid crystals & columnar organization

The history of *liquid crystals* started at the end of the nineteenth century, when Reinitzer⁴ and Lehmann,⁵ discovered the first compound (cholesteryl benzoate) with *mesomorphic* properties (“*mezo*” in Greek means *middle*). Upon heating, these materials exhibit a middle phase

(mesophase) between a highly ordered solid crystal and an isotropic liquid. These new *liquid crystalline* compounds, seen as “*liquids with high degree of ordering*”, have several general and attractive features:

1. relatively easy synthesis
2. easy processability within their mesophase
3. self-organization within their LC phase, leading to highly organized materials
4. high anisotropy of specific properties (i.e., reflection of light)

LC molecules usually consist of partially rigid and partially flexible moieties, while the overall molecular shape can be rod-like or disk-shaped.⁶ In this chapter an overview of the liquid-crystalline properties of disk-shaped molecules is given, with focus on the synthesis and mesomorphic properties of triphenylene derivatives.

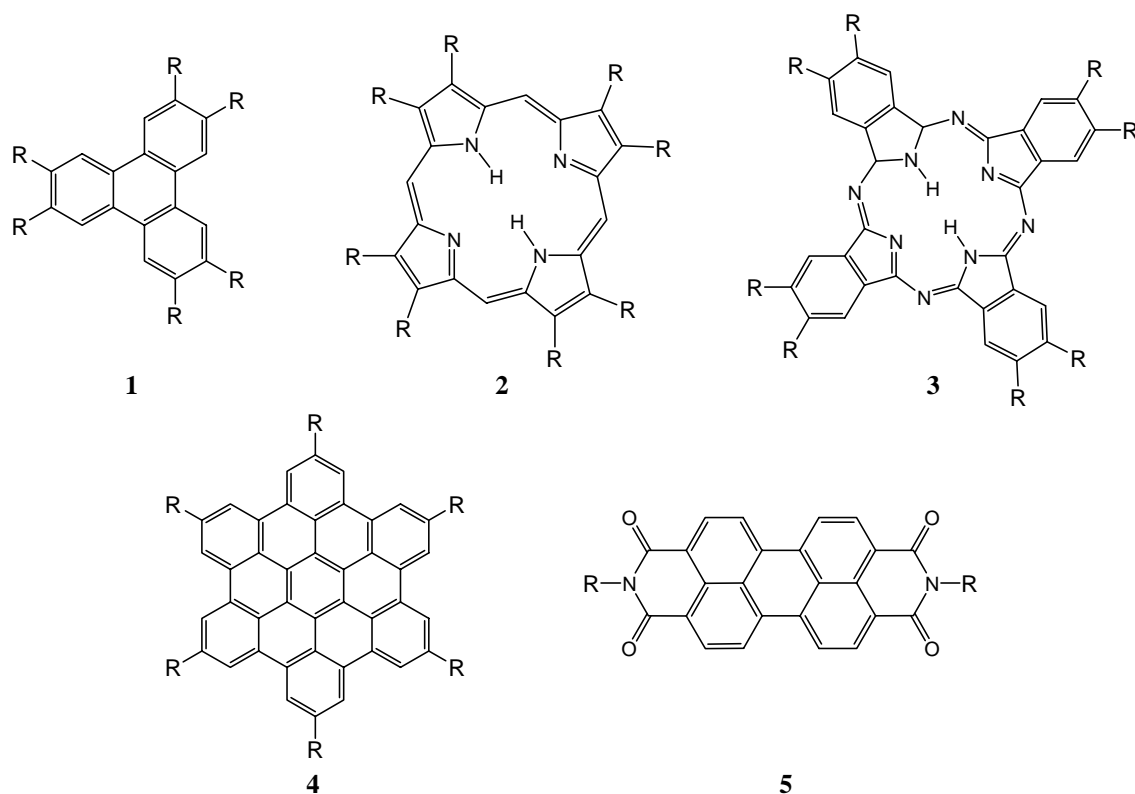


Figure 2. Examples of disk-shaped mesogens with peripheral substituents R: **1** - triphenylenes; **2** - porphyrins; **3** - phthalocyanines; **4** - hexabenzocoronenes; **5** - carboxydiimido-perylenes.

Disk-like (discotic) LC materials, discovered in 1977 by Chandrasekhar,⁷ and rapidly investigated by a variety of groups,⁸ have attracted considerable attention over the years regarding their potential applications. These materials consist of disk-shaped molecules that usually have polycyclic aromatic cores (Figure 2), which stack one in top of each other in a columnar fashion.⁹

This stacking is based on extensive and highly stabilizing overlap of molecular π -orbitals of rigid aromatic moieties that are ~ 3.5 Å apart. This central aromatic core represents the rigid part of the molecule, and is surrounded by long alkyl or other peripheral substituents, which provide the flexibility to the molecule. Variation of either the core or these peripheral substituents yields new materials with mesomorphic properties that can be varied in a controllable fashion.¹⁰

In the case of disk-shaped molecules two main types of liquid crystalline mesophases can be distinguished: nematic discotic (N_D) phases, in which molecules show only 2D orientational ordering and no positional ordering, and columnar (Col) organizations, which display a combination of orientational and positional ordering, as indicated in Figure 3. Among nematic phases additional sub-categories can be distinguished, such as: nematic discotic, nematic columnar (N_{Col}), and nematic lateral (N_L). For the last mentioned nematic phase relatively small disk-shaped molecules form larger disk-shaped assemblies, which organize into a nematic fashion.¹¹

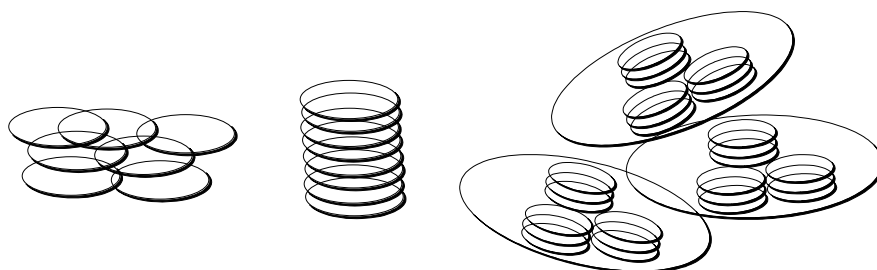


Figure 3. Two different mesophases of discotic liquid crystals: nematic discotic (N_D) (left), columnar discotic (Col_D) (middle) and nematic lateral (N_L) (right).

Most frequently, disk-like molecules with a flexible periphery organize into a columnar (discotic) mesophase, in which molecules self-organize into columnar stacks. Within these columns the π -systems of neighboring aromatic cores overlap and a one-dimensional pathway for charge transport along the axis of the columns is created. These “*molecular wires*” are interconnected through their long alkyl substituents.

It is rather important to realize that the main interaction between the aromatic cores is π - π interaction, which is the result of a combination of dipole-dipole (electrostatic), van der Waals, and dipole-induced attractive forces, and Pauli repulsion (short-range repulsion), none of them being predominant.¹²

In many materials with a discotic LC phase, the discotic molecules organize into a tilted columnar structure in the solid phase (Figure 4a) and a horizontal columnar organization in

their liquid crystalline state (Figure 4b). In both solid and LC phases, the cofacial distance takes values between $d_c = 3.18^{13}$ and 3.60 \AA^{14}

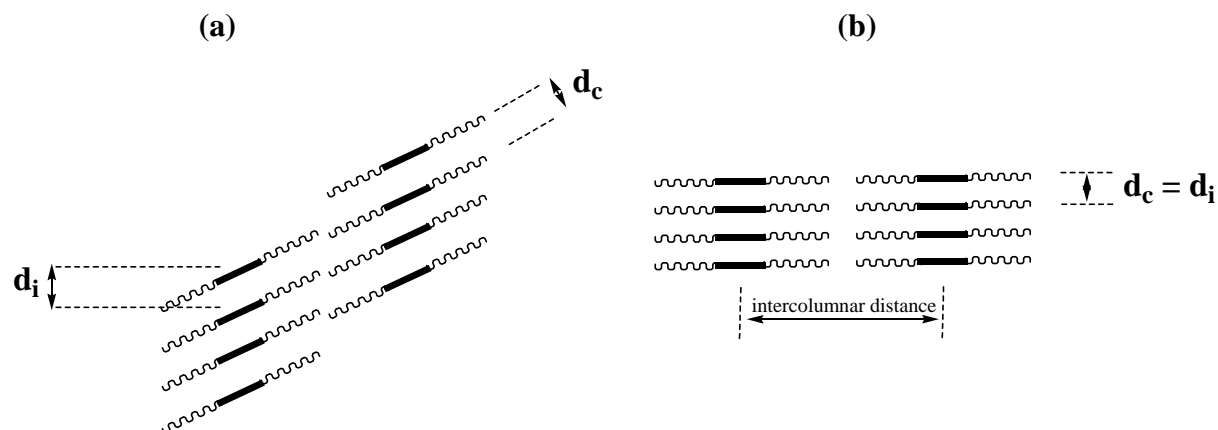


Figure 4. A side-view representation of the solid (a) and liquid crystalline (b) state of columnar stacks of discotics substituted with long peripheral side chains (d_i = intracolumnar distance; d_c = cofacial distance).

Different columnar organizations are possible taking into consideration the degree of ordering within the columns and the order between the columns. Often columnar orderings are classified as ordered (disks are equidistant within the same column) (Col_o) or disordered (disks are not equidistant within the same column) (Col_d), but the most accurate classification is given by the two-dimensional arrangements that can be discerned in the columnar packing: columnar hexagonal (Col_h), columnar rectangular (Col_r) or columnar oblique (Col_{ob}) (Figure 5). For the last two columnar phases (Col_r and Col_{ob}) disk-like molecules are tilted within the columns being represented by ellipses, as shown in Figure 5. Transitions between different columnar phases and even between columnar phases and non-typical discotic phases are possible. These phase transitions are accompanied by structural fluctuations such as tilting of the disks, lateral displacement, and rotation around the columnar axis. These fluctuations are deduced from NMR studies.¹⁵

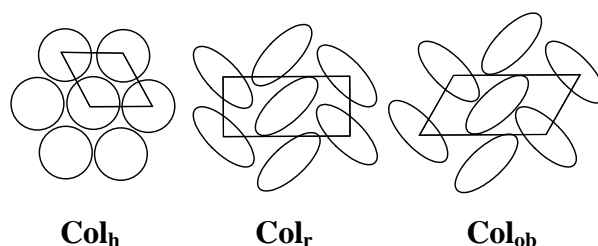


Figure 5. A top-view representation of two-dimensional organizations of columnar packing for disk-like molecules (Col_h = columnar hexagonal; Col_r = columnar rectangular; Col_{ob} = columnar oblique).

Columnar hexagonal plastic (Col_{hp}) is another particular columnar organization, in which the fluctuations of molecules are very much suppressed within the columnar stacks. The term “plastic” describes a particular class of mesophases, in which the molecules show suppressed fluctuations inside a certain lattice. These molecules illustrate a three-dimensional positional order, as in the crystalline phase, and a rotational mobility.¹⁶

1.3 Charge carrier transport in discotic molecules

The electrical conductivity of a material, σ (S m⁻¹), represents *the amount of charge carriers transported through a unit cross-sectional area, per second and per unit of applied electric field*. Taking into account the concentration of charge carriers present in a material, the conductivity σ can be described using equation (1).

$$\sigma = n_e \times \mu_e \times |e^-| + n_h \times \mu_h \times |h^+| \quad (1)$$

Equation (1) indicates the conductivity σ of a material, when n_e and n_h represent the electron and hole concentrations (m⁻³), μ_e and μ_h their mobilities (m² V⁻¹ s⁻¹), and $|e^-|$ or $|h^+|$ is the elementary charge (1.602 x 10⁻¹⁹ C).

With respect to their conductivity σ , materials can be classified in three categories: *insulators* with $\sigma \leq 10^{-12}$ S cm⁻¹, *semiconductors* with $10^{-12} \leq \sigma \leq 10^3$ S cm⁻¹, and *metals* with $\sigma \geq 10^3$ S cm⁻¹.

For a good conductivity a material needs to provide:

- a highly organized and stable pathway that can support the migration of charges;
- as high as possible concentration of charge carriers;

In most organic materials the concentration of charges is very low due to their high ionization potential (energies of at least a few electronvolts are required for ionization); additionally, the low dielectric constant of most organic materials restricts very much the electron-hole pair separation processes. As a direct result, the charge carrier concentrations, at room temperature are very low and a negligible dark conductivity is detected for most molecular materials.

In the late 1940s, Eley and Vartanian¹⁷ measured for the first time the electron conductivity in organic materials. A few years later conductivities on the order of 1 S cm⁻¹ had been reported for a donor-acceptor perylene-bromine complex,¹⁸ while it took another 20 years to obtain a conductivity as high as 5 x 10² S cm⁻¹ (for a TTF-TCNQ complex).¹⁹ An important breakthrough for the field of organic conductors was made when a huge increase in conductivity (100 S cm⁻¹) was found for polydiacetylene upon doping with oxidizing agents.²⁰

A few years ago a new class of materials was introduced, so-called “*synthetic metals*”, which besides their semiconductive properties, electroluminescence and lasing made them more attractive for electronic devices.²¹

To obtain high conductivities for discotic materials two factors play a role:

1). π -stacking must be achieved for large aromatic molecules that display a low internal reorganization energy upon electron transfer or hole transfer.²² Columnar discotic materials with such features yield mobilities upto $\sim 1 \text{ cm}^2 \text{ V}^{-1} \text{ s}^{-1}$. For typical charge densities of $1.08 \times 10^{19} \text{ cm}^{-3}$, this shows conductivity of $1.47 \times 10^{-4} \text{ S cm}^{-1}$ (charge carrier mobility is $\mu = 8.5 \times 10^{-5} \text{ cm}^2 \text{ V}^{-1} \text{ s}^{-1}$).²³

2). a high stability of the discotic stacks is required, to obtain a perfect columnar organization and thus minimize dislocations that disrupt the charge transfer.

Optimization of this latter feature is the focal point of this thesis. Using a series of smaller model compounds for the LC core moieties, polyaromatic triphenylenes moieties, a series of novel compounds with additional stabilization features is made. These molecules are easy to process and exhibit low clearing points, allowing homeotropic alignment, which is required for photoconductivity and time-of-flight (TOF) measurements.^{23, 24}

According to previous studies, charge transport in columnar phases exhibits a high anisotropy, showing up to 3 orders of magnitude higher conductivity in the direction of the columnar stacks.

A high charge carrier mobility, of $0.26 \text{ cm}^2 \text{ V}^{-1} \text{ s}^{-1}$, was found for a hexahexylthiotriphenylene (HHTT)²⁵ derivative in its crystalline phase. This value is considerably higher than found for the corresponding alkyloxy derivative, which is between 6×10^{-3} and $3 \times 10^{-2} \text{ cm}^2 \text{ V}^{-1} \text{ s}^{-1}$.²⁶

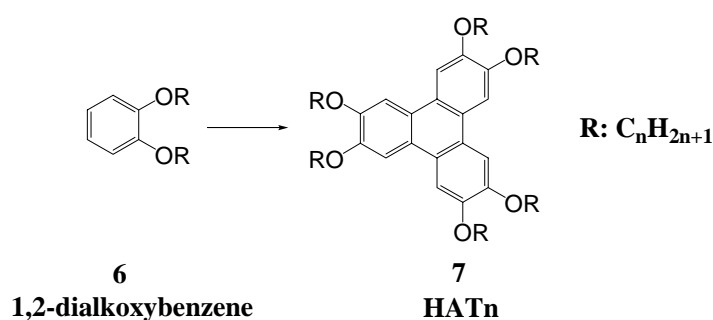
This difference, which is attributed to the larger reorganization energy required by the alkyloxy derivative in the crystalline state,²⁷ does not exist anymore in their columnar hexagonal mesophases (Col_h), where charge carrier mobilities between 2×10^{-3} and $2 \times 10^{-2} \text{ cm}^2 \text{ V}^{-1} \text{ s}^{-1}$ were found respectively.²⁸

For the design of electronic devices that are based on columnar discotic materials, higher charge carrier mobility, through one-dimensional pathways of aromatic cores, is very much desirable.

The use of larger aromatic central moieties, however, is usually accompanied by a decreased processability. As a result, the improvement of the stabilization of columnar mesophases without this decreased processability is asked for, and precisely this is the goal of the work described in this thesis.

1.4 Synthesis of triphenylene-based columnar discotic derivatives

Since the work presented in this thesis is entirely on new triphenylene-based materials, a short overview of the possible synthetic routes is described in this paragraph. A large amount of synthetic information exists on **HAT6** and its derivatives, and several, quite different preparation methods have been employed in the literature. One method to synthesize triphenylene molecules is the oxidative coupling reaction of *o*-dialkoxybenzene, using oxidative agents such as FeCl_3 ²⁹, VOCl_3 ³⁰, MoCl_5 (Scheme 1).³¹ The final product is obtained after quenching with methanol of the triphenylene radical cation, formed during the coupling reaction.



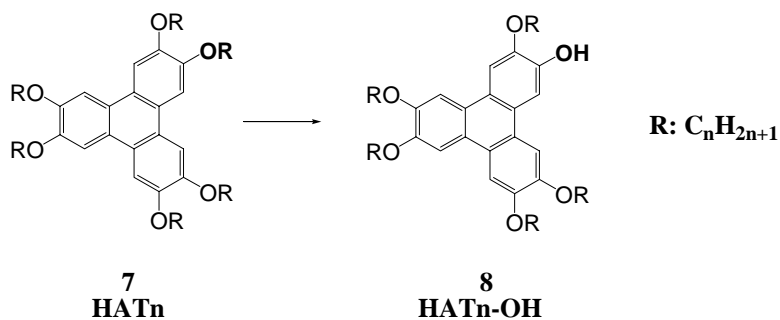
Scheme1. Synthetic route for symmetrical triphenylene (**HATn**) molecules.

This method is mostly used for the synthesis of symmetrically substituted triphenylene derivatives, which mostly exhibit a columnar discotic mesophase.³¹

When two 1,2-dialkoxybenzene derivatives with two different alkoxy substituents are used, then a mixture of two different triphenylene isomers is obtained.³² The separation of these positional isomers is possible with column chromatography. This method is tedious and unpractical when large amounts of pure isomer are needed.

For further derivatization of the **HATn** molecule, different methods can be used. One possible route is the selective ether cleavage reaction using a stoichiometric amount of a hindered Lewis acid like *B*-bromocatecholborane³³ or 9-bromo-9-borabicyclo[3.3.1]nonane (9-Br-BBN).³⁴

After the ether cleavage reaction a monohydroxy-triphenylene derivative (**HATn-OH**) can be obtained (Scheme 2). This hydroxyl group is a diversification point for further functionalization reactions.



Scheme 2. Ether cleavage reaction of a hexaalkoxytriphenylene derivative **HATn** with a stoichiometric amount of dealkylation agent, such as *B*-bromocatecholborane or 9-Br-BBN.

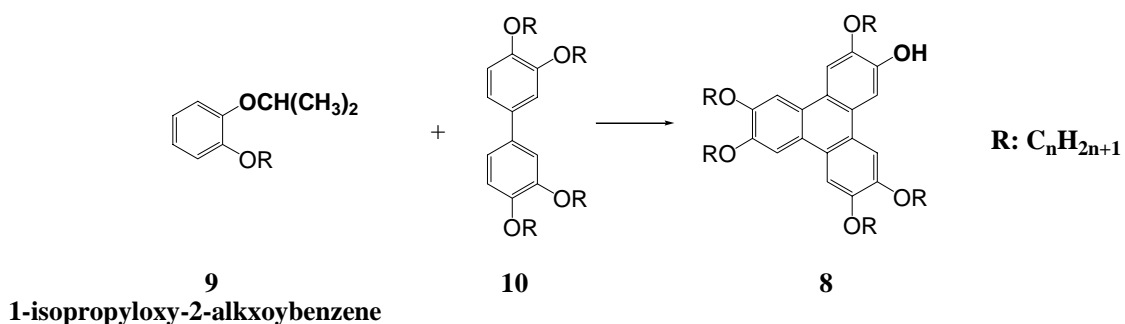
Several interesting examples of LC triphenylene-based compounds are referred, which use as a starting material **HATn-OH** derivative: (a) star-like discotic liquid crystals, which do not crystallize and resemble a well-defined structure with a discotic polymer system;³⁵ (b) triphenylene-containing side chain liquid crystalline ladder-like polysiloxane;³⁶ (c) sugar-coated discotics, a symmetrically hexasubstituted triphenylene with sugar molecules;³⁷ (d) a high diversity of polymeric liquid crystals including triphenylene derivatives;³⁸ (e) extended triphenylenes³⁹ *etc.*

Symmetrically substituted triphenylene **HATn** together with **HATn-OH** derivative have been obtained recently in relatively good yield, by performing the oxidative coupling reaction of 1,2-dialkoxybenzene with trifluoroacetic acid (TFA) in nitromethane.⁴⁰

Moreover, **HATn-OH** derivatives can be obtained by selective monodemethylation of a methoxytriphenylene derivative, using lithium diphenylphosphide.⁴¹

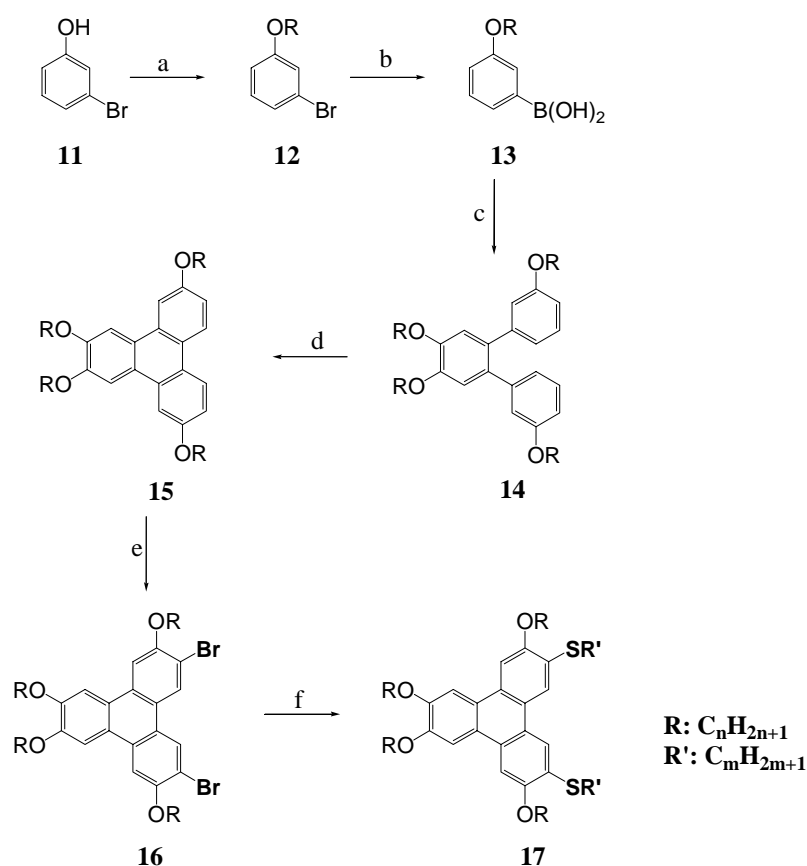
Another synthetic route used to introduce different substituents around **HATn** core is the biphenyl route, illustrated in Scheme 3.⁴² This consists of an oxidative coupling reaction between a 1,2-dialkoxybenzene derivative and a 3,3',4,4'-tetraalkoxybiphenyl molecule. The latter compound can be synthesized *via* an Ullmann coupling reaction,⁴³ between two 1,2-dialkoxybenzene molecules with Cu powder at high temperatures. The same kind of reaction under very mild reaction conditions can be performed when Zn and Pd/C, in acetone / water are used.⁴⁴

Scheme 3 illustrates a more efficient reaction route for the formation of the **HATn-OH** compound, when an isopropyl group is used instead of an *n*-alkoxy substituent. In this particular case, **HATn-OH** derivative is directly obtained after quenching the oxidative coupling reaction with methanol, without the additional ether cleavage step.⁴⁵



Scheme 3. Synthesis route for asymmetrically substituted **HATn-OH (8)** derivative.

Several other unsymmetrical triphenylene derivatives have been prepared via other synthetic pathways. An example is given in Scheme 4.⁴⁶



Scheme 4. Synthetic route for asymmetrically substituted derivatives **17**, with different substituents with $n \neq m$ / $n = m$: (a) RBr , $EtOH$, K_2CO_3 , reflux; (b): (i) Mg , Et_2O ; (ii) $B(OCH_3)_3$; (iii) H_3O^+ ; (c) $PdCl_2$, Na_2CO_3 , PPh_3 , toluene- $EtOH-H_2O$, reflux; (d) $FeCl_3$, CH_2Cl_2 , r.t.; (e) Br_2 , CH_2Cl_2 , $0\text{ }^\circ C$; (f) $R'SH$, KO^tBu , NMP , $70\text{ }^\circ C$.

For instance, the synthesis of compound **17** was achieved starting with 3-bromophenol **11**, which was alkylated and then converted to the corresponding boronic acid. A double Suzuki coupling with 1,2-dibromo-3,4-bis(alkoxy)benzene gave terphenyl derivative **14**. Treatment

of **14** with FeCl_3 results in the formation of triphenylene **15**. Bromination of **15** at the free β -positions provides triphenylene derivative **16**. Finally, substitution of Br with alkanethiol gives the final triphenylene product **17**.

When due to electronic effects, formation of triphenylene ring cannot occur with a Pd catalyst (reaction step d, Scheme 4), photochemical cyclisation can be used as an alternative.⁴⁷

A relatively short overview of triphenylene **8** and HATn (**7**) derivatives preparation, *via* different synthetic pathways was reported recently.⁴⁸

1.5 Hydrogen bonding in columnar discotic materials

H-bonding is an important tool for building molecular architectures with liquid-crystalline properties.⁴⁹

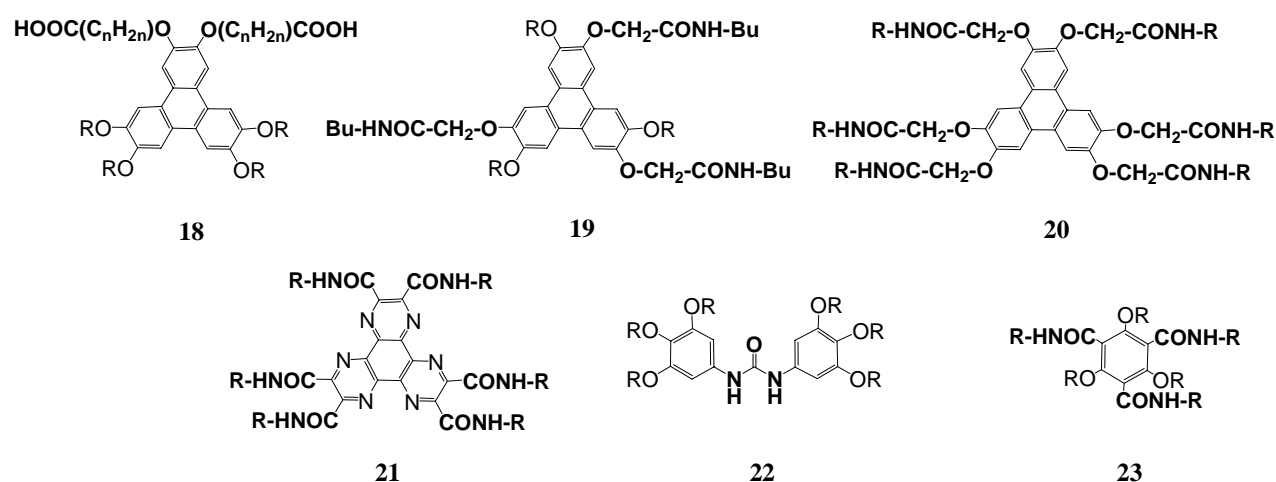


Figure 6. H-bonding in discotic molecules, which form columnar mesophases: **18-20** – derivatives of triphenylene; **21** – hexaazatriphenylene; **22** – N,N'-bis(3,4,5-trialkoxyphenyl)urea; **23** – 1,3,5-benzenetrisamide.

Considerable efforts have been made to construct disk-like molecules that can form columnar mesophases, using H-bonding as a direct tool for the stabilization of their mesophases. Several attractive examples are shown in Figure 6.

A carboxylic acid-terminated triphenylene derivative (**18**) shows columnar hexagonal mesophases, when dimers are formed *via* H-bonding between the two carboxylic functionalities.⁵⁰ Amide H-bonding stabilizes the columnar mesophase of triphenylene derivatives (**19**), for which higher clearing temperatures than for the corresponding ester derivatives have been found.⁵¹

Furthermore, two amide-containing triphenylene derivatives (**20**) have been shown to form a columnar hexagonal mesophase characterized by a π - π stacking distance of 3.6 Å.⁵² As for improving the charge carrier mobility of columnar mesophases, decreasing the π - π stacking distance is highly desired.⁵³ A very short interdisk distance of 3.18 Å has been found for a hexaamide derivative of hexaazatriphenylene (**21**), with a charge carrier mobility of only 0.08 cm² V⁻¹ s⁻¹ at 200 °C.¹³

N, N'-bisurea compounds (**22**) show both rectangular and hexagonal columnar mesophases, based on stacking and strong H-bonding along the columnar axis. Derivatives of 1,3,5-benzenetrisamide (**23**) have attracted considerable attention due to their columnar organization reinforced by amide-H-bonding, which induces a 60 ° rotation between adjacent disk-like molecules.⁵⁴

1.6 Characterization of liquid crystals

The properties of liquid crystalline materials can be investigated with several techniques. For the study of the thermotropic phase transitions, usually differential scanning calorimetry (DSC) is used. This gives information about the phase transition temperatures and the enthalpies accompanying these phase transitions, both on heating and cooling the sample.

For the identification of the liquid crystalline mesophases, very often the texture observed by optical polarizing microscopy (OPM) is analyzed.

However, in order to find out the exact type of mesophase, X-ray diffraction (XRD) is used. This technique provides detailed information about the molecular organization within a given (meso)phase at a certain temperature.

In the case of liquid crystals that exhibit specific interactions, such as H-bonding, Fourier Transform Infrared spectroscopy (FTIR) is used to investigate the relevance of H-bonding within a certain (meso)phase, at a given temperature. In order to quantify the overall mobility of holes and electrons in liquid crystalline materials, pulse radiolysis time resolved microwave conductivity (PR-TRMC)⁵⁵ is often used.

It is important to mention that other techniques, such as solid-state nuclear magnetic resonance (SS-NMR) spectroscopy, neutron and light scattering, dynamic mechanical analysis (DMA) or dielectric spectroscopy, which were not used in this thesis, can also provide important information for the characterization of the liquid crystal mesophases.

1.7 Thesis Outlook

The aim of the research described in this thesis is the preparation of novel discotic materials, by using urea, amide or thiourea H-bonding as a tool for their columnar mesophase stabilization. These new discotics are triphenylene-based compounds, derivatives of 2,3,6,7,10,11-hexakis(hexyloxy)triphenylene (**HAT6**). The structures of these novel materials are given below (Figure 7-10). Their synthesis is detailed in chapters 2 to 5, using different synthetic approaches. Their thermotropic properties have been investigated in order to establish structure-property relationships, for each structure type. Furthermore, their charge carrier transport properties of several compounds have been investigated.

Chapter 1 is an introduction into the field of liquid crystals (LCs), with focus on discotic LCs and their molecular organization. An overview of several synthetic routes to triphenylene-based LCs is given. The relevance of the columnar discotic mesophases stabilization for application of such materials in organic-based electronic devices is outlined.

In **Chapter 2** three different synthetic approaches are described to prepare a series of amide, urea and thiourea-triphenylene derivatives (Figure 7). Regarding the mesomorphic properties of these materials, the influence of H-bonding on the π - π stacking between triphenylene cores is investigated.

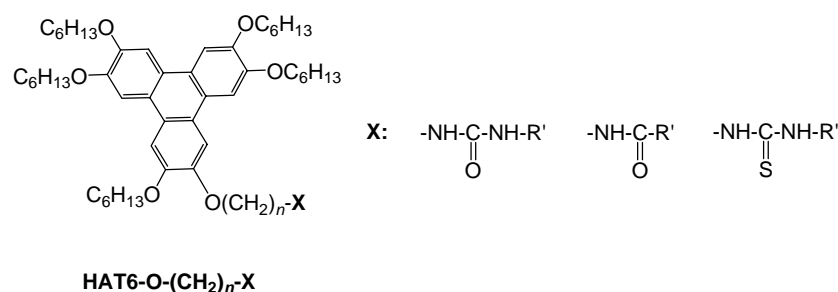
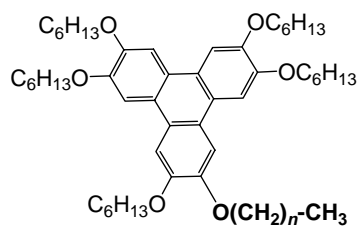


Figure 7. Structure of the amide, urea and thiourea triphenylenes investigated in Chapter 2 (R': alkyl end chains with different length).

Chapter 3 brings forward the importance of symmetry and tail length for obtaining a columnar discotic liquid crystalline material. The subject regarding van der Waals interactions *versus* π - π stacking interactions is the focus point in this chapter.

Even if this investigation does not implicate H-bonding, it shows how sensitive liquid-crystalline properties of triphenylene molecules are upon changing, slightly, the molecular symmetry (Figure 8).



HAT6-O-(CH₂)_n-CH₃

Figure 8. Structure of asymmetrically substituted triphenylenes investigated in Chapter 3.

In **Chapter 4** the synthesis of a 1,3,5-benzenetrisamide with pendant triphenylene groups (Figure 9) is reported. A detailed characterization of its highly ordered mesophase is given in this chapter. For this particular compound, sum charge carrier mobilities have been determined upto temperatures of 200 °C.

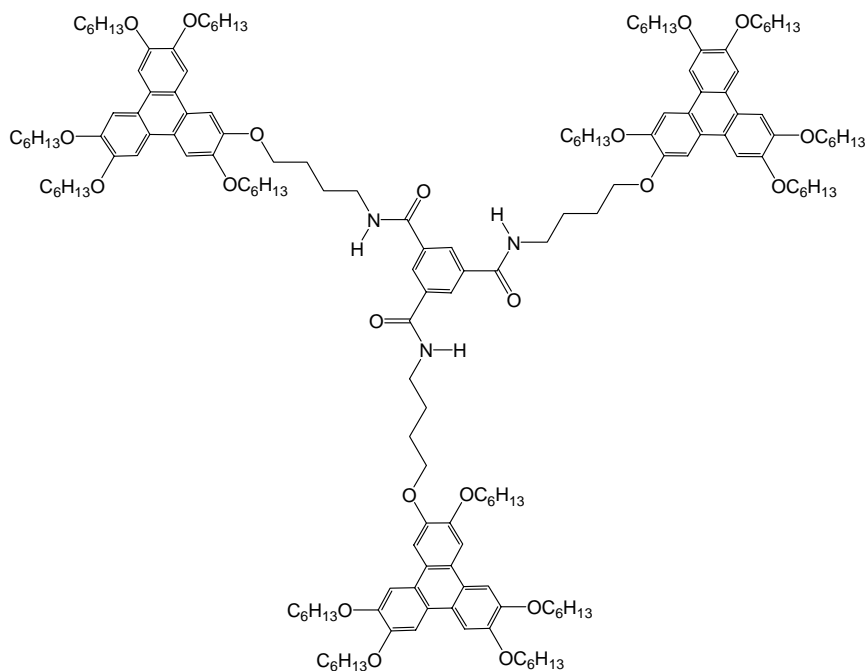


Figure 9. Structure of 1,3,5-benzenetrisamide triphenylene derivative investigated in Chapter 4.

Chapter 5 is an extension of the work presented in Chapter 4. In this chapter the influence of the flexible spacer length (given by n) and the size of the *ortho*-substituent (R') on the columnar packing, is described (Figure 10).

The columnar organization inside the aggregates formed by a chiral 1,3,5-benzenetrisamide triphenylene derivative in an apolar solvent is investigated by circular dichroism (CD) spectroscopy.

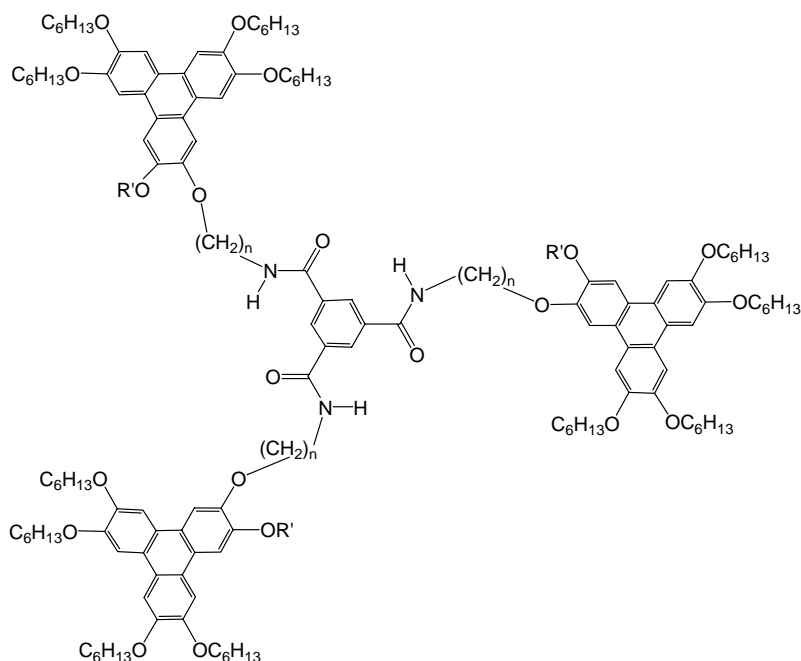


Figure 10. Structure of additional 1,3,5-benzenetrisamide triphenylenes investigated (R': an n-alkyl or a chiral alkyl substituent).

1.8 References

- ¹ (a) Christ, T.; Glösen, B.; Greiner, A.; Kettner, A.; Sander, R.; Stümpflen, V.; Tsukruk, V.; Wendorff, J. H. *Adv. Mater.* **1997**, *9*, 48-52. (b) Bacher, A.; Erdelen, C. H.; Haarer, D.; Paulus, W.; Schmidt, H. W. *SPIE*, **2003**, 313-320. (c) Freudenmann, R.; Behnisch, B.; Hanack, M. *J. Mater. Chem.* **2001**, *11*, 1618-1624. (d) Boden, N.; Bushby, R. J.; Clements, J.; Movaghar, B. *J. Mater. Chem.* **1999**, *9*, 2081-2086.
- ² (a) Petritsch, K.; Friend, R. H.; Lux, A.; Rozenberg, G.; Moratti, S. C.; Holmes, A. B. *Synth. Met.* **1999**, *102*, 1776-1777. (b) Kumar, S.; Schumhacher, P.; Henderson, P.; Rego, J.; Ringsdorf, H. *Mol. Cryst. Liq. Cryst.* **1996**, *288*, 211-222. (c) Schmidt-Mende, L.; Fechtenkötter, A.; Müllen, K.; Moons, E.; Friend, R. H.; MacKenzie, J. D. *Science* **2001**, *293*, 1119-1122.
- ³ Horowitz, G. *J. Mater. Res.* **2004**, *19*, 1946-1962.
- ⁴ Reinitzer, F. *Monatsch Chem.* **1888**, *9*, 421.
- ⁵ Lehmann, O. *Z. Physikal. Chem.* **1889**, *4*, 462.

- ⁶ (a) Chandrasekhar, S. “*Liquid Crystals*” **1992**, 2nd Edition, Cambridge University Press. (b) Demus, D.; Goodby, J. W. G.; Gray, G. W.; Spiess, H. W. “*Handbook of Liquid Crystals*” **1998**, Wiley-VCH.
- ⁷ Chandrasekhar, S.; Sadashiva, B. K.; Suresh, K. A. *Pramana* **1977**, 9, 471-480.
- ⁸ (a) Billard, J.; Dubois, J. C.; Tinh, N. H.; Zann, A. *Nouv. J. Chim.* **1978**, 2, 535-540. (b) Tinh, N. H.; Bernaud, M. C.; Sigaud, G.; Destrade, C. *Mol. Cryst. Liq. Cryst.* **1981**, 65, 307-316. (c) Tinh, N. H.; Gasparoux, H.; Destrade, C. *Mol. Cryst. Liq. Cryst.* **1981**, 68, 101-111.
- ⁹ Bushby, R. J.; Lozman, O. R. *Curr. Opinion Coll. & Interface Sci.* **2002**, 7, 343-354.
- ¹⁰ (a) Kumar, S. *Liq. Cryst.* **2005**, 32, 1089-1113. (b) Kumar, S. *Chem. Soc. Rev.* **2006**, 35, 83-109.
- ¹¹ (a) Kouwer, P. H. J.; Jager, W. F.; Mijs, W. J.; Picken, S. J. *Macromolecules* **2001**, 34, 7582-7584. (b) Kouwer, P. H. J.; Mijs, W. J.; Jager, W. F.; Picken, S. J. *Macromolecules* **2000**, 33, 4336-4342. (c) Kouwer, P. H. J.; Gast, J.; Jager, W. F.; Mijs, W. J.; Picken, S. J. *Mol. Cryst. Liq. Cryst.* **2001**, 364, 225-234.
- ¹² (a) Hunter, C. A.; Sanders, J. K. M. *J. Am. Chem. Soc.* **1990**, 112, 5525-5534. (b) Sinnokrot, M. O.; Sherrill, C. D. *J. Phys. Chem. A* **2006**, 110, 10656-10668.
- ¹³ Gearba, R. I.; Lehmann, M.; Levin, J.; Ivanov, D. A. Koch, M. H. J.; Barbera, J.; Debije, M. G.; Piris, J.; Geerts, Y. H. *Adv. Mater.* **2003**, 15, 1614-1618.
- ¹⁴ Paraschiv, I.; Delforterie, P.; Giesbers, M.; Posthumus, M. A.; Marcelis, A. T. M.; Zuilhof, H.; Sudhölter, E. J. R. *Liq. Cryst.* **2005**, 32, 977-983.
- ¹⁵ (a) Leisen, J.; Werth, M.; Boeffel, C.; Spiess, H. W. *J. Chem. Phys.* **1992**, 97, 3749-3759. (b) Brown, S. P.; Schnell, I.; Brand, J. D.; Müllen, K.; Spiess, H. W. *J. Molec. Struct.* **2000**, 521, 179-195.
- ¹⁶ (a) Simmerer, J.; Glösen, B.; Paulus, W.; Kettner, A.; Schuhmacher, P.; Adam, D.; Eitzbach, K. H.; Siemensmeyer, K.; Wendorff, J. H.; Ringsdorf, H.; Haarer, D. *Adv. Mater.* **1996**, 8, 815-819. (b) Glösen, B.; Heitz, W.; Kettner, A.; Wendorff, J. H. *Liq. Cryst.* **1996**, 20, 627-633. (c) Kopitzke, J.; Wendorff, J. H.; Glösen, B. *Liq. Cryst.* **2000**, 27, 643-648.
- ¹⁷ (a) Eley, D. D. *Nature* **1948**, 162, 819. (b) Vartanyan, A. T. *Zhur. Fiz. Kim.* **1948**, 22, 769-782.
- ¹⁸ Akamatu, H.; Inokutchi, H. Matsunaga, Y. *Nature* **1954**, 173, 168-169.
- ¹⁹ Ferraris, J.; Cowan, D. O.; Walatka, V. V.; Perstein, J. H. *J. Am. Chem. Soc.* **1973**, 95, 948-949.

- ²⁰ Chiang, C. K.; Fincher, C. R.; Jr., Park, Y. W.; Heeger, A. J.; Shirakawa, H.; Louis, E. J.; Gau, S. G.; MacDiarmid, A. G. *Phys. Rev. Lett.* **1977**, *39*, 1098-1101.
- ²¹ Friend, R. H.; Gymer, R. W.; Holmes, A. B.; Burroughes, J. H.; Marks, R. N.; Taliani, C.; Bradley, D. D. C.; Dos Santos, D. A.; Bredas, J. L.; Löglund, M.; Salaneck, W. R. *Nature*, **1999**, *397*, 121-128.
- ²² (a) Warman, J. M.; Schouten, P. G. *Appl. Organometal. Chem.* **1996**, *10*, 637-647. (b) van de Craats, A. M.; Warman, J. M.; Fechtenkötter, A.; Brand, J. D.; Harbison, M. A.; Müllen, K. *Adv. Mater.* **1999**, *11*, 1469-1472.
- ²³ Boden, N.; Bushby, R. J.; Clements, J.; Movaghar, B.; Donovan, K. J.; Kreouzis, T. *Phys. Rev. B* **1995**, *52*, 13274-13280.
- ²⁴ (a) Adam, D.; Chuhmacher, P.; Simmerer, J.; Häußlinger, L.; Siemensmeyer, K.; Etzbach, K. H.; Ringsdorf, H.; Haarer, D. *Nature* **1994**, *371*, 141-143. (b) Kreouzis, T.; Donovan, K. J.; Boden, N.; Bushby, R. J.; Lozman, O. R.; Liu, Q. *J. Chem. Phys.* **2001**, *114*, 1797-1802.
- ²⁵ (a) Heiney, P. A.; Fontes, E.; De Jeu, W. H.; Riera, A., Carroll, P.; Smith, A. B. *III. J. Phys. France* **1989**, *50*, 461-483. (b) Fontes, E.; Heiney, P. A.; De Jeu, W. H.; *Phys. Rev. Lett.* **1988**, *61*, 1202-1205.
- ²⁶ van de Craats, A. M.; Warman, J. M.; de Haas, M. P.; Adam, D.; Simmerer, J.; Haarer, D.; Schuhmacher, P. *Adv. Mater.* **1996**, *8*, 823-826.
- ²⁷ Lemaure, V.; da Silva Filho, D. A.; Coropceanu, V.; Lehmann, M.; Geerts, Y. H.; Piris, J.; Debije, M. D.; van de Craats, A. M.; Senthilkumar, K.; Siebbeles, L. D. A.; Warman, J. M.; Brédas, J. L.; Cornil, J. *J. Am. Chem. Soc.* **2004**, *126*, 3271-3279.
- ²⁸ Warman, J. M.; van de Craats, A. M. *Mol. Cryst. Liq. Cryst.* **2003**, *396*, 41-72.
- ²⁹ Naarmann, H.; Hanack, M.; Mattmer, R. *Synthesis* **1994**, 477-478.
- ³⁰ Kumar, S.; Varshney, S. K. *Liq. Cryst.* **1999**, *26*, 1841-1843.
- ³¹ Kumar, S.; Manickam, M. *Chem. Commun.* **1997**, 1615-1616.
- ³² (a) Paraschiv, I.; Tomkinson, A.; Posthumus, M. A.; Giesbers, M.; Marcelis, A. T. M.; Zuilhof, H.; Sudhölter, E. J. R., *manuscript in preparation*. (b) Tinh, N. H.; Bernaud, M. C.; Sigaud, G.; Destrade, C. *Mol. Cryst. Liq. Cryst.* **1981**, *65*, 307-316.
- ³³ Kumar, S.; Manickam, M. *Synthesis*, **1998**, 1119-1122.
- ³⁴ (a) Closs, F.; Häußling, L.; Henderson, P.; Ringsdorf, H.; Schumhmacher, P. *J. Chem. Soc., Perkin Trans. I.* **1995**, 829-837. (b) Wright, P. T.; Gillies, I.; Kilburn, J. D. *Synthesis* **1997**, 1007-1009.
- ³⁵ Plesnivý, T.; Ringsdorf, H.; Schuhmacher, P. *Liq. Cryst.* **1995**, *18*, 185-190.

- ³⁶ Ba, C. Y.; Shen, Z. R.; Gu, H. W.; Guo, G. Q.; Xie, P.; Zhang, R. B.; Zhu, C. F.; Wan, L. J.; Li, F. Y.; Huang, C. H. *Liq. Cryst.* **2003**, *30*, 391-397.
- ³⁷ Barberá, J.; Garcés, A. C.; Jayaraman, N.; Omenat, A.; Serrano, J. L.; Stoddart, J. F. *Adv. Mater.* **2001**, *13*, 175-180.
- ³⁸ (a) Disch, S.; Finkelmann, H.; Ringsdorf, H.; Schumhacher, P. *Macromolecules* **1995**, *28*, 2424-2428. (b) Wan, W.; Monobe, H.; Tanaka, Y.; Shimizu, Y. *Liq. Cryst.* **2003**, *30*, 571-578. (c) Otmakhova, O. A.; Kuptsov, S. A.; Talroze, R. V.; Patten, T. E. *Macromolecules* **2003**, *36*, 3432-3435.
- ³⁹ Yatabe, T.; Harbison, M. A.; Brand, J. D.; Wagner, M.; Müllen, K.; Samori, P.; Rabe, J. P. *J. Mater. Chem.* **2000**, *10*, 1519-1525.
- ⁴⁰ Kumar, S.; Lakshmi, B. *Tetrahedron Lett.* **2005**, *15*, 2603-2605.
- ⁴¹ Boden, N.; Bushby, R. J.; Cammidge, A. N.; Martin, P. S. *J. Mater. Chem.* **1995**, *5*, 1857-1860.
- ⁴² (a) Boden, N.; Bushby, R. J.; Cammidge, A. N.; Headdock, G. *Synthesis* **1995**, 31-32. (b) Boden, N.; Bushby, R. J.; Cammidge, A. N.; El-Mansoury, A.; Martin, P. S.; Lu, Z. *J. Mater. Chem.* **1999**, *9*, 1391-1402.
- ⁴³ Nelson, T. D.; Crouch, R. D. “*Organic Reactions*”, **2004**, *63*, 265-555.
- ⁴⁴ Rose, A.; Lugmair, C. G.; Swager, T. M. *J. Am. Chem. Soc.* **2001**, *123*, 11298-11299.
- ⁴⁵ Bushby, R. J.; Zhibao, L. *Synthesis* **2001**, *5*, 763-767.
- ⁴⁶ (a) Cammidge, A. N.; Goppe, H. *J. Mater. Chem.* **2001**, *11*, 2773-2783. (b) Cammidge, A. N.; Goppe, H. *Chem. Commun.* **2002**, 966-967.
- ⁴⁷ Bushby, R. J.; Hardy, C. *J. Chem. Soc., Perkin Trans.*, **1986**, *1*, 721-723.
- ⁴⁸ Mao, H. X.; He, Z. Q.; Zhang, C. X. *Chin. J. Org. Chem.* **2006**, *26*, 413-418.
- ⁴⁹ (a) Kato, T. “*Structure and Bonding*”, **2000**, *96*, 95-146, Springer Verlag Berlin Heilderberg. (b) Beginn, U. *Prog. Polym. Sci.* **2003**, *28*, 1049-1105.
- ⁵⁰ Wan, W.; Monobe, H.; Sugino, T.; Tanaka, Y.; Shimizu, Y. *Mol. Cryst. Liq. Cryst.* **2001**, *364*, 597-603.
- ⁵¹ Zhao, K. Q.; Gao, C. Y.; Hu, P.; Wang, B. Q.; Li, Q. *Acta Chimica Sinica* **2006**, *64*, 1051-1062.
- ⁵² Ikeda, M.; Takeuchi, M.; Shinkai, S. *Chem. Commun.* **2003**, 1354-1355.
- ⁵³ Liu, C. Y.; Bard, A. J. *Nature*, **2002**, *418*, 162-164.
- ⁵⁴ Bushey, M. L.; Hwang, A.; Stephens, P. W.; Nuckolls, C. *Angew. Chem. Int. Ed.* **2002**, *41*, 2828-2831.

⁵⁵ (a) Warman, J. M.; Gellinck, G. H.; de Haas, M. P. *J. Phys.: Condens. Matter.* **2002**, *14*, 9935-9954. (b) Watson, M. D.; Debije, M. G.; Warman, J. M.; Müllen, K. *J. Am. Chem. Soc.* **2004**, *126*, 766-771. (c) Warman, J. M.; de Haas, M. P.; Dicker, G.; Grozema, F. C.; Piris, J.; Debije, M. G. *Chem. Mater.* **2004**, *16*, 4600-4609.

Chapter 2

Amide, Urea and Thiourea-Triphenylene Derivatives: Synthesis and Mesomorphic Properties*

Abstract – *The synthesis and thermotropic properties of a series of hexaalkoxytriphenylenes that contain an amide, urea or thiourea group in one of their alkoxy tails are reported. Three different routes were explored for the synthesis of these compounds; the biphenyl route proved to be the best with respect to yields and versatility. The intermolecular hydrogen bonding abilities of these molecules have a negative influence on the formation and stability of the columnar liquid crystalline phases. The stronger the hydrogen bonding, the more the liquid crystallinity is suppressed, probably due to disturbance of the π - π stacking of the triphenylene disks. As a direct result, urea and amide containing triphenylene derivatives do not exhibit liquid crystalline properties, while several thiourea derivatives revealed columnar hexagonal mesophases, as shown by differential scanning calorimetry, optical polarization microscopy and X-ray diffraction.*

* This chapter is based on:

Paraschiv, I.; Tomkinson, A.; Posthumus, M. A.; Giesbers, M.; Marcelis, A. T. M.; Zuilhof, H.; Sudhölter, E. J. R. - *manuscript in preparation.*

2.1 Introduction

Discotic molecules, such as 2,3,6,7,10,11-hexakis(hexyloxy)triphenylene (**HAT6**) and several of its derivatives,¹ self-assemble into columns based on favorable π - π interactions between their polyaromatic cores.² This particular type of interaction leads to the formation of a one-dimensional pathway for transport of charge carriers along the columns.³ Based on their semiconducting properties,⁴ these π -conjugated materials offer a remarkable potential as active elements in electronic devices such as field effect transistors (FETs), photovoltaic solar cells, and light-emitting diodes (LEDs).⁵

One of the key factors for a good performance of organic-based electronic devices is the *efficiency of charge transport through self-assembled columnar stacks* of molecules, from one electrode to another.⁶ This efficiency is strongly correlated with the degree of ordering inside the organic-based active layer(s), which is regularly used inside an electronic device, as a thin film or as a crystal.⁷ Given the fact that inside the columns disk-like molecules can still oscillate, slide out of the column or rotate around the columnar axis,⁸ it is still a challenge to obtain electronic devices with high performance by using disk-like molecules. In order to restrict these movements inside the columnar stacks, the stabilization of disk-like molecules in a highly stable and ordered columnar phase is strongly desired.

One possible way of stabilizing disk-like molecules inside its columnar organization is to make use of H-bonding interactions. These interactions play an important role in supramolecular chemistry of self-assembled molecules,⁹ and are considered to be an important tool to construct interesting functional liquid-crystalline assemblies.¹⁰

A good example of well-defined molecular architectures that make use of the H-bonding properties of a urea moiety is a recently reported urea-containing tetraphenoxy-substituted perylenebisamide, which self-assembles by hydrogen-bonding and π - π stacking interactions leading to the formation of a fluorescent organogel in toluene and CCl_4 .¹¹ Additional examples such as bisurea gelators, which can form one-dimensional fibers, based on π -stacked molecular assembling with well-defined directionality of urea-H-bond interactions are known.¹² Furthermore, ferroelectrically switchable columnar liquid crystals containing urea groups have been obtained, based on favorable H-bonding and π - π stacking interactions.¹³

In the columnar liquid crystalline state, polyaromatic molecules stack one in top of each other with an intermolecular π - π stacking distance of about 3.6 Å.¹⁴ In the case of H-bonding enforced discotic mesophases, the π - π stacking distance can be reduced to 3.18 Å,¹⁵ which

expected to lead to higher charge mobilities.¹⁶ However, even in this case of very close π - π distances, as obtained for hexaazatriphenylene derivatives,¹⁷ a disappointing charge carrier mobility of only $0.08 \text{ cm}^2 \text{ V}^{-1} \text{ s}^{-1}$ was found at $200 \text{ }^\circ\text{C}$.¹⁵

A more efficient H-bond stabilization of triphenylene molecules has recently been realized using a C_3 -symmetrical 1,3,5-benzenetrisamide central unit, surrounded by three pendant triphenylene groups.¹⁸ In this particular case, successive triphenylene cores in the columnar stacks rotate as little as 15° with respect to each other. This small rotation of successive triphenylene cores allowed charge carrier mobilities as high as $0.12 \text{ cm}^2 \text{ V}^{-1} \text{ s}^{-1}$ at $180 \text{ }^\circ\text{C}$. Theoretically, a small rotation results in a large splitting of the frontier electronic levels (HOMO, LUMO), which is favorable for a high charge carrier mobility.¹⁹

The amide hydrogen bonds²⁰ have very often been used to decrease the intra-columnar distance and lock the movements of the disk-like molecules inside the columns, as seen by the work of Meijer and Nuckolls.²¹ This results in higher clearing points of the amides than of the corresponding ester derivatives, as observed for a series of symmetrically substituted triphenylenes.²² **HAT6** molecules have also been immobilized by hydrogen-bonded fibrous aggregates of two amino acids. In these aggregates, the hole mobility of **HAT6** was nearly three times as high as that observed for pure **HAT6**.²³ Furthermore, intra-columnar H-bonding has been used to stabilize columnar assemblies of carboxylic acid-terminated triphenylene and hexabenzocoronene derivatives, by locking the disk-like molecules into a stable columnar phase.²⁴

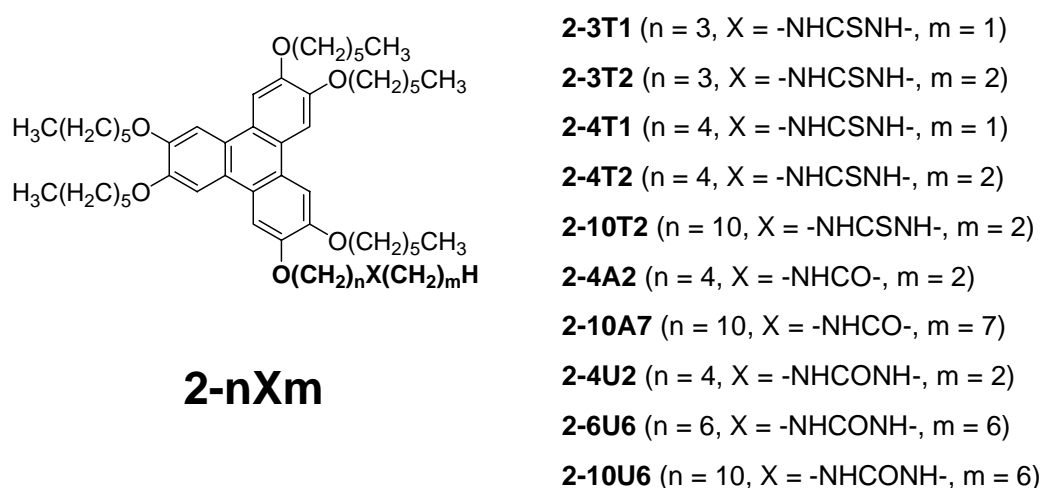
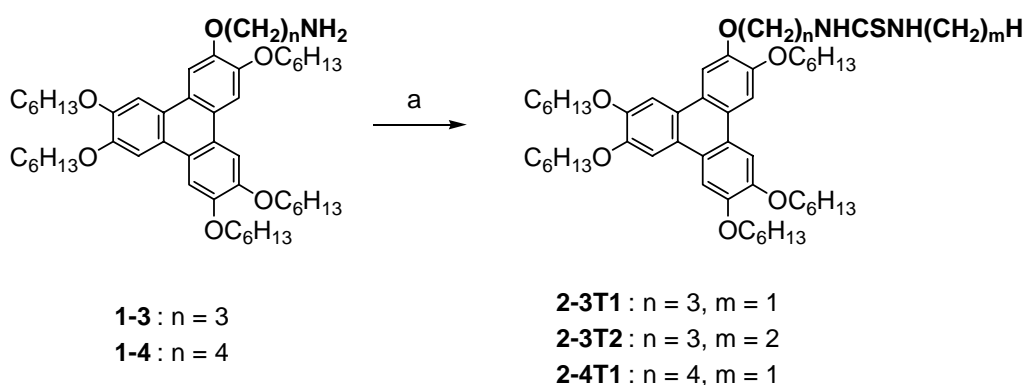


Figure 1. Structure of the H-bond-tailoring triphenylene derivatives, **2-nXm**, under investigation (X: T = thiourea; U = urea; A = amide derivative).

2.2 Results and Discussions

2.2.1 Synthesis

Compounds **2-3T1**, **2-3T2** and **2-4T1** have been synthesized using amino-terminated triphenylenes **1-3** and **1-4**, respectively, which will be described in more detail in Chapters 4 and 5 of this thesis. The final reaction step, which is relevant for this chapter, is shown in Scheme 2.



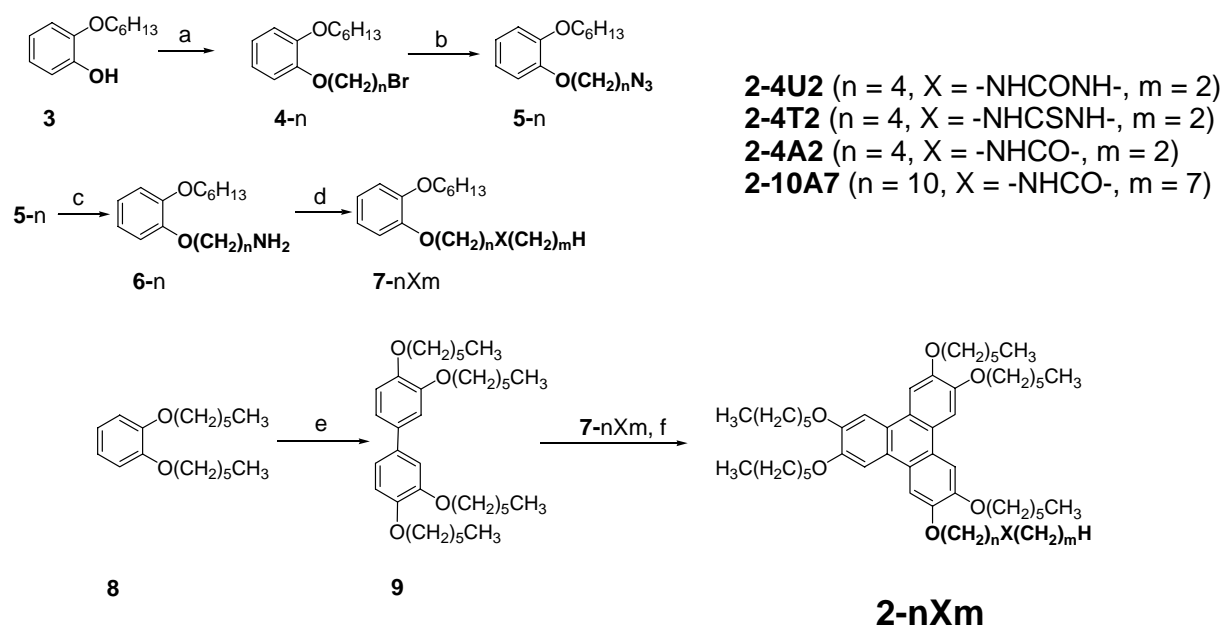
Scheme 2. Reaction scheme for the synthesis of **2-3T1** : (a). CH_3NCS , benzene, pyridine; **2-3T2**, **2-4T1** : (a). $\text{C}_2\text{H}_5\text{NCS}$, and respectively CH_3NCS , CH_2Cl_2 , Et_3N .

Compounds **2-4U2**, **2-4T2**, **2-4A2**, **2-10A7** were synthesized using the biphenyl route (Scheme 3).¹⁴ The synthesis of biphenyl **9** will be reported in Chapter 3 of this thesis.

The final reaction step depicted in Scheme 3 is an oxidative coupling using FeCl_3 in CH_2Cl_2 under anhydrous conditions.

Intermediary compounds **2-6U6** and **2-10U6** have been synthesized using the reaction route presented in Scheme 4, which consists of a trimerization reaction using MoCl_5 .²⁵ Compounds **7-6U6** and **7-10U6**, required for this last step, have been prepared using the method shown in Scheme 3.

For compound **7-10U6**, catechol was reacted with 1-bromohexane to form both 2-hexyloxyphenol **3** (35 %) and 1,2-bis-hexyloxybenzene **8** (51 %), which were separated by column chromatography. In case only compound **8** was required, a higher yield was obtained when Cs_2CO_3 in acetonitrile was used, with an excess of bromohexane.²⁶

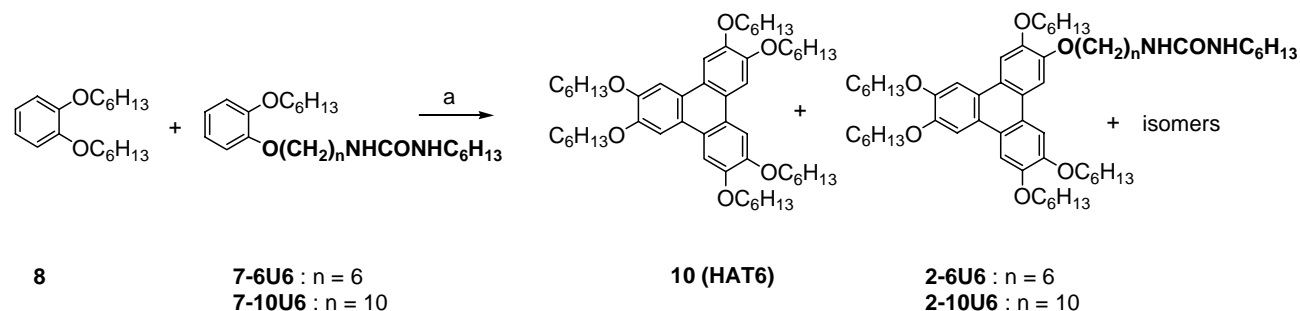


Scheme 3. Reaction scheme for the synthesis of compounds **2-4U2**, **2-4T2**, **2-4A2** and **2-10A7**:

(a). $\text{Br}(\text{CH}_2)_n\text{Br}$, 2-butanone (ethanol or acetonitrile), K_2CO_3 or Cs_2CO_3 ; (b). NaN_3 , ethanol; (c). LiAlH_4 , THF, $\text{Na}_2\text{SO}_4 \times 10 \text{H}_2\text{O}$; (d). $\text{CH}_3(\text{CH}_2)_{m-1}\text{NCO}$ (for ureas), $\text{CH}_3(\text{CH}_2)_{m-1}\text{COCl}$ (for amides) or $\text{CH}_3(\text{CH}_2)_{m-1}\text{NCS}$ (for thioureas), CH_2Cl_2 ; (e). ICl , CHCl_3 ; Cu , heat; (f). FeCl_3 , CH_2Cl_2 ; MeOH .

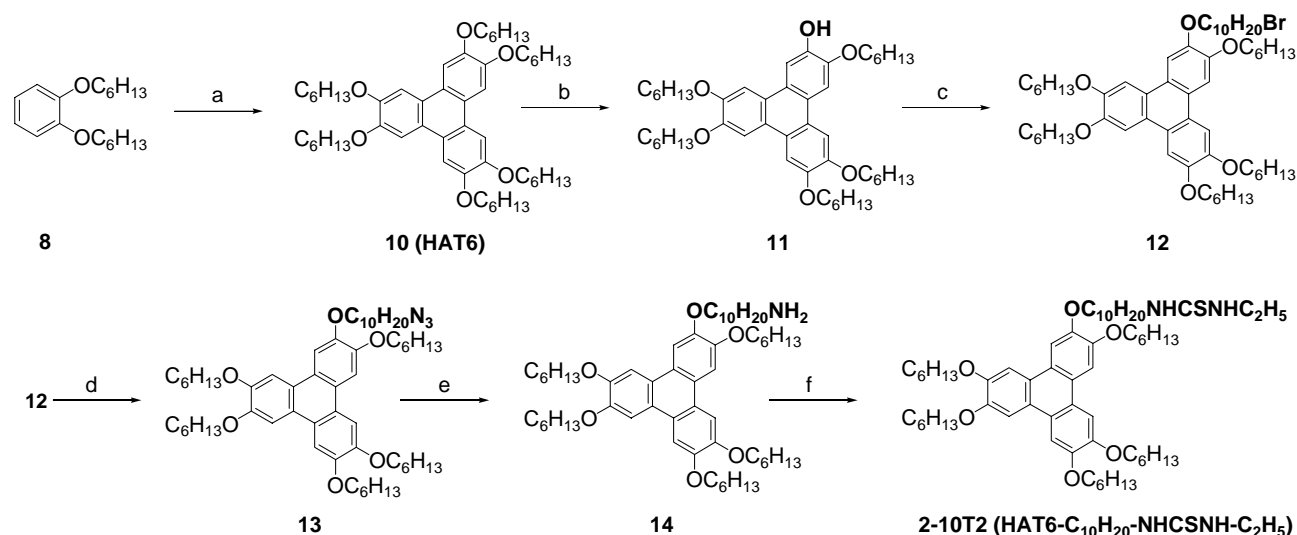
2-Hexyloxyphenol **3** has been further reacted with 1,10-dibromodecane to give 1-(10-bromodecyloxy)-2-hexyloxybenzene **4-10**, (62 %). In the next step, this bromo-derivative **4-10** was reacted with sodium azide to give 1-(10-azidodecyloxy)-2-hexyloxybenzene **5-10** (95 %). Subsequently, the azide was reduced with LiAlH_4 to give 10-(2-hexyloxyphenoxy)decylamine **6-10** (93 %).

1-Hexyl-3-(10-[2-hexyloxyphenoxy]decyl)urea **7-10U6** was obtained in an 85 % yield by reaction of **6-10** with hexyl isocyanate. Under strictly anhydrous conditions, a mixture of mainly 2,3,6,7,10,11-hexakis-hexyloxytriphenylene **10 (HAT6)** and 1-hexyl-3-(10-[2,5,6,9,10-pentahexyloxytriphenylene]decyl)urea **2-10U6** has been obtained as shown in Scheme 4.



Scheme 4. Reaction scheme for the synthesis of **10 (HAT6)** and **2-6U6**, **2-10U6**: (a). MoCl_5 , CH_2Cl_2 ; methanol.

The last triphenylene derivative **2-10T2** was synthesized according to Scheme 5. The oxidative coupling reaction has been applied to 1,2-dihexyloxybenzene **8**, in order to obtain the symmetrically hexasubstituted triphenylene, **10 (HAT6)** in 45 % yield.²⁷ After the selective ether cleavage reaction of **10 (HAT6)** with *B*-bromocatecholborane, **11 (HAT6OH)** has been obtained in 48 % yield, following a modified method reported in the literature.²⁸ Next, the monohydroxy-triphenylene derivative **11** has been reacted with 1,10-dibromodecane in order to obtain the bromo-terminated triphenylene **12**.²⁹ Compound **12** has been further refluxed with sodium azide in ethanol, to afford compound **13**, which was reduced with lithium aluminium hydride to obtain amino-terminated triphenylene **14**. This was finally reacted in dichloromethane with ethyl isothiocyanate to obtain thiourea triphenylene derivative **2-10T2** in 49 % yield.



Scheme 5. Reaction scheme for the synthesis of **2-10T2**: (a). MoCl₅, CH₂Cl₂; MeOH; (b). C₆H₄O₂BBr (3 eq), CH₂Cl₂; H₂O; (c). Br-C₁₀H₂₀-Br, EtOH, K₂CO₃; (d). NaN₃, EtOH; (e). LiAlH₄, THF, NaOH, H₂O, Na₂SO₄ x 10 H₂O; (f). C₂H₅NCS, CH₂Cl₂.

Regarding the practicability of all the different synthetic routes that have been explored for the synthesis of compounds **2-nXm**, it is important to mention that in the hands of the author the most efficient method is the biphenyl route shown in Scheme 3. It should be stressed that rigorous anhydrous conditions are required for handling anhydrous FeCl₃. The presence of small traces of water, gives rise to the formation of a mixture of several triphenylene isomers due to unselective ether cleavage reactions at the **HAT6** core, which are difficult to separate by column chromatography using silica gel.

By using the synthetic route presented in Scheme 4 always a mixture of several triphenylene isomers is obtained, dramatically decreasing the reaction yield, and making the purification procedure tedious.

The difficulties of the route shown in Scheme 5 lie in the selective ether cleavage reaction, which is highly sensitive towards moisture and reaction time; additionally the separation of **11** from **HAT6 (10)** requires extensive column separations on silica gel.

2.2.2 Characterization

The structures and purity of the synthesized products were confirmed by ¹H-NMR, ¹³C-NMR, mass spectroscopy and thin layer chromatography (TLC). For the exact mass determination of **2-3T1**, **2-10T2** and **2-6U6** the molecular ion peak was not observed, while only several fragments were found. However, the correct structure of these materials have been confirmed by NMR, TLC and Fourier Transform Infrared (FTIR) investigations. The properties of **2-nXm** compounds were investigated using optical polarization microscopy (OPM), differential scanning calorimetry (DSC), temperature-dependent FTIR spectroscopy and X-ray diffraction (XRD).

OPM shows that not all synthesized compounds exhibit mesophase formation. The compounds with an amide or urea group do not show liquid crystalline behavior, while the compounds with a thiourea group show a columnar discotic texture. The thiourea with the longest spacer, **2-10T2**, shows no mesophase. Compounds **2-3T1**, **2-3T2** and **2-4T1** are enantiotropic, while **2-4T2** shows a monotropic behavior.

The fan-like textures of the liquid crystalline thiourea compounds in the series (**2-3T1**, **2-3T2**, **2-4T1**) are typical for a hexagonal columnar discotic mesophase (Col_h) (Figure 2), regularly observed for triphenylene derivatives.³⁰

The DSC results are shown in Table 1 for all **2-nXm** compounds. Within the series of compounds that have a butyl spacer and an ethyl terminal group, the urea derivative **2-4U2** shows the highest melting point (135 °C), followed by the amide derivative **2-4A2** (112 °C) and then by the thiourea derivative **2-4T2** (73 °C). A similar trend is observed among all compounds under present study: the urea derivatives show the highest melting points followed by the amide and then by the thiourea compounds. This thermal stability hierarchy corresponds with the H-bonding strength, which is the strongest between urea groups,³¹ weaker between amide groups (one H-bond less than between urea groups), and even weaker between thiourea groups.³² From this point of view, the H-bonding interactions between urea or amide groups turned out to be detrimental for the formation of a mesophase.



Figure 2. Polarized optical microphotographs of (a) **2-3T1** at 64 °C, (b) **2-3T2** at 63 °C, (c) **2-4T1** at 57 °C, all indicating a Col_h phase (See the Appendix at the end of the thesis for the color pictures).

Table 1. Transition temperatures (°C) and transition enthalpies (kJ mol⁻¹, between square brackets) of the triphenylene derivatives **2-nXm** (DSC, 10 °C min⁻¹) and **HAT6** (DSC, 5 °C min⁻¹).

Compound	Heating				Cooling		
	Cr ₁ ^d	Cr ₂ ^d	Col _h	I	I	Col _h	Cr ₃ ^d
HAT6*	• 67 [40]		• 98 [5]	•	•	96 [5]	• 48 [42] •
2-3T1	• 55 [3]	• 64 [3]	• 75 [2]	•	•	67 [3]	• - ^a •
2-3T2	• 60 [29]		• 69 [2]	•	•	60 [2]	• - ^a •
2-4T1	• 60 [30]		• 65 [1]	•	•	59 [1]	• 35 [-] ^c •
2-4T2	• 61	• 73 [23] ^b		•	•	54 [2]	• 37 [-] ^c •
2-10T2	• 37 [15]	• 41 [6]		•	•		19 [-] ^c •
2-4A2	• 112 [56]			•	•		67 [49] •
2-10A7	• 55	• 74 [41] ^b		•	•		- ^a •
2-4U2	• 135 [54]			•	•		119 [35] •
2-6U6	• 84	• 91 [30] ^b		•	•		61 [36] •
2-10U6	• 68	• 77 [37] ^b		•	•		47 [-] ^c •

Notes: ^aNo crystallization was observed upon cooling to room temperature; ^b ΔH corresponds to Cr₁ - Cr₂ and Cr₂ - I transitions; ^ccould not be determined due to only partial crystallization; ^dunknown crystalline phases (Cr₁, Cr₂, Cr₃).

The H-bonding interactions appear to be, in this particular case, a perturbing factor for the π -stacking of the triphenylene cores, which in fact is essential for obtaining the columnar

* **HAT6**, previously reported in Chapter 3, as compound **4-6**.

discotic mesophase.³³ The four thiourea compounds that show liquid crystalline behavior were also studied by X-ray powder diffraction. They all show a columnar hexagonal phase (Col_h), as very often observed for triphenylenes, confirming the conclusion from OPM.³⁴ As can be seen in Table 2, the intercolumnar distance slightly increases with increasing total tail length, as expected.¹⁴ Compared to the corresponding alkyl derivatives with the same total tail length the intercolumnar distance is about 0.6 Å shorter. This may be caused by intermolecular hydrogen bonding that has a compacting effect on the fluid alkyl tails of these compounds.

Comparison of these thiourea compounds with molecules having only methylene moieties in the tail (Chapter 3), shows that the melting points in the thiourea compounds are higher and the isotropization temperatures are lower for compounds with the same tail lengths.

It therefore seems that hydrogen bonding in these materials stabilizes the crystalline state and destabilizes the liquid crystalline ordering. This trend seems to hold also for the amide and urea derivatives; the melting points become higher for compounds that give stronger H-bonding, while for these two classes of materials the liquid crystallinity even disappears completely.

Table 2. X-ray data for the liquid crystalline thiourea derivatives.

Comp.	Temperature (°C)	Type of mesophase	Interdisk distance (Å)	<i>d</i> – spacing (intercolumn distance) ^a (Å)
HAT6*	90	Col _h	3.61	18.34 (21.17)
2-3T1	50	Col _h	3.60	18.04 (20.83)
2-3T2	45	Col _h	3.60	18.20 (21.01)
2-4T1	60	Col _h	3.65	18.20 (21.01)
2-4T2	64	Col _h	3.95	18.40 (21.24)

^a – intercolumn distance is $2/\sqrt{3} \times d$.

Hydrogen bonding in **2-nXm** molecules was investigated, for different phases, by FTIR spectroscopy.³⁵ FTIR spectra for three different triphenylene derivatives (**2-10U6**, **2-4A2** and **2-3T2**) with different H-bonding groups were recorded at room temperature, using dried

* **HAT6**, previously reported in Chapter 3, as compound **4-6**.

powder samples as obtained after recrystallization from a polar organic solvent (i.e. acetonitrile).

FTIR spectra were recorded for CDCl_3 solutions. The $\nu(\text{N-H})$ stretching bands appear as double sharp peaks at 3430 and 3363 cm^{-1} for **2-3T2**, as a single peak at 3448 cm^{-1} for **2-10U6** and as double sharp peaks at 3451 and 3409 cm^{-1} for **2-4A2**, respectively, which correspond to *non-H-bonded* N-H functionalities, as the molecules are solubilized in CDCl_3 (which is a good solvent for these molecules). As regards the $\nu(\text{C=O})$ stretching (amide I) band, for **2-10U6** derivative appears at 1664 cm^{-1} and for **2-4A2** at 1663 cm^{-1} .

FTIR were recorded for the neat samples, at room temperature, onto KBr pellet, when *H-bonded* N-H functionalities were evidenced. The $\nu(\text{N-H})$ stretching vibration band appears as a broad band at 3282 cm^{-1} for **2-3T2**, as a sharp peak at 3344 cm^{-1} for **2-10U6** and as a sharp peak at 3305 cm^{-1} for **2-4A2**. The $\nu(\text{C=O})$ stretching (amide I) band appears at 1621 cm^{-1} for **2-10U6** and at 1642 cm^{-1} for **2-4A2**.

These differences clearly demonstrate a weakening of H-bonding interactions between molecules dissolved into CDCl_3 .³⁶ Much stronger H-bonding interactions are found in neat samples at room temperature.

Temperature-dependent FTIR spectra of compound **2-3T2** (neat) were recorded upon cooling from 80 °C, which is 20 °C higher than its isotropic point. At 80 °C, the free N-H functionalities are indicated by a small shoulder at 3351 cm^{-1} , which is somewhat lower as compared to the value found for CDCl_3 solution. Matching up the peaks representative of free and bonded N-H functionalities, it can be concluded that H-bonding, between the thiourea groups, persists over a wide temperature range. This H-bonding cannot be totally disrupted even at temperatures far above the isotropization point, proving once more the relevance of the thiourea H-bonding interactions for the formation of a stable columnar mesophase.

Based on these properties, observed for compounds **2-nXm**, a model for the intermolecular interactions is proposed.

The strength and relation between these interactions are important for obtaining liquid crystalline behavior, for this type of molecules. A columnar mesophase is obtained for the combination of rigid central cores that display π - π stacking interactions and flexible chains at the periphery. If the π - π stacking, which is vital for a columnar organization is disturbed, the mesophase range narrows or is completely suppressed. This last situation is observed in the case of urea and amide-containing triphenylene derivatives. In these two cases, the H-bond interactions are too strong disturbing the π - π stacking between the triphenylene disks.

It was shown previously that asymmetry in the alkyl tail lengths can also be a disturbing factor for formation of columnar phases of **HAT** derivatives. Replacement of one of the six hexyloxy substituents, around **HAT6**, with another alkoxy substituent with more than twelve carbon atoms, completely suppresses the liquid crystalline behavior.¹⁴ The properties of compounds **2-nXm** constitute the second evidence, in this respect. This is the reason for the non-mesomorphic behavior of **2-10T2**, the thiourea compound with the longest total tail length. These results represent an additional confirmation for the dramatic disturbance of the columnar organization, which is produced by changing the structure of only one substituent around the **HAT6** core. Comparable results were found for 2,3,6,7,10,11-hexakispendyloxytriphenylene (**HAT5**) derivatives, for which bulky or polar substituents were found to destabilize the columnar mesophase.³⁷

2.3 Conclusions

Several novel triphenylene derivatives with urea, amide or thiourea groups in one of their tails have been successfully synthesized using different synthetic approaches. The most efficient route for these compounds is the biphenyl route. Among the new materials only the thiourea-containing triphenylenes (**2-3T1**, **2-3T2**, **2-4T1** and **2-4T2**) show a columnar hexagonal (Col_h) mesophase, while the urea and amide-containing triphenylenes do not possess a liquid crystalline phase. It seems that for these series of compounds, hydrogen bonding stabilizes the crystalline state and destabilizes the columnar liquid crystalline organization (higher melting points and lower liquid crystal to isotropic transition). Only for thioureas-containing triphenylenes, the π - π stacking interaction is stronger relative to the thiourea hydrogen bonding (which is the weakest in the series studied in this chapter). In addition, the total length of the tail containing the hydrogen bond-forming group is also important for observing liquid crystallinity. If this tail becomes too long, liquid crystallinity is also lost.

2.4 Experimental

2.4.1 Measurements

¹H-NMR (300 MHz and 400 MHz) and ¹³C-NMR (75 MHz and 100 MHz) spectra were obtained with a Bruker spectrometer, using CDCl₃ as a solvent. Melting points, thermal phase transition temperatures and optical investigation of the liquid crystalline phases were determined on samples between ordinary glass slides using an Olympus BH-2 polarization

microscope equipped with a Mettler FP82HT hot stage, which was controlled by a Mettler FP80HT central processor.

Differential scanning calorimetry (DSC) thermograms were obtained on a Perkin Elmer DSC-7 system using 2-5 mg samples in 30 μl sample pans and a scan rate of 10 $^{\circ}\text{C min}^{-1}$. ΔH is calculated in kJ mol^{-1} .

Temperature-dependent X-ray curves were measured on a Philips X'pert Pro MRD machine equipped with an Anton Paar camera for temperature control. For the measurements in the small angle region, the sample was spread in the isotropic or the liquid crystalline phase on a thin glass slide (about 15 μm thick), which was placed on a temperature regulated flat copper sample stage.

This sample preparation sometimes caused very high intensities of X-ray reflections ($> 500 \text{ kc s}^{-1}$) because of preferential orientation of the molecules in the liquid crystalline state.

The accurate masses were obtained using a Finnigan MAT 95 mass spectrometer operating in the 70 eV EI mode at a resolution of 5500. The matrix-assisted laser desorption/ionization time-of-flight mass spectrometer (Maldi-Tof MS) mass spectra were obtained on an Ultraflex spectrometer, using 2,5-dihydroxybenzoic acid (DHB; Sigma-Aldrich) as a matrix.

Infrared spectra (FTIR) were obtained using a Bruker Vector 22 spectrometer. The sample was dropcast from CH_2Cl_2 solution onto a KBr window, when recorded as a function of temperature, on cooling to room temperature.

At room temperature, FT-IR spectra were recorded on powder samples homogeneously distributed into a KBr pellet, as obtained after recrystallization, without melting them at all.

2.4.2 Synthesis

All solvents were PA quality. All reactions were carried out under a nitrogen or argon atmosphere, if required. Dry dichloromethane was freshly distilled from anhydrous calcium hydride. All starting materials were obtained from Sigma-Aldrich and used as received.

1-Methyl-3-(3-[3,6,7,10,11-pentakis-hexyloxytriphenylen-2-yloxy]propyl)thiourea, 2-3T1

A solution of methyl isothiocyanate (0.23 g, 3.15 mmol) in 100 ml benzene was added dropwise to a stirred solution of 3-(3,6,7,10,11-pentakis-hexyloxytriphenylen-2-yloxy)propan-1-amine **1-3** (1.23 g, 1.53 mmol) in benzene (100 ml), containing 1.50 g pyridine as base. The reaction was at room temperature overnight. Then the reaction mixture was poured in ice water and hydrochloric acid was added until the pH was lower than 4. The reaction mixture

was then extracted with dichloromethane (2 x 50 ml). The organic layer was washed with a saturated sodium chloride solution and dried over anhydrous sodium sulfate. After evaporation of the solvent a pale yellow oil was obtained, which crystallized immediately. The crude compound was purified by column chromatography (silica-gel, dichloromethane-methanol (20:1)). The final product was recrystallized from methanol, yielding 0.46 g (35 %) of **2-3T1**.

¹H NMR: δ 7.85-7.80 (6H, m, ArH), 6.77, 6.39 (2H, bs, 2 x NH), 4.35 (2H, t, J = 5.60 Hz, OCH₂), 4.27-4.17 (10H, m, OCH₂), 3.83 (2H, broad signal, CH₂NH), 2.98 (3H, d, J = 4.71 Hz, NHCH₃), 2.21 (2H, m, OCH₂CH₂CH₂NH), 2.00-1.90 (10H, m, OCH₂CH₂), 1.62-1.54 (10H, m, CH₂), 1.43-1.42 (20H, m, CH₂), 0.98-0.95 (15H, m, CH₃).

¹³C NMR: δ 182.70 (C=S), 149.20-147.60 (2,3,6,7,10,11-ArC-O), 124.11-123.17 (ArC-C), 107.68-106.61 (ArC-H), 70.11-69.47 (OCH₂), 42.50 (CH₂NH), 31.67-31.03 (CH₂), 30.17 (CH₃NH), 29.66-29.33 (CH₂), 28.84 (OCH₂CH₂CH₂NH), 25.83-22.63 (CH₂), 14.03 (CH₃).

MS (Maldi-tof) [M]⁺: calculated for C₅₃H₈₂N₂O₆S: 874.589 amu; found [M-NH₂CH₃]⁺ 843.244 amu.

1-Ethyl-3-(3-[3,6,7,10,11-pentakishexyloxytriphenylen-2-yloxy]propyl)thiourea, 2-3T2

A solution of ethyl isothiocyanate (0.15 g, 1.72 mmol) in dry dichloromethane was added dropwise to a stirred solution of 3-(3,6,7,10,11-pentakishexyloxytriphenylen-2-yloxy)propan-1-amine **1-3** (0.85 g, 1.06 mmol) in dry dichloromethane (20 ml), containing 2.50 g triethylamine as base. The reaction mixture was stirred at room temperature under argon, and its progress monitored by TLC. Once the reaction was complete, the solvent and excess of triethylamine were evaporated under vacuum. The crude compound was purified by column chromatography (silica-gel, dichloromethane-methanol (1.5 % methanol)). The final product was recrystallized from methanol, yielding 0.45 g (48 %) of **2-3T2**.

¹H NMR: δ 7.86-7.81 (6H, m, ArH), 6.70, 6.20 (2H, bs, 2 x NH), 4.35 (2H, t, J = 5.20 Hz, OCH₂CH₂CH₂NH), 4.27-4.23 (10H, m, OCH₂), 3.84 (2H, broad signal, CH₂NH), 3.44 (2H, m, NHCH₂CH₃), 2.21 (2H, m, NHCH₂CH₂CH₂O), 2.00-1.91 (10H, m, OCH₂CH₂), 1.61-1.42 (30H, m, CH₂), 1.14 (3H, t, J = 7.20 Hz, NHCH₂CH₃), 0.98-0.95 (15H, m, CH₃).

¹³C NMR: δ 181.70 (C=S), 149.20-147.71 (2,3,6,7,10,11-ArC-O), 124.13-123.18 (ArC-C), 107.80-106.69 (ArC-H), 69.76-69.49 (OCH₂), 68.24 (OCH₂), 42.27, 39.05 (CH₂NH), 31.67-29.33 (CH₂), 28.86 (OCH₂CH₂CH₂NH), 25.83-22.63 (CH₂), 14.15 (CH₃), 14.03 (CH₃).

MS (Maldi-tof) [M+H]⁺: calculated for C₅₄H₈₅N₂O₆S: 889.613 amu; found [M+H]⁺ 889.572 amu.

1-Methyl-3-[4-(3,6,7,10,11-pentakis-hexyloxytriphenyl-2-yloxy)butyl]thiourea, 2-4T1

A solution of methyl isothiocyanate (0.05 g, 0.68 mmol) in dry dichloromethane was added dropwise to a stirred solution of 4-(3,6,7,10,11-pentakis-hexyloxytriphenyl-2-yloxy)-butylamine **1-4** (0.56 g, 0.68 mmol) in dry dichloromethane (20 ml), containing 4.50 g triethylamine as base. The reaction mixture was stirred at room temperature under argon, and its progress monitored by TLC. Once the reaction was complete, the solvent and excess of triethylamine were evaporated under vacuum. The crude compound was separated by column chromatography (silica-gel, dichloromethane-methanol (2 % methanol)). Recrystallization from methanol / dichloromethane yielded 0.20 g (33 %) of **2-4T1**.

¹H NMR: δ 7.86-7.83 (6H, m, ArH), 6.38, 6.14 (2H, broad m, 2 x NH), 4.34-4.23 (12H, m, OCH₂), 3.72 (2H, m, CH₂CH₂NH), 2.98 (3H, m, NHCH₃), 2.04-1.92 (14H, m, CH₂), 1.62-1.38 (30H, m, CH₂), 0.97-0.94 (15H, m, CH₃).

¹³C NMR: δ 182.57 (C=S), 149.24-148.09 (2,3,6,7,10,11-ArC-O), 123.82-123.36 (ArC-C), 107.52-106.58 (ArC-H), 69.87-69.56 (OCH₂), 44.09 (CH₂NH), 31.69 (CH₃NH), 31.63 -29.25 (CH₂), 26.75, 26.15 (OCH₂CH₂CH₂CH₂NH), 25.86-22.66 (CH₂), 14.05 (CH₃).

MS (Maldi-tof) [M+H]⁺: calculated for C₅₄H₈₅N₂O₆S: 889.613 amu; found [M+H]⁺ 889.865 amu.

1,2-Bishexyloxybenzene, 8 and 2-Hexyloxyphenol, 3

A stirred mixture of catechol (1,2-dihydroxybenzene) (7.10 g, 65.0 mmol), 1-bromohexane (10.7 g, 65.0 mmol) and anhydrous potassium carbonate (20.0 g), in ethanol (320 ml) was refluxed for 21 h under nitrogen. The solvent was evaporated and the crude product purified by column chromatography on silica gel, eluting with light petroleum - dichloromethane (2:1) to give 2-hexyloxyphenol **3** (4.43 g, 35 %) and 1,2-bishexyloxybenzene **8** (4.62 g, 51 %), both as pale yellow oil.

3: **¹H NMR:** δ 6.99 - 6.85 (4H, m, ArH), 5.75 (1H, s, OH), 4.04 (2H, t, J = 6.56 Hz, OCH₂), 1.89-1.76 (2H, m, CH₂CH₂O), 1.55-1.32 (6H, m, CH₂), 0.94 (3H, t, J = 6.40 Hz, CH₃).

¹³C NMR: δ 146.0 (1-ArC-OH), 145.9 (2-ArC-O), 121.3 (6-ArC-H), 120.1 (3-ArC-H), 114.5 (5-ArC-H), 111.6 (4-ArC-H), 68.9 (OCH₂), 31.6-22.7 (CH₂), 14.1 (CH₃).

MS [M]⁺: calculated for C₁₂H₁₈O₂: 194.1307 amu; found 194.1309 amu.

8: **¹H NMR:** δ 6.91 (4H, s, ArH), 4.02 (4H, t, J = 6.01 Hz, OCH₂), 1.92-1.78 (4H, m, CH₂CH₂O), 1.56-1.34 (12H, m, CH₂), 0.95 (6H, t, J = 6.69 Hz, CH₃).

¹³C NMR: δ 149.2 (1,2-ArC-O), 120.9 (3,6-ArC-H), 114.0 (4,5-ArC-H), 69.2 (OCH₂), 31.6-22.6 (CH₂), 14.0 (CH₃).

MS [M]⁺: calculated for C₁₈H₃₀O₂: 278.2246 amu; found 278.2248 amu.

1-(4-Bromobutoxy)-2-hexyloxybenzene, 4-4

A stirred mixture of 2-hexyloxyphenol **3** (7.70 g, 0.04 mol), 1,4-dibromobutane (25.7 g, 0.12 mol) and cesium carbonate (20.0 g) in acetonitrile (100 ml) was refluxed for 8 h under nitrogen. After evaporating about half the solvent from the reaction mixture, 150 ml water was added and the product was extracted with 3 x 50 ml dichloromethane. The evaporated organic layers were dried over anhydrous sodium sulfate and the crude product was purified by column chromatography on silica gel eluting with light petroleum - dichloromethane (2:1), to obtain **4-4** as pale yellow oil (11.9 g, 91 %).

¹H-NMR: δ 6.91 (4H, s, ArH), 4.06-3.97 (4H, dt, J = 6.10 Hz, OCH₂), 3.54 (2H, t, J = 6.00 Hz, CH₂Br), 2.15-1.38 (12H, m, CH₂), 0.95 (3H, t, J = 5.61 Hz, CH₃).

¹³C-NMR: δ 149.35, 148.83 (1,2-ArC-O), 121.41 (6-ArC-H), 120.90 (3-ArC-H), 114.24 (5-ArC-H), 113.70 (4-ArC-H), 69.00, 68.31 (OCH₂), 33.67 (CH₂Br), 31.67-22.71 (CH₂), 14.13 (CH₃).

MS [M]⁺: calculated for C₁₆H₂₅BrO₂: 328.1038 amu; found 328.1038 amu.

1-(4-Azidobutoxy)-2-hexyloxybenzene, 5-4

A stirred mixture of 1-(4-bromobutoxy)-2-hexyloxybenzene **4-4** (4.98 g, 15.0 mmol) and sodium azide (2.95 g, 45.0 mmol) in ethanol (50 ml) was refluxed for 8 h. After partial evaporation of the solvent, the reaction mixture was poured into water (150 ml) and the product was extracted with 2 x 50 ml of dichloromethane. The organic layer was then dried on anhydrous sodium sulfate and the solvent was evaporated under vacuum. 1-(4-azidobutoxy)-2-hexyloxybenzene **5-4** (2.55 g, 56 %) was obtained as pale yellow oil, after purification on a silica gel column with light petroleum – dichloromethane (2:1).

¹H-NMR: δ 6.90 (4H, s, ArH), 4.06-3.96 (4H, dt, J = 5.83 Hz, OCH₂), 3.39 (2H, t, J = 6.32 Hz, CH₂N₃), 1.94-1.31 (12H, m, CH₂), 0.92 (3H, t, J = 6.64 Hz, CH₃).

¹³C-NMR: δ 149.32 (1-ArC-O), 148.79 (2-ArC-O), 121.40 (6-ArC-H), 120.88 (3-ArC-H), 114.24 (5-ArC-H), 113.72 (4-ArC-H), 69.02, 68.58 (OCH₂), 51.26 (CH₂N₃), 31.61-22.65 (CH₂), 14.05 (CH₃).

MS [M]⁺: calculated for C₁₆H₂₅N₃O₂: 291.1947 amu; found 291.1949 amu.

4-(2-Hexyloxy-phenoxy)-butylamine, 6-4

A stirred mixture of 1-(4-azidobutoxy)-2-hexyloxybenzene **5-4** (5.41 g, 18.0 mmol) and lithium aluminum hydride (0.36 g, 94.0 mmol) in dry tetrahydrofuran (50 ml) was reacted for 3 h under nitrogen. The excess of lithium aluminum hydride was destroyed with sodium sulfate decahydrate (0.50 g) by stirring for 16 h at room temperature. The salts were filtered off and the solvent evaporated to give 4-(2-hexyloxyphenoxy)-butylamine **6-4**, as yellow oil (4.70 g, 98 %), which crystallizes overnight at room temperature. The amine was used directly for the synthesis of **7-4U2**, **7-4T2** and **7-4A2** without any further purification. M.p. 80 °C.

¹H-NMR: δ 6.86 (4H, s, ArH), 4.00-3.94 (4H, m, OCH₂), 3.74 (2H, broad s, NH₂), 2.85 (2H, t, J = 6.39 Hz, CH₂NH₂), 1.90-1.30 (12H, m, CH₂), 0.87 (3H, t, J = 5.21 Hz, CH₃).

¹³C-NMR: δ 148.97, 148.64 (1,2-ArC-O), 121.23, 120.89 (3,6-ArC-H), 113.95, 113.62 (4, 5-ArC-H), 69.02, 68.75 (OCH₂), 41.12 (CH₂NH₂), 31.53-22.60 (CH₂), 14.01 (CH₃).

MS [M]⁺: calculated for C₁₆H₂₇NO₂: 265.2042 amu; found 265.2034 amu.

1-Ethyl-3-(4-[2-hexyloxyphenoxy]-butyl)urea, 7-4U2

A solution of ethyl isocyanate (0.40 g, 5.63 mmol) in dry dichloromethane (10 ml) was slowly added to a vigorously stirred solution of 4-(2-hexyloxy-phenoxy)-butylamine **6-4** (0.79 g, 2.98 mmol) in dry dichloromethane (30 ml). The mixture was stirred at room temperature, under nitrogen for 12 h. The product was purified by column chromatography on silica gel eluting with dichloromethane - methanol (10 % methanol), yielding 0.46 g (46 %) of **7-4U2** as yellow oil, which crystallizes immediately at room temperature. M.p. 109 °C.

¹H-NMR: δ 6.85 (4H, m, ArH), 5.36 (1H, bt, J = 5.38 Hz, NH), 5.05 (1H, bt, J = 5.36 Hz, NH), 3.96 (4H, t, J = 6.64 Hz, OCH₂), 3.27-3.07 (4H, m, CH₂NH), 1.85-1.25 (12H, m, CH₂), 1.04 (3H, t, J = 7.24 Hz, CH₃CH₂), 0.87 (3H, t, J = 6.67 Hz, CH₃).

¹³C-NMR: δ 158.87 (C=O), 148.81 (1-ArC-O), 148.78 (2-ArC-O), 121.16 (3,6-ArC-H), 113.86 (5-ArC-H), 113.75 (4-ArC-H), 69.28 (OCH₂), 68.92 (OCH₂), 39.90 (CH₂NH), 35.01-22.62 (CH₂), 15.55 (CH₃), 14.03 (CH₃).

MS [M]⁺: calculated for C₁₉H₃₂N₂O₃: 336.2413 amu; found 336.2417 amu.

1-Ethyl-3-(4-[3,6,7,10,11-pentakishexyloxytriphenylen-2-yloxy]butyl)urea, 2-4U2

A mixture of 1-ethyl-3-(4-[2-hexyloxyphenoxy]butyl)urea **7-4U2** (0.33 g, 0.98 mmol), 0.81 g (1.46 mmol) biphenyl **9** and iron(III)chloride (1.00 g) in dry dichloromethane (40 ml) was stirred for 35 min under nitrogen at room temperature. Then the reaction was quenched with 100 ml cold methanol. After filtration, the gray precipitate was purified by column chromatography using dichloromethane-methanol (2.5 % methanol). Subsequent recrystallization from methanol yielded 0.51 g (60 %) of **2-4U2**.

¹H NMR: δ 7.82 (6H, m, ArH), 4.85 (2H, bs, NH), 4.22 (12H, t, J = 6.51 Hz, OCH₂), 3.34 (2H, t, J = 6.33 Hz, NHCH₂), 3.19-3.15 (2H, q, J = 7.20 Hz, CH₃CH₂NH), 2.00-1.24 (44H, m, CH₂), 1.07 (3H, t, J = 7.24 Hz, CH₂CH₃), 0.92 (15H, t, J = 6.98 Hz, CH₃).

¹³C NMR: δ 157.35 (C=O), 149.06-148.38 (2,3,6,7,10,11-ArC-O), 123.70-123.45 (ArC-C), 107.40-106.76 (ArC-H), 69.73-69.31 (OCH₂), 40.18 (CH₂NH), 35.28-22.65 (CH₂), 15.45, 14.04 (CH₃).

MS [M]⁺: calculated for C₅₅H₈₆N₂O₇: 886.64 amu; found 886.66 amu.

1-Ethyl-3-(4-[2-hexyloxyphenoxy]butyl)thiourea, 7-4T2

A mixture of 4-(2-hexyloxyphenoxy)-butylamine **6-4** (4.20 g, 16.0 mmol), ethyl isothiocyanate (1.68 g, 19.0 mmol) in dry dichloromethane (40 ml) was stirred for 3 h under nitrogen at room temperature. After completion of the reaction the solvent was evaporated under vacuum and the resulted yellow oil was then purified by column chromatography using dichloromethane – methanol (0.5 % methanol), yielding 4.19 g (75 %) of **7-4T2**, as a yellow oil.

¹H-NMR: δ 6.88 (4H, s, ArH), 6.45 (1H, bt, NH), 6.14 (1H, bt, NH), 4.04-3.94 (4H, m, OCH₂), 3.61 (2H, q, J = 5.36 Hz, CH₃CH₂NH), 3.40 (2H, bt, NHCH₂CH₂), 1.89-1.29 (12H, m, CH₂), 1.10 (3H, t, J = 7.32 Hz, CH₃CH₂), 0.87 (3H, t, J = 6.34 Hz, CH₃).

¹³C-NMR: δ 181.19 (C=S), 148.44 (1-ArC-O), 148.26 (2-ArC-O), 121.32 (6-ArC-H), 121.09 (3-ArC-H), 113.43 (4,5-ArC-H), 69.09, 69.04 (OCH₂), 53.36, 43.82 (CH₂NH), 38.93-22.51 (CH₂), 14.09 (CH₃), 13.91 (CH₃).

MS [M]⁺: calculated for C₁₉H₃₂N₂O₂S: 352.2184 amu; found 352.2186 amu.

1-Ethyl-3-(4-[3,6,7,10,11-pentakishexyloxytriphenylen-2-yloxy]butyl)thiourea, 2-4T2

A mixture of 1-ethyl-3-(4-[2-hexyloxyphenoxy]butyl)thiourea **7-4T2** (0.57 g, 1.62 mmol), biphenyl **9** (1.44 g, 2.60 mmol) and iron(III)chloride (2.00 g) in dry dichloromethane (30 ml) was stirred for 30 min under nitrogen at room temperature. The reaction was quenched with

100 ml cold methanol. After filtration, the gray precipitate was purified using column chromatography with dichloromethane - methanol (0.5 % methanol). Subsequent recrystallization from acetonitrile yielded 0.77 g (53 %) of **2-4T2** as white crystals.

¹H NMR: δ 7.82 (6H, s, ArH), 6.31 (1H, bs, NH), 6.00 (1H, bs, NH), 4.30-4.19 (12H, m, OCH₂), 3.72 (2H, q, CH₃CH₂NH), 3.39 (2H, bt, NHCH₂CH₂), 1.97-1.24 (44H, m, CH₂), 1.10 (3H, t, J = 7.20 Hz, CH₂CH₃), 0.92 (15H, t, J = 6.76 Hz, CH₃).

¹³C NMR: δ 181.41 (C=S), 149.25-148.09 (2,3,6,7,10,11-ArC-O), 123.83-123.36 (ArC-C), 107.54-106.59 (ArC-H), 69.88-69.53 (OCH₂), 44.02, 39.06 (CH₂NH), 26.68, 26.21 (OCH₂CH₂CH₂CH₂NH), 25.86-22.66 (CH₂), 14.19 (CH₃), 14.05 (CH₃).

MS (Maldi-tof) [M+H]⁺: calculated for C₅₅H₈₇N₂O₆S: 903.628 amu; found [M+H]⁺ 903.3770 amu.

1-Ethyl-3-(4-[2-Hexyloxyphenoxy]butyl)amide, 7-4A2

A mixture of 4-(2-hexyloxyphenoxy)butylamine **6-4** (1.15 g, 4.33 mmol), propionyl chloride (0.35 g, 3.80 mmol) in dry dichloromethane (15 ml) was stirred for 3 h under nitrogen at room temperature. After completion of the reaction, the solvent was evaporated and the resulted yellow oil was then purified by column chromatography, using dichloromethane - methanol (10 % methanol), yielding 0.96 g (79 %) of **7-4A2** as a yellow oil, which crystallizes overnight at room temperature. M.p. 59 °C.

¹H-NMR: δ 6.87 (4H, s, ArH), 6.02 (1H, broad s, NH), 4.03-3.95 (4H, dt, J = 6.65 Hz, OCH₂), 3.33 (2H, q, J = 6.11 Hz, CH₂NHCO), 2.16 (2H, q, J = 7.53 Hz, COCH₂CH₃), 1.88-1.29 (12H, m, CH₂), 1.12 (3H, t, J = 7.60 Hz, CH₃CH₂), 0.88 (3H, t, J = 7.58 Hz, CH₃).

¹³C-NMR: δ 174.00 (C=O), 148.85 (1-ArC-O), 148.55 (2-ArC-O), 121.17 (6-ArC-H), 120.92 (3-ArC-H), 113.65 (5-ArC-H), 113.42 (4-ArC-H), 68.93 (OCH₂), 68.69 (OCH₂), 38.94 (CH₂NH), 31.51-22.56 (CH₂), 13.96 (CH₃), 9.95 (CH₃).

MS [M]⁺: calculated for C₁₉H₃₁NO₃: 321.2304 amu; found 321.2303 amu.

1-Ethyl-2-(4-[3,6,7,10,11-pentakishexyloxytriphenylen-2-yloxy]butyl)amide, 2-4A2

A mixture of 1-ethyl-3-(4-[2-hexyloxyphenoxy]butyl)amide **7-4A2** (0.96 g, 3.00 mmol), 3,4,3',4'-tetrakis-hexyloxybiphenyl **9** (1.65 g, 3.03 mmol) and iron(III)chloride (2.50 g) in dry dichloromethane (40 ml) was stirred for 35 min under nitrogen at room temperature. The reaction was quenched with 100 ml cold methanol. After filtration, the gray precipitate was

purified by column chromatography using dichloromethane - methanol (2.5 % methanol). Subsequent recrystallization from methanol yielded 0.80 g (31%) of **2-4A2**.

¹H NMR: δ 7.83-7.81 (6H, m, ArH), 6.21 (1H, bs, NH), 4.22 (12H, t, J = 6.50 Hz, OCH₂), 3.43 (2H, q, J = 5.96 Hz, CH₂NHCO), 2.24 (2H, q, J = 7.58 Hz, CH₃CH₂CO), 2.02-1.36 (44H, m, CH₂), 1.15 (3H, t, J = 7.63 Hz, CH₃), 0.92 (15H, t, J = 7.03 Hz, CH₃).

¹³C NMR: δ 173.90 (C=O), 148.98, 148.52, 148.28 (2,3,6,7,10,11-ArC-O), 123.65, 123.42 (ArC-C), 107.36-106.61 (ArC-H), 69.63-69.10 (OCH₂), 39.12 (CH₂NH), 31.66-22.65 (CH₂), 14.05 (CH₃), 9.98 (CH₃).

MS [M]⁺: calculated for C₅₅H₈₅NO₇: 871.6326 amu; found 871.6309 amu.

1-(6-Bromohexyloxy)-2-hexyloxybenzene, 4-6

A stirred mixture of 2-hexyloxyphenol **3** (2.00 g, 10.4 mmol), 1,6-dibromohexane (6.94 g, 28.5 mmol) and potassium carbonate (15.0 g) in 2-butanone (100 ml) was refluxed for 8 h under nitrogen. After removing about half of the solvent, 150 ml water was added and the product was extracted with 3 x 50 ml dichloromethane. The crude compound was then dried over anhydrous sodium sulfate and purified by column chromatography on silica gel eluting with light petroleum - dichloromethane (2:1), yielding 2.53 g (69 %) of **4-6** as pale yellow oil.

¹H NMR: δ 6.88 (4H, s, ArH), 4.03-3.95 (4H, dt, J = 6.66 Hz, OCH₂), 3.42 (2H, t, J = 6.75 Hz, CH₂Br), 1.89-1.78 (4H, m, CH₂CH₂O), 1.55-1.31 (12H, m, CH₂), 0.90 (3H, t, J = 6.83 Hz, CH₃).

¹³C NMR: δ 149.22, 149.03 (1,2-ArC-O), 121.14, 120.95 (3,6-ArC-H), 114.08, 113.88 (4,5-ArC-H), 69.15, 68.98 (OCH₂), 33.85 (CH₂Br), 32.75-22.67 (CH₂), 14.09 (CH₃).

MS [M]⁺: calculated for C₁₈H₂₉BrO₂: 356.1351 amu; found 356.1346 amu.

1-(6-Azidohexyloxy)-2-hexyloxybenzene, 5-6

A stirred mixture of 1-(6-bromohexyloxy)-2-hexyloxybenzene **4-6** (3.00 g, 8.40 mmol) and sodium azide (0.64 g, 9.84 mmol) in ethanol (80 ml) was refluxed for 7 h. After partial evaporation of the solvent, the reaction mixture was poured in water (150 ml) and the product was extracted with 3 x 50 ml of dichloromethane. The organic layer was then dried on anhydrous sodium sulfate and the solvent was evaporated under vacuum. 1-(6-Azidohexyloxy)-2-hexyloxybenzene **5-6** (2.35 g, 88 %) was obtained as a pale-yellow oil, after purification on a silica gel column with light petroleum - dichloromethane (1:2).

¹H NMR: δ 6.93 (4H, s, ArH), 4.04 (4H, t, J = 5.86 Hz, OCH₂), 3.31 (2H, t, J = 6.84 Hz, CH₂N₃), 1.94-1.61 (4H, m, CH₂CH₂O), 1.54-1.36 (12H, m, CH₂), 0.97 (3H, t, J = 6.82 Hz, CH₃).

¹³C NMR: δ 149.10, 148.92 (1,2-ArC-O), 121.02 (3,6-ArC-H), 113.96, 113.76 (4,5-ArC-H), 69.01, 68.84 (OCH₂), 51.25 (CH₂N₃), 31.51-22.54 (CH₂), 13.94 (CH₃).

MS [M]⁺: calculated for C₁₈H₂₉N₃O₂: 319.2260 amu; found 319.2263 amu.

6-(2-Hexyloxyphenoxy)hexylamine, 6-6

A stirred mixture of 1-(6-azidohexyloxy)-2-hexyloxybenzene **5-6** (2.00 g, 6.30 mmol) and lithium aluminum hydride (0.29 g, 7.80 mmol) in dry tetrahydrofuran (50 ml) was reacted for 2 h under nitrogen at room temperature. The excess of lithium aluminum hydride was destroyed with sodium sulfate decahydrate (0.50 g), followed by stirring for 16 h at room temperature. The salts were filtered off and the solvent evaporated to give 6-(2-hexyloxyphenoxy)hexylamine **6-6**, as a yellow oil, (1.62 g, 88 %), which crystallizes overnight at room temperature. M.p. 55 °C.

¹H NMR: δ 6.85 (4H, s, ArH), 3.96 (4H, t, J = 6.36 Hz, OCH₂), 2.66 (2H, m, CH₂NH₂), 2.25-1.72 (4H, m, CH₂CH₂O), 1.62-1.20 (14H, m, CH₂), 0.89 (3H, t, J = 6.34 Hz, CH₃).

¹³C NMR: δ 149.19-148.63 (1,2-ArC-O), 121.56-121.02 (3,6-ArC-H), 114.32-114.04 (4,5-ArC-H), 69.21-68.97 (OCH₂), 39.85 (CH₂NH₂), 31.56-21.18 (CH₂), 14.05 (CH₃).

MS [M]⁺: calculated for C₁₈H₃₁NO₂: 293.2355 amu; found 293.2351 amu.

1-Hexyl-3-(6-[2-hexyloxyphenoxy]hexyl)urea, 7-6U6

A solution of hexyl isocyanate (0.67 g, 5.30 mmol) in dry dichloromethane (10 ml) was slowly added to a vigorously stirred solution of 6-(2-hexyloxyphenoxy)hexylamine **6-6** (1.04 g, 3.60 mmol) in dry dichloromethane (30 ml). The mixture was stirred at room temperature under nitrogen for 12 h. The white crystals were formed were filtered and purified by column chromatography on silica gel eluting with dichloromethane-methanol (20:1) to give 1-hexyl-3-(6-[2-hexyloxyphenoxy]hexyl)urea **7-6U6** (1.20 g, 81 %), as a white powder. M.p. 79 °C.

¹H NMR: δ 6.89 (4H, s, ArH), 4.47 (2H, bs, 2 x NH), 4.01 (4H, t, J = 6.84 Hz, OCH₂), 3.14-3.04 (4H, bq, NHCH₂), 1.85-1.71 (4H, m, CH₂CH₂O), 1.45-1.25 (20H, m, CH₂), 0.90-0.81 (6H, dt, J = 6.34 Hz, CH₃).

^{13}C NMR: δ 158.45 (C=O), 148.99, 148.92 (1,2-ArC-O), 121.05, 121.03 (3,6-ArC-H), 113.96, 113.88 (4,5-ArC-H), 69.23, 68.93 (OCH₂), 40.47, 40.25 (CH₂NH), 31.54-22.54 (CH₂), 13.99 (CH₃).

MS [M]⁺: calculated for C₂₅H₄₄N₂O₃: 420.3352 amu; found 420.3358 amu.

1-Hexyl-3-(6-[3,6,7,10,11-pentakishexyloxytriphenylen-2-yloxy]hexyl)urea, 2-6U6

To a mixture of **8** (1.00 g, 3.60 mmol) and **7-6U6** (1.51 g, 3.60 mmol) in 10 ml dry CH₂Cl₂ was added 1.60 g molybdenum chloride and the reaction mixture has been stirred for 1 h. Then 15 ml cold methanol and 20 ml water were added. **HAT6 (10)** was extracted from the water phase with light petroleum in which urea compound **2-6U6** does not dissolve. When **HAT6 (10)** was removed, the urea derivative **2-6U6** was extracted with dichloromethane. Both **HAT6 (10)** and **2-6U6** were further purified by column chromatography on silica gel, eluting with dichloromethane - methanol (20:1), followed by recrystallization. **HAT6 (10)** was recrystallized from ethanol and urea derivative **2-6U6** from methanol to give white crystals (**HAT6 (10)**: 0.65 g, 65 %) and (**2-6U6**: 0.23 g, 20 %). For the characterization of **HAT6 (10)** compound, see compound **4-6** in Chapter 3 of this thesis.

2-6U6: ^1H NMR: δ 7.82 (6H, s, ArH), 4.22 (12H, t, J = 6.52 Hz, OCH₂), 3.21-3.08 (6H, m, 2 x CH₂NH, 2 x NH), 2.00-1.86 (12H, m, OCH₂CH₂), 1.58-1.23 (44H, m, CH₂), 0.96-0.80 (18H, m, CH₃).

^{13}C NMR: δ 158.27 (C=O), 148.95, 148.92, 148.89, 148.73, 148.69 (2,3,6,7,10,11-ArC-O), 123.58, 123.53, 123.45 (ArC-C), 107.32, 107.16 (ArC-H), 69.73, 69.60, 69.30 (OCH₂), 40.53, 40.30 (CH₂NH), 31.64-22.52 (CH₂), 14.02, 13.97 (CH₃).

MS [M]⁺: calculated for C₆₁H₉₈N₂O₇: 970.7374 amu; found [M-NHC₆H₁₃]⁺: 869.6142 amu.

1-Heptyl-2-(10-[2-hexyloxyphenoxy]decyl)amide, 7-10A7

A solution of octanoyl chloride (0.60 g, 3.70 mmol) in dry dichloromethane (10 ml) was slowly added to a vigorously stirred solution of 10-(2-hexyloxyphenoxy)decylamine **6-10** (1.00 g, 2.86 mmol) in dry dichloromethane (30 ml). The mixture was stirred at room temperature, under nitrogen for 12 h. The white crystals were formed were filtered off and purified by column chromatography on silica gel eluting with dichloromethane - methanol (10:1) to give 1-heptyl-2-(10-[2-hexyloxyphenoxy]decyl)amide **7-10A7** (0.57 g, 48 %), as a white powder. M.p. = 68 °C.

¹H NMR: δ 6.84 (4H, s, ArH), 5.91 (1H, bt, NH), 3.94 (4H, t, J = 6.60 Hz, OCH₂), 3.18 (2H, q, J = 6.31 Hz, CH₂NH), 2.11 (2H, t, J = 7.14 Hz, CH₂CO), 1.81-1.70 (4H, m, CH₂CH₂O), 1.58-1.25 (30H, m, CH₂), 0.90-0.81 (6H, dt, J = 6.66 Hz, CH₃).

¹³C NMR: δ 173.00 (C=O), 148.96 (1,2-ArC-O), 120.81 (3,6-ArC-H), 113.84 (4,5-ArC-H), 68.99 (OCH₂), 39.27 (CH₂NH), 36.60-22.44 (CH₂), 13.86 (CH₃).

MS [M]⁺: calculated for C₃₀H₅₃NO₃: 475.4025 amu; found 475.4029 amu.

1-Heptyl-2-(10-[3,6,7,10,11-pentakishexyloxytriphenylen-2-yloxy]decyl)amide, 2-10A7

To a solution of **7-10A7** (0.25 g, 0.52 mmol) in 10 ml dry dichloromethane was added 0.45 g (0.81 mmol) biphenyl **9** and 0.65 g iron(III)chloride. The reaction mixture has been stirred for 90 min and then 15 ml cold methanol was added. From the grey precipitate, **2-10A7** was further purified by column chromatography on silica gel, eluting with dichloromethane – methanol (1% methanol). Recrystallization from ethanol yielded 0.26 g (50 %) of **2-10A7** as white crystals.

¹H NMR: δ 7.82 (6H, s, ArH), 5.51 (1H, bt, J = 4.18 Hz, NH), 4.22 (12H, t, J = 6.49 Hz, OCH₂), 3.18 (2H, q, J = 6.56 Hz, CH₂NH), 2.12-1.25 (68H, m, CH₂), 0.96-0.75 (18H, m, CH₃).

¹³C NMR: δ 173.06 (C=O), 148.97 (2,3,6,7,10,11-ArC-O), 123.60 (ArC-C), 107.31 (ArC-H), 69.69 (OCH₂), 39.49 (CH₂NH), 36.87 (CH₂CO), 31.72-22.63 (CH₂), 14.08 (CH₃).

MS [M]⁺: calculated for C₆₆H₁₀₇NO₇: 1025.8048 amu; found 1025.8073 amu.

1-(10-Bromodecyloxy)-2-hexyloxybenzene, 4-10

A stirred mixture of 2-hexyloxyphenol **3** (4.02 g, 20.7 mmol), 1,10-dibromodecane (10.4 g, 35.0 mmol) and potassium carbonate (15.0 g) in 2-butanone (150 ml) was refluxed for 8 h under nitrogen. After removing about half of the solvent from the reaction mixture, 150 ml water was added and the product was extracted with 3 x 50 ml dichloromethane. The crude compound was dried over anhydrous sodium sulfate and purified by column chromatography on silica gel eluting with light petroleum - dichloromethane (1:2), to obtain 1-(10-bromodecyloxy)-2-hexyloxybenzene **4-10** (5.34 g, 62 %) as pale yellow oil.

¹H NMR: δ 6.88 (4H, s, ArH), 3.99 (4H, t, J = 6.58 Hz, OCH₂), 3.39 (2H, t, J = 6.82 Hz, CH₂Br), 1.92-1.69 (4H, m, CH₂CH₂O), 1.55-1.31 (20H, m, CH₂), 0.91 (3H, t, J = 6.62 Hz, CH₃).

¹³C NMR: δ 149.2 (1,2-ArC-O), 121.0 (3,6-ArC-H), 114.0 (4,5-ArC-H), 69.2 (OCH₂), 34.0 (CH₂Br), 32.8-22.7 (CH₂), 14.0 (CH₃).

MS [M]⁺: calculated for C₂₂H₃₇O₂Br: 412.1977 amu; found 412.1984 amu.

1-(10-Azidodecyloxy)-2-hexyloxybenzene, 5-10

A stirred mixture of 1-(10-bromodecyloxy)-2-hexyloxybenzene **4-10** (4.63 g, 11.2 mmol) and sodium azide (2.20 g, 33.9 mmol) in ethanol (80 ml) was refluxed for 7 h. After partial evaporation of the solvent, the reaction mixture was poured in water (150 ml) and the product was extracted with 3 x 50 ml of dichloromethane. After drying the organic layer on anhydrous sodium sulfate and evaporation of the solvent, 1-(10-azidodecyloxy)-2-hexyloxybenzene **5-10** (4.00 g, 95 %) was obtained as a pale-yellow oil.

¹H NMR: δ 6.89 (4H, s, ArH), 4.00 (4H, t, J = 6.56 Hz, OCH₂), 3.25 (2H, t, J = 6.81 Hz, CH₂N₃), 1.86-1.75 (4H, m, CH₂CH₂O), 1.60-1.32 (20H, m, CH₂), 0.92 (3H, t, J = 6.73 Hz, CH₃).

¹³C NMR: δ 149.1 (1,2-ArC-O), 121.0 (3,6-ArC-H), 114.0 (4,5-ArC-H), 69.2 (OCH₂), 51.4 (CH₂N₃), 31.6-22.7 (CH₂), 14.0 (CH₃).

MS [M]⁺: calculated for C₂₂H₃₇N₃O₂: 375.2886 amu; found 375.2884 amu.

10-(2-Hexyloxyphenoxy)decylamine, 6-10

A stirred mixture of 1-(10-azidodecyloxy)-2-hexyloxybenzene **5-10** (3.20 g, 8.50 mmol) and lithium aluminum hydride (0.50 g, 13.0 mmol) in dry tetrahydrofuran (50 ml) was reacted for 2 h under nitrogen at room temperature. The excess of lithium aluminum hydride was quenched with sodium sulfate decahydrate (15.0 g), followed by stirring for 16 h at room temperature. The salts were filtered off and the solvent evaporated to give 10-(2-hexyloxyphenoxy)decylamine **6-10**, as a colorless oil, which crystallizes overnight at room temperature as white crystals (2.80 g, 93 %). M.p. 57 °C.

¹H NMR: δ 7.84 (2H, bs, NH₂), 6.84 (4H, s, ArH), 3.99-3.90 (4H, m, OCH₂), 2.97 (2H, bt, J = 7.80 Hz, CH₂NH₂), 1.81-1.71 (4H, m, CH₂CH₂O), 1.43-1.28 (20H, m, CH₂), 0.88 (3H, t, J = 6.65 Hz, CH₃).

¹³C NMR: δ 149.20 (1,2-ArC-O), 120.97 (3,6-ArC-H), 114.15 (4,5-ArC-H), 69.22 (OCH₂), 39.98 (CH₂NH₂), 31.54-22.56 (CH₂), 13.98 (CH₃).

MS [M]⁺: calculated for C₂₂H₃₉NO₂: 349.2981 amu; found 349.2986 amu.

1-Hexyl-3-(10-[2-hexyloxyphenoxy]decyl)urea, 7-10U6

A solution of hexyl isocyanate (0.28 g, 2.20 mmol) in dry dichloromethane (10 ml) was slowly added to a vigorously stirred solution of 10-(2-hexyloxyphenoxy)decylamine **6-10** (0.55 g, 1.60 mmol) in dry dichloromethane (30 ml). The mixture was stirred at room temperature under nitrogen for 40 min. The white crystals were formed were filtered off and purified by column chromatography on silica gel eluting with dichloromethane - methanol (20:1) to give 1-hexyl-3-(10-[2-hexyloxyphenoxy]decyl)urea **7-10U6** (0.64 g, 85 %) as a white powder. M.p. 90 °C.

¹H NMR: δ 6.87 (4H, s, ArH), 4.43 (2H, bt, J = 4.88 Hz, NH), 3.97 (4H, t, J = 6.67 Hz, OCH₂), 3.12 (4H, q, J = 6.83 Hz, CH₂NH), 1.83-1.73 (4H, m, CH₂CH₂O), 1.49-1.27 (28H, m, CH₂), 0.92-0.83 (6H, m, CH₃).

¹³C NMR: δ 158.34 (C=O), 149.10 (1,2-ArC-O), 120.97 (3,6-ArC-H), 113.96 (4,5-ArC-H), 69.19 (OCH₂), 40.57 (CH₂NH), 31.52-22.58 (CH₂), 14.01 (CH₃).

MS [M]⁺: calculated for C₂₉H₅₂N₂O₃: 476.3978 amu; found 476.3981 amu.

1-Hexyl-3-(10-[3,6,7,10,11-pentakishexyloxytriphenylen-2-yloxy]decyl)urea, 2-10U6

To a mixture of **8** (0.28 g, 0.99 mmol) and **7-10U6** (0.47 g, 0.99 mmol) in 10 ml dry dichloromethane was added 0.58 g molybdenum chloride (2.13 mmol) and the reaction mixture has been stirred for 20 min. Then 15 ml cold methanol and 20 ml water were added. **HAT6 (10)** was extracted from the water phase with light petroleum in which urea compound **2-10U6** does not dissolve. When **HAT6 (10)** was removed, the urea derivative **2-10U6** was extracted with dichloromethane. Both **HAT6 (10)** and **2-10U6** were further purified by column chromatography on silica gel eluting with dichloromethane - methanol (40:1), followed by recrystallization. **HAT6 (10)** was recrystallized from ethanol and urea derivative **2-10U6** from methanol, yielding 0.15 g (55 %) of **HAT6 (10)** and 0.10 g (30 %) of **2-10U6**. For the characterization of **HAT6 (10)** compound, see compound **4-6** in Chapter 3 of this thesis.

2-10U6: **¹H NMR:** δ 7.82 (6H, s, ArH), 4.53 (2H, bs, 2 x NH), 4.22 (12H, t, J = 6.49 Hz, OCH₂), 3.10-3.08 (4H, bq, J = 5.08 Hz, 2 x CH₂NH), 2.00-1.86 (12H, m, OCH₂CH₂), 1.60-1.24 (52H, m, CH₂), 0.96-0.82 (18H, m, CH₃).

¹³C NMR: δ 158.40 (C=O), 148.85 (2,3,6,7,10,11-ArC-O), 123.50 (ArC-C), 107.18 (ArC-H), 69.61 (OCH₂), 40.48 (CH₂NH), 31.66-22.64 (CH₂), 14.04 (CH₃).

MS [M]⁺: calculated for C₆₅H₁₀₆N₂O₇: 1026.800 amu; found 1026.804 amu.

3,6,7,10,11-Pentakishexyloxytriphenylen-2-ol, 11

Amide, Urea and Thiourea-Triphenylene Derivatives

To a solution of 35 ml dry dichloromethane with 1.40 g (1.69 mmol) **10** (**HAT6**) has been carefully added 11 ml (3 eq.) of dichloromethane solution containing *B*-bromocatecholborane (cat-*B*-Br) (0.5 M). The reaction mixture has been refluxed for 5 h under nitrogen. Then the reaction mixture was poured in ice/water and the crude product has been extracted with 3 x 30 ml dichloromethane, washed with 30 ml of saturated solution of sodium chloride and dried over anhydrous sodium sulfate. Extensive column chromatography separations on silica gel, using dichloromethane - light petroleum (1:1) ($R_f = 0.4$), have been performed, yielding 0.60 g (48 %) of **11** after recrystallization from ethanol. M.p. 58 °C.

$^1\text{H NMR}$: δ 7.95-7.76 (6H, m, ArH), 5.90 (1H, OH), 4.31-4.19 (10H, m, OCH₂), 1.97-1.90 (10H, m, OCH₂CH₂), 1.55-1.24 (30H, m, CH₂), 0.92 (15H, bt, $J = 6.37$ Hz, CH₃).

$^{13}\text{C NMR}$: δ , 149.06-148.64, 145.79-145.19 (2,3,6,7,10,11-ArC-O), 123.83-122.90 (ArC-C), 107.35-107.16, 106.37-106.16, 104.25-104.07 (ArC-H), 69.78-68.98 (OCH₂), 31.71, 29.44, 25.85, 22.68 (CH₂), 14.07 (CH₃).

MS [M]⁺: calculated for C₄₈H₇₂O₆: 744.5329 amu; found 744.5317 amu.

2-(10-Bromodecyloxy)-3,6,7,10,11-pentakishexyloxytriphenylene, 12

A stirred mixture of **11** (0.19 g, 0.26 mmol), 0.38 g (1.30 mmol) of 1,10-dibromodecane and 7.00 g of potassium carbonate has been refluxed in 40 ml ethanol for 4 h under nitrogen. After evaporating about half of the solvent from the reaction mixture, 50ml water was added and the product was extracted with 2 x 50 ml dichloromethane. The organic layers were washed with 50 ml of saturated solution of sodium chloride and then dried over anhydrous sodium sulfate. After concentration under vacuum of the organic layer, the crude product was subjected to a column chromatography separation on silica gel using dichloromethane - light petroleum (1:1), yielding 0.11 g (45 %) of **12** after recrystallization from ethanol. Cr 44 °C Col_h 54 °C I.

$^1\text{H NMR}$: δ 7.84 (6H, s, ArH), 4.24 (12H, t, $J = 6.43$ Hz, OCH₂), 3.38 (2H, t, $J = 6.81$ Hz, CH₂Br), 2.03-1.33 (56H, m, CH₂), 0.96 (15H, bt, $J = 6.94$ Hz, CH₃).

$^{13}\text{C NMR}$: δ 148.35 (2,3,6,7,10,11-ArC-O), 124.00 (ArC-C), 107.65 (ArC-H), 70.05 (OCH₂), 37.24 (CH₂Br), 34.39-23.12 (CH₂), 14.52 (CH₃).

MS [M]⁺: calculated for C₅₈H₉₁BrO₆: 962.5999 amu; found 962.5994 amu.

2-(10-Azidodecyloxy)-3,6,7,10,11-pentakishexyloxytriphenylene, 13

A stirred mixture of **12** (0.57 g, 0.59 mmol) and 0.18 g (2.76 mmol) of sodium azide in 50 ml ethanol was refluxed for 12 h. After partial evaporation of the solvent, 50 ml of water was added to the reaction mixture. The crude product was extracted with 2 x 50 ml dichloromethane, washed with 50 ml of saturated solution of sodium chloride and then dried over anhydrous sodium sulfate. The solvent was evaporated and the crude product subjected to a column chromatography separation on silica gel using dichloromethane - light petroleum (1:1), yielding 0.52 g (95 %) of **13** after recrystallization from ethanol. M.p. 57 °C.

¹H NMR: δ 7.76 (6H, s, ArH), 4.15 (12H, t, J = 6.57 Hz, OCH₂), 3.17 (2H, t, J = 6.93 Hz, CH₂N₃), 1.91-1.83 (12H, m, OCH₂CH₂), 1.51-1.17 (44H, m, CH₂), 0.85 (15H, bt, J = 6.90 Hz, CH₃).

¹³C NMR: δ 147.13, 147.11 (2,3,6,7,10,11-ArC-O), 123.93 (ArC-C), 105.57, 105.51 (ArC-H), 67.85 (OCH₂), 49.61 (CH₂N₃), 29.82-20.79 (CH₂), 12.18 (CH₃).

MS [M]⁺: calculated for C₅₈H₉₁N₃O₆: 925.6908 amu; found 925.6919 amu.

10-(3,6,7,10,11-Pentakishexyloxytriphenylen-2-yloxy)decylamine, 14

A stirred mixture of **13** (0.49 g, 0.53 mmol) and 0.08 g (2.10 mmol) of lithium aluminum hydride in 40 ml dry tetrahydrofuran was reacted for 4 h under nitrogen atmosphere, at room temperature. After completion of the reaction, the excess of lithium aluminum hydride has been destroyed with 0.50 g of sodium sulfate decahydrate and 1 ml of 0.1 M sodium hydroxide solution. After filtration of the salts, the crude product was recrystallized from ethyl acetate, yielding 0.24 g (50 %) of **14**. M.p. 79 °C.

¹H NMR: δ 7.82 (6H, s, ArH), 4.21 (12H, t, J = 6.50 Hz, OCH₂), 3.09 (2H, bs, NH₂), 2.73 (2H, t, J = 6.89 Hz, CH₂NH₂), 1.99-1.86 (12H, m, OCH₂CH₂), 1.66-1.21 (44H, m, CH₂), 0.92 (15H, t, J = 6.97 Hz, CH₃).

¹³C NMR: δ 148.94 (2,3,6,7,10,11-ArC-O), 123.58 (ArC-C), 107.27 (ArC-H), 69.68 (OCH₂), 41.67 (CH₂NH₂), 32.32-22.69 (CH₂), 14.09 (CH₃).

MS [M]⁺: calculated for C₅₈H₉₃NO₆: 899.7003 amu; found 899.6989 amu.

1-Ethyl-3-(10-[3,6,7,10,11-pentakishexyloxytriphenylen-2-yloxy]decyl)thiourea, 2-10T2

A mixture of **14** (0.40 g, 0.44 mmol) and ethyl isothiocyanate (0.05 g, 0.57 mmol) in 15 ml dry dichloromethane was reacted for 12 h at room temperature under nitrogen. After completion of the reaction the solvent was evaporated and the product purified by column

chromatography on silica gel, eluting with dichloromethane – methanol (1 % methanol), yielding 0.21 g (49 %) of **2-10T2** as white crystals after recrystallization from methanol.

¹H NMR: δ 7.82 (6H, s, ArH), 5.74 (2H, bs, NH), 4.22 (12H, t, $J = 6.52$ Hz, OCH₂), 3.44-3.34 (4H, m, CH₂NH), 1.96-1.86 (12H, m, OCH₂CH₂), 1.60-1.00 (44H, m, CH₂), 1.17 (3H, t, $J = 7.21$ Hz, CH₃CH₂NHCS), 0.89 (15H, t, $J = 7.12$ Hz, CH₃).

¹³C NMR: δ 181.30 (C=S), 148.96, 148.91 (2,3,6,7,10,11-ArC-O), 123.56 (ArC-C), 107.24 (ArC-H), 69.67 (OCH₂), 44.39, 39.12 (2 x CH₂NHCS), 31.71-22.69 (CH₂), 14.27, 14.09 (CH₃).

MS [M]⁺: calculated for C₆₁H₉₈N₂O₆S: 986.7 amu; found [M-(NH-CS-C₂H₅)⁺ 899.5 amu.

2.5 Acknowledgements

The author would like to thank Mr. Barend van Lagen and Mr. Beb van Veldhuizen for helping with the NMR measurements and Dr. Maarten A. Posthumus for the exact mass determinations.

2.6 References

¹ (a) Boden, N.; Bushby, R. J.; Cammidge, A. N.; Headdock, G. *J. Mater. Chem.* **1995**, *12*, 2275-2281. (b) Kumar, S. *Liq. Cryst.* **2005**, *32*, 1089-1113. (c) Kumar, S. *Chem. Soc. Rev.* **2006**, *35*, 83-109.

² Grimsdale, A. C.; Müllen, K. *Angew. Chem. Int. Ed.* **2005**, *44*, 5592-5629.

³ (a) Adam, D.; Schuhmacher, P.; Simmerer, J.; Häussling, L.; Siemensmeyer, K.; Eitzbach, K. H.; Ringsdorf, H.; Haarer, D. *Nature* **1994**, *371*, 141-143. (b) Struijk, C. W.; Sieval, A. B.; Dakhorst, J. E. J.; van Dijk, M.; Kimkes, P.; Koehorst, R. B. M.; Donker, H.; Schaafsma, T. J.; Picken, S. J.; van de Craats, A. M.; Warman, J. M.; Zuilhof, H.; Sudhölter, E. J. R. *J. Am. Chem. Soc.* **2000**, *122*, 11057-11066.

⁴ Brédas, J. L.; Calbert, J. P.; da Silva Filho, D. A.; Cornil, J. *PNAS* **2002**, *99*, 5804-5809.

⁵ (a) Lüssem, G.; Wendorff, J. H.; *Polym. Adv. Technol.* **1998**, *9*, 443-460. (b) Seguy, I.; Destruel, P.; Boch, H. *Synth. Met.* **2000**, *111-112*, 15-18. (c) Seguy, I.; Jolinat, P.; Farenc, J.; Mamy, R.; Bock, H.; Ip, J.; Nguyen, T. P. *J. Appl. Phys.* **2001**, *89*, 5442-5448. (d) Schmidt-Mende, L.; Fechtenkötter, A.; Müllen, K.; Moons, E.; Friend, R. H.; MacKenzie, J. D. *Science* **2001**, *293*, 1119-1122. (e) Schmidt-Mende, L.; Fechtenkötter, A.; Müllen, K.; Friend, R. H.;

MacKenzie, J. D. *Physica E* **2002**, *14*, 263-267. (f) Stutzmann, N.; Friend, R. H.; Siringhaus, H. *Science* **2003**, *299*, 1881-1884.

⁶ Itaka, K.; Yamashiro, M.; Yamaguchi, J.; Haemori, M.; Yaginuma, S.; Matsumoto, Y.; Kondo, M.; Koinuma, H. *Adv. Mater.* **2006**, *18*, 1713-1716.

⁷ Boden, N.; Bushby, R. J.; Clements, J.; Movaghar, B. *J. Mater. Chem.* **1999**, *9*, 2081-2086.

⁸ (a) Mulder, F. M.; Stride, J.; Picken, S. J.; Kouwer, P. H. J.; de Haas, M. P.; Siebbeles, L. D. A.; Kearly, G. J. *J. Am. Chem. Soc.* **2003**, *125*, 3860-3866. (b) Kearly, G. J.; Mulder, F. M.; Picken, S. J.; Kouwer, P. H. J.; Stride, J. *Chem. Phys.* **2003**, *292*, 185-190. (c) Cinacchi, G.; Colle, R.; Tani, A. *J. Phys. Chem. B* **2004**, *108*, 7969-7977. (d) Lehmann, M.; Kestemont, G.; Aspe, R. G.; Buess-Herman, C.; Koch, M. H. J.; Debije, M. G.; Piris, J.; de Haas, M. P.; Warman, J. M.; Watson, M. D.; Lemaur, V.; Cornil, J.; Geerts, Y. H.; Gearba, R.; Ivanov, D. *A. Chem. Eur. J.* **2005**, *11*, 3349-3362.

⁹ (a) Percec, V.; Mitchell, C. M.; Cho, W. D.; Uchida, S.; Glodde, M.; Ungar, G.; Zeng, X.; Liu, Y.; Balagurusamy, V. S. K.; Heiney, P. A. *J. Am. Chem. Soc.* **2004**, *126*, 6078-6094. (b) Kajitani, T.; Kohmoto, S.; Yamamoto, M.; Kishikawa, K. *J. Mater. Chem.* **2004**, *14*, 3449-3456.

¹⁰ (a) Suárez, M.; Lehn, J. M.; Zimmerman, S. C.; Skoulios, A.; Heinrich, B. *J. Am. Chem. Soc.* **1998**, *120*, 9526-9532. (b) Kato, T. *Structure and Bonding* **2000**, *96*, 95-146. (c) Prins, L. J.; Reinhoudt, D. N.; Timmerman, P. *Angew. Chem. Int. Ed.* **2001**, *40*, 2382-2426. (d) Beginn, U. *Prog. Polym. Sci.* **2003**, *28*, 1049-1105. (e) Kato, T.; Mizoshita, N.; Kishimoto, K. *Angew. Chem. Int. Ed.* **2006**, *45*, 38-68. (f) Kato, T.; Mizoshita, N.; Kishimoto, K. *Angew. Chem. Int. Ed.* **2006**, *45*, 38-68.

¹¹ Würthner, F.; Hanke, B.; Lysetska, M.; Lambright, G.; Harms, G. S. *Org. Lett.* **2005**, *7*, 967-970.

¹² Yabuuchi, K.; Marfo-Owusu, E.; Kato, T. *Org. Biomol. Chem.* **2003**, *1*, 3464-3469.

¹³ (a) Kishikawa, K.; Nakahara, S.; Nishikawa, Y.; Kohmoto, S.; Yamamoto, M. *J. Am. Chem. Soc.* **2005**, *127*, 2565-2571. (b) Takezoe, H.; Kishikawa, K.; Gorecka, E. *J. Mater. Chem.* **2006**, *16*, 2412-2416.

¹⁴ Paraschiv, I.; Delforterie, P.; Giesbers, M.; Posthumus, M. A.; Marcelis, A. T. M.; Zuilhof, H.; Sudhölter, E. J. R. *Liq. Cryst.* **2005**, *32*, 977-983.

¹⁵ Gearba, R. I.; Lehmann, M.; Levin, J.; Ivanov, D. A.; Koch, M. H. J.; Barberá, J.; Debije, M. G.; Piris, J.; Geerts, Y. H. *Adv. Mater.* **2003**, *15*, 1614-1618.

¹⁶ Liu, C. Y.; Bard, A. J. *Nature* **2002**, *418*, 162-164.

- ¹⁷ Beeson, J. C.; Fitzgerald, L. J.; Gallucci, J. C.; Gerkin, R. E.; Rademacher, J. T.; Czarnik, A. W. *J. Am. Chem. Soc.* **1994**, *116*, 4621-4622.
- ¹⁸ Paraschiv, I.; Giesbers, M.; van Lagen, B.; Grozema, F. C.; Abellon, R. D.; Siebbeles, L. D. A.; Marcelis, A. T. M.; Zuilhof, H.; Sudhölter, E. J. R. *Chem. Mater.* **2006**, *18*, 968-974.
- ¹⁹ (a) Cornil, J.; Lemaury, V.; Calbert, J. P.; Brédas, J. L. *Adv. Mater.* **2002**, *14*, 726-729. (b) Tant, J.; Geerts, Y. H.; Lehmann, M.; De Cupere, V.; Zucchi, G.; Laursen, B. W.; Bjørnholm, T.; Lemaury, V.; Marcq, V.; Burquel, A.; Hennebicq, E.; Gardebien, F.; Viville, P.; Beljonne, D.; Lazzaroni, R.; Cornil, J. *J. Phys. Chem. B* **2005**, *109*, 20315-20323.
- ²⁰ Matsunaga, Y.; Miyajima, N.; Nakayasu, Y.; Sakai, S.; Yonenaga, M. *Bull. Chem. Soc. Jpn.* **1988**, *61*, 207-210.
- ²¹ (a) Matsunaga, Y.; Miyajima, N.; Nakayasu, Y.; Sakai, S.; Yonenaga, M. *Bull. Chem. Soc. Jpn.* **1988**, *61*, 207-210. (b) Brunsfeld, L.; Folmer, B. J. B.; Meijer, E. W.; Sijbesma, R. P. *Chem. Rev.* **2001**, *101*, 4071-4097. (c) Nguyen, T. Q.; Bushey, M. L.; Brus, L. E.; Nuckolls, C. *J. Am. Chem. Soc.* **2002**, *124*, 15051-15054. (d) van Gorp, J. J.; Vekemans, J. A. J. M.; Meijer, E. W.; *J. Am. Chem. Soc.* **2002**, *124*, 14759-14769. (e) Bushey, M. L.; Hwang, A.; Stephens, P. W.; Nuckolls, C. *Angew. Chem. Int. Ed.* **2002**, *41*, 2828-2831.
- ²² Zhao, K. Q.; Gao, C. Y.; Hu, P.; Wang, B. Q.; Li, Q. *Acta Chimica Sinica* **2006**, *64*, 1051-1062.
- ²³ Mizoshita, N.; Monobe, H.; Inoue, M.; Ukon, M.; Watanabe, T.; Shimizu, Y.; Hanabusa, K.; Kato, T. *Chem. Commun.* **2002**, 428-429.
- ²⁴ (a) Brown, S. P.; Schnell, I.; Brand, J. D.; Müllen, K.; Spiess, H. W. *Phys. Chem. Chem. Phys.* **2000**, *2*, 1735-1745. (b) Wan, W.; Monobe, H.; Sugino, T.; Tanaka, Y.; Shimizu, Y. *Mol. Cryst. Liq. Cryst.* **2001**, *364*, 597-603. (c) Setoguchi, Y.; Monobe, H.; Wan, W.; Terasawa, N.; Kiyohara, K.; Nakamura, N.; Shimizu, Y. *Thin Solid Films* **2003**, *438-439*, 407-413.
- ²⁵ Tinh, N. H.; Bernaud, M. C.; Sigaud, G.; Destrade, C. *Mol. Cryst. Liq. Cryst.* **1981**, *65*, 307-316.
- ²⁶ Lee, J. C.; Yuk, J. Y.; Cho, S. H. *Synth. Commun.* **1995**, *25*, 1367-1370.
- ²⁷ Kumar, S.; Manickam, M. *Chem. Commun.* **1997**, *17*, 1614-1616.
- ²⁸ Kumar, S.; Manickam, M. *Synthesis* **1998**, 1119-1122.
- ²⁹ Boden, N.; Bushby, R.K.; Cammidge, A. N.; El-Mansoury, A.; Martin, P. S.; Lu, Z. *J. Mater. Chem.* **1999**, *9*, 1391-1402.

- ³⁰ (a) Boden, N.; Bushby, R. J.; Lu, Z.; Lozman, O. R. *Liq. Cryst.* **2001**, *28*, 657-661. (b) Dierking, I. *Textures of Liquid Crystals* **2003**, Wiley-VCH. (c) Bushby, R. J.; Boden, N.; Kilner, C. A.; Lozman, O. R.; Lu, Z.; Liu, Q.; Thornton-Pett, M. A. *J. Mater. Chem.* **2003**, *13*, 470-474.
- ³¹ (a) van Esch, J. H.; De Feyter, S.; Kellogg, R. M.; De Schryver, F.; Feringa, B. L. *Chem. Eur. J.* **1997**, *3*, 1238-1234. (b) van Esch, J.; Schoonbeek, F.; de Loos, M.; Kooijman, H.; Spek, A. L.; Kellogg, R. M.; Feringa, B. L. *Chem. Eur. J.* **1999**, *5*, 937-950. (c) Schoonbeek, F. S.; van Esch, J. H.; Wegewijs, B.; Rep, D. B. A.; de Haas, M. P.; Klapwijk, T. M.; Kellogg, R. M.; Feringa, B. L. *Angew. Chem. Int. Ed.* **1999**, *38*, 1393-1397. (d) Schoonbeek, F. S.; van Esch, J. H.; Hulst, R.; Kellogg, R. M.; Feringa, B. L. *Chem. Eur. J.* **2000**, *6*, 2633-2643.
- ³² Results were confirmed by crystal structure data of thiourea and urea, respectively, and also computational results: Masunov, A.; Dannenberg, J. J. *J. Phys. Chem. B* **2000**, *104*, 806-810.
- ³³ (a) Brown, S. P.; Schnell, I.; Brand, J. D.; Müllen, K.; Spiess, H. W. *J. Molec. Struct.* **2000**, *521*, 179-195. (b) Watson, M. D.; Jäckel, F.; Severin, N.; Rabe, J. P.; Müllen, K. *J. Am. Chem. Soc.* **2004**, *126*, 1402-1407.
- ³⁴ (a) Fimmen, W.; Glösen, B.; Kettner, A.; Wittenberg, M.; Wendorff, J. H. *Liq. Cryst.* **1997**, *23*, 569-573. (b) Terasawa, N.; Monobe, H.; Kiyohara, K.; Shimizu, Y. *Chem. Lett.* **2003**, *32*, 214-215. (c) Motoyanagi, J.; Fukushima, T.; Aida, T. *Chem. Commun.* **2005**, 101-103.
- ³⁵ (a) Kardan, M.; Reinhold, B. B.; Hsu, S. L.; Thakur, R.; Lillya, C. P. *Macromolecules* **1986**, *19*, 616-621. (b) Perova, T. S.; Vij, J. K.; Kocot, A. *Advances in Liquid Crystals: A Special Volume of Advances in Chemical Physics*, **2000**, *113*, 341-486.
- ³⁶ (a) Skrovanek, D. J.; Howe, S. E.; Painter, P. C.; Coleman, M. M. *Macromolecules* **1985**, *18*, 1676-1683. (b) Xue, C.; Jin, S.; Weng, X.; Ge, J. J.; Shen, Z.; Shen, H.; Graham, M. J.; Jeong, K. U.; Huang, H.; Zhang, D.; Guo, M.; Harris, F. W.; Cheng, S. Z. D.; Li, C. Y.; Zhu, L. *Chem. Mater.* **2004**, *16*, 1014-1025. (c) Shen, H.; Jeong, K. U.; Xiong, H.; Graham, M. J.; Leng, S.; Zheng, J. X.; Huang, H.; Guo, M.; Harris, F. W.; Cheng, S. Z. D. *Soft Matter* **2006**, *2*, 232-242.
- ³⁷ Kettner, A.; Wendorff, J. H. *Liq. Cryst.* **1999**, *26*, 483-487.

Chapter 3

Asymmetry in Liquid Crystalline Hexaalkoxy-triphenylene Discotics*

Abstract – In the current chapter, the synthesis and phase behaviour of a new series of unsymmetrically substituted hexaalkoxytriphenylene-based liquid crystals are reported. One of the hexyloxy chains in hexa-hexyloxytriphenylene (**HAT6**) is replaced by either a shorter or longer chain, HAT-(OC₆H₁₃)₅-(OC_nH_{2n+1}). Compounds with chain lengths *n* of 2 - 14, 16 and 18 were prepared and investigated.

Compounds with *n* ≥ 13 were not liquid crystalline. For all compounds with *n* ≤ 12 Col_h textures were observed by polarizing microscopy. X-ray investigations showed that the intercolumnar distance gradually increased from 20.19 Å to 22.03 Å with *n* from *n* = 2 to 12, while the interdisk distance (3.6 Å) remained constant. A small odd-even effect on the increase of the intercolumn distance with *n* was observed. This effect was also found in the change of Δ*H* of isotropization with *n*.

* This chapter is based on:

Paraschiv, I.; Delforterie, P.; Giesbers, M.; Posthumus, M. A.; Marcelis, A. T. M.; Zuilhof, H.; Sudhölter, E. J. R. *Liq. Cryst.* **2005**, 32, 977-983.

3.1 Introduction

Columnar discotic mesophases have attracted considerable interest in the last decade, which has led to a detailed characterization and classification of these phases.¹ Such materials could be interesting as one-dimensional (hole) conductors and find application in, for example, nanowires. The possibility for strong $\pi - \pi$ interactions between the polyaromatic cores of hexaalkoxytriphenylenes (HATs) in the hexagonal columnar (Col_h) phase can lead to highly organized columns and a relatively high charge carrier mobility.^{2,3,4} Additional stabilization of the columnar mesophase is expected to lead to improved charge mobility, thus making these materials potential candidates for application in photovoltaic devices.⁵

In the Col_h phase the motions of the core and the alkyl tails are strongly correlated.⁶ Due to this coupling, an important factor that determines the stability of the columns is the length of the alkyl chains, which surround the disk-like aromatic cores. The interplay between these two motions originates from tail - tail van der Waals interactions and core - core $\pi - \pi$ interactions, and results in the potential of HATs to act as molecular wires.

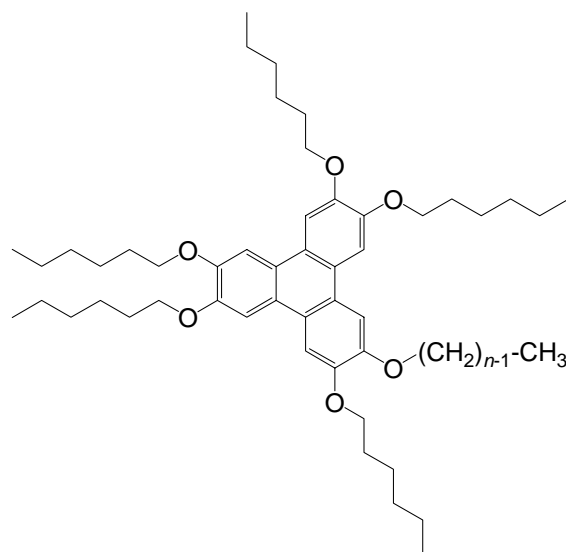


Figure 1. Structure of the triphenylenes studied ($n = 2 - 14, 16, 18$).

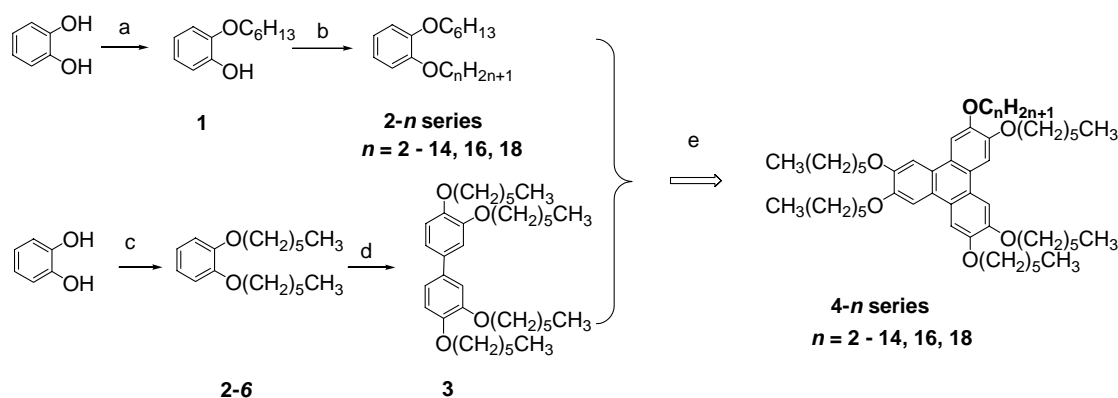
In this study we report the synthesis of a series of novel triphenylene molecules (Figure 1), which contain an element of asymmetry due to the presence of five hexyloxy chains and one alkyl chain that is either shorter or longer.

We studied the liquid crystalline phase behaviour by polarizing optical microscopy (POM), X-ray diffraction (XRD) and differential scanning calorimetry (DSC).

3.2 Results and Discussions

3.2.1 Synthesis

The compounds (series **4-n**) were synthesized via the biphenyl route, starting from tetrakis(hexyloxy)biphenyl and the appropriate 1-hexyloxy-2-alkoxybenzene (see Scheme 1).⁷ 2-Hexyloxyphenol was obtained by reacting 1-bromohexane with a tenfold excess of catechol. Subsequent reaction with another 1-bromoalkane gave the appropriate 1-hexyloxy-2-alkoxybenzenes (**2-n**) in good yield. The biphenyl derivative **3** was obtained in two steps from 1,2-bis(hexyloxy)benzene in overall 19% yield. First, 1,2-bis(hexyloxy)-4-iodobenzene was obtained in almost quantitative yield by reaction with iodine monochloride. Reaction with copper powder at 275 °C gave the biphenyl derivative. The coupling towards the triphenylene derivatives (series **4-n**) was carried out with FeCl₃ as a catalyst under anhydrous conditions. In order to avoid dealkylation, anhydrous conditions and a short reaction time (0.5 – 1 h) was used.



Scheme 1. General procedure for the synthesis of HAT-(OC₆H₁₃)₅(OC_nH_{2n+1}) derivatives **4-n**. (a) C₆H₁₃Br, ethanol, K₂CO₃; (b) C_nH_{2n+1}Br, 2-butanone (CH₃CN), K₂CO₃ (Cs₂CO₃); (c) C₆H₁₃Br, CH₃CN, Cs₂CO₃; (d) ICl, CHCl₃; Cu powder, heat; (e) FeCl₃, CH₂Cl₂, CH₃OH.

3.2.2 Characterization

POM shows that all members of the **4-n** series of compounds with $n \leq 12$ exhibit enantiotropic liquid crystalline phases. The fan-like optical texture is typical for a hexagonal columnar discotic mesophase (Col_h), commonly observed for triphenylene derivatives (Figure 2).⁸

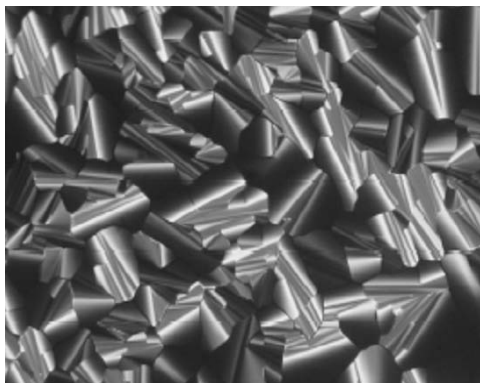


Figure 2. Polarized optical microphotograph of **4-2** at 78 °C, indicative of a Col_h phase (See the Appendix at the end of the thesis for the color picture).

As a typical example, the DSC thermogram of compound **4-12** is shown in Figure 3. The Cr-Col_h and Col_h-I transitions upon heating, and the I-Col_h and Col_h-Cr transitions upon cooling, respectively, are seen. Compound **4-12** could be cooled significantly below the melting point, with a crystallization point at about 26 °C (Table 1).

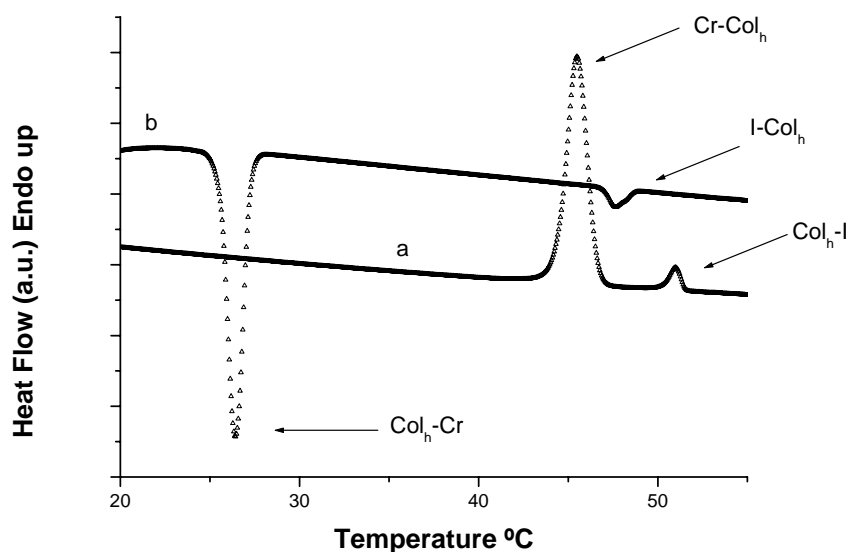


Figure 3. DSC traces of compound **4-12** (a) the second heating and (b) cooling runs (5 °C min⁻¹).

The transition temperatures and corresponding enthalpies of all compounds in the **4-*n*** series are given in Table 1. The melting points and isotropization temperatures of this series are plotted in Figure 4.

Table 1. Transition temperatures (°C) and transition enthalpies (kJ mol⁻¹; in parentheses) of the **4-*n*** series of compounds, obtained from the second DSC runs, 5 °C min⁻¹.

Compound	Heating			Cooling			
	Cr	Col _h	I	I	Col _h	Cr	
4-2	• 58.7 [37.9]	•	81.3 [4.0]	•	• 79.2 [3.8]	• 33.4 [36.0]	•
4-3	• 62.3 [42.5]	•	87.9 [4.6]	•	• 84.7 [4.5]	• 36.6 [38.2]	•
4-4	• 61.0 [44.1]	•	98.4 [5.8]	•	• 96.1 [5.8]	• 35.7 [38.1]	•
4-5	• 59.0 [35.5]	•	100.8 [5.7]	•	• 98.8 [5.8]	• 39.9 [36.7]	•
4-6	• 66.6 [39.6]	•	98.1 [4.9]	•	• 96.1 [4.8]	• 48.1 [42.1]	•
4-7	• 59.6 [38.2]	•	97.2 [4.9]	•	• 95.3 [4.7]	• 44.0 [38.7]	•
4-8	• 54.8 [40.1]	•	91.3 [4.5]	•	• 86.2 [4.5]	• 33.9 [39.1]	•
4-9	• 49.7 [40.2]	•	82.4 [4.4]	•	• 79.9 [4.2]	• 29.1 [38.2]	•
4-10	• 45.0 [37.8]	•	71.8 [3.2]	•	• 68.3 [3.2]	• 23.3 [36.1]	•
4-11	• 46.8 [41.2]	•	62.9 [3.1]	•	• 59.6 [3.2]	• 25.8 [39.2]	•
4-12	• 45.5 [43.9]	•	50.9 [2.6]	•	• 47.6 [2.6]	• 26.4 [41.2]	•
4-13	• 41.0 [32.3]			•		27.1 [26.9]	•
4-14	• 39.7 [29.2]			•		25.3 [27.7]	•
4-16	• 38.4 [23.7]			•		24.9 [22.9]	•
4-18	• 36.1 [35.5]			•		19.7 [31.0]	•

All the compounds, with $n \leq 12$, exhibit a liquid crystalline Col_h phase. As can be seen from Table 1 and Figure 4, compounds **4-13** to **4-18** are not liquid crystalline, although they can be supercooled considerably before crystallization occurs. The highest melting point is found for **4-6**. This is not unreasonable, since the 6-fold symmetry probably allows an optimal packing in regard of both $\pi - \pi$ interactions and intercolumn interference. With increasing the tail length of one of the alkyloxy chains, the melting points gradually decrease to below 40 °C.

The isotropization temperatures have a maximum for **4-5** and decrease both for shorter and longer chains. For longer chains than hexyloxy the asymmetry increases and the isotropization temperatures decrease rapidly. This leads to a gradual decrease of the temperature range for the LC phase, with the result that for $n \geq 13$ no liquid crystalline phases are observed anymore. The isotropization temperatures do not have their maximum for the fully symmetrical **4-6** but for **4-5**. For the class of 6-fold symmetrical HATs it was found that the isotropization temperatures decrease strongly with longer alkyl tails.⁹ For compound **4-5** the balance between a higher isotropization temperature due to a shorter chain, and a lower isotropization temperature due to asymmetry, is apparently just in favor of the first effect. For **4-4**, **4-3**, and **4-2** the increasing asymmetry leads to a lowering of the isotropization temperature.

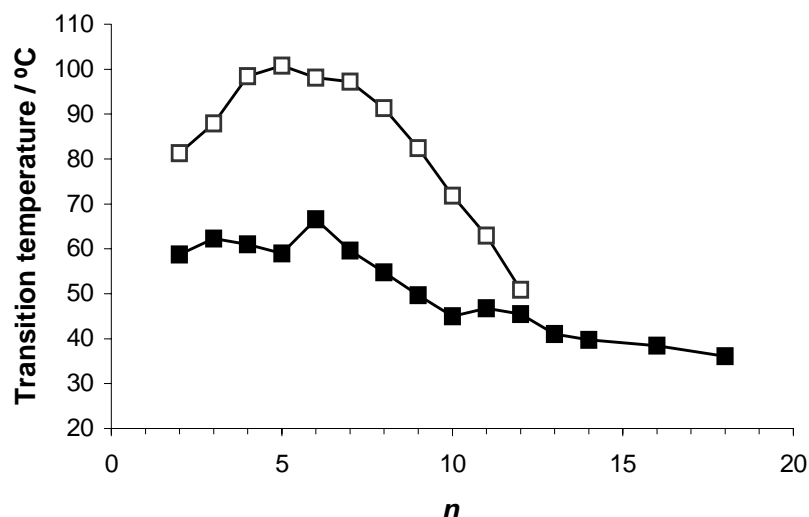


Figure 4. Dependence of the melting points (■) and isotropization temperatures (□) of series **4-*n*** on *n*.

Figure 5 shows the isotropization enthalpy as a function of *n*. Less energy is required for molecules with longer alkyl tail to go into highly disordered isotropic state, indicating a lower thermal stability of the liquid crystalline phase. With increase of *n* the asymmetry of the system increases also, which results in a less stable mesophase, and a smaller mesophase region.

For the systems with smaller *n*, such as **4-4**, where the isotropization enthalpy is comparable to that of **4-5**, close packing of molecules plays an important role. Going to smaller values of *n*, the intercalation of the other five hexyloxy chains around the triphenylene core will progressively disturb the system, resulting in a strong decrease of transition temperatures and isotropization enthalpies, as shown in Figure 4 and 5.

XRD of the liquid crystalline phases was used to determine the intercolumn and interdisk distances. The *d*-spacings obtained by X-ray diffraction are given in Table 2.

Intercolumn distances were calculated from the small angle peaks, assuming that a Col_h phase is present. The intracolumn distance follows directly from the wide-angle (001) peak in the diffractograms.

For all liquid crystalline compounds the interdisk distance was the same (3.6 Å), the typical value for the π - π stacking of triphenylene discotics.¹⁰

For a few of the analyzed compounds, the interdisk spacing could not be deduced from the X-ray measurements, due to high tendency of these compounds to align with the columns parallel to the surface during sample preparation. The intercolumn distances increase with *n*, as can be seen in Figure 6.

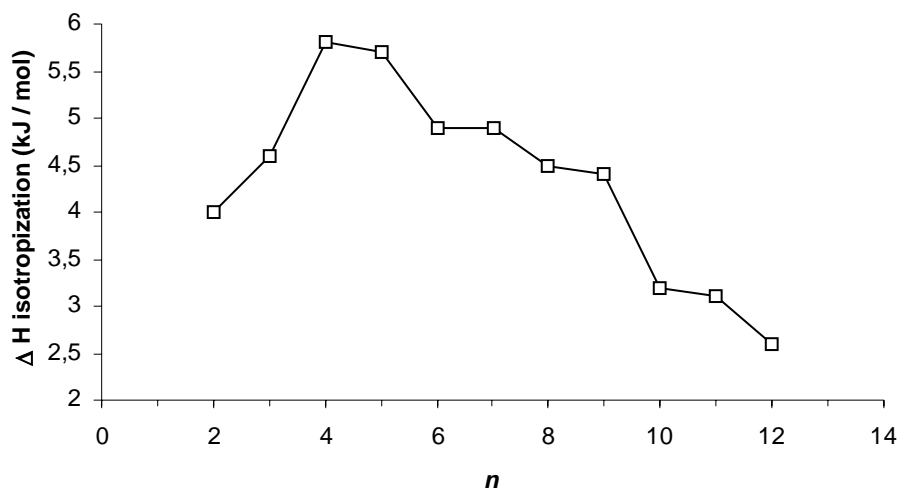


Figure 5. Dependence of the isotropization enthalpy ΔH of series **4-*n*** on *n*.

In addition, upon increasing *n* the concomitant increase of the intercolumn distance levels off. This suggests that upon further increase of the chain length ($n \geq 7$), the chain that is sticking out is largely bent upwards or downwards, but will still have a component parallel to the plane of the aromatic core.

Table 2. Layer spacing and columnar distances for the mesophase of series **4-*n***, deduced from X-ray measurements.

Compound	<i>d</i> - spacing (Å)	Intercolumn distance (Å) ^b	Interdisk distance (Å)
4-2	17.49	20.19	- ^a
4-3	17.72	20.46	- ^a
4-4	17.92	20.69	3.62
4-5	18.13	20.93	3.60
4-6	18.34	21.17	3.61
4-7	18.43	21.28	- ^a
4-8	18.64	21.52	3.66
4-9	18.76	21.66	- ^a
4-10	18.98	21.91	3.65
4-11	19.00	21.93	3.63
4-12	19.08	22.03	3.60

^a could not be determined. ^b intercolumnar distance is $2/\sqrt{3} \times d$.

As a result, the disks themselves become asymmetric, which will lead to a decrease of the

core-core overlap between the disks in the columns. Therefore, the $\pi - \pi$ interactions will be diminished, and this will lead to a destabilization of the columnar phase.

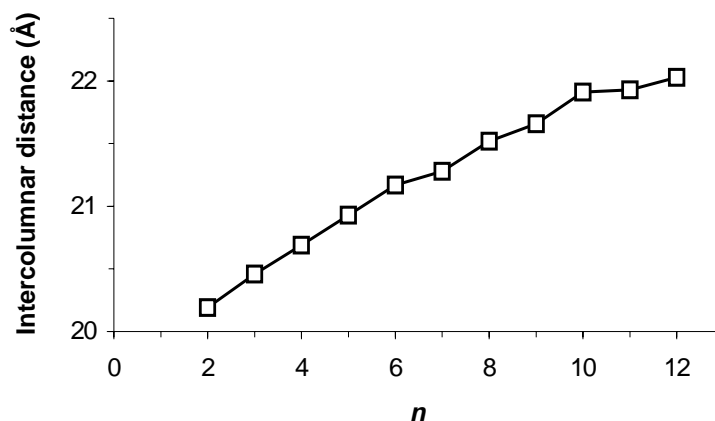


Figure 6. The intercolumnar distances for the **4-n** series as a function of n .

Furthermore, a small but distinct odd-even effect becomes apparent in the increase of the intercolumnar distance above $n = 6$. This increase is larger on going from odd n to the next even n , than from an even spacer length to the next odd one. This is probably related to the observation that, seen from a fixed point, the increase of the distance of the atom in the alkyl chain that is furthest removed from that point of reference is different in going from an odd to an even spacer length than from an even to an odd spacer length. This is schematically depicted in Figure 7. This can be clarified by the distance of a carbon atom in the alkyl tail to the aromatic core. These distances are depicted in Figure 7 for a model compound with a heptyloxy chain. As can be seen, the increase from an odd n to the next even value of n ($1 \rightarrow 2$, $3 \rightarrow 4$, $5 \rightarrow 6$) is $\sim 1.31 \text{ \AA}$, and therefore distinctly larger than that from an even n to the next odd value of n ($2 \rightarrow 3$, $4 \rightarrow 5$, $6 \rightarrow 7$), which is $\sim 1.23 \text{ \AA}$.

Preece *et al.* have observed similar odd-even effects for a series of HAT5-derived compounds.^{8,11} In fact, related odd-even effects can also be discerned in Figure 4 (isotropization temperatures) and more clearly in Figure 5 (isotropization enthalpies). Upon going from $n = 6$ to $n = 12$ the change in ΔH values upon going from odd n to even n are much larger than upon going from even n to odd n . For $n < 5$ the reverse effect seems to take place. These trends for both $n < 5$ and $n > 6$ indicate that the stability of the mesophase is strongly related to the actual distance between the aromatic core and the terminal atoms in the spacer, rather than to the number of carbon atoms in the tail. This specific study has been conducted to determine the influence of variation of the length of only one tail around the triphenylene disk on the thermotropic liquid-crystalline properties of **HAT6** derivatives.

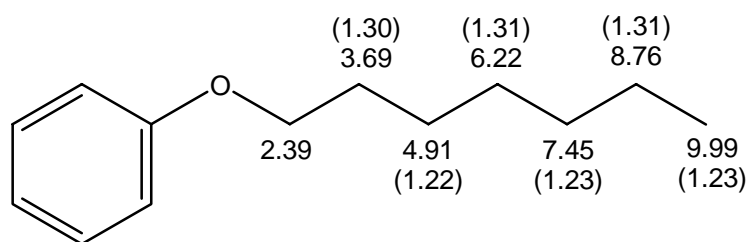


Figure 7. Geometrical basis of odd - even effects: distance between *ipso* C atom in aromatic core and the designated C atom in the spacer, and (in parentheses) the increase in distance (all in Å).

3.3 Conclusions

In this chapter, a new series of columnar discotic LC materials is reported, based on a triphenylene core with five hexyloxy chains and one alkoxy chain with n carbon atoms. For $n \leq 12$ this class of materials exhibits a Col_h mesophase. For compounds with $n \geq 13$ no mesophase is present. The observed maxima in isotropization temperatures and isotropization enthalpies display an intricate balance between the π - π stacking of the triphenylene cores and the organization of the alkyl chain (interpenetration, orientation with respect to the aromatic core, intercolumn distance). Finally, distinct odd-even effects on the intercolumn distances are observed, which are related to the direct spatial distance between the aromatic core and the terminal atom in the alkyl chain.

3.4 Experimental

3.4.1 Measurements

$^1\text{H-NMR}$ (200 MHz) and $^{13}\text{C-NMR}$ (50 MHz) spectra were obtained with a Bruker spectrometer, using CDCl_3 as a solvent. Melting points, thermal phase transition temperatures and optical investigation of the liquid crystalline phases were determined on samples between ordinary glass slides using an Olympus BH-2 polarizing microscope equipped with a Mettler FP82HT hot stage, which was controlled by a Mettler FP80HT central processor. DSC thermograms were obtained on a Perkin-Elmer DSC-7 system using 2-5 mg samples in 30 μl sample pans and a scan rate of 5 $^\circ\text{C min}^{-1}$. ΔH is calculated in kJ mol^{-1} . Temperature-dependent X-ray curves were measured on a Philips X'pert Pro MRD machine equipped with an Anton Paar camera for temperature control. For the measurements in the small angle

region, the sample was spread in the isotropic or the liquid crystalline phase on a thin glass slide (about 15 μm thick), which was placed on a temperature regulated flat copper sample stage. This sample preparation sometimes caused very high intensities of X-ray reflections because of partial or complete surface alignment of the molecules in the liquid crystalline state. The accurate masses were obtained using a Finnigan MAT 95 mass spectrometer operating in the 70 eV EI mode at a resolution 5500.

3.4.2 Synthesis

All solvents were PA quality. All reactions were carried out under nitrogen atmosphere. Dry CH_2Cl_2 was freshly distilled from CaH_2 . All compounds gave NMR spectra that are in agreement with the proposed structure and show correct elemental analyses or accurate masses. All the synthesis details are given below.

2-Hexyloxyphenol, 1¹²

A mixture of catechol (10.1 g, 92.0 mmol), 1-bromohexane (3.10 g, 19.0 mmol) and anhydrous potassium carbonate (15.0 g) in ethanol (100 ml) was stirred under reflux for 26 h. The solvent was partially evaporated and 250 ml of water was added to the system. After extraction with 3 x 100 ml CH_2Cl_2 and washing with brine (200 ml), the organic layer was dried on anhydrous Na_2SO_4 and then concentrated. The crude product was purified by column chromatography on silica, eluting with petroleum ether 40/60 – CH_2Cl_2 , in a (2:1) ratio, to give 2-hexyloxyphenol as a pale yellow oil (2.02 g, 10.4 mmol, 55 %).

¹H NMR: δ 7.04-6.87 (4H, m, ArH), 5.86 (1H, s, OH), 4.05 (2H, t, $J = 6.49$ Hz, OCH_2), 1.91-1.77 (2H, m, $\text{CH}_2\text{CH}_2\text{O}$), 1.54-1.35 (6H, m, CH_2), 0.98 (3H, t, $J = 6.38$ Hz, CH_3).

¹³C NMR: δ 146.04 (1-ArCOH), 145.85 (2-ArCO-R), 121.31 (6-ArC), 120.11 (3-ArC), 114.51 (5-ArC), 111.65 (4-ArC), 68.90 (OCH_2), 31.62-22.66 (CH_2), 14.08 (CH_3).

1-Ethoxy-2-hexyloxybenzene, 2-2

A solution of 5.90 g (30.0 mmol) of **1**, 11.3 g (0.10 mol) of bromoethane, 10.0 g K_2CO_3 and a catalytic amount of KI in 30 ml of 2-butanone was refluxed for 2 days under anhydrous conditions. After refluxing, the reaction mixture was worked up using the same procedure as for compound **1**. Compound **2-2** was obtained as pale yellow oil, 6.07 g (27.0 mmol, 89 %).

¹H NMR: δ 6.91 (4H, bs, ArH), 4.45-3.65 (4H, m (t + q overlap), OCH_2), 2.34-1.71 (2H, m, $\text{CH}_2\text{CH}_2\text{O}$), 1.59-1.10 (9H, m, 1 x CH_3 and 3 x CH_2), 0.96 (3H, t, $J = 6.25$ Hz, CH_3).

^{13}C NMR: δ 150.14 (1-ArC-O), 149.92 (2-ArC-O), 122.04 (6-ArCH), 121.94 (3-ArCH), 114.93 (5-ArCH), 111.83 (4-ArCH), 70.15 (OCH_2CH_2), 65.55 (OCH_2CH_3), 32.64, 30.27, 26.73, 23.65 (CH_2), 15.92 (CH_3 , OCH_2CH_3), 15.04 (CH_3).

2-Hexyloxy-1-propyloxybenzene, 2-3

From 19.5 g (0.10 mol) of **1**, 16.6 g (0.13 mol) of 1-bromopropane, 11.4 g K_2CO_3 and a catalytic amount of KI in 100 ml 2-butanone, 7.61 g (32.0 mmol, 32 %) of **2-3** was obtained as a pale yellow oil.

^1H NMR: δ 6.91 (4H, s, ArH), 4.05-3.95 (4H, m, OCH_2), 1.92-1.82 (4H, m, $\text{CH}_2\text{CH}_2\text{O}$), 1.42-1.35 (6H, m, CH_2), 1.08 (3H, t, $J = 7.39$ Hz, $\text{OCH}_2\text{CH}_2\text{CH}_3$), 0.94 (3H, t, $J = 6.43$ Hz, CH_3).

^{13}C NMR: δ 149.27 (1-ArC-O), 149.23 (2-ArC-O), 121.05 (6-ArCH), 121.02 (3-ArCH), 114.09 (5-ArCH), 114.05 (4-ArCH), 70.72 (OCH_2CH_2), 69.24 ($\text{OCH}_2\text{CH}_2\text{CH}_3$), 31.68, 29.36, 25.79, 22.72, 22.70 (CH_2), 14.09 (CH_3 , $\text{OCH}_2\text{CH}_2\text{CH}_3$), 10.56 (CH_3).

1-Butyloxy-2-hexyloxybenzene, 2-4

From 1.02 g (5.25 mmol) of **1**, 1.44 g (10.5 mmol) of 1-bromobutane, 5.00 g K_2CO_3 and a catalytic amount of KI in 100 ml 2-butanone, 1.20 g (4.80 mmol, 91 %) of **2-4** was obtained as pale yellow oil.

^1H NMR: δ 6.87 (4H, s, ArH), 4.00 (4H, t, $J = 6.50$ Hz, OCH_2), 1.95-1.75 (4H, m, OCH_2CH_2), 1.62-1.24 (8H, m, CH_2), 1.00-0.85 (6H, m, CH_3).

^{13}C NMR: δ 149.2 (1,2-ArC-O), 120.96 (3,6-ArCH), 114.03 (4,5-ArCH), 69.2 (OCH_2), 31.63-22.64 (CH_2), 14.1 (CH_3).

2-Hexyloxy-1-pentyloxybenzene, 2-5

From 3.50 g (18.0 mmol) of **1**, 3.30 g (22.0 mmol) of 1-bromopentane, 3.00 g K_2CO_3 as base and a catalytic amount of KI in 100 ml 2-butanone, 4.00 g (15.0 mmol, 84 %) of **2-5** was obtained as pale yellow oil.

^1H NMR: δ 6.90 (4H, s, ArH), 4.01 (4H, t, $J = 6.52$ Hz, OCH_2), 1.92-1.78 (4H, m, OCH_2CH_2), 1.55-1.32 (10H, m, CH_2), 1.20-0.90 (6H, m, CH_3).

^{13}C NMR: δ 149.30 (1,2-ArC-O), 121.02 (3,6-ArCH), 114.05 (4,5-ArCH), 69.19 (OCH_2), 31.71-22.57 (CH_2), 14.09 (CH_3).

1-Heptyloxy-2-hexyloxybenzene, 2-7

From 5.30 g (27.3 mmol) of **1**, 5.80 g (32.0 mmol) of 1-bromoheptane, 5.00 g K_2CO_3 and a

Asymmetry in Hexaalkoxy Triphenylenes

catalytic amount of KI in 100 ml 2-butanone, 6.40 g (22.0 mmol, 80 %) of **2-7** was obtained as pale yellow oil.

¹H NMR: δ 6.90 (4H, s, ArH), 4.00 (4H, t, J = 6.55 Hz, OCH₂), 1.91-1.77 (4H, m, OCH₂CH₂), 1.51-1.34 (14H, m, CH₂), 0.95-0.93 (6H, m, CH₃).

¹³C NMR: δ 149.22 (1,2-ArC-O), 120.95 (3,6-ArCH), 113.97 (4,5-ArCH), 69.14 (OCH₂), 32.85-22.68 (CH₂), 14.04 (CH₃).

1-Hexyloxy-2-octyloxybenzene, 2-8

From 9.30 g (48.0 mmol) of **1**, 11.90 g (62.0 mmol) of 1-bromooctane, 9.00 g K₂CO₃ and a catalytic amount of KI in 100 ml 2-butanone, 13.4 g (43.8 mmol, 91 %) of **2-8** was obtained as pale yellow oil.

¹H NMR: δ 6.91 (4H, s, ArH), 4.02 (4H, t, J = 6.56 Hz, OCH₂), 1.92-1.78 (4H, m, OCH₂CH₂), 1.56-1.35 (16H, m, CH₂), 1.00-0.91 (6H, m, CH₃).

¹³C NMR: δ 149.22 (1,2-ArC-O), 120.95 (3,6-ArCH), 113.97 (4,5-ArCH), 69.14 (OCH₂), 32.85-22.68 (CH₂), 14.04 (CH₃).

1-Hexyloxy-2-nonyloxybenzene, 2-9

From 7.02 g (36.2 mmol) of **1**, 18.6 g (90.0 mmol) of 1-bromononane, 8.00 g K₂CO₃ and a catalytic amount of KI in 60 ml 2-butanone, 11.5 g (35.9 mmol, quantitative yield) of **2-9** was obtained as pale yellow oil.

¹H NMR: δ 6.90 (4H, s, ArH), 4.01 (4H, t, J = 6.55 Hz, OCH₂), 1.91-1.77 (4H, m, OCH₂CH₂), 1.58-1.32 (18H, m, CH₂), 0.97-0.89 (6H, m, CH₃).

¹³C NMR: δ 149.27 (1,2-ArC-O), 121.01 (3,6-ArCH), 114.04 (4,5-ArCH), 69.23 (OCH₂), 31.99-22.71 (CH₂), 14.17, 14.09 (CH₃).

1-Decyloxy-2-hexyloxybenzene, 2-10

From 6.70 g (34.5 mmol) of **1**, 9.20 g (42.0 mmol) of 1-bromodecane, 7.00 g K₂CO₃ and a catalytic amount of KI in 100 ml 2-butanone, 6.20 g (18.6 mmol, 54 %) of **2-10** was obtained as pale yellow oil.

¹H NMR: δ 6.88 (4H, s, ArH), 3.99 (4H, t, J = 6.62 Hz, OCH₂), 1.85-1.74 (4H, m, OCH₂CH₂), 1.60-1.27 (20H, m, CH₂), 0.93-0.85 (6H, m, CH₃).

¹³C NMR: δ 149.22 (1,2-ArC-O), 120.98 (3,6-ArCH), 114.03 (4,5-ArCH), 69.24 (OCH₂), 31.94-22.66 (CH₂), 14.15, 14.07 (CH₃).

1-Hexyloxy-2-undecyloxybenzene, 2-11

From 1.80 g (9.30 mmol) of **1**, 3.30 g (14.0 mmol) of 1-bromoundecane, 2.00 g K₂CO₃ and a catalytic amount of KI in 100 ml 2-butanone, 2.54 g (7.29 mmol, 78 %) of **2-11** was obtained as pale yellow oil.

¹H NMR: δ 6.90 (4H, s, ArH), 4.01 (4H, t, J = 6.55 Hz, OCH₂), 1.87-1.77 (4H, m, OCH₂CH₂), 1.49-1.29 (22H, m, CH₂), 0.93-0.91 (6H, m, CH₃).

¹³C NMR: δ 149.20 (1,2-ArC-O), 120.96 (3,6-ArCH), 114.03 (4,5-ArCH), 69.20 (OCH₂), 31.63-22.64 (CH₂), 14.1 (CH₃).

1-Dodecyloxy-2-hexyloxybenzene, 2-12

From 5.00 g (26.0 mmol) of **1**, 8.20 g (33.0 mmol) of 1-bromododecane, 5.00 g K₂CO₃ and a catalytic amount of KI in 100 ml 2-butanone, 8.77 g (24.0 mmol, 94 %) of **2-12** was obtained as pale yellow oil.

¹H NMR: δ 6.89 (4H, s, ArH), 4.01 (4H, t, J = 6.57 Hz, OCH₂), 1.86-1.79 (4H, m, OCH₂CH₂), 1.51-1.28 (24H, m, CH₂), 0.95-0.86 (6H, m, CH₃).

¹³C NMR: δ 149.23 (1,2-ArC-O), 120.99 (3,6-ArCH), 114.03 (4,5-ArCH), 69.24 (OCH₂), 22.68-31.96 (CH₂), 14.08, 14.16 (CH₃).

1-Hexyloxy-2-tridecyloxybenzene, 2-13

From 3.60 g (18.6 mmol) of **1**, 5.00 g (19.0 mmol) of 1-bromotridecane, 4.00 g K₂CO₃ and a catalytic amount of KI in 100 ml 2-butanone, 6.70g (17.8 mmol, 96 %) of **2-13** was obtained as pale yellow oil.

¹H NMR: δ 6.88 (4H, s, ArH), 4.01 (4H, t, J = 6.56 Hz, OCH₂), 1.89-1.71 (4H, m, OCH₂CH₂), 1.48-1.27 (26H, m, CH₂), 0.95-0.86 (6H, m, CH₃).

¹³C NMR: δ 149.23 (1,2-ArC-O), 120.99 (3,6-ArCH), 114.03 (4,5-ArCH), 69.24 (OCH₂), 31.97-22.68 (CH₂), 14.16, 14.08 (CH₃).

1-Hexyloxy-2-tetradecyloxybenzene, 2-14

From 4.85 g (25.0 mmol) of **1**, 9.00 g (32.0 mmol) of 1-bromotetradecane, 5.00 g K₂CO₃ and a catalytic amount of KI in 100 ml 2-butanone, 6.14 g (15.7 mmol, 63 %) of **2-14** was obtained as a white solid. M.p. 28 °C.

¹H NMR: δ 6.88 (4H, s, ArH), 3.99 (4H, t, J = 6.62 Hz, OCH₂), 1.85-1.78 (4H, m, OCH₂CH₂), 1.38-1.26 (28H, m, CH₂), 0.94-0.88 (6H, m, CH₃).

Asymmetry in Hexaalkoxy Triphenylenes

¹³C NMR: δ 149.22 (1,2-ArC-O), 120.98 (3,6-ArCH), 114.03 (4,5-ArCH), 69.24 (OCH₂), 31.96-22.67 (CH₂), 14.16, 14.07 (CH₃).

1-Hexadecyloxy-2-hexyloxybenzene, 2-16

From 3.40 g (17.5 mmol) of **1**, 7.00 g (23.0 mmol) of 1-bromohexadecane, 4.00 g K₂CO₃ and a catalytic amount of KI in 100 ml 2-butanone, 4.90 g (11.7 mmol, 67 %) of **2-16** was obtained as a white solid. M.p. 35 °C.

¹H NMR: δ 6.87 (4H, s, ArH), 3.98 (4H, t, J = 6.64 Hz, OCH₂), 1.80-1.76 (4H, m, OCH₂CH₂), 1.41-1.24 (32H, m, CH₂), 0.89-0.83 (6H, m, CH₃).

¹³C NMR: δ 149.20 (1,2-ArC-O), 120.97 (3,6-ArCH), 114.02 (4,5-ArCH), 69.25 (OCH₂), 31.94-22.71 (CH₂), 14.15, 14.06 (CH₃).

1-Hexyloxy-2-octadecyloxybenzene, 2-18

From 7.00 g (36.0 mmol) of **1**, 15.6 g (46.8 mmol) of 1-bromooctadecane, 7.00 g K₂CO₃ and a catalytic amount of KI in 100 ml 2-butanone, 10.9 g (24.4 mmol, 68 %) of **2-18** was obtained as white solid. M.p. 43 °C.

¹H NMR: δ 6.87 (4H, s, ArH), 3.98 (4H, t, J = 6.84 Hz, OCH₂), 1.87-1.73 (4H, m, OCH₂CH₂), 1.45-1.24 (36H, m, CH₂), 0.92-0.83 (6H, m, CH₃).

¹³C NMR: δ 149.20 (1,2-ArC-O), 120.98 (3,6-ArCH), 114.03 (4,5-ArCH), 69.25 (OCH₂), 31.94-22.65 (CH₂), 14.15, 14.06 (CH₃).

3,3',4,4'-Tetrakis-hexyloxybiphenyl, 3¹²

A mixture of **2-6** (10.0 g, 36.0 mmol) and iodine monochloride (8.80 g, 54.0 mmol) in CHCl₃ was stirred at room temperature for 2.5 h. The mixture was washed twice with 150 ml of 1M sodium metabisulphite solution followed by washing with 100 ml of water. The organic phase was dried on anhydrous Na₂SO₄. The solvent was evaporated and the crude product (1,2-bis-hexyloxy-4-iodobenzene) was obtained (13.0 g, 89 %) as an intermediate for the synthesis of **3**. The crude compound was used in the next reaction without further purification.

For the coupling reaction a mixture of 9.00 g (22.0 mmol) of 1,2-bis-hexyloxy-4-iodobenzene and 6.30 g (0.10 mol) copper powder were heated at 275 °C for 1h, while the reaction mixture was vigorously stirred. After cooling the mixture to room temperature, 250 ml of CH₂Cl₂ was added and the reaction mixture was filtered through Hyflo. The crude compound was

recrystallized from a mixture of methanol and ethanol (1:1) yielding 2.35 g (4.24 mmol, 38 %) of **3**. M.p. 79 °C.

¹H NMR: δ 7.10-7.06 (4H, dd, ArH), 6.95-6.91 (2H, dd, ArH), 4.11-4.00 (8H, m, OCH₂), 1.92-1.78 (8H, m, OCH₂CH₂), 1.51-1.28 (24H, m, CH₂), 0.94 (12H, t, J = 6.82 Hz, CH₃).

¹³C NMR: δ 149.24 (3,3'-ArC-O), 148.44 (4,4'-ArC-O), 134.31 (6,6'-ArC-CAr), 119.28 (5,5'-ArCH), 114.07 (2,2'-ArCH), 113.06 (1,1'-ArCH), 69.35 (OCH₂), 31.63, 29.34, 25.75, 22.65 (CH₂), 14.04 (CH₃).

2-Ethoxy-3,6,7,10,11-pentakishexyloxytriphenylene, 4-2

To a solution of **2-2** (5.70 g, 25.7 mmol) and 9.24 g (16.7 mmol) of **3** in 50 ml of dry CH₂Cl₂ was carefully added 14.0 g of FeCl₃ under anhydrous conditions. The mixture was stirred under N₂ for 0.5 – 1 h at 35 °C. Upon addition of 300 ml of methanol to the reaction mixture the triphenylene compound crystallized from the solution. The mixture was cooled to -35 °C and then filtered. The crystals were washed several times with cold methanol. The crude product has been subjected to column chromatography eluting with CH₂Cl₂ : PE 40/60, in a (1:1) ratio. After recrystallization from a mixture of ethanol, methanol and 2-butanone, 3.70 g (29 %) of **4-2** was obtained.

¹H NMR: δ 7.83 (6H, s, ArH), 4.35-4.19 (12H, m, OCH₂), 2.00-1.86 (10H, m, OCH₂CH₂), 1.59-1.36 (33H, m, CH₂ and CH₃), 0.93 (15H, t, J = 6.71 Hz, CH₃).

¹³C NMR: δ 148.98-148.66 (2,3,6,7,10,11-ArC-O), 123.63-123.56 (ArC-C), 107.31-107.16 (ArC-H), 69.71 (OCH₂), 65.20 (OCH₂CH₃), 31.71, 29.35, 25.87, 22.68 (CH₂), 15.04 (OCH₂CH₃), 14.01(CH₃).

MS [M]⁺: calculated for C₅₀H₇₆O₆: 772.5642 amu; found 772.5660 amu.

3,6,7,10,11-Pentakishexyloxy-2-propyloxytriphenylene, 4-3

From 3.90 g (16.5 mmol) of **2-3**, 5.90 g (10.6 mmol) of **3** and 8.00 g FeCl₃, 1.70 g (2.16 mmol, 20 %) of **4-3** was obtained by the same procedure as described for **4-2**.

¹H NMR: δ 7.83 (6H, s, ArH), 4.26-4.16 (12H, m, OCH₂), 1.97-1.86 (12H, m, OCH₂CH₂), 1.55-1.36 (30H, m, CH₂), 1.14 (3H, t, J = 7.39 Hz, OCH₂CH₂CH₃), 0.94 (15H, t, J = 6.77 Hz, CH₃).

¹³C NMR: δ 148.92 (2,3,6,7,10,11-ArC-O), 123.57 (ArC-C), 107.27 (ArC-H), 71.14 (OCH₂CH₂CH₃), 69.67 (OCH₂CH₂), 31.68, 29.41, 25.85, 22.66 (CH₂), 14.06 (CH₃), 10.66 (CH₃). Elem. anal: calculated for C₅₁H₇₈O₆: C 77.81, H 9.98 %; found C 77.42, H 10.10 %.

MS [M]⁺: calculated 786.5798 amu; found 786.5810 amu.

2-Butyloxy-3,6,7,10,11-pentakishexyloxytriphenylene, 4-4

From 1.20 g (4.80 mmol) of **2-4**, 1.73 g (3.10 mmol) of **3** and 2.30 g FeCl₃, 1.05 g (1.31 mmol, 42 %) of **4-4** was obtained by the same procedure as described for **4-2**.

¹H NMR: δ 7.83 (6H, s, ArH), 4.23 (12H, t, J = 6.54 Hz, OCH₂), 1.97-1.86 (12H, m, OCH₂CH₂), 1.58-1.36 (32H, m, CH₂), 1.04 (3H, t, J = 7.27 Hz, CH₃), 0.93 (15H, t, J = 6.79 Hz, CH₃).

¹³C NMR: δ 148.94 (2,3,6,7,10,11-ArC-O), 123.58 (ArC-C), 107.27 (ArC-H), 69.69 (OCH₂), 69.35 (OCH₂), 31.71-19.40 (CH₂), 14.09 (CH₃). Elem. anal: calculated for C₅₂H₈₀O₆: C 77.95, H 10.06 %; found C 77.99, H 10.33 %.

MS [M]⁺: calculated: 800.5954 amu; found 800.5958 amu.

3,6,7,10,11-Pentakishexyloxy-2-pentyloxytriphenylene, 4-5

From 2.23 g (8.40 mmol) of **2-5**, 2.84 g (5.10 mmol) of **3** and 5.10 g FeCl₃, 0.70 g (0.85 mmol, 17 %) of **4-5** was obtained by the same procedure as described for **4-2**.

¹H NMR: δ 7.83 (6H, s, ArH), 4.23 (12H, t, J = 6.53 Hz, OCH₂), 2.01-1.87 (12H, m, OCH₂CH₂), 1.57-1.36 (34H, m, CH₂), 1.00-0.89 (18H, m, CH₃).

¹³C NMR: δ 148.95 (2,3,6,7,10,11-ArC-O), 123.59 (ArC-C), 107.28 (ArC-H), 69.69 (OCH₂), 31.71-22.59 (CH₂), 14.09 (CH₃). Elem. anal: calculated for C₅₃H₈₂O₆: C 78.08, H 10.13 %; found: C 78.01, H 10.38 %.

MS [M]⁺: calculated 814.6111 amu; found 814.6120 amu.

2,3,6,7,10,11-Hexakishexyloxytriphenylene (HAT6), 4-6¹³

From 1.50 g (5.40 mmol) of **2-6**, 1.20 g (2.16 mmol) of **3** and 2.80 g FeCl₃, 0.95 g (1.14 mmol, 53 %) of **4-6** was obtained by the same procedure as described for **4-2**.

¹H NMR: δ 7.82 (6H, s, ArH), 4.22 (12H, t, J = 6.53 Hz, OCH₂), 1.96-1.86 (12H, m, OCH₂CH₂), 1.43-1.35 (36H, m, CH₂), 0.92 (18H, t, J = 6.73 Hz, CH₃).

¹³C NMR: δ 148.95 (2,3,6,7,10,11-ArC-O), 123.59 (ArC-C), 107.30 (ArC-H), 69.70 (OCH₂), 31.70, 29.43, 25.86, 22.68 (CH₂), 14.07 (CH₃). Elem. anal: calculated for C₅₄H₈₄O₆: C 78.21, H 10.20 %; found C 78.24, H 10.43 %.

MS [M]⁺: calculated 828.6260 amu; found 828.6270 amu.

2-Heptyloxy-3,6,7,10,11-pentakishexyloxytriphenylene, 4-7

From 2.30 g (7.90 mmol) of **2-7**, 5.10 g (9.20 mmol) of **3** and 8.35 g FeCl₃, 2.65 g (3.14 mmol, 39 %) of **4-7** was obtained by the same procedure as described for **4-2**.

¹H NMR: δ 7.82 (6H, s, ArH), 4.22 (12H, t, J = 6.55 Hz, OCH₂), 2.00-1.86 (12H, m, OCH₂CH₂), 1.61-1.36 (38H, m, CH₂), 0.93 (18H, t, J = 6.70 Hz, CH₃).

¹³C NMR: δ 148.95 (2,3,6,7,10,11-ArC-O), 123.59 (ArC-C), 107.28 (ArC-H), 69.69 (OCH₂), 31.89-22.69 (CH₂), 14.09 (CH₃). Elem. anal: calculated for C₅₅H₈₆O₆: C 78.33, H 10.27 %; found: C 78.15, H 10.44 %.

MS [M]⁺: calculated 842.6424 amu; found 842.6405 amu.

11-Octyloxy-2,3,6,7,10-pentakishexyloxytriphenylene, 4-8

From 0.40 g (1.30 mmol) of **2-8**, 0.55 g (0.99 mmol) of **3** and 1.00 g FeCl₃, 140 mg (0.16 mmol, 16 %) of **4-8** was obtained by the same procedure as described for **4-2**.

¹H NMR: δ 7.83 (6H, s, ArH), 4.22 (12H, t, J = 6.49 Hz, OCH₂), 1.97-1.90 (12H, m, OCH₂CH₂), 1.56-1.36 (40H, m, CH₂), 0.93 (18H, bt, J = 6.77 Hz, CH₃).

¹³C NMR: δ 148.95 (2,3,6,7,10,11-ArC-O), 123.59 (ArC-C), 107.29 (ArC-H), 69.70 (OCH₂), 31.87-22.69 (CH₂), 14.10 (CH₃). Elem. anal: calculated for C₅₆H₈₈O₆: C 78.45, H 10.34 %; found C 77.70, H 10.41 %.

MS [M]⁺: calculated 856.6581 amu; found 856.6546 amu.

11-Nonyloxy-2,3,6,7,10-pentakishexyloxytriphenylene, 4-9

From 2.50 g (7.80 mmol) of **2-9**, 2.40 g (4.30 mmol) of **3** and 5.90 g FeCl₃, 0.50 g (0.57 mmol, 13 %) of **4-9** was obtained by the same procedure as described for **4-2**.

¹H NMR: δ 7.83 (6H, s, ArH), 4.22 (12H, t, J = 6.52 Hz, OCH₂), 2.00-1.86 (12H, m, OCH₂CH₂), 1.60-1.29 (42H, m, CH₂), 0.90 (18H, bt, J = 6.75 Hz, CH₃).

¹³C NMR: δ 148.95 (2,3,6,7,10,11-ArC-O), 123.59 (ArC-C), 107.29 (ArC-H), 69.70 (OCH₂), 31.94-22.69 (CH₂), 14.11 (CH₃). Elem. anal: calculated for C₅₇H₉₀O₆: C 78.57, H 10.41 %; found: C 79.38, H 10.90 %.

MS [M]⁺: calculated: 870.6737 amu; found 870.6730 amu.

2-Decyloxy-3,6,7,10,11-pentakishexyloxytriphenylene, 4-10

From 0.55 g (1.64 mmol) of **2-10**, 0.80 g (1.44 mmol) of **3** and 1.50 g FeCl₃, 150 mg (0.16 mmol, 11 %) of **4-10** was obtained by the same procedure as described for **4-2**.

Asymmetry in Hexaalkoxy Triphenylenes

¹H NMR: δ 7.83 (6H, s, ArH), 4.22 (12H, t, J = 6.49 Hz, OCH₂), 1.97-1.90 (12H, m, OCH₂CH₂), 1.56-1.27 (44H, m, CH₂), 0.97 (18H, t, J = 6.75 Hz, CH₃).

¹³C NMR: δ 148.95 (2,3,6,7,10,11-ArC-O), 123.60 (ArC-C), 107.30 (ArC-H), 69.70 (OCH₂), 31.94-22.69 (CH₂), 14.10 (CH₃).

MS [M]⁺: calculated for C₅₈H₉₂O₆: 884.6894 amu; found 884.6925 amu.

2,3,6,7,10-Pentakishexyloxy-11-undecyloxytriphenylene, 4-11

From 2.54 g (7.30 mmol) of **2-11**, 2.60 g (4.70 mmol) of **3** and 5.00 g FeCl₃, 1.30 g (1.44 mmol, 30 %) of **4-11** was obtained by the same procedure as described for **4-2**.

¹H NMR: δ 7.83 (6H, s, ArH), 4.22 (12H, t, J = 6.56 Hz, OCH₂), 2.00-1.86 (12H, m, OCH₂CH₂), 1.56-1.26 (46H, m, CH₂), 1.01-0.84 (18H, m, CH₃).

¹³C NMR: δ 148.93 (2,3,6,7,10,11-ArC-O), 123.58 (ArC-C), 107.27 (ArC-H), 69.69 (OCH₂), 31.95-22.69 (CH₂), 14.09 (CH₃). Elem. anal: calculated for C₅₉H₉₄O₆: C 78.79, H 10.53 %; found C 78.55, H 10.51 %.

MS [M]⁺: calculated 898.7050 amu; found 898.7040 amu.

2-Dodecyloxy-3,6,7,10,11-pentakishexyloxytriphenylene, 4-12

From 2.14 g (5.90 mmol) of **2-12**, 2.80 g (5.10 mmol) of **3** and 5.00 g FeCl₃, 0.90 g (0.98 mmol, 19 %) of **4-12** was obtained by the same procedure as described for **4-2**.

¹H NMR: δ 7.83 (6H, s, ArH), 4.23 (12H, t, J = 6.55 Hz, OCH₂), 1.97-1.86 (12H, m, OCH₂CH₂), 1.57-1.26 (48H, m, CH₂), 0.96-0.87 (18H, m, CH₃).

¹³C NMR: δ 148.95 (2,3,6,7,10,11-ArC-O), 123.60 (ArC-C), 107.29 (ArC-H), 69.70 (OCH₂), 31.95-22.70 (CH₂), 14.10 (CH₃).

MS [M]⁺: calculated for C₆₀H₉₆O₆: 912.7207 amu; found 912.7225 amu.

2,3,6,7,10-Pentakishexyloxy-11-tridecyloxytriphenylene, 4-13

From 5.10 g (13.6 mmol) of **2-13**, 6.40 g (11.6 mmol) of **3** and 10.6 g FeCl₃, 1.01 g (1.07 mmol, 9.3 %) of **4-13** was obtained by the same procedure as described for **4-2**.

¹H NMR: δ 7.83 (6H, s, ArH), 4.23 (12H, t, J = 6.51 Hz, OCH₂), 2.00-1.86 (12H, m, OCH₂CH₂), 1.60-1.25 (50H, m, CH₂), 0.96-0.83 (18H, m, CH₃).

¹³C NMR: δ 148.95 (2,3,6,7,10,11-ArC-O), 123.59 (ArC-C), 107.29 (ArC-H), 69.69 (OCH₂), 31.95-22.69 (CH₂), 14.09 (CH₃). Elem. anal: calculated for C₆₁H₉₈O₆: C 78.99, H 10.65 %; found C 79.07, H 10.86%.

MS [M]⁺: calculated 926.7363 amu; found 926.7366 amu.

2,3,6,7,10-Pentakishexyloxy-11-tetradecyloxytriphenylene, 4-14

From 0.33 g (0.85 mmol) of **2-14**, 0.47 g (0.85 mmol) of **3** and 0.90 g FeCl₃, 0.17 g (0.18 mmol, 21 %) of **4-14** was obtained by the same procedure as described for **4-2**.

¹H NMR: δ 7.83 (6H, s, ArH), 4.23 (12H, t, J = 6.5 Hz, OCH₂), 2.00-1.87 (12H, m, OCH₂CH₂), 1.57-1.25 (52H, m, CH₂), 0.96-0.84 (18H, m, CH₃).

¹³C NMR: δ 148.95 (2,3,6,7,10,11-ArC-O), 123.60 (ArC-C), 107.29 (ArC-H), 69.70 (OCH₂), 31.96-22.70 (CH₂), 14.10 (CH₃). Elem. anal: calculated for C₆₂H₁₀₀O₆: C 79.09, H 10.70 %; found C 78.96, H 11.03 %.

MS [M]⁺: calculated 940.7520 amu; found 940.7541 amu.

2-Hexadecyloxy-3,,6,7,10,11-pentakishexyloxytriphenylene, 4-16

From 0.70 g (1.70 mmol) of **2-16**, 0.80 g (1.44 mmol) of **3** and 1.50 g FeCl₃, 0.40 g (0.41 mmol, 28 %) of **4-16** was obtained by the same procedure as described for **4-2**.

¹H NMR: δ 7.83 (6H, s, ArH), 4.23 (12H, t, J = 6.45 Hz, OCH₂), 1.97-1.87 (12H, m, OCH₂CH₂), 1.57-1.25 (56H, m, CH₂), 0.96-0.87 (18H, m, CH₃).

¹³C NMR: δ 148.95 (2,3,6,7,10,11-ArC-O), 123.60 (ArC-C), 107.29 (ArC-H), 69.70 (OCH₂), 31.96-22.70 (CH₂), 14.10 (CH₃). Elem. anal: calculated for C₆₄H₁₀₄O₆: C 79.28, H 10.81 %; found C 79.59, H 11.15 %.

MS [M]⁺: calculated 968.7833 amu; found 968.7855 amu.

11-Octadecyloxy-2,3,6,7,10-pentakishexyloxytriphenylene, 4-18

From 0.53 g (1.20 mmol) of **2-18**, 0.22 g (0.41 mmol) of **3** and 1.00 g FeCl₃, 0.11 g (0.11 mmol, 28 %) of **4-18** was obtained by the same procedure as described for **4-2**.

¹H NMR: δ 7.83 (6H, s, ArH), 4.23 (12H, t, J = 6.50 Hz, OCH₂), 1.97-1.90 (12H, m, OCH₂CH₂), 1.57-1.25 (60H, m, CH₂), 0.96-0.87 (18H, m, CH₃).

¹³C NMR: δ 148.95 (2,3,6,7,10,11-ArC-O), 123.60 (ArC-C), 107.29 (ArC-H), 69.70 (OCH₂), 31.95-22.70 (CH₂), 14.16, 14.10 (CH₃).

MS [M]⁺: calculated for C₆₆H₁₀₈O₆: 996.8146 amu; found 996.8145 amu.

3.5 Acknowledgements

The authors would like to thank Mr. Barend van Lagen and Mr. Beb van Veldhuizen for help with the NMR measurements, Mr. Elbert van der Klift for the elemental analyses.

3.6 References

- ¹ (a) Chandrasekhar, S.; Sadashiva, B. K.; Suresh, K. A. *Pramana* **1977**, *9*, 471-480. (b) Chandrasekhar, S.; Sadashiva, B. K.; Suresh, K. A. *Mol. Cryst. Liq. Cryst.* **2003**, *397*, 595-605. (c) Chandrasekhar, S. *Liq. Cryst.* **1993**, *14*, 3-14. (d) Kumar, S. *Liq. Cryst.* **2004**, *31*, 1037-1059.
- ² (a) Gearba, R. I.; Lehmann, M.; Levin, J.; Ivanov, D. A.; Koch, M. H. J.; Barberá, J.; Debije, M. G.; Piris, J.; Geerts, Y. H. *Adv. Mater.* **2003**, *15*, 1614-1618. (b) Wan, W.; Monobe, H.; Sugino, T.; Tanaka, Y.; Shimizu, Y. *Mol. Cryst. Liq. Cryst.* **2001**, *364*, 597-603.
- ³ van de Craats, A. M. “*Charge Transport in Self-Assembling Discotic Liquid Crystalline Materials*”, *Ph.D. thesis*, **2000**, Chapter 3, 57-78, Delft University Press, The Netherlands.
- ⁴ Senthilkumar, K.; Grozema, F. C.; Bickelhaupt, F. M.; Siebbeles, L. D. A. *J. Chem. Phys.* **2003**, *119*, 9809-9817.
- ⁵ Mulder, F. M.; Stride, J.; Picken, S. J.; Kouwer, P. H. J.; de Haas, M. P.; Siebbeles, L. D. A.; Kearley, G. J. *J. Am. Chem. Soc.* **2003**, *125*, 3860-3866.
- ⁶ Nelson, J. *Science* **2001**, *293*, 1059-1060.
- ⁷ Boden, N.; Bushby, R. J.; Cammidge, A. N.; El-Mansoury, A.; Martin, P.S.; Lu, Z. *J. Mater. Chem.* **1999**, *9*, 1391-1402.
- ⁸ Allen, M. T.; Diele, S.; Harris, K. D. M.; Hegmann, T.; Kariuki, B. M.; Lose, D.; Preece, J. A.; Tschierske, C. *J. Mater. Chem.* **2001**, *11*, 302-311.
- ⁹ Kranig, W.; Hüser, B.; Spiess, H. W.; Kreuder, W.; Ringsdorf, R.; Zimmerman, H. *Adv. Mater.* **1990**, *2*, 36.
- ¹⁰ Bengs, H.; Closs, F.; Frey, T.; Funhoff, D.; Ringsdorf, H.; Siemensmeyer, K. *Liq. Cryst.* **1993**, *15*, 565-574.
- ¹¹ Allen, M. T.; Harris, K. D. M.; Kariuki, B. M.; Kumari, N.; Preece, J. A.; Diele, S.; Lose, D.; Hegmann, T.; Tschierske, C. *Liq. Cryst.* **2000**, *27*, 689-692.
- ¹² Wan, W.; Monobe, H.; Tanaka, Y.; Shimizu, Y. *Liq. Cryst.* **2003**, *30*, 571-578.
- ¹³ Kumar, S.; Manickam, M. *Chem. Commun.* **1997**, 1615-1616.

Chapter 4

A H-Bond Stabilized Hexagonal Plastic Columnar (Col_{hp}) Discotic Phase*

Abstract – *This chapter describes a 1,3,5-benzenetrisamide with three pendant hexaalkoxytriphenylene groups, which has been synthesized as an example of an interesting class of intermolecular H-bond-stabilized columnar discotic liquid crystalline materials. The material forms a plastic hexagonal discotic phase that does not crystallize on cooling from the isotropic phase, even after annealing for a few days at room temperature. X-ray and computational studies provide a detailed model for the organization of this material. The observed charge carrier mobility of $0.12 \text{ cm}^2 \text{ V}^{-1} \text{ s}^{-1}$ at $180 \text{ }^\circ\text{C}$, is the second highest ever reported for liquid crystalline triphenylene systems, and even increases with temperature. The factors responsible for this behavior are discussed.*

* This chapter is based on:

Paraschiv, I.; Giesbers, M.; van Lagen, B.; Grozema, F. C.; Abellon, R. D.; Siebbeles, L. D. A.; Marcelis, A. T. M.; Zuilhof, H.; Sudhölter, E. J. R. *Chem. Mater.* **2006**, 18, 968-974.

4.1 Introduction

Columnar discotic liquid crystals have received considerable interest as functional materials for applications as photovoltaic solar cells¹, light emitting diodes² and field effect transistors.³ The interest stems from the high charge carrier mobilities that have been obtained for some of these materials, even up to the level of amorphous silicon.⁴ Generally, the high charge carrier mobility is related to the property of discotic liquid crystals to self-organize into a columnar phase.⁵ An advantage of columnar discotic liquid crystals over inorganic materials is their ease of processing, the possibility of alignment by shear forces or electrical fields, and their capability of self-healing. The high charge carrier mobility of these materials stems from the organization in columns with concomitant π - π stacking of two adjacent aromatic systems, which yields significant splitting of the aromatic HOMO (LUMO) levels. When these aromatic systems approach each other closely, the HOMO (LUMO) splitting increases and a higher charge carrier mobility ensues. Another factor that is important for charge transfer is the rotational angle between two adjacent discotic molecules. For C_3 -symmetrical compounds, such as triphenylenes and hexaazatriphenylenes, the optimal rotational angles for high charge carrier transport are 0, 120, and 240°, i.e. orientations in which the side chains attached to such aromatic cores are also right on top of each other.⁶ Finally, the charge carrier mobility is increased if the π - π stacking is as large as possible^{5b}, i.e., slippage of molecules from the columns via a lateral displacement from the center of the column rapidly decreases the charge carrier mobility.

To obtain materials with improved charge carrier mobilities, stabilization of the columns is therefore desirable, as this will decrease the disk-disk distances and the lateral slippage.⁷ An elegant method to enhance the attractive interactions between the discotic mesogens is by introducing hydrogen bonding. Especially amide groups have been used by several groups to obtain stabilized columnar phases. Intermolecular H-bonding in discotic 1,3,5-trisamide derivatives was demonstrated some time ago.⁸ More recently, Meijer *et al.*⁹ prepared several 1,3,5-benzenetrisamides that form columnar discotic phases, but in these compounds there is often a competition between inter- and intramolecular hydrogen bonding. Furthermore, the aromatic groups that are connected to these benzenetrisamides become more or less part of the rigid cores since their motions are not decoupled from the central group by a flexible spacer. Nuckolls *et al.* investigated several discotic columnar materials based on 2,4,6-trialkoxy-1,3,5-benzenetrisamides with intermolecular hydrogen bonding along the columns.¹⁰ Modeling of the hydrogen bond interactions showed that the adjacent

benzenetrisamides are rotated almost 60° with respect to each other to give a helically stacked column. However, the benzene aromatic groups are not suitable for charge carrier transport. High charge carrier mobilities were obtained by Gearba *et al.* for an intermolecularly hydrogen-bond stabilized hexaazatriphenylene discotic.¹¹ Due to the 6-fold intermolecular hydrogen bonding motifs in these assemblies, the rotational angle between two adjacent discotics is fixed.

In the approach described in the present paper we investigate compound **1** (Figure 1) which forms an intermolecular benzenetrisamide hydrogen-bonding motif along a central column. The central core is connected via spacers to three triphenylene groups, which preferably organize in three outer π -stacked columns that are capable of charge carrier transport. In this way the triphenylene columns will be stabilized and the possibilities for slippage will be reduced. On the other hand, the motions of the triphenylene groups are decoupled from those of the central benzenetrisamide group through the presence of a flexible spacer and will therefore still have flexibility to optimize their $\pi - \pi$ interactions.

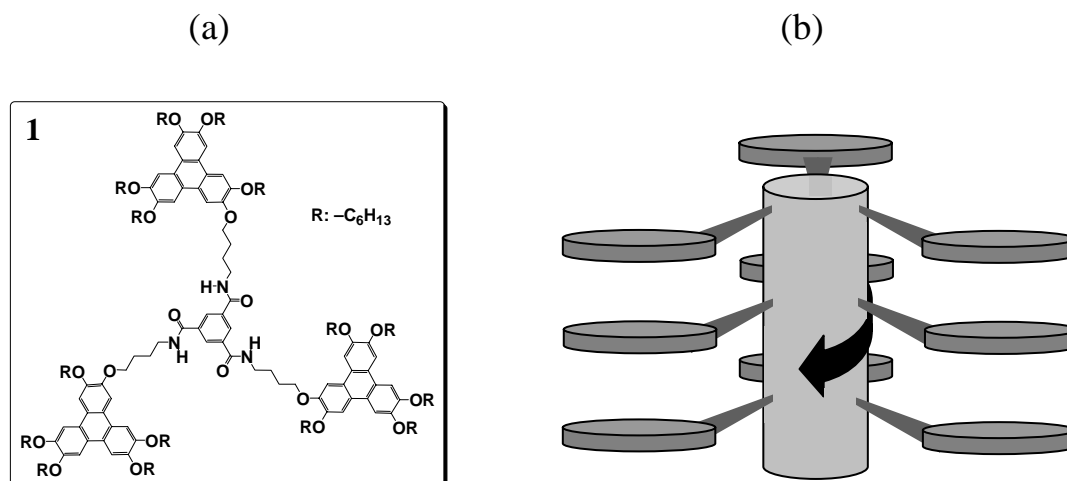
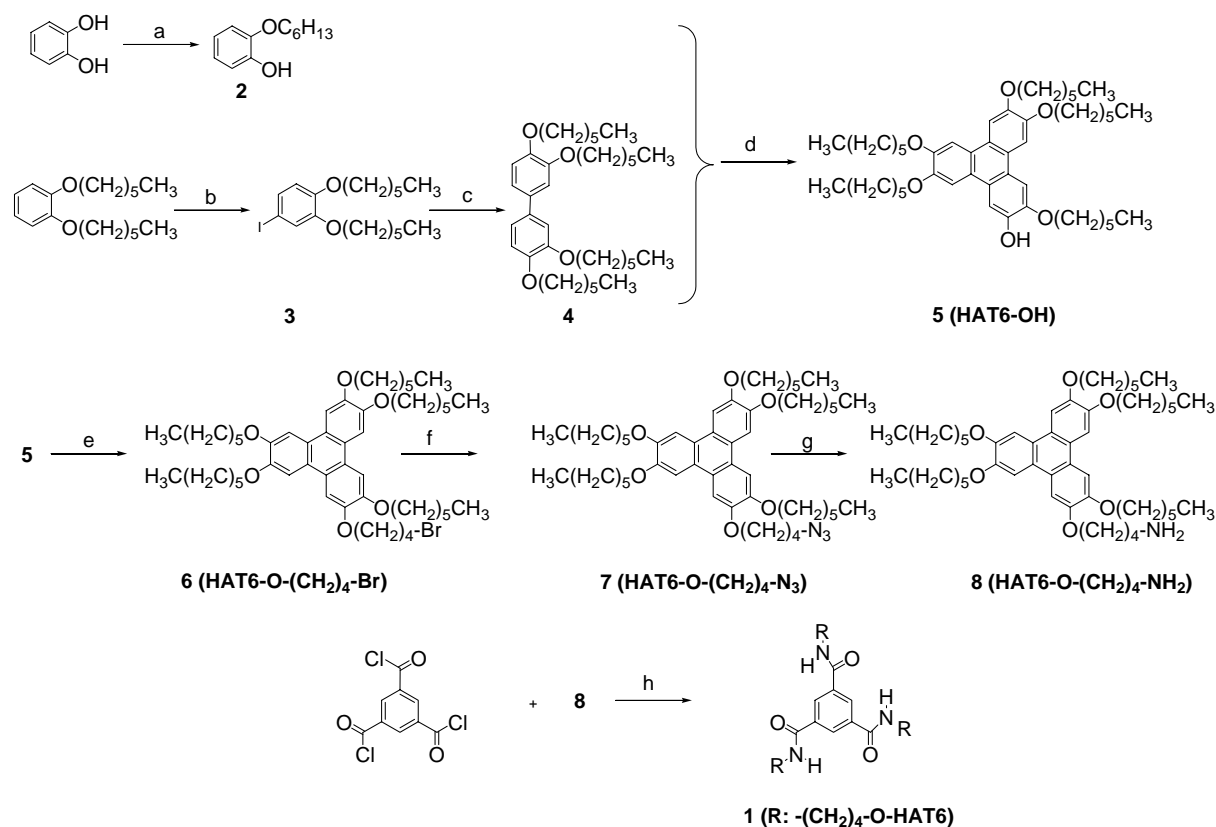


Figure 1. (a) Structure of C_3 -symmetrical trisamide derivative **1**. (b) Image showing the central trisamide hydrogen-bond stabilized column (light grey) surrounded by three triphenylene π -stacked columns (dark grey). The hydrogen bond helical network is indicated by the black arrow.

4.2 Results and Discussions

4.2.1 Synthesis

Compound **1** was synthesized from benzene-1,3,5-tricarboxylic acid trichloride and triphenylene **8** with five hexyloxy chains and one amine-terminated butyloxy chain. Synthetic details are given in Scheme 1.



Scheme 1. Synthetic route for the synthesis of **1**: (a) $\text{C}_6\text{H}_{13}\text{Br}$, 2-butanone, K_2CO_3 ; (b) I_2 , H_5IO_6 , CHCl_3 , CH_3COOH , H_2SO_4 , H_2O ; (c) Cu powder, heat; (d) FeCl_3 , CH_2Cl_2 ; methanol; (e) $\text{Br}(\text{CH}_2)_4\text{Br}$, K_2CO_3 , 2-butanone; (f); NaN_3 , ethanol; (g) LiAlH_4 , THF; NaOH , H_2O , $\text{Na}_2\text{SO}_4 \cdot 10\text{H}_2\text{O}$; (h) $\text{N}(\text{CH}_2\text{CH}_3)_3$, CH_2Cl_2 , room temperature.

4.2.2 Characterization

Trisamide **1** displays only one liquid crystalline phase, with an isotropization temperature of 208 °C. Upon cooling to room temperature, no crystallization occurs and the sample can be kept at room temperature for weeks without crystallization.

Optical polarization microscopy shows broad ribbon-like textures with alternating bright and dark domains upon cooling from the isotropic state (Figure 2). DSC (Figure 3) confirmed the reversibility of the isotropization transition with a ΔH of isotropization of 88 kJ mol^{-1} , and here also no transitions at lower temperatures were found.

XRD measurements of compound **1** (Figure 4) at 182 °C indicate a highly ordered hexagonal columnar phase. Of specific interest are the two peaks at 3.54 and 3.62 Å.

Together with the lower angle reflections these point to a liquid crystalline phase that is characterized by diminished movements of the discotic units within the stack, a so-called plastic columnar discotic hexagonal phase (Col_{hp})¹² or sometimes called hexagonal plastic crystal.¹³



Figure 2. Polarized optical microphotograph of **1** at 196 °C (See the Appendix at the end of the thesis for the color picture).

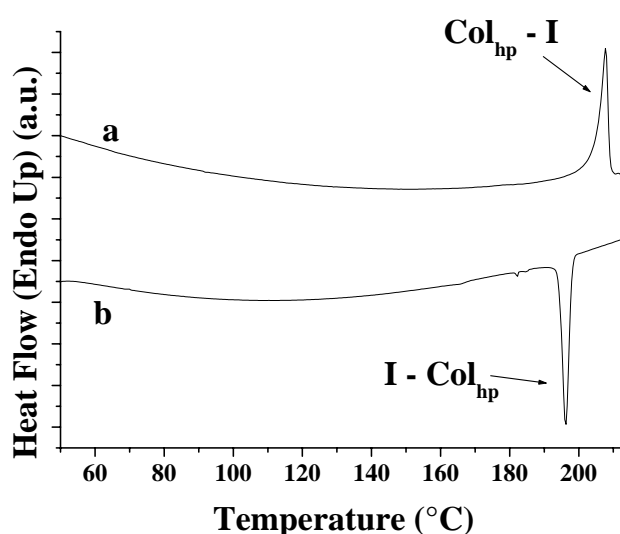


Figure 3. DSC thermograms of compound **1**, showing (a) the second heating and (b) the second cooling run; rate 10 °C min⁻¹.

The peaks in the X-ray diagram can be indexed using lattice parameters of 18.63 Å and 7.23 Å. For the HAT columns this leads to an intercolumn distance of 21.5 Å and an interdisk distance of 3.62 Å.

The liquid crystalline order is preserved upon cooling to room temperature as seen from temperature-dependent X-ray measurements. Upon cooling the lattice parameters decrease slightly to 18.33 and 6.96 Å, respectively, at 25 °C. The broad reflection at about $2\theta = 2.5^\circ$ (~ 35 Å) points towards a *superstructural ordering* (*vide infra*) of the liquid crystalline phase.¹⁴

In order to investigate the hydrogen bonding, compound **1** was studied by FT-IR. The IR spectrum of a dilute CCl₄ solution of **1** shows the $\nu(\text{N-H})$ stretching vibration band at 3404 cm⁻¹, together with the $\nu(\text{C=O})$ (amide I) stretching band at 1666 cm⁻¹.

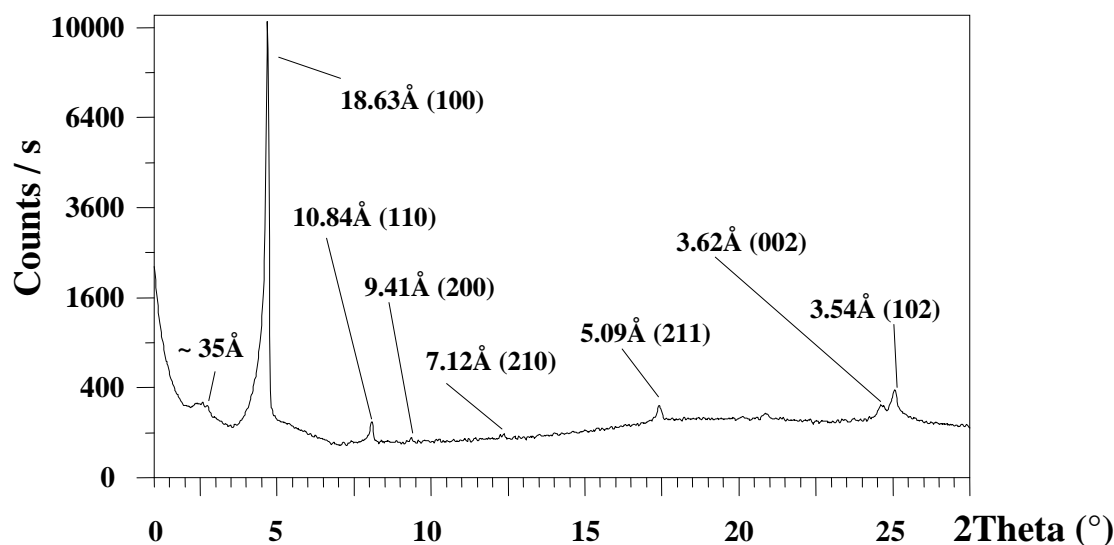


Figure 4. X-ray pattern of compound **1** at 182 °C.

These values indicate that there is no inter- or intramolecular H-bonding in CCl_4 solution and these values also agree with those reported for other 1,3,5-trisamides.¹⁵ In case of intermolecular H-bonding these values would have been shifted.¹⁶

We determined the positions of these three IR-bands of compound **1** without solvent (in KBr) as a function of temperature (Figure 5).

A very clear change can be seen at the transition from the isotropic to the Col_{hp} phase: upon cooling from 220 °C to room temperature $\nu(\text{N-H})$ band shifts about 107 cm^{-1} to lower wavenumbers. A shift of 40 cm^{-1} was observed for the $\nu(\text{C=O})$ stretching vibration signal (amide I), from 1674 cm^{-1} in the isotropic phase to 1634 cm^{-1} at room temperature, with a sharp change at the isotropization temperature. These changes at the isotropization transition indicate that intermolecular hydrogen bonding does exist in the columnar phase.

To investigate both the hydrogen bonding and the ordering in the columnar phase, complementary molecular modeling studies were done.

Quantum chemical B3LYP/6-311++G(d,p)//B3LYP/6-311G(d,p) computations¹⁷ were performed on two π -stacked benzene trisamides, which represent the central benzenetrisamide core of π -stacked **1** (Figure 6).

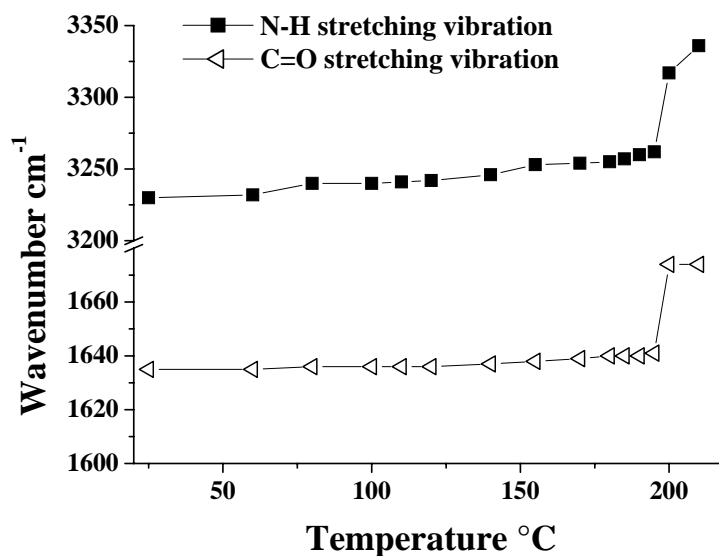


Figure 5. The variation of the $\nu(\text{N-H})$ and $\nu(\text{C=O})$ stretching (amide I) vibrations of trisamide **1** as a function of temperature, upon cooling from the isotropic state.

Figure 6a clearly shows that interdisk H-bonding is feasible. In the optimized structure of the dimer, the distance between the π - π stacked benzene cores is calculated to be 3.69 Å, in good agreement with the experimental X-ray result of 3.62 Å, and in line with values usually found for π - π distances in triphenylene discotics.^{6,7} The combination of π - π stacking and H-bonding effects a helix-like rotation over precisely 60° of the two stacked benzene cores (see Figure 6b), with a tilt angle of 45° for the H-bond with the plane of the benzene trisamide core, as has also been found for other H-bonding molecules with 3-fold symmetry.^{9, 10} This π - π stacking distance fits in almost perfectly with the interdisk N-H \cdots O hydrogen bonds, which are optimized at $r(\text{N-O}) = 3.04$ Å, a near-optimum length for such an H-bond.¹⁸ These results are comparable with those reported by Nuckolls for a 2,4,6-trialkoxy-1,3,5-benzenetrisamide, which displays 3.8 Å for the stacking distance between the benzene cores and 2.8 Å for the $r(\text{N-O})$ distance; also in that case, the amides twist out of the aromatic plane by ca. 45°.¹⁰

Although the orientation of the spacers of two successive trisamides is twisted by 60°, this core orientation still allows for a large overlap of triphenylene moieties that are attached via a flexible spacer, as can be seen from the optimized mono-triphenylene substituted benzene trisamide model in Figure 7. This means that the hydrogen-bond stabilization of the trisamide cores is not hampering a discotic ordering of the triphenylene moieties.

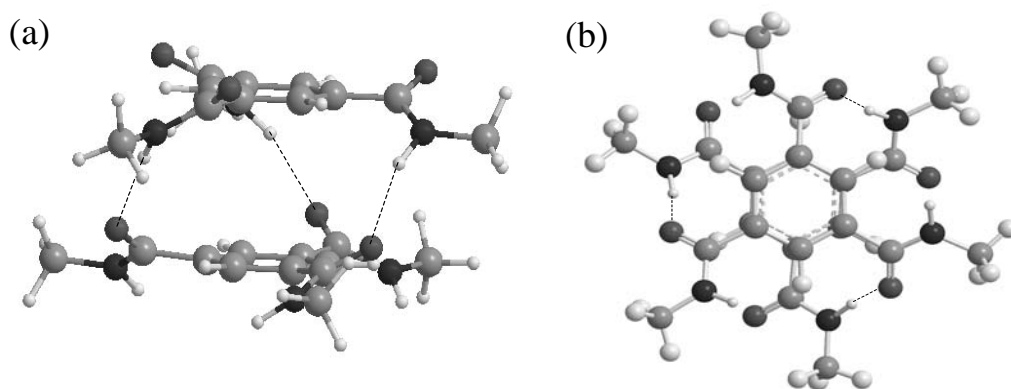


Figure 6. Molecular modeling representation of two π -stacked trimethyl 1,3,5-benzenetrisamide molecules: (a) side view and (b) top view.

Combining the results from X-ray and modeling provides a model for the ordering of the molecules in the liquid crystalline phase. A strong hydrogen bond interaction leads to helix-like columns of benzenetrisamides in which the cores of successive molecules are rotated by 60° . The triphenylene columns are located on a hexagonal grid (Figure 8a), as deduced from the X-ray diffractograms. The space between the triphenylene columns is filled with either alkyl groups or the central benzenetrisamide columns. The presence of these latter columns gives rise to a superstructure, which is observed via the presence of a peak at 35 \AA in the X-ray diffractogram. The attached triphenylenes can stack on top of each other by a small conformational adaptation of the flexible spacer. In this way, three columns of triphenylenes surround the central benzenetrisamide core (Figure 8b). In the model compound in Figure 7, the distance from the center of the benzenetrisamide to the center of the triphenylene group is about 11.8 \AA . This distance can also be deduced from the model based on the X-ray data (Figure 8a), and this distance (12.4 \AA) agrees well with the computational result. When two molecules stack on top of each other, the spacers have to adopt a curved conformation in order to allow for the $\pi - \pi$ stacking of the triphenylene groups. Since the benzenetrisamide cores are twisted about 60° with respect to one another, the bending of the spacers has to be to the left and to the right for successive molecules in the stack. This is represented schematically in Figure 8b.

Molecular modeling (Figures 6 and 7) quantifies the stabilization of the interdisk H-bond formation to be $10.2 \text{ kcal mol}^{-1}$. Each of these H-bonds is slightly weaker than normal ($4\text{-}7 \text{ kcal mol}^{-1}$)^{18,19} as result of the compromise between optimal $\pi - \pi$ stacking of the benzene cores and optimal H-bonds. However, the combination of these three H-bonds yields a significant strengthening of the total stacking interactions. This can be seen by comparing the

isotropization temperature and ΔH of compound **1** with those of corresponding triesters without H-bonds.²⁰

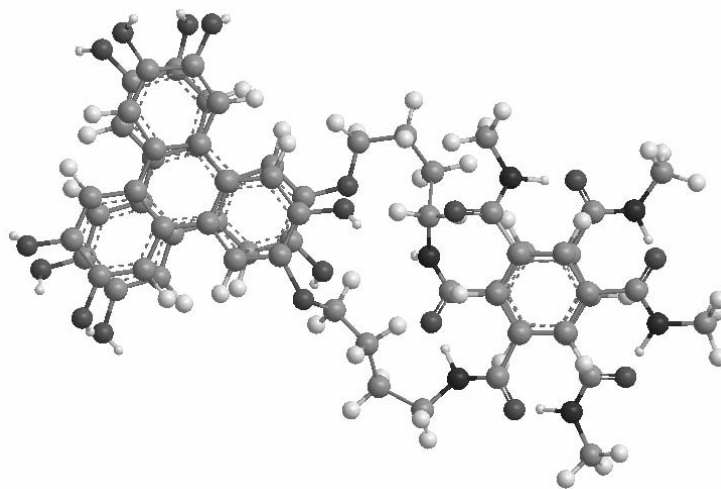


Figure 7. Stack of two dimethyl 1,3,5-benzenetrisamide molecules with one triphenylene-containing sidearm.

The isotropization temperature of **1** is much higher than that of a corresponding benzene triester with propyloxy spacers and pentyloxy tails of the triphenylene has an isotropization temperature of 129 °C.^{20a} For this latter compound a ΔH of isotropization was found of about 19.5 kJ mol⁻¹. We find a ΔH of isotropization of about 88 kJ mol⁻¹.

This high value is to be expected, as the stabilization by hydrogen bonding alone is already calculated to be 45 kJ mol⁻¹ (10.2 kcal mol⁻¹).

To investigate the potential of the additional stabilization by the H-bonds on the charge carrier mobility, pulse-radiolysis time-resolved microwave conductivity (PR-TRMC) measurements of **1** were performed.²¹ In this technique, pulse radiolysis yields charge carriers, and from the time-resolved microwave conductivity, the mobility and life-time of these charge carriers can be derived.

Long-lived conductivity signals were observed with a half-life time of ~100 ns (Figure 9a), which is much longer than the half-life time observed for (crystalline) **HAT6**.²¹ The decay kinetics were not found to change with variations in the radiation dose, indicating a clean, first-order decay process.

The charge carrier mobility of **1** at room temperature is 0.06 cm² V⁻¹ s⁻¹ (Figure 9b), which is already 5 times higher than previously observed for (crystalline) **HAT6**.^{22a} The increase can be attributed to two factors:

(a) The additional H-bonds diminish the movements of disks in the stack of molecules, i.e., they restrict rotations of a molecule in the π -stack, and also provide a much higher activation

energy barrier for molecules to slide out of a column. As a result, fewer or shorter-lived defects are present in such a π -stack, which leads to a higher charge mobility.

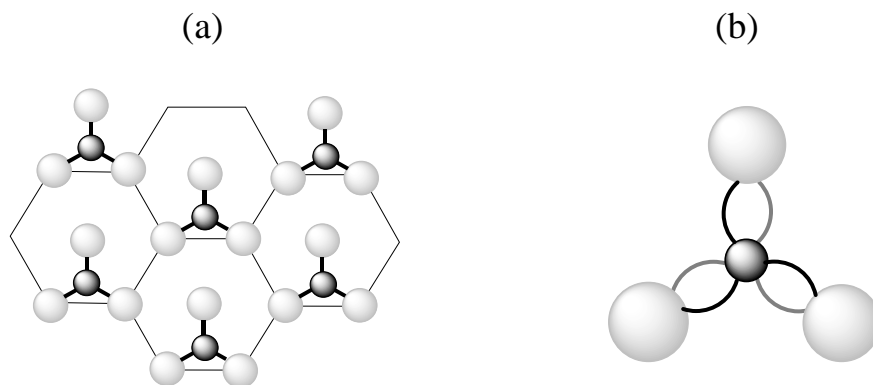


Figure 8. (a) Model for the liquid crystalline ordering of **1**, with the cores of the HAT moieties (light grey) on a hexagonal grid and the superstructure determined by the trisamide cores (dark grey). (b) Schematic top view of two stacked molecules showing that the spacers of two π -stacked molecules (black and grey) have to bend successively left and right to allow the formation of the triphenylene columns. In reality, the HAT disks are much larger than depicted due to the presence of the alkoxy tails.

(b) As Figure 7 reveals, the triphenylene moieties can stack with only a small rotation between adjacent triphenylenes: when the central cores are rotated 60° with respect to each other, then the triphenylene moieties are rotated as little as 15° . It has been reported⁶ that the charge-transfer integral displays a periodicity of 120° , with maxima at $0, 120,$ and 240° , and minima at $60, 180,$ and 300° . The value obtained by modeling (Figure 7) is close to 15° , which yields a value of the charge-transfer integral that is $\sim 85\%$ of the maximally obtainable value. The rotation angle between successive triphenylene moieties in the triphenylene stacks (15°) is considerably smaller than that in the parent compound (**HAT6**), where the rotation angle is close to 45° . From electronic structure calculations it was found that the charge transfer integral increases by roughly a factor of 2 when decreasing the rotation angle from 45 to 15° .^{6b} This implies an increase of the charge carrier mobility by a factor of 4, close to the factor of 5 difference in mobility found experimentally.

From Figure 9b it can be seen that the charge carrier mobility increases considerably with increasing temperature, up to $0.12 \text{ cm}^2 \text{ V}^{-1} \text{ s}^{-1}$ at 180°C (the instrumental limit). A similar increase in charge carrier mobility with temperature was found in the case of a hydrogen-bond enforced hexaazatriphenylene columnar discotic.¹¹ Even so, the intracolumnar mobility of the charge carriers in that case reaches only an absolute value of $0.08 \text{ cm}^2 \text{ V}^{-1} \text{ s}^{-1}$ at 200°C .¹¹ In

the current study, the charge carrier mobility of $0.12 \text{ cm}^2 \text{ V}^{-1} \text{ s}^{-1}$ is the second highest ever reported value for any liquid crystalline triphenylene system, even higher than that observed for the helical liquid crystalline phase of the sulfur analogue 2,3,6,7,10,11-hexakis(hexylthio)triphenylene (HHTT), $0.087 \text{ cm}^2 \text{ V}^{-1} \text{ s}^{-1}$.^{22b}

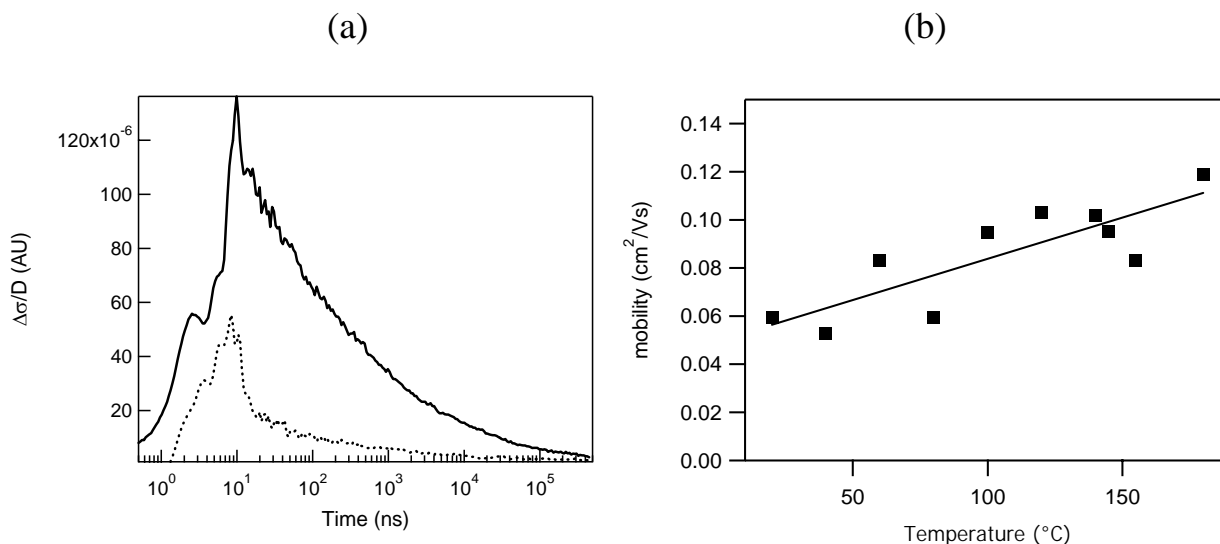


Figure 9. (a) TRMC decay kinetics of **1** (full line; 60 °C) and crystalline **HAT6** (dashed line; RT). (b) Charge carrier mobility of **1** as a function of temperature.

We tentatively attribute this remarkable increase with temperature to increased conformational mobility of the butyl linker between the central benzene core and the triphenylene moieties. At higher temperatures the thermal energy can more easily provide the means to overcome conformational barriers of this chain, to the effect that the triphenylene moieties can overlap better, leading to an increased charge carrier mobility. Research to investigate this hypothesis via the study of S-for-O substitution and via variation of the spacer length are recommended (see also Chapter 5), with the aim to even further increase the charge carrier mobility in the columnar liquid crystalline phase.

4.3 Conclusions

The columnar organization of triphenylene moieties has been successfully stabilized by intermolecular H-bonding, without losing the ease of processing provided by a liquid crystalline phase. The resulting, highly ordered liquid crystalline material, with a so-called plastic columnar discotic hexagonal phase (Col_{hp}), yields the second highest charge carrier

mobility measured for *any* liquid crystalline triphenylene derivative. In addition, elucidation of the factors behind this (minimization of columnar defects and optimization of the relative orientation of π -stacked triphenylene moieties) provides a route towards finding even higher charge mobilities for these and related π -systems.

4.4 Experimental

4.4.1 Measurements

$^1\text{H-NMR}$ (200 MHz and 400 MHz) and $^{13}\text{C-NMR}$ (50 MHz and 100 MHz) spectra were obtained with a Bruker spectrometer, using CDCl_3 as a solvent. Melting points, thermal phase transition temperatures and optical investigation of the liquid crystalline phases were determined on samples between ordinary glass slides using an Olympus BH-2 polarization microscope equipped with a Mettler FP82HT hot stage, which was controlled by a Mettler FP80HT central processor.

Differential scanning calorimetry (DSC) thermograms were obtained on a Perkin Elmer DSC-7 system using 2-5 mg samples in 30 μl sample pans and a scan rate of 10 $^\circ\text{C min}^{-1}$. ΔH is calculated in kJ mol^{-1} .

Temperature dependent X-ray curves were measured on a Philips X'pert Pro MRD machine equipped with an Anton Paar camera for temperature control. For the measurements in the small angle region, the sample was spread in the isotropic or the liquid crystalline phase on a thin glass slide (about 15 μm thick), which was placed on a temperature regulated flat copper sample stage. This sample preparation sometimes caused very high intensities of X-ray reflections ($> 500 \text{ kc s}^{-1}$) because of partial or complete orientation of the molecules in the liquid crystalline state.

The accurate masses were obtained using a Finnigan MAT 95 mass spectrometer operating in the 70 eV EI mode at a resolution 5500. The matrix-assisted laser desorption/ionization time-of-flight mass spectrometer (Maldi-Tof MS) mass spectra was obtained on an Ultraflex spectrometer using 2,5-dihydroxybenzoic acid (DHB; Sigma-Aldrich) as a matrix.

Infrared spectra (FTIR) were obtained using a Bruker Vector 22 spectrometer. The sample was cast from CH_2Cl_2 solution onto a KBr window. After evaporation of the solvent the KBr pellet was heated at 220 $^\circ\text{C}$, almost 10 $^\circ\text{C}$ above the isotropisation temperature. The spectra were recorded as a function of decreasing temperature.

4.4.2 Synthesis

All solvents were PA quality. All reactions were carried out under a nitrogen or argon atmosphere, if required. Dry CH₂Cl₂ was freshly distilled from CaH₂. All starting materials were obtained from Sigma-Aldrich and used as received. The synthetic route of the compounds is shown in Scheme 1. Compounds **2** - **4** were synthesized as reported before in Chapter 2 and Chapter 3²³ of this thesis. Compound **5** was obtained by an oxidative coupling reaction with anhydrous FeCl₃.²⁴

2-(4-Bromobutoxy)-3,6,7,10,11-pentakishexyloxytriphenylene, 6

A mixture of 3.00 g (4.03 mmol) of 2-hydroxy-3,6,7,10,11-pentakishexyloxytriphenylene **5** and 8.00 g of 1,4-dibromobutane (37.0 mmol) was refluxed in 2-butanone, under nitrogen, for 14 h in the presence of 2.00 g of K₂CO₃ as base. After filtration of the salts and removal of the solvent, recrystallization of the residue from acetonitrile gave 3.06 g (3.43 mmol; 86 %) of **6** as colorless crystals. Cr - 62 °C - Col_h - 84 °C - I.

¹H-NMR : δ 7.86-7.85 (6H, s, ArH), 4.27 (12H, t, J = 6,40 Hz, CH₂O), 3.75 (2H, t, J = 6.00 Hz, CH₂Br), 2.13-1.27 (44H, m, CH₂), 0.91 (15H, t, J = 6.80 Hz, CH₃).

¹³C-NMR : δ 149.48-148.96 (ArC-O), 124.27-123.88 (ArC-C), 107.92-107.33 (ArC-H), 70.17-69.27 (OCH₂), 45.33 (CH₂Br), 34.12-23.07 (CH₂), 14.47 (CH₃).

MS [M]⁺: calculated for C₅₂H₇₉BrO₆: 878.5060 amu; found: 878.5060 amu.

2-(4-Azidobutoxy)-3,6,7,10,11-pentakishexyloxytriphenylene, 7

A solution of 2.12 g (2.41 mmol) of **6** and 1.56 g (24.0 mmol) of NaN₃ in ethanol was refluxed for 20 h. After the reaction was complete the solvent was evaporated. After addition of 20 ml of water the reaction mixture was extracted with 2 x 20 ml of CH₂Cl₂; the organic layer was dried on anhydrous Na₂SO₄ and the solvent was evaporated under vacuum. After recrystallization from ethanol, 1.97 g (2.34 mmol; 98 %) of compound **7** was obtained as colorless crystals. Cr - 60 °C - Col_h - 83 °C - I.

¹H-NMR : δ 7.83 (6H, s, ArH), 4.25 (12H, t, J = 6.62 Hz, CH₂O), 3.45 (2H, t, J = 6.65 Hz, CH₂N₃), 1.98-1.25 (44H, m, CH₂), 0.90-0.85 (15H, m, CH₃).

¹³C-NMR : δ 149.02-148.54 (ArC-O), 123.87-123.54 (ArC-C), 107.26-106.89 (ArC-H), 69.71-69.02 (OCH₂), 51.31 (CH₂N₃), 31.71-22.69 (CH₂), 14.09 (CH₃).

MS [M]⁺: calculated for C₅₂H₇₉N₃O₆: 841.5969 amu; found: 841.5973 amu.

A Hexagonal Plastic Columnar Discotic Phase

N,N',N''-Tris(2-butyloxy-3,6,7,10,11-pentakishexyloxytriphenylene)benzene-1,3,5-tricarboxamide, 1

To a stirred solution of compound **7** (1.97 g; 2.34 mmol), dissolved in 20 ml of dry tetrahydrofuran, was added 0.97 g (25.5 mmol) of LiAlH₄. The reaction mixture was stirred under an argon atmosphere for 4 h. The excess of LiAlH₄ was destroyed by addition of Na₂SO₄ · 10H₂O and 1 ml of 0.1 M NaOH in water. After filtration of the salts and evaporation of the solvent, 1.68 g (2.06 mmol; 88 %) of amine-terminated **8** was obtained as highly viscous yellow oil, which slowly crystallized at room temperature. **MS** [M]⁺: calculated for C₅₂H₈₁NO₆: 815.6064 amu; found: 815.6060 amu.

Crude amine-terminated triphenylene **8** (0.83 g; 1.02 mmol) was dissolved in 10 ml of dry CH₂Cl₂. To this solution was first added 2.30 ml of a CH₂Cl₂ solution containing 90.0 mg (0.34 mmol) of 1,3,5-benzenetricarboxylic acid trichloride and then 0.50 g of triethylamine. After 24 h the solvent was evaporated under reduced pressure and the crude compound was purified by column chromatography using silica gel eluting with CH₂Cl₂ : MeOH (gradual increase from 0 to 4% MeOH). The obtained material was subsequently precipitated from an acetonitrile / acetone mixture and from an isopropyl ether / acetonitrile (1:4) mixture. After filtration 0.51 g (0.19 mmol; 58 %) of compound **1** was obtained.

¹H-NMR (400 MHz): δ 8.47 (3H, s, Ar-H benzene), 7.92-7.65 (12H, m, ArC-H triphenylene), 7.57-7.54 (6H, m, ArC-H triphenylene), 7.10 (3H, bt, J = 5.20 Hz, NH), 4.41-4.00 (36H, m, OCH₂), 3.59-3.57 (6H, q, J = 6.00 Hz, CH₂NH), 1.96-1.27 (132H, m, CH₂), 0.97-0.87 (45H, m, CH₃).

¹³C-NMR (100 MHz): δ 166.08 (C=O), 149.50-148.52 (ArC-O triphenylene), 135.95 (ArC-C=O benzene), 128.60 (ArC-H benzene), 124.13-123.74 (ArC-C triphenylene), 107.77-106.59 (ArC-H triphenylene), 70.19-69.42 (OCH₂), 40.04 (CH₂NH), 32.14-23.00 (CH₂), 14.48, 14.43 (CH₃).

¹H-¹H COSY and **HETCOR NMR** measurements also confirm the structure of compound **1**.

FT-IR (KBr, RT) ν_{max} (cm⁻¹): 3246 (N-H stretching), 2931, 2858 (CH₂ stretching), 1643 (C=O, amide I band), 1518, 1468, 1437 (C-H bending, alkyl tails), 1391, 1262, 1170, 1044, 828 (1,3,5-trisubstituted benzene).

MS - MALDI-ToF: calculated for C₁₆₅H₂₄₃N₃O₂₁: 2602.80 amu, found [M+H]⁺ 2603.56 amu.

4.5 Acknowledgments

The author thank to Dr. M. A. Posthumus for the exact mass determinations and Mr. Edwin Bakx from the Food Chemistry Laboratory (WUR) for help with the Maldi-ToF measurements.

4.6 References

- ¹ (a) Nelson, J. *Science* **2001**, *293*, 1059-1060. (b) Schmidt-Mende, L.; Fechtenkötter, A.; Müllen, K.; Moons, E.; Friend, R. H.; MacKenzie, J. D. *Science* **2001**, *293*, 1119-1122. (c) Schmidt-Mende, L.; Watson, M.; Müllen, K.; Friend, R. H. *Mol. Cryst. Liq. Cryst.* **2003**, *396*, 73-90. (d) Haßheider, T.; Benning, S. A.; Lauhof, M. W.; Kitzerow, H. S.; Bock, H.; Watson, M. D.; Müllen, K. *Mol. Cryst. Liq. Cryst.* **2004**, *413*, 461-472. (e) Oukachmih, M.; Destruel, P.; Seguy, I.; Ablart, G.; Jolinat, P.; Archambeau, S.; Mabiala, M.; Fouet, S.; Bock, H. *Sol. Energ. Mat. Sol. C.* **2005**, *85*, 535-543.
- ² (a) Freudenmann, R.; Behnisch, B.; Hanack, M. *J. Mater. Chem.* **2001**, *11*, 1618-1624. (b) Bayer, A.; Zimmermann, S.; Wendorff, J. H. *Molec. Cryst. Liq. Cryst.* **2003**, *396*, 1-22.
- ³ (a) van de Craats, A. M.; Stutzmann, N.; Bunk, O.; Nielsen, M. M.; Watson, M.; Müllen, K.; Chanzy, H. D.; Sirringhaus, H.; Friend, R. H. *Adv. Mater.* **2003**, *15*, 495-499. (b) Katsuhara, M.; Aoyagi, I.; Nakajima, H.; Mori, T.; Kambayashi, T.; Ofuji, M.; Takanishi, Y.; Ishikawa, K.; Takezoe, H.; Hosono, H. *Synth. Met.* **2005**, *149*, 219-223.
- ⁴ van de Craats, A. M.; Warman, J. M.; Fechtenkötter A.; Brand, J. D.; Harbison, M. A.; Müllen, K. *Adv. Mater.* **1999**, *11*, 1469-1472.
- ⁵ (a) Struijk, C. W.; Sieval, A. B.; Dakhorst, J. E. J.; Kimkes, P.; Koehorst, R. B. M.; Donker, H.; Schaafsma, T. J.; Picken, S. J.; van de Craats, A. M.; Warman, J. M.; Zuilhof, H.; Sudhölter, E. J. R. *J. Am. Chem. Soc.* **2000**, *122*, 11057-11066. (b) Grimsdale, A. C.; Müllen, K. *Angew. Chem. Int. Ed.* **2005**, *44*, 5592-5629.
- ⁶ (a) Cornil, J.; Lemaur, V.; Calbert, J.-P.; Brédas, J.-L. *Adv. Mater.* **2002**, *14*, 726-729. (b) Senthilkumar K.; Grozema F. C.; Bickelhaupt F. M.; Siebbeles L. D. A. *J. Chem. Phys.* **2003**, *119*, 9809-9817.
- ⁷ (a) Fontes, E.; Heiney, P. A.; de Jeu, W. H. *Phys. Rev. Lett.* **1988**, *61*, 1202-1205. (b) Adam, D.; Schuhmacher, P.; Simmerer, J.; Häußling, L.; Siemensmeyer, K.; Eitzbach, K. H.; Ringsdorf, H.; Haarer, D. *Nature* **1994**, *371*, 141-143.

- ⁸ Matsunaga, Y.; Miyajima, N.; Nakayasu, Y.; Sakai, S.; Yonenaga, M. *Bull. Chem. Soc. Jpn.* **1988**, *61*, 207-210.
- ⁹ (a) Brunsveld, L.; Schenning, A. P. H. J.; Broeren, M. A. C.; Janssen, H. M.; Vekemans, J. A. J. M.; Meijer, E. W. *Chem. Lett.* **2000**, *29*, 292-293. (b) van Gorp, J. J.; Vekemans, J. A. J. M.; Meijer, E. W. *J. Am. Chem. Soc.* **2002**, *124*, 14759-14769. (c) van Gestel, J.; Palmans, A. R. A.; Titulaer, B.; Vekemans, J. A. J. M.; Meijer, E. W. *J. Am. Chem. Soc.* **2005**, *127*, 5490-5494.
- ¹⁰ (a) Bushey, M. L.; Hwang, A.; Stephens, P. W.; Nuckolls, C. *J. Am. Chem. Soc.* **2001**, *123*, 8157-8158. (b) Bushey, M. L.; Hwang, A.; Stephens, P. W.; Nuckolls, C. *Angew. Chem. Int. Ed.* **2002**, *41*, 2828-2831.
- ¹¹ Gearba, R. I.; Lehmann, M.; Levin, J.; Ivanov, Dimitri A.; Koch, M. H. J.; Barberá, J.; Debije, Michael G.; Piris, J.; Geerts, Y. H. *Adv. Mater.* **2003**, *15*, 1614-1618.
- ¹² (a) Krishna Prasad, S.; Shankar Rao, D. S.; Chandrasekhar, S.; Kumar, S. *Mol. Cryst. Liq. Cryst.* **2003**, *396*, 121-139. (b) Glösen, B.; Heitz, W.; Kettner, A.; Wendorff, J. H. *Liq. Cryst.* **1996**, *20*, 627-633.
- ¹³ Simmerer, J.; Glösen, B.; Paulus, W.; Kettner, A.; Schuhmacher, P.; Adam, D.; Etzbach, K.-H.; Siemensmeyer, K.; Wendorff, J. H.; Ringsdorf, H.; Haarer, D. *Adv. Mater.* **1996**, *8*, 815-819.
- ¹⁴ Kettner, A.; Wendorff, J. H. *Liq. Cryst.* **1999**, *26*, 483-487.
- ¹⁵ (a) Yasuda, Y.; Iishi, E.; Inada, H.; Shirota, Y. *Chem. Lett.* **1996**, 575-576. (b) Fan, E.; Yang, J.; Geib, S. J.; Stoner, T. C.; Hopkins, M. D.; Hamilton, A. D. *J. Chem. Soc., Chem. Commun.* **1995**, 1251-1252. (c) Lightfoot, M. P.; Mair, F. S.; Pritchard, R. G.; Warren, J. E. *Chem. Commun.* **1999**, 1945-1946. (d) Hanabusa, K.; Kawakami, A.; Kimura, M.; Shirai, H. *Chem. Lett.* **1997**, *28*, 191-192. (e) Hanabusa, K.; Koto, C.; Kimura, M.; Shirai, H.; Kakehi, A. *Chem. Lett.* **1997**, *26*, 429-430. (f) Camerel, F.; Faul, C. F. J. *Chem. Commun.* **2003**, 1958-1959.
- ¹⁶ (a) Xue, C.; Jin, S.; Weng, X.; Ge, J. J.; Shen, Z.; Shen, H.; Graham, M. J.; Jeong, K.-U.; Huang, H.; Zhang, D.; Guo, M.; Harris, F. W.; Cheng, S. Z. D.; Li, C. Y.; Zhu, L. *Chem. Mater.* **2004**, *16*, 1014-1025. (b) Xue, C.; Ilhan, F.; Jin, S.; Cheng, S. Z. D.; Meador, M. A.; Eby, R. K. *Polym. Prep.* **2004**, 820-821.
- ¹⁷ (a) Gaussian 03, Revision C.02, Frisch, M. J.; Trucks, G. W.; Schlegel, H. B.; Scuseria, G. E.; Robb, M. A.; Cheeseman, J. R.; Montgomery, Jr., J. A.; Vreven, T.; Kudin, K. N.; Burant, J. C.; Millam, J. M.; Iyengar, S. S.; Tomasi, J.; Barone, V.; Mennucci, B.; Cossi, M.;

Scalmani, G.; Rega, N.; Petersson, G. A.; Nakatsuji, H.; Hada, M.; Ehara, M.; Toyota, K.; Fukuda, R.; Hasegawa, J.; Ishida, M.; Nakajima, T.; Honda, Y.; Kitao, O.; Nakai, H.; Klene, M.; Li, X.; Knox, J. E.; Hratchian, H. P.; Cross, J. B.; Bakken, V.; Adamo, C.; Jaramillo, J.; Gomperts, R.; Stratmann, R. E.; Yazyev, O.; Austin, A. J.; Cammi, R.; Pomelli, C.; Ochterski, J. W.; Ayala, P. Y.; Morokuma, K.; Voth, G. A.; Salvador, P.; Dannenberg, J. J.; Zakrzewski, V. G.; Dapprich, S.; Daniels, A. D.; Strain, M. C.; Farkas, O.; Malick, D. K.; Rabuck, A. D.; Raghavachari, K.; Foresman, J. B.; Ortiz, J. V.; Cui, Q.; Baboul, A. G.; Clifford, S.; Cioslowski, J.; Stefanov, B. B.; Liu, G.; Liashenko, A.; Piskorz, P.; Komaromi, I.; Martin, R. L.; Fox, D. J.; Keith, T.; Al-Laham, M. A.; Peng, C. Y.; Nanayakkara, A.; Challacombe, M.; Gill, P. M. W.; Johnson, B.; Chen, W.; Wong, M. W.; Gonzalez, C.; Pople, J. A. Gaussian, Inc., Wallingford CT, **2004**. (b) This level of theory was previously shown to yield accurate results for systems with simultaneous H-bonding and π -stacking interactions, reference 19 c) and d). (c) Zuilhof, H.; Morokuma, K. *Org. Lett.* **2003**, *5*, 3081-3084. (d) Guo, D.; Sijbesma, R. P.; Zuilhof, H. *Org. Lett.* **2004**, *6*, 3667-3670.

¹⁸ Jeffrey, G. A. *An Introduction to Hydrogen Bonding*, Oxford University Press, **1997**.

¹⁹ Kato, T.; Mizoshita, N.; Kanie, K. *Macromol. Rapid Commun.* **2001**, *22*, 797-814.

²⁰ (a) Blanton, T. N.; Chen, H. P.; Mastrangelo, J.; Chen, S. H. *Adv. X-ray Anal.* **2001**, *44*, 18-23. (b) Kumar, S.; Manickam, M. *Liq. Cryst.* **1999**, *26*, 939-941. (c) Grafe, A.; Janietz, D.; Frese, T.; Wendorff, J. H. *Chem. Mater.* **2005**, *17*, 4979-4984.

²¹ Warman, J. M.; van de Craats, A. M. *Mol. Cryst. Liq. Cryst.* **2003**, *396*, 41-72.

²² (a) van de Craats, A. M.; de Haas, M. P.; Warman, J. M. *Synth. Met.* **1997**, *86*, 2125-2126. (b) van de Craats, A. M.; Warman, J. M.; de Haas, M. P.; Adam, D.; Simmerer, J.; Haarer, D.; Schuhmacher, P. *Adv. Mater.* **1996**, *8*, 823-826.

²³ Paraschiv, I.; Delforterie, P.; Giesbers, M.; Posthumus, M. A.; Marcelis, A. T. M.; Zuilhof H.; Sudhölter, E. J. R. *Liq. Cryst.* **2006**, *32*, 977-983.

²⁴ (a) Wan, W.; Monobe, H.; Tanaka, Y.; Shimizu, Y. *Liq. Cryst.* **2003**, *30*, 571-578. (b) Kumar, S. *Liq. Cryst.* **2004**, *31*, 1037-1059.

Chapter 5

High Charge Carrier Mobility in H-Bond Stabilized Columnar Discotic Triphenylene Derivatives*

Abstract – A new series of 1,3,5-benzenetrisamide derivatives with three hexaalkoxy triphenylene (**HAT6**) pendant groups was prepared. **HAT6** groups are connected to the central 1,3,5-benzenetrisamide core through a flexible spacer. The length of this spacer, as well as the size of the ortho-substituent at the triphenylene core, influences the columnar packing of these molecules. All materials show liquid crystalline behavior with high isotropization temperatures. Different columnar hexagonal phases have been identified using optical polarization microscopy, differential scanning calorimetry and X-ray diffraction. A chiral 1,3,5-benzenetrisamide derivative forms columnar stacks with a single helical orientation, both in an apolar solvent and in a film, as observed by circular dichroism studies. By using pulse-radiolysis time resolved microwave conductivity, charge carrier mobilities as high as $0.25 \text{ cm}^2 \text{ V}^{-1} \text{ s}^{-1}$ have been determined for the liquid crystalline phase of the chiral derivative. This mobility is twice the highest value ever reported for triphenylene-based liquid crystalline materials, approaching mobilities found for hexabenzocoronene-based liquid crystals.

* This chapter is based on:

Paraschiv, I.; de Lange, K.; Yildirim, Z.; Mendes, E.; Picken, S. J.; Grozema, F. C.; Giesbers, M.; Marcelis, A. T. M.; Zuilhof, H.; Sudhölter, E. J. R. - *manuscript in preparation*.

5.1 Introduction

Discotic liquid crystals (DLCs) are a particularly interesting class of compounds in the category of self-organized soft materials.¹ Discotic mesogens are mostly² geometrically rigid poly-aromatic molecules³ surrounded by alkyl chains that provide the flexibility required for the liquid crystalline properties.⁴ Several classes of DLCs have been described in the literature; two of the most studied ones are triphenylene⁵ and hexabenzocoronene⁶ derivatives. Through π -stacking of the aromatic cores, these molecules often form columnar aggregates and as a direct consequence of this organization, charge carrier migration along the columns is possible.^{7,8} Significant advantages of organic conducting materials are their flexible synthesis, easy processability and low production costs. Therefore, these organic optoelectronic materials are of interest for a number of applications,⁹ such as photovoltaic solar cells,¹⁰ electroluminescent displays,¹¹ and field-effect transistors.¹² Because charge transport across the organic layer(s), quantified by the charge carrier mobility,¹³ plays a key role in the performance of such devices,¹⁴ the *stability* of the organization of DLC molecules in the columnar stacking is very important.

For obtaining DLC materials with optimal processability and high charge carrier mobilities,¹⁵ a *controlled balance* is required between the π - π stacking of the aromatic central cores and alkyl-alkyl interactions between the liquid-like chains around the disk-like molecule.¹⁶ In the last years, more complex architectures have been constructed in order to obtain better performing DLCs,¹⁷ useful for building up organic-based electronic devices.¹⁸ Nevertheless, the more complex the molecules will become, the more difficult it will be to control the intermolecular forces.¹⁹ Among these intermolecular interactions hydrogen bonds constitute an attractive and tunable interaction in the stabilization of columnar organizations of disk-like molecules.²⁰

In this chapter, a series of 1,3,5-benzenetrisamide derivatives with three pendant **HAT6** moieties is investigated, as new examples of H-bond-stabilized self-assembled disk-like molecules. This type of C_3 -symmetrical trisamide molecules that associate into supramolecular stacks through H-bonding has been previously described for smaller disk-like molecules.²¹

As reported in Chapter 4 of this thesis, the synergetic effects of 1,3,5-benzenetrisamide groups slowed down considerably the dynamics of the attached triphenylene (**HAT6**) molecules, resulting in a highly ordered columnar hexagonal plastic phase (Col_{hp}).²² In this columnar phase, hydrogen bonding intermolecularly connects the central benzene cores, in

such a way that adjacent central benzene cores are rotated over 60° , therefore giving rise to a helical orientation of the intermolecular H-bonding (see Figure 1a and 1b).^{21d, 22} Furthermore, in this particular phase molecular modeling calculations indicate that adjacent triphenylene disks are rotated 15° with respect to each other. This would correspond to $\sim 85\%$ of the maximum of the charge transfer integral.²³ As a result, this particular highly-stable mesophase is characterized by a charge carrier mobility of $0.12 \text{ cm}^2 \text{ V}^{-1} \text{ s}^{-1}$, being the second highest ever reported for triphenylene-based liquid crystalline materials.²²

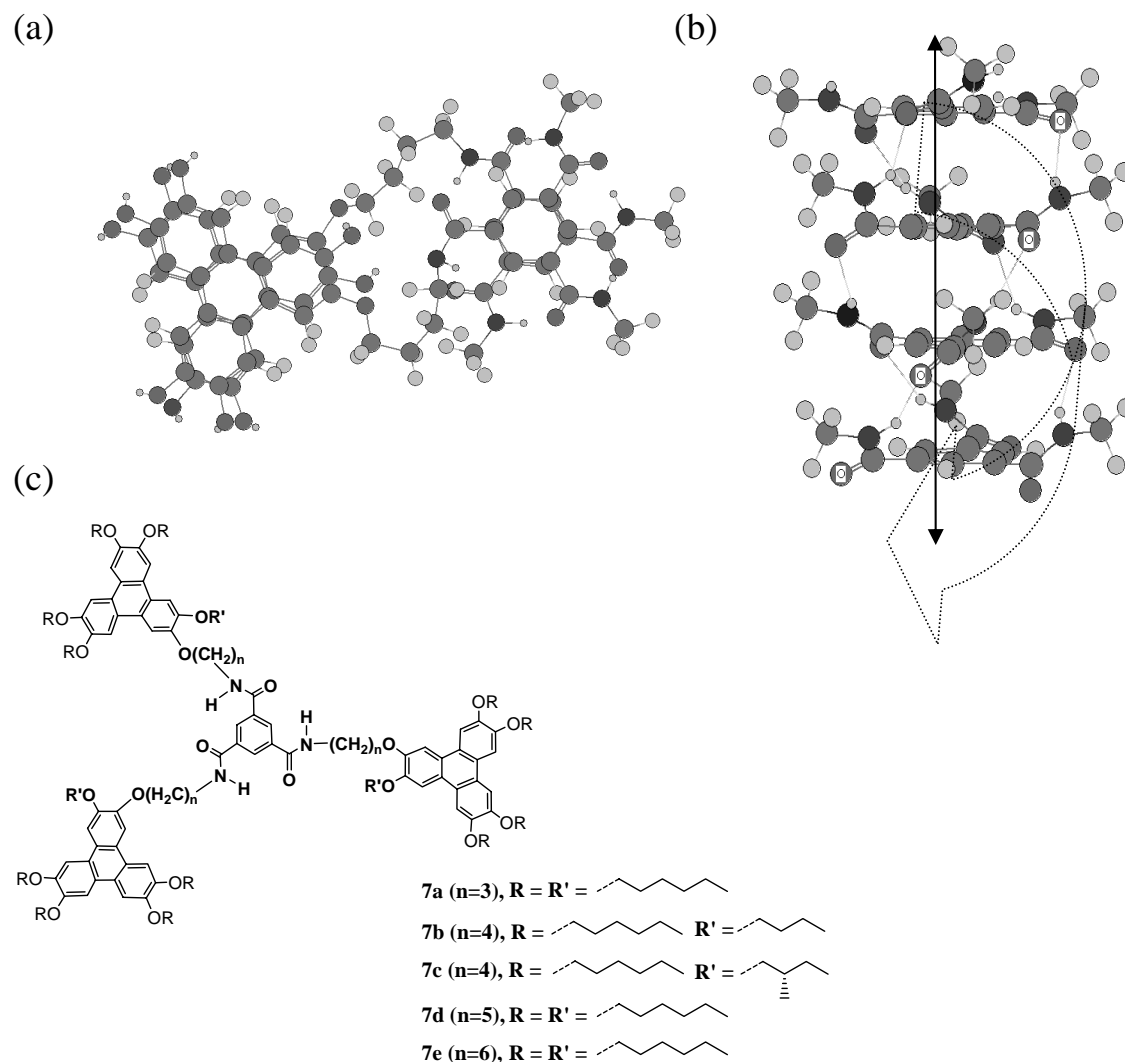


Figure 1. Molecular modeling representation of two stacked dimethyl 1,3,5-benzenetrisamide molecules with one triphenylene-containing sidearm (a) and four π -stacked trimethyl 1,3,5-benzenetrisamide molecules (b), indicating the H-bond helix formation. Structures of the C_3 -benzenetrisamide compounds under study (c).

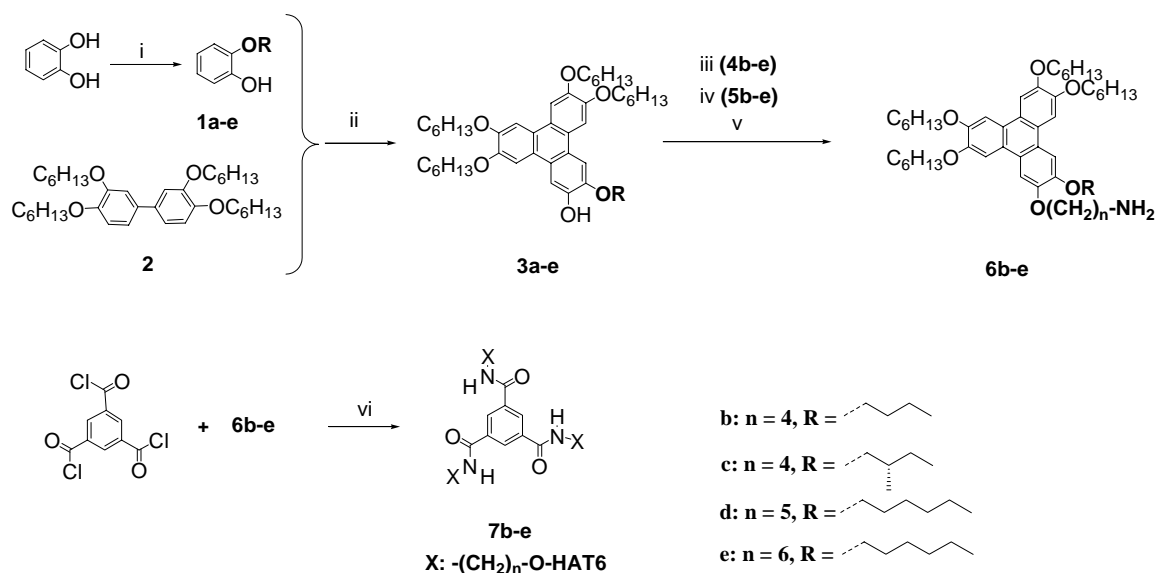
Our modeling studies suggested that the conformation of the butyl spacer dictates the π - π overlap of **HAT6** units within the liquid crystalline phase (Figure 1a).²² A better overlap of

the π -orbitals would result in a larger splitting of the HOMO (LUMO) levels, and ultimately in a higher charge transfer integral.^{8,15,23} Therefore, it can be expected that variation of the spacer length, as well as the size of the *ortho*-substituent of the **HAT6** core will have a significant influence on the aggregation (degree of ordering), and charge carrier mobility, of 1,3,5-benzenetrisamide triphenylene molecules. Therefore, several new trisamide compounds with various spacer lengths (Figure 1c) were synthesized and investigated with respect to their liquid crystalline organization and charge conduction. Since we were specifically interested in forming a single helical orientation for the columnar organization, a chiral 1,3,5-benzenetrisamide triphenylene derivative has been synthesized, by introduction of a chiral center in one of the *ortho*-substituents of the **HAT6** core. For this compound, the effects of the chirality on the molecular packing and the resulting charge carrier mobility as a function of temperature have been investigated in detail.

5.2 Results and Discussion

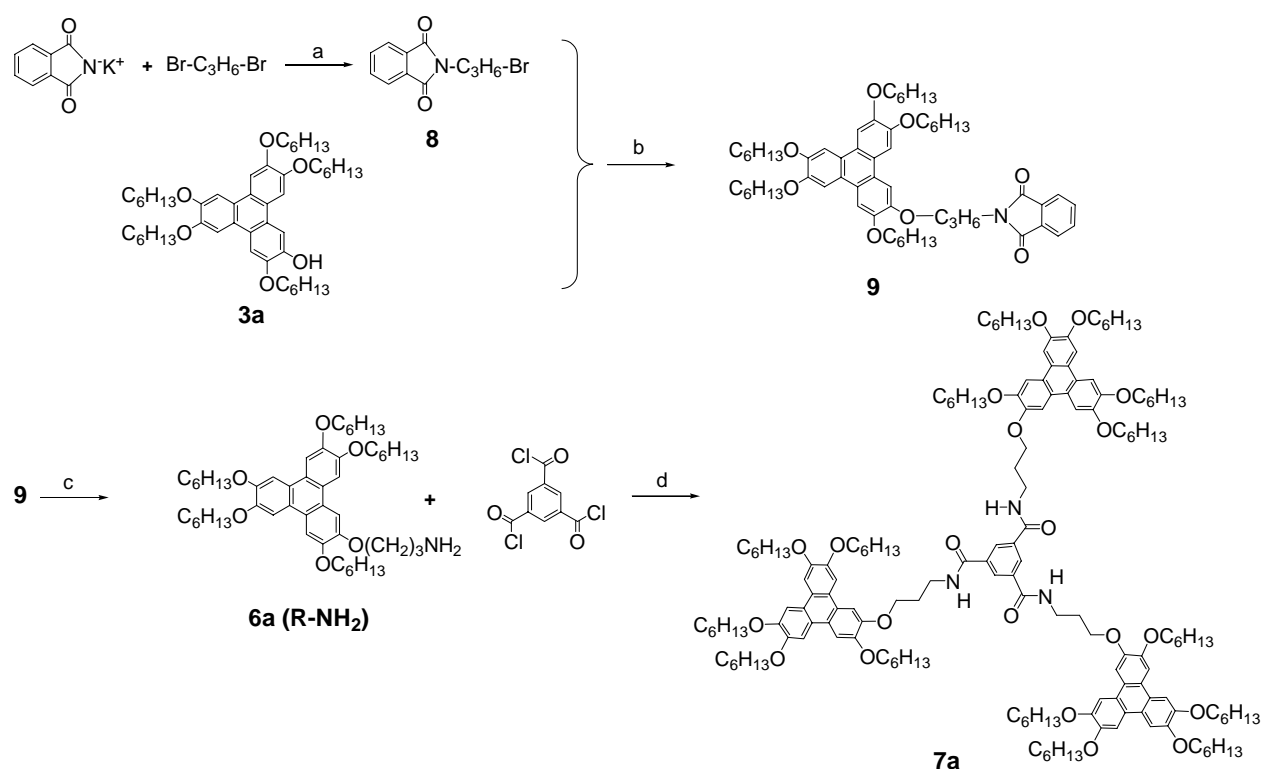
5.2.1 Synthesis

The synthesis of compounds **7b-e** is analogous to that reported before for a similar 1,3,5-benzenetrisamide with three pendant hexaalkoxytriphenylenes (Chapter 4),²² and is depicted in Scheme 1.



Scheme 1. Reagents and conditions for the synthesis of compounds **7b-e**: (i) **1a-e**: R-Br, 2-butanone, K_2CO_3 or Cs_2CO_3 ; (ii) FeCl_3 , CH_2Cl_2 ; methanol; (iii) **4b-d**: $\text{Br}(\text{CH}_2)_n\text{Br}$, K_2CO_3 , 2-butanone; **4e**: $\text{Br}(\text{CH}_2)_6\text{Br}$, Cs_2CO_3 , acetonitrile; (iv) NaN_3 , ethanol; (v) LiAlH_4 , THF; NaOH , H_2O , $\text{Na}_2\text{SO}_4 \cdot 10\text{H}_2\text{O}$; (vi) **7b-c**: $\text{N}(\text{CH}_2\text{CH}_3)_3$, CH_2Cl_2 , R. T.; **7d-e**: benzene, pyridine, R. T.

The synthetic route presented in Scheme 1 was not successful in the case of compound **7a**, which has the shortest alkyl spacer ($-\text{C}_3\text{H}_6-$) within the studied materials. In reaction step (iii) (Scheme 1), both of the bromide atoms from 1,3-dibromopropane react with triphenylene derivative **3a**, even when a large excess of the alkylating agent is used. Therefore an alternative route to the synthesis of compound **7a** was developed, via the monobromo propane derivative **8** (Scheme 2). Phthalimido-protected bromopropane **8** reacts with **3a** to give triphenylene derivate **9**. Deprotection with hydrazine hydrate gives amine **6a**, which was further reacted with 1,3,5-benzenetricarbonyl trichloride to finally yield compound **7a**.



Scheme 2. Reagents and conditions for the synthesis of compound **7a**: (a) reflux, acetone; (b) K_2CO_3 , 2-butanone; (c) $\text{NH}_2-\text{NH}_2 \cdot \text{H}_2\text{O}$, ethanol; (d) CH_2Cl_2 , $(\text{CH}_3\text{CH}_2)_3\text{N}$.

5.2.2 Characterization

The structure for each of the intermediary compounds and final products has been confirmed by ^1H -NMR, ^{13}C -NMR and exact mass measurements. Additionally, ^1H - ^1H COSY and HETCOR NMR measurements were used for further confirmation if so required. The properties of compounds **7a-e** were investigated using optical polarization microscopy (OPM), differential scanning calorimetry (DSC), temperature-dependent Fourier Transform Infrared spectroscopy (FTIR) and X-ray diffraction (XRD) techniques. Additionally, circular dichroism (CD) studies have been performed on the chiral derivative **7c**.

The charge carrier mobility as a function of temperature was measured using pulse radiolysis time-resolved microwave conductivity (PR-TRMC).²⁴

Part of the HETCOR NMR correlation spectrum of compound **7a** is shown in Figure 2, which shows the CH₂O- and CH₂N- groups from the flexible spacer and CH₂ groups from the alkoxy substituents around the **HAT6** units.

The CH₂N group can be observed as a quartet around $\delta = 3.82$ ppm, which is linked to the CH₂NH signal in ¹³C-NMR at $\delta = 38.75$ ppm; the integrated intensity of this peak shows complete 3-fold substitution of HAT moieties to the central core.

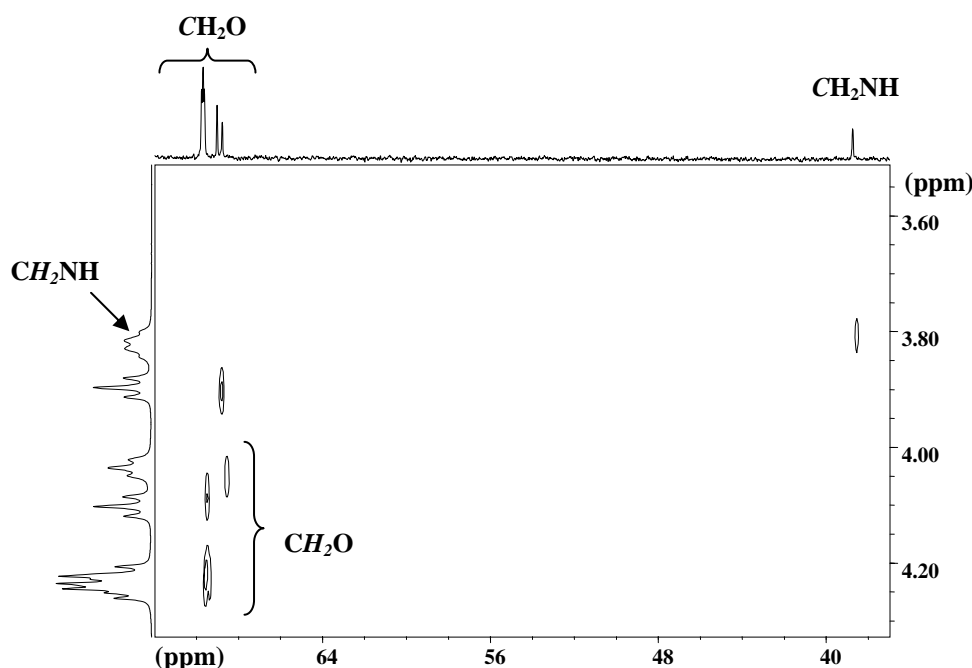


Figure 2. HETCOR NMR correlation spectrum of compound **7a**, showing a part of the CH₂ area.

All compounds **7a-e** display liquid crystalline behavior. Optical polarization microscopy shows fan-like textures both upon heating to or upon cooling from the isotropic state (Figure 3). Particularly compound **7a** exhibits a dendritic growth,²⁵ as shown in Figure 3a. The observed micrographs are indicative for a columnar mesophase.^{25c} Below the isotropization temperature, compound **7b** exhibits one-dimensionally growing needles, as shown in Figures 3b₁ and 3b₂. In this case, the growth direction of the needles in the direction of the arrow (Figure 3b₂) is remarkably faster than in the perpendicular direction.

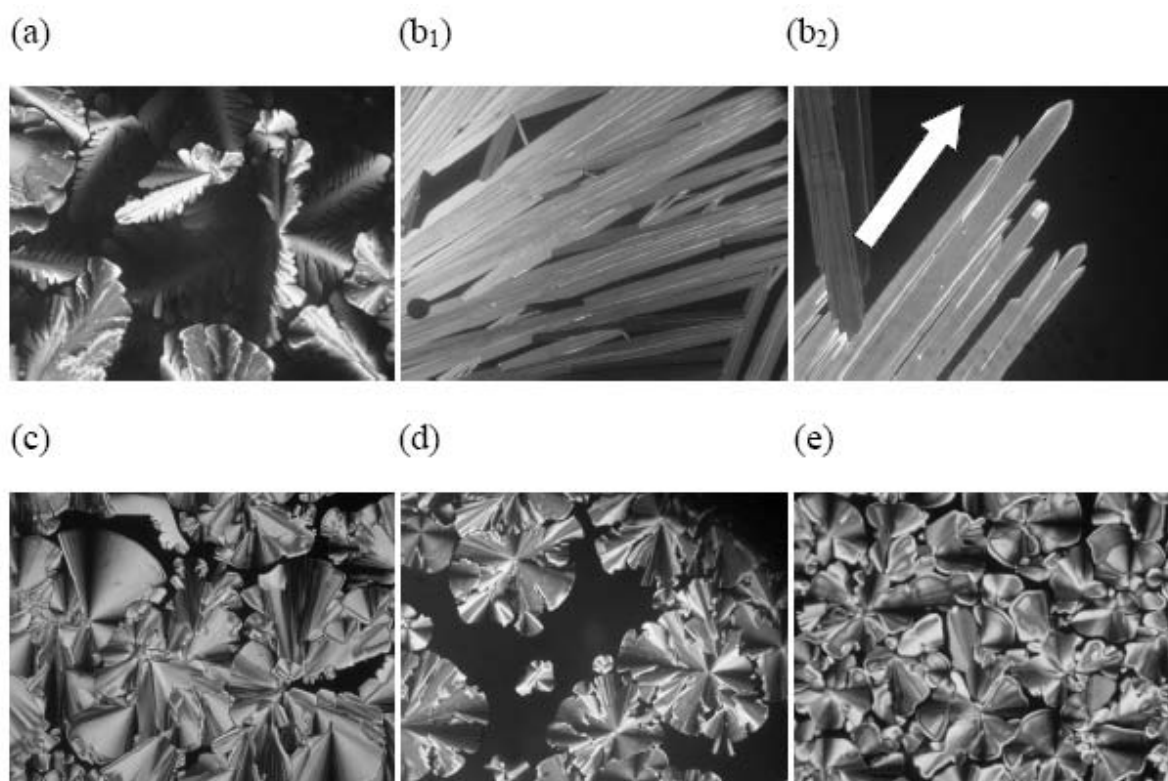


Figure 3. Polarized optical micrographs of the compounds **7a** at 169 °C (a), **7b** at 193 °C (b₁ and b₂), **7c** at 172 °C (c), **7d** at 187 °C (d) and **7e** at 177 °C (e) (See the Appendix at the end of the thesis for the color picture).

DSC thermograms of trisamides **7a** and **7b** show a single transition upon heating. For all compounds **7a-e** the DSC curves of the 2nd cooling run are given in Figure 4. Upon cooling to room temperature, no crystallization occurs for any of the investigated compounds.

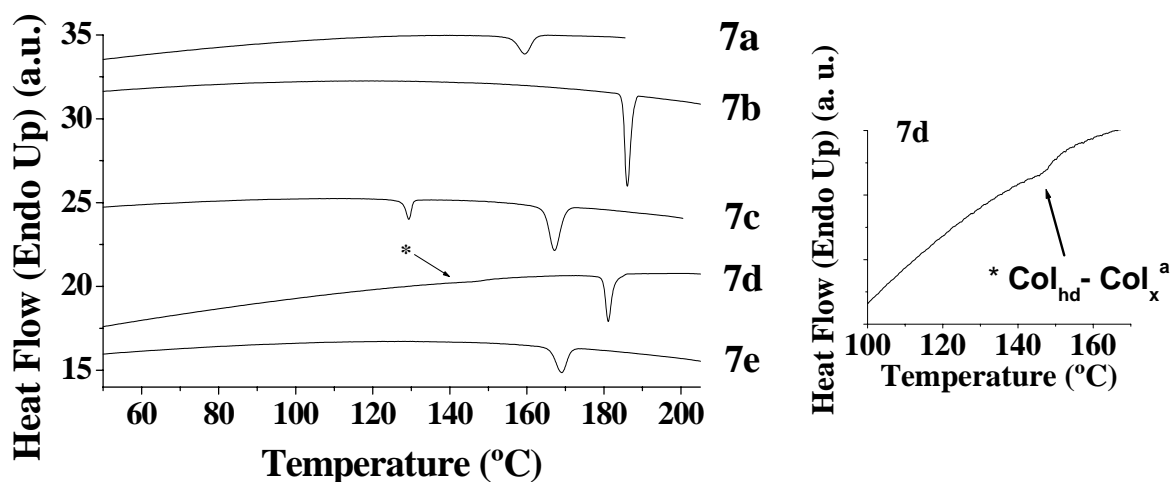


Figure 4. DSC thermograms of compounds **7a-e** (left figure).

Note: *Col_{hd} to Col_x transition for compound **7d** (right figure); second cooling at 10 °C min⁻¹.

Additionally, these samples can be kept at room temperature for weeks without crystallization. The absence of crystallization could be a result of the H-bonding network formed between the amide groups, which brings the molecules into an H-bond reinforced “glassy” state.

As shown in Table 1, the isotropization temperatures and the corresponding heat effects (ΔH) are rather similar, upon spacer length variation, with the exception for **7b**. All these compounds show similar thermal stability, the isotropization points being in the temperature range of 172 – 200 °C.

Table 1. Type of mesophases, phase transition temperatures (°C) and enthalpies (kJ mol⁻¹, in parentheses) of compounds **7a-e** as determined by DSC; scanning rate 10 °C min⁻¹.

Comp.	Heating			Cooling					
7a	Col _h •		172 [29] • I	I •	160 [29] •	Col _h			
7b	Col _{hp} •		199 [102] • I	I •	186 [99] •	Col _{hp}			
7c	Col _{hd} •	135 [11] •	Col _h •	182 [42] •	I •	167 [37] •	Col _h •	129 [10] •	Col _{hd}
7d	Col _x ^a •	162 [7] •	Col _{hd} •	190 [41] •	I •	181 [35] •	Col _{hd} •	146 [3] •	Col _x ^a
7e	Col _x ^a •	154 [3] •	Col _h •	183 [39] •	I •	170 [35] •	Col _h		

^aUnidentified columnar phase; Col_h = columnar hexagonal; Col_{hp} = columnar hexagonal plastic; Col_{hd} = columnar hexagonal disordered.

The DSC analysis confirms the reversibility of the isotropization transition with ΔH values between 30 - 45 kJ mol⁻¹, values which are relatively high for the isotropization processes comparing to literature values for H-bonded triphenylene derivatives.²⁶ Compound **7b** shows the highest isotropization heat effect (102 kJ mol⁻¹) within the series. A lower heat effect of 88 kJ mol⁻¹, was previously observed for another 1,3,5-benzenetrisamide derivative, which showed a highly ordered columnar hexagonal plastic mesophase.²²

The difference of 14 kJ mol⁻¹ between these two relatively large heat effects suggests an even better packing for molecules **7b** in the liquid crystalline phase. Since compound **7b** bears a shorter, butyloxy *ortho*-substituent, instead of a hexyloxy substituent as in the previously reported 1,3,5-benzenetrisamide,²² a stronger interdigitation of the **HAT6** triphenylene units could give rise to a more compact organization of the molecules within the liquid crystalline phase. In other words, a better interconnection between adjacent columns is expected to take place in this case (*vide infra* – the X-ray results), yielding high isotropization heat effects.

Compound **7c**, which differs from **7b** only in the addition of one methyl group in a side chain, displays a slightly lower transition temperature than **7b**. Most likely, the presence of a chiral center and the addition of a side chain even if only small, creates some disturbance in the packing, which also could be the reason for the second transition at lower temperature (see Table 1).

As the spacer length increases up to $n = 5$ or 6 (compounds **7d** and **7e**, respectively), the molecules become more flexible, and phase transitions are found at lower temperatures. Additionally, the flexibility of the hexyl spacer in compound **7e**, allows a reorganization of the molecules within a Col_h phase, which is relatively better ordered than the Col_{hd} phase found for compound **7d**.

XRD analysis was performed on compounds **7a-e** to elucidate the mode of self-assembly within their mesophase.

The lattice parameters (a , b , c and γ) have been experimentally derived from the X-ray patterns and theoretically estimated using equation (1).

$$d_{hkl} = \left[\left(h^2 / a^2 + k^2 / b^2 + 2hk \cos \gamma / ab \right) / \sin^2 \gamma + l^2 / c^2 \right]^{-0.5} \quad (1)$$

This equation, corresponding to a monoclinic system,²⁷ has been used to approximate the theoretical values for the distances between different reflection planes, with a given set of Miller indices (hkl). The (001) reflection plane has been fixed for the $\pi - \pi$ stacking distance, as determined experimentally. For comparison, both the experimental and estimated results using equation (1) are listed in Table 2.

Generally, all the X-ray patterns are characterized by the presence of several sharp peaks in the low-angle region, corresponding to several reflection planes as indicated in Table 2. The lattice parameters (distances a , b , c and angle γ) of the various compounds are very similar. These values generally indicate a two-dimensional hexagonal lattice, since a and b values are equal or only slightly different from each other, and the angle γ is 60° for all compounds.

One or two reflection peaks have been identified in all the X-ray spectra of the investigated compounds, corresponding to distances of 32 \AA for **7b**, up to almost 37 \AA for **7a** and **7d**. These peaks can be representative of a superstructural ordering (see also Chapter 4) of the liquid crystalline phase.²⁸

Table 2. X-ray Diffraction Data for the Liquid Crystalline Phases of compounds **7a-e**.

Comp.	X-ray lattice parameters (a, b, c, γ)	Phase	Temp. (°C)	d_{exp} (Å)	d_{calc} (Å)	Miller indices
7a	a = b = 41.82 Å c = 3.70 Å $\gamma = 60^\circ$	Col _h	150	36.22	36.22	(100)
				18.25	18.11	(200)
				9.10	9.05	(400)
				3.70	3.70	(001)
7b	a = b = 36.85 Å c = 3.50 Å $\gamma = 60^\circ$	Col _{hp}	140	31.91	31.91	(100)
				18.41	18.43	(110)
				16.01	15.96	(200)
				10.60	10.64	(300)
				6.98	6.96	(410)
				4.98	5.11	(520)
				4.15	4.02	(630)
				3.56	3.42	(201)
				3.50	3.50	(001)
7c	a = b = 37.60 Å c = 3.51 Å $\gamma = 60^\circ$	Col _h	150	32.61	32.56	(100)
				18.78	18.80	(110)
				16.23	16.28	(200)
				12.34	12.31	(120)
				10.89	10.85	(300)
				9.02	9.03	(310)
				8.18	8.14	(040)
				4.00	4.10	(630)
				3.51	3.51	(001)
7d	a = 42.00 Å b = 35.85 Å c* $\gamma = 60^\circ$	Col _{hd}	170	36.45	36.37	(100)
				31.03	31.05	(010)
				18.10	18.19	(200)
				15.37	15.52	(020)
				12.05	12.24	(120)
7e	a = b = 39.45 Å c = 3.53 Å $\gamma = 60^\circ$	Col _h	120	34.20	34.16	(100)
				19.58	19.73	(110)
				16.84	17.08	(020)
				12.80	12.91	(210)
				11.23	11.39	(300)
				3.53	3.53	(001)

*could not be determined.

It should be pointed out that the lattice parameters given in Table 2 strongly depend on the correct Miller indices attributed to a certain peak. To index the peaks with more certainty, 2D XRD studies on oriented samples are still required.

For compound **7a**, which has the shortest spacer ($-\text{C}_3\text{H}_6-$), a columnar hexagonal (Col_h) organization characterized by relatively large lattice parameters, $a = b = 41.82 \text{ \AA}$ and $c = 3.70 \text{ \AA}$, is found for its liquid crystalline phase. Unfortunately, no real explanation could be found for this particular large lattice, since a relatively short spacer has been used ($-\text{C}_3\text{H}_6-$). Furthermore, it should be pointed out that the π - π distance for this particular compound is the largest in the series.

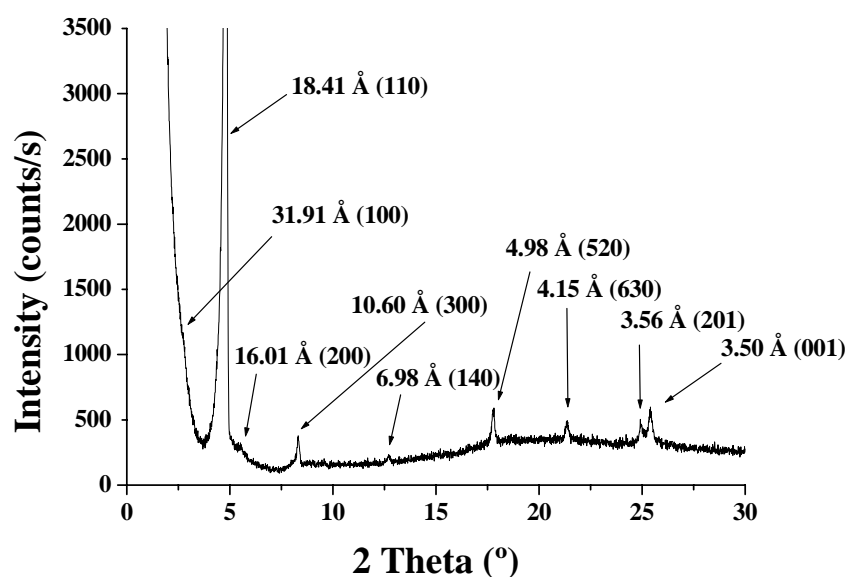


Figure 5. X-ray pattern of compound **7b** at 140 °C, indicating a columnar hexagonal plastic (Col_{hp}) phase.

The XRD diagram of compound **7b** (Figure 5), which is characterized by several sharp peaks up to the (630) reflection plane, corresponds to a highly ordered hexagonal lattice. This diagram points towards a *columnar hexagonal plastic* discotic (Col_{hp}) mesophase, with lattice parameters: $a = b = 36.85 \text{ \AA}$, $c = 3.50 \text{ \AA}$, $\gamma = 60^\circ$. The presence of two specific sharp reflections at 3.56 \AA (201) and 3.50 \AA (001) is particularly indicative for this LC phase,^{22, 29} in which only minor positional fluctuations of the molecules are possible.³⁰

The introduction of a less bulky group (which might reduce also the steric hindrance) in the *ortho* position of the triphenylene mesogenic units, allows the molecules to organize in a highly ordered columnar hexagonal phase (Col_{hp}), as an appropriate size of the *ortho*-substituent can yield to an overall tighter packing.

Based on these arguments, the introduction e.g. of a methyl or ethyl group in the *ortho* position of the triphenylene core is strongly recommended for obtaining a highly ordered columnar hexagonal mesophase.

In the diffractogram of the chiral compound **7c**, taken at 150 °C, several peaks with relatively high intensity are present (Figure 6). The diffractogram reveals reflections with a reciprocal spacing ratio of $1:\sqrt{3}:2:\sqrt{7}:3$ indicative of a two-dimensional hexagonal lattice.^{4a} The broad X-ray halo observed in the range of $2\theta = 15 - 30^\circ$ (Figure 6) shows, that introduction of a branched alkoxy substituent around the triphenylene cores is a factor of disturbance as compared to situation of **7b**.³¹ This can be related to a higher mobility of the alkyl tails around the triphenylene cores, which could be the origin of the second transition detected by DSC.

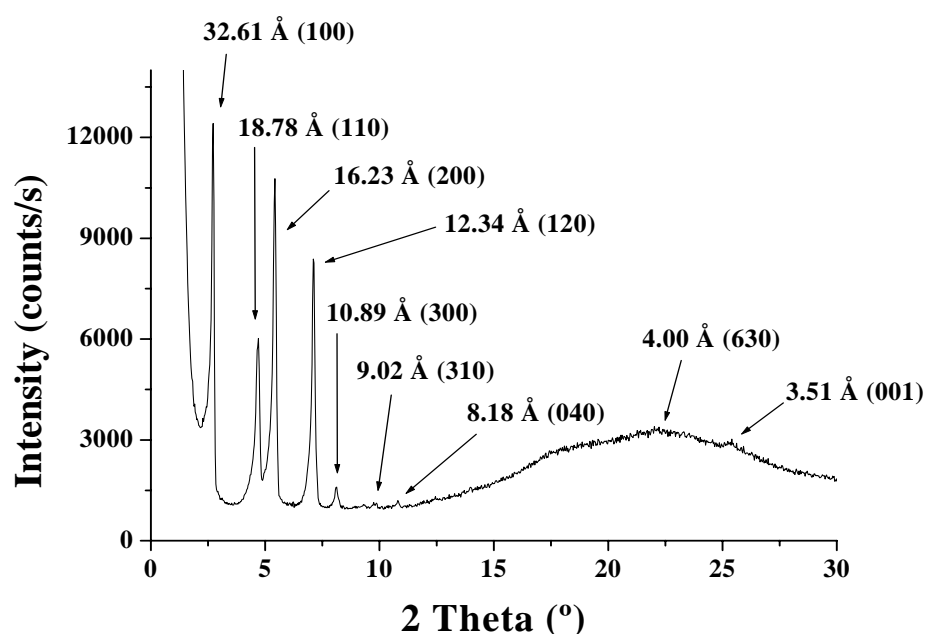


Figure 6. X-ray pattern of compound **7c** at 150 °C.

The XRD diagram of compound **7c**, taken at 110 °C, below the first transition point, shows several sharp peaks. These point towards a columnar hexagonal disordered (Col_{hd}) lattice, since $a = 38.40 \text{ \AA}$, $b = 37.25 \text{ \AA}$ and $\gamma = 60^\circ$, i.e. slightly different than those at 150 °C ($a = b = 37.60 \text{ \AA}$, $c = 3.51 \text{ \AA}$, $\gamma = 60^\circ$). Additionally, the superstructural peak at $\sim 32.6 \text{ \AA}$ is sharper than observed for compounds **7a**, **7b**, **7d** and **7e**, which might point towards a highly ordered mesophase over a larger domain, as compared to the other investigated compounds.

The X-ray diffractogram of compound **7d** shows, for its liquid crystalline state, a slightly disordered columnar hexagonal phase (Col_{hd}), where distances a and b are not equal anymore, but the angle γ is still 60° .

Compound **7e**, which bears the longest alkyl spacer ($-\text{C}_6\text{H}_{12}-$), shows a columnar hexagonal mesophase with equal distances a and b , and a typical $\pi - \pi$ stacking distance of 3.53 Å. This is again an indication that a longer spacer, such as hexyl spacer, allows a better packing of the **7e** molecules within their liquid crystalline phase, based on their much higher flexibility, as compared to the situation of **7d**.

Since there is a possibility that small stacks of molecules still exist in the optically isotropic phase, X-ray diffractograms have also been measured above the isotropization temperature (Figure 7). In these plots, at 200 °C, two types of reflections are still present: a featureless peak just below 4 Å indicating both the closeness of alkyl tails and any remaining π - π interactions, and broad peaks at about 31 Å and 17 Å. The presence of these latter peaks indeed suggests that short columns of stacked benzenetrisamides exist in the isotropic phase, but their correlation length is too short to give optical anisotropy. Such “*quasi-isotropic*” *columnar* phases have previously been observed for other discotic molecules, such as hexabenzocoronenes.³²

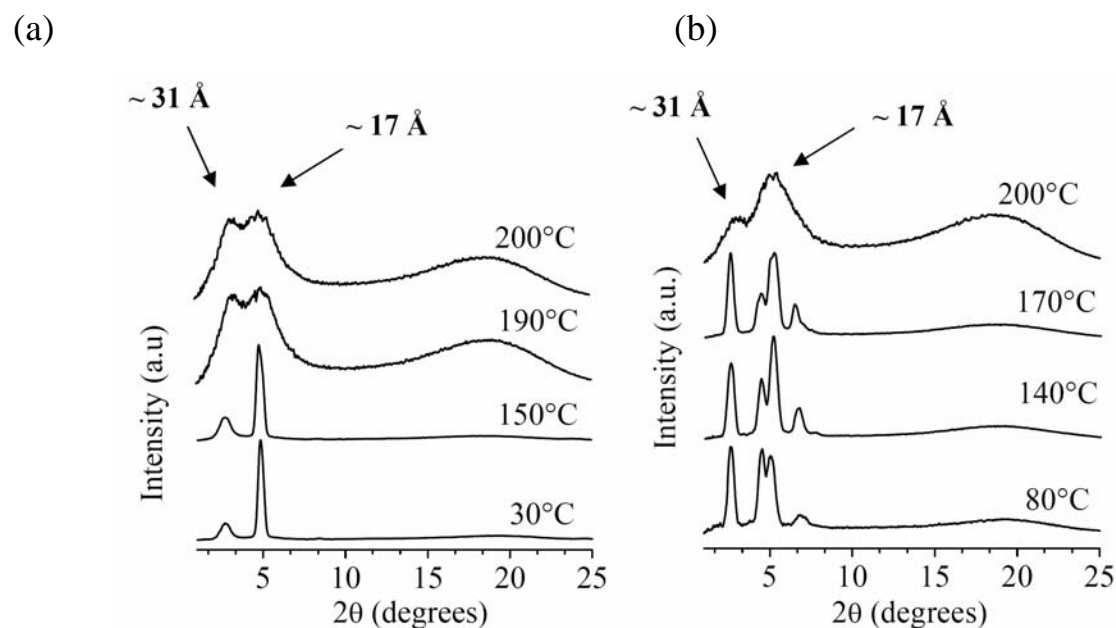


Figure 7. XRD diagrams of compounds **7a** (a) and **7e** (b) at several temperatures, clearly indicating the *quasi-isotropic* phase at 200 °C.*

The X-ray investigation allowed a detailed study on the molecular packing within the columnar mesophase of compounds **7a-e**. No significant changes have been observed upon variation of flexible spacer length, regarding the packing of the molecules within the

* Figure courtesy of Zeynep Yildirim and Stephen J. Picken, TU Delft.

columnar organization. For all the compounds, the π - π distance is between 3.50 and 3.70 Å and the intercolumnar triphenylene-triphenylene distances are around 20 Å. The best ordering was seen for compound **7b**, for which a Col_{hp} phase is found.

Based on the X-ray results a model is proposed (Figure 8) for the molecular organization of molecules **7a-e**, in their mesophases. This model includes basically $1\frac{1}{3}$ 1,3,5-benzenetrisamide molecules inside one cell, indicated by thin lines, since the lateral distance between two **HAT6** units is around 20 Å. A hexagonal grid is also indicated by a larger lattice (thick lines), which includes 2 molecules instead of only $1\frac{1}{3}$. The later lattice might be closer to the real organization of the 1,3,5-benzenetrisamide triphenylene derivatives within their mesophase, as regards the repeating unit of a hexagonal cell.

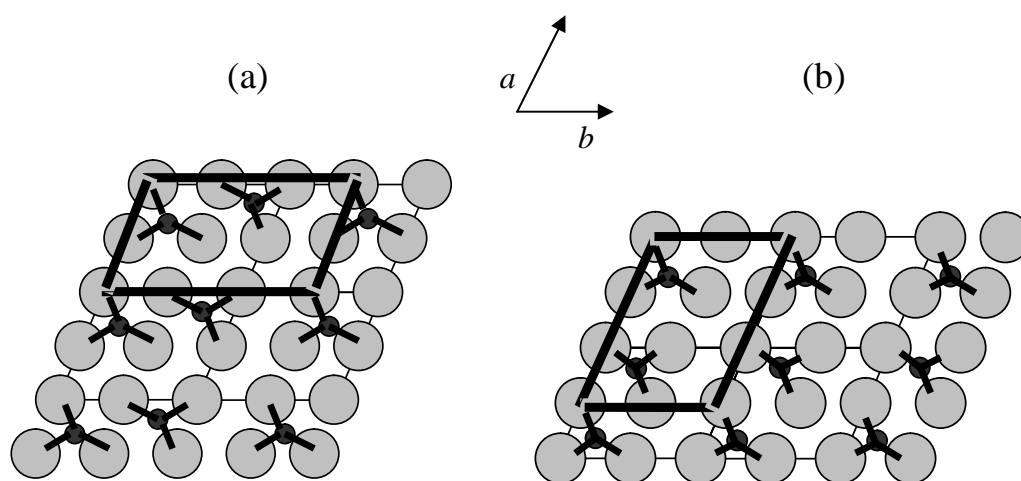


Figure 8. Possible models for the liquid crystalline ordering of **7a-e** compounds, with the cores of the **HAT6** moieties (big grey spheres) and the superstructure determined by the benzenetrisamide cores (small black spheres).

The presence of H-bonding in the self-assembly of these discotic molecules within their mesophases is demonstrated by temperature-dependent FT-IR studies.³³ The infrared spectra were recorded upon cooling from the isotropic (I) state down to room temperature (R.T.). The wavenumber variations of indicative bands, corresponding to the N-H and C=O stretching vibrations, are shown in Table 3.

Upon decreasing the temperature, specifically at the isotropic (I) to columnar mesophase (Col_h) transition point, a strong decrease of the wavenumbers is observed for the characteristic C=O (amide I) and N-H stretching bands, as shown in Figure 10. These differences clearly show a strengthening of the H-bonding interactions within the liquid crystalline phase (Col_h), as the temperature decreases from the isotropic point, which confirms the reinforcement by H-bonding indicated by X-ray results (see Figure 7).

Above the isotropization point the N-H stretching vibrations displays characteristics in between those of strong hydrogen bonding (at R.T.) and very weak to absent hydrogen bonding (in CHCl_3).^{33c,34} This indicates that some hydrogen bonding is still present in this state. The observation that this state just above the isotropization point is *optically* isotropic implies that any form of aggregation has to take place with length scales significantly below 100 nm, but this, of course, does not exclude the presence of smaller aggregates (i.e. in the 5 – 50 nm range), which are held together by a combination of van der Waals, π - π , and hydrogen bonding interactions. Due to the sensitivity of the N-H stretching vibration to hydrogen bond formation, the observed wavenumbers for this state can therefore be interpreted to confirm the observation by X-ray that some form of aggregation is still present just above the temperature at which optical isotropization occurs.

This conclusion can not be drawn from variations in the C=O stretching bands. The intrinsically much smaller effects of hydrogen bonding – in comparison to the effects on N-H stretching – are in this case overshadowed by the combined effects of variations in medium polarity, temperature (with implications on the molecular conformation) and concentration. In other words: this variation can not be used to draw any conclusion regarding the presence or absence of aggregates in the optically isotropic state.

Table 3. Wavenumbers of the N-H and C=O stretching bands in CDCl_3 solution, in as pure materials in the isotropic phase at elevated temperature (I) and at room temperature (R.T.) for the compounds 7a-e.

Comp.	(N-H) stretching vibration (cm^{-1})			(C=O) stretching vibration (cm^{-1})		
	CDCl_3	I	R.T.	CDCl_3	I	R.T.
7a	3402	3400 (190 °C)	3247	1665	1674 (190 °C)	1646
7b	3407	3369 (205 °C)	3233	1664	1673 (205 °C)	1633
7c	3449	3385 (200 °C)	3240	1665	1673 (200 °C)	1643
7d	3451	3318 (200 °C)	3239	1665	1672 (200 °C)	1638
7e	3451	3339 (197 °C)	3237	1665	1673 (197 °C)	1633

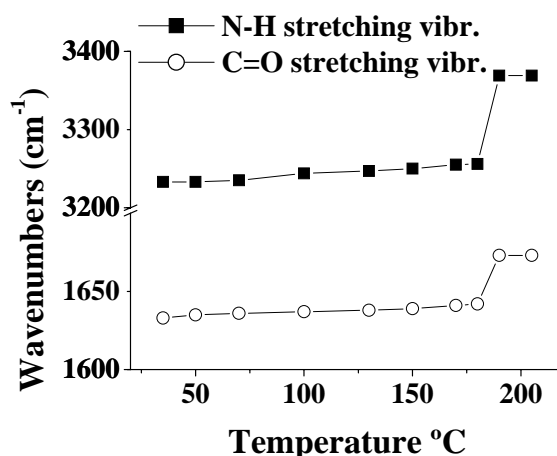


Figure 9. The variation of the wavenumber of the N-H and C=O stretching vibrations of trisamide **7b**, as a function of temperature, upon cooling from the isotropic state.

Similar variations to those shown in Figure 9 for compound **7b**, have been obtained around the isotropization point for all of the 1,3,5-benzenetrisamide triphenylene compounds. Additionally, it is important to mention that for compounds **7c** and **7d** no significant variations in either the N-H or the C=O stretching bands were found for the transitions occurring at lower temperature (Col_h to Col_{hd} (**7c**), and Col_{hd} to Col_x (**7d**), respectively). At those phase transitions, thus no large changes in H-bonding occur, in line with the relatively small structural differences between those mesophases.

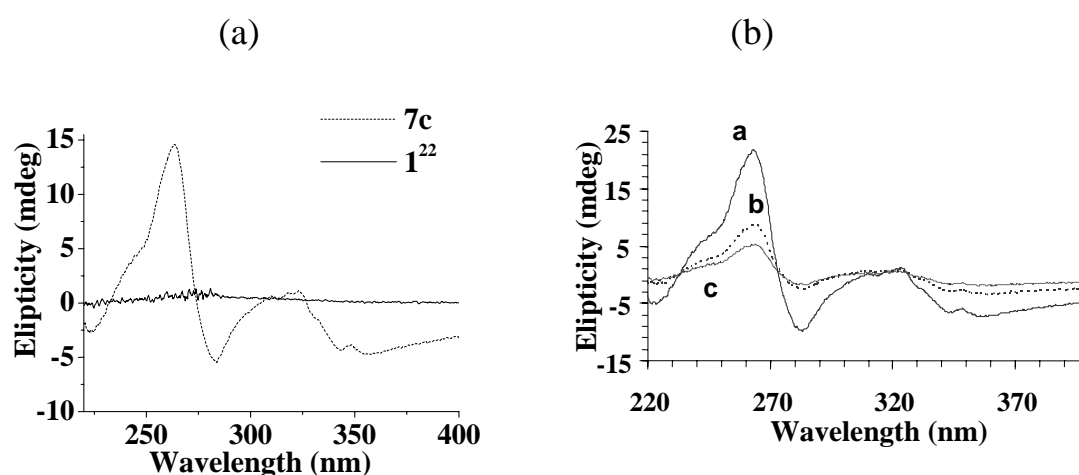


Figure 10. (a) CD spectra of a 5×10^{-5} M hexane solution of **7c** and the 1,3,5-benzenetrisamide **1** reported in Chapter 4.²² (b) CD spectra of hexane solutions of **7c** with different amounts of CH_2Cl_2 : (a) 5×10^{-5} M, 4% CH_2Cl_2 ; (b) 5×10^{-5} M, 4.8% CH_2Cl_2 ; (c) 5×10^{-5} M, 6% CH_2Cl_2 .

With a chiral side chain, such as in compound **7c**, helical orientations such as depicted in Figure 1b might have a preferred direction, which should in principle be observable by circular dichroism (CD). CD measurements³⁵ were performed in order to investigate the aggregation of the chiral derivative **7c** in a hexane diluted solution (5×10^{-5} M) and the expression of chirality in the columnar aggregates. As can be observed in Figure 10a, compound **7c** shows a very strong CD effect, which points to oriented helical aggregates in hexane. The strong CD effect can only be caused by a single helical orientation of the columns inside the aggregates, which is effected by the chiral center of the *ortho*-substituent of the **HAT6** core. The previously reported achiral derivative **1**²² (Chapter 4) does not give a CD signal. By adding dichloromethane to the hexane solution, the CD effect decreases as can be expected, since the aggregates initially present in hexane solution are solubilized by the dichloromethane. Since the CD signal is proportional to the amount of the helically oriented aggregates, its intensity decreases with increasing the dichloromethane concentration (Figure 10b).

These samples were also measured as neat films on a quartz plate at room temperature, after cooling from the isotropic phase. In this situation, again a similar CD effect has been observed, indicating aggregated columnar stacks that obviously exhibit a single helical orientation. These results show that transfer of chirality occurs from the chiral center, introduced in one of the substituents in *ortho* position of the triphenylene core, to the columnar (Col_x) organization. Since this sample does not crystallize on cooling from the isotropic state, the columnar organization is preserved down to room temperature and therefore this organization likely resembles the organization at higher temperatures (see also Figure 7).

The high degree of ordering that is indicated by the H-bonding stabilization of the liquid-crystalline phase was expected to effect a relatively high conductivity along the π -stack of molecules over a wide range of temperatures. Therefore, the one-dimensional charge carrier mobility in compounds **7a-e** was measured as a function of temperature using pulse-radiolysis time resolved microwave conductivity (PR-TRMC) measurements.³⁶ In this technique, pulse radiolysis yields the charge carriers, and from the time-resolved microwave conductivity, the mobility and life-time of these charge carriers can be derived.

Figure 11 shows the dependence of the normalized absorbed microwave power as a function of time. In this graph the change in absorbed microwave power for compound **7a** is measured at 20 °C, when an electron pulse length of 10 ns is used.

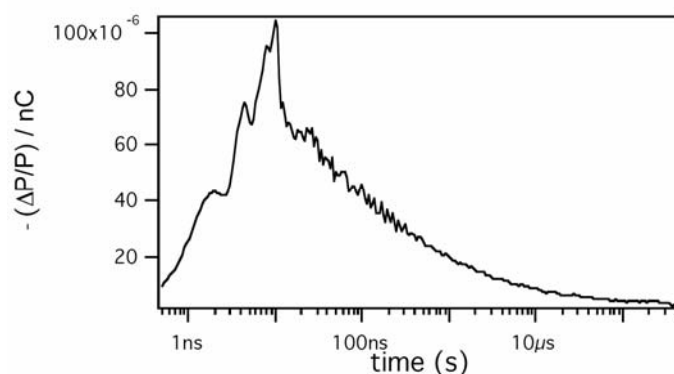


Figure 11. Normalized change in microwave power of **7a** as a function of time, at 20 °C.

The decay kinetics follow a first-order process, since similar decay transients are found when pulses of 2, 5, or 20 ns are used.²² This graph also shows that the half-life of the mobile charge carriers in **7a** is ~100 ns. This time is two times higher than the half-life of pure **HAT6**,²⁴ and this relatively long life time thus confirms the very good stabilization of the molecules within their mesophase.

Figure 12 shows the dependence of the charge carrier mobility on temperature for compounds **7a-e**. Interestingly, the charge carrier mobility keeps increasing with increasing temperature, up to about the clearing point. The relatively high mobilities detected around the isotropization point show values, in accordance with the *quasi*-isotropic state discussed before (*vide supra* – see the X-ray section).³² Apparently, at these high temperatures, stacks of a few molecules are indeed still present, which are enough to provide a relatively high short-range charge carrier mobility as is detected by the PR-TRMC technique.

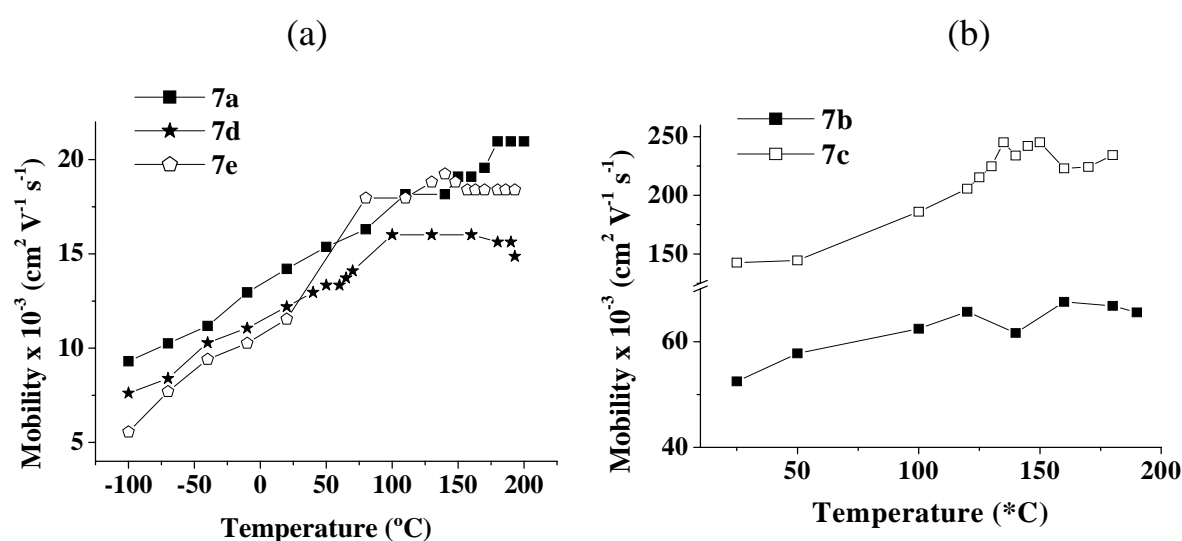


Figure 12. PR-TRMC charge carrier mobility of compounds: (a) **7a**, **7d** and **7e**; (b) **7b** and **7c**, as function of temperature.

As shown also in Table 4, similar mobilities were measured for compounds **7a**, **7d** and **7e** bearing spacers shorter or longer than a butyl one. For compounds with a butyl spacer, i.e. **7b**, **7c** and a previously reported derivative,²² significantly higher mobility values are found. Thus, the length of the butyl spacer it is very important for obtaining the best overlapping of the **HAT6** units, and thus high mobilities.

By changing the length of the substituent in the *ortho* position of the triphenylene core a strong influence on the intracolumnar mobility is found. By shortening the length of this particular substituent a lower mobility in the liquid crystalline phase is obtained ($0.06 \text{ cm}^2 \text{ V}^{-1} \text{ s}^{-1}$ for **7b** versus $0.12 \text{ cm}^2 \text{ V}^{-1} \text{ s}^{-1}$ for a previously reported 1,3,5-benzenetrisamide²²).

Table 4. Charge carrier mobilities for compounds **7a-e**, in different phases.

Comp.	Temperature, °C (phase type)	Mobility ($\text{cm}^2 \text{ V}^{-1} \text{ s}^{-1}$)
7a	20 (glassy state)	0.014
	150 (Col_h)	0.019
	190 (<i>quasi isotropic</i>)	0.021
7b	25 (glassy state)	0.052
	140 (Col_{hp})	0.062
	190 (close to I)	0.066
7c	25 (glassy state)	0.143
	150 (Col_h)	0.245
	180 (close to I)	0.234
7d	20 (glassy state)	0.012
	180 (Col_{dh})	0.016
	193 (<i>quasi isotropic</i>)	0.015
7e	20 (glassy state)	0.012
	170 (Col_h)	0.018
	193 (<i>quasi isotropic</i>)	0.018

When a chiral center at the substituent in the *ortho* position of the triphenylene core is present, a very high charge carrier mobility is obtained for the liquid crystalline phase (**7c**). This mesophase is characterized by a single helical orientation of the columnar packing. This mobility of almost $0.25 \text{ cm}^2 \text{ V}^{-1} \text{ s}^{-1}$ is by far the highest ever reported for *any crystalline or liquid crystalline* triphenylene derivatives. Moreover, this value is close to the charge carrier mobilities of about $0.3 \text{ cm}^2 \text{ V}^{-1} \text{ s}^{-1}$ measured for columnar disordered liquid crystalline phases of several hexabenzocoronene derivatives.^{13,23,37}

Apparently, the introduction of a chiral center effects a single directionality in the helix, and thus improves the long-range overlap of triphenylene moieties. As a result, the conductivity will be improved, and this effect is rather significant. This clearly points to further chances to obtain higher charge conductivities in related materials that could, in principle, display helical organizations, such as benzenetrisamides with peripheral benzocoronenes.

5.3 Conclusions

Five new 1,3,5-benzenetrisamide triphenylene derivatives **7a-e** with different flexible spacers have been synthesized and characterized. All these materials exhibit liquid crystalline properties over a wide temperature range. The isotropization points are between 172 - 200 °C, and the corresponding heat effects are between 30 - 45 kJ mol⁻¹, with the exception of **7b**. This compound has a higher ordered Col_{hp} phase, hence a much higher 102 kJ mol⁻¹ isotropization enthalpy.

XRD analysis has shown that as the spacer length increases, the molecules become more flexible, when the well-ordered Col_h mesophase becomes a Col_{hd} phase. Since similar mobilities have been measured for compounds **7a**, **7d** and **7e**, and significantly higher values for **7b**, **7c** and the compound previously reported in Chapter 4, it can be concluded that using a butyl spacer between the 1,3,5-benzenetrisamide central core and the **HAT6** units is the best choice for obtaining high charge carrier mobilities and also highly ordered columnar hexagonal mesophases.

The introduction of a chiral center in the *ortho* position of the triphenylene ring induces the formation of columnar stacks with a single helical orientation, as shown in the case of compound **7c** by CD spectroscopy. This resulting highly ordered columnar hexagonal (Col_h) phase of the chiral derivative **7c** yields the highest ever reported charge carrier mobility of 0.25 cm² V⁻¹ s⁻¹ for the liquid crystalline triphenylene derivatives. Taking into account this very high value, it is obvious that a very strong H-bonding stabilization of the columnar organization has been successfully achieved for triphenylene moieties, since the monomeric unit (**HAT6**) indicates a charge carrier mobility of only 2 x 10⁻³ cm² V⁻¹ s⁻¹ at 80 °C.²²

In addition, by making use of this rather simple 1,3,5-benzenetrisamide motif, highly tunable stability of the columnar mesophases, *without extremely large π -systems*,³⁷ can be successfully obtained.

5.4 Experimental

5.4.1 Measurements

^1H -NMR (300 MHz and 400 MHz) and ^{13}C -NMR (75 MHz and 100 MHz) spectra were obtained with a Bruker spectrometer, using CDCl_3 as a solvent. Melting points, thermal phase transition temperatures and optical investigation of the liquid crystalline phases were determined on samples between ordinary glass slides using an Olympus BH-2 polarization microscope equipped with a Mettler FP82HT hot stage, which was controlled by a Mettler FP80HT central processor. Differential scanning calorimetry (DSC) thermograms were obtained on a Perkin Elmer DSC-7 system using 2-5 mg samples in 30 μl sample pans and a scan rate of 10 $^\circ\text{C min}^{-1}$. ΔH is calculated in kJ mol^{-1} .

Temperature dependent X-ray curves were measured on a Philips X'pert Pro MRD machine equipped with an Anton Paar camera for temperature control. For the measurements in the small angle region, the sample was spread in the isotropic phase on a thin glass slide (about 15 μm thick), which was placed on a temperature regulated flat copper sample stage.

The accurate masses were obtained using a Finnigan MAT 95 mass spectrometer operating in the 70 eV EI mode at a resolution 5500. Matrix-assisted laser desorption/ionization time-of-flight mass spectra (Maldi-Tof MS) were obtained on an Ultraflex spectrometer using 2,5-dihydroxybenzoic acid (DHB; Sigma-Aldrich) as a matrix.

Infrared spectra (FTIR) were obtained using a Bruker Vector 22 spectrometer. Samples for the temperature-dependent studies were cast from CH_2Cl_2 solution onto a KBr window. The KBr window was kept for some time at a temperature of about 10 $^\circ\text{C}$ above the isotropisation temperature in order to remove residual water and solvents. The spectra were recorded as a function of decreasing temperature.

Circular dichroism studies were performed on aggregates formed in hexane solutions, at room temperature, on a Jasco J-715 polarimeter. The spectra were recorded in a 0.1 cm path length cell, between 400/450 and 220/195 nm, using a step size of 0.5 nm and a bandwidth of 2 nm. The scan rate was 50 nm min^{-1} and 10 scans were averaged.

Charge carriers are created in the materials by high energy radiation (3 MeV) from a van de Graaf accelerator and the mobile charges are detected by monitoring adsorbed microwave power. The electron pulse lengths were varied from 2 to 20 ns, and the maximum beam current is 4 A. The samples were put in a cavity of 6 x 3 x 2 mm^3 in a polyimide block. This block was introduced in a gold plated copper cell, which gives a negligible conductivity signal on irradiation.

5.4.2 Synthesis

All solvents were PA quality. All reactions were carried out under a nitrogen or argon atmosphere. Dry CH₂Cl₂ was freshly distilled from CaH₂. All starting materials were obtained from Sigma-Aldrich and used as received. Synthesis of compounds **1a** = **1d** = **1e**, **2**, **3a** = **3d** = **3e**, and **2** have been previously reported.²²

2-Butyloxyphenol, 1b

A mixture of 20.4 g of catechol (0.19 mol), 5.00 g of 1-bromobutane (36.8 mmol) and 5.00 g of K₂CO₃ was refluxed in 150 ml 2-butanone, under nitrogen, for 24 h. The reaction mixture was cooled and solids were removed by filtration over Hyflo. The filtrate was concentrated under *vacuum* and purified by column chromatography using silica gel eluting with dichloromethane / petroleum ether (40/60), in a (1:1) ratio. Finally, 2.65 g of product (16.0 mmol, 43 %) as a pale yellow oil, was obtained.

¹H-NMR: δ 7.01-6.87 (4H, m, ArH), 5.76 (1H, s, OH), 4.08 (2H, t, J = 6.00 Hz, OCH₂), 1.89-1.80 (2H, m, OCH₂CH₂), 1.58-1.54 (2H, m, CH₂CH₂CH₃), 1.04 (3H, t, J = 6.00 Hz, CH₃).

¹³C-NMR: δ 146.03-145.88 (ArC-O), 121.32 (6-ArC-H), 120.10 (3-ArC-H), 114.50 (5-ArC-H), 111.68 (4-ArC-H), 68.60 (OCH₂), 31.32 (OCH₂CH₂), 19.27 (CH₂CH₂CH₃), 13.85 (CH₃).

MS [M]⁺: calculated for C₁₀H₁₄O₂: 166.0994 amu; found [M]⁺ 166.0993 amu.

(S)-2-(2-Methylbutoxy)phenol, 1c

A mixture of 35.0 g catechol (0.32 mol), 5.00 g (S)-(+)-1-bromo-2-methylbutane (33.1 mmol) and 3.50 g Cs₂CO₃ was refluxed in 200 ml 2-butanone, under nitrogen, for 72 h. The reaction mixture was cooled and solids were removed by filtration over Hyflo. The filtrate was concentrated under *vacuum* and purified by column chromatography using silica gel eluting with dichloromethane / petroleum ether (40/60), in a (1:1) ratio. Finally, 2.52 g (42 %) of **1c** as a pale yellow oil, was obtained.

¹H-NMR: δ 6.97-6.86 (4H, m, ArH), 5.70 (1H, s, OH), 3.97-3.83 (2H, m, OCH₂CH, prochiral Hs), 1.96 (1H, m, CH chiral), 1.63-1.56 (1H, m, CHCH₂CH₃, prochiral H), 1.38-1.31 (1H, m, CHCH₂CH₃, prochiral H), 1.07 (3H, d, J = 6.78 Hz, CHCH₃), 1.00 (3H, t, J = 7.53 Hz, CH₂CH₃).

¹³C-NMR: δ 146.11 (1-ArC-OH), 145.86 (2-ArC-OCH₂), 121.30 (6-ArC-H), 120.10 (3-ArC-H), 114.47 (5-ArC-H), 111.64 (4-ArC-H), 73.65-73.39 (OCH₂), 34.94-34.71 (CH chiral), 26.18-25.94 (CH₂CH₃), 16.58-16.33 (CHCH₃), 11.31 (CH₂CH₃).

MS $[M]^+$: calculated for $C_{11}H_{16}O_2$: 180.1150 amu; found $[M]^+$ 180.1148 amu.

2-(3-Bromopropyl)isoindoline-1,3-dione, 8

A mixture of 8.25 g potassium phthalimide (44.0 mmol), 50.0 g of 1,3-dibromopropane (0.24 mol), 3.13 g of benzyltriethylammonium chloride as phase-transfer catalyst was refluxed in 30 ml acetone for 24 h. After filtration of the salts, the crude product was purified by column chromatography on silica gel eluting with petroleum ether 40/60 and ethyl acetate, in a (10:1) ratio. Finally, 8.37 g (31.0 mmol, 70 %) of **8**, as white crystals, was obtained. M. p. 76 °C.

1H -NMR: δ 9.20-9.03 (4H, m, ArH), 5.16 (2H, t, J = 6.00 Hz, CH_2N), 4.73 (2H, t, J = 6.00 Hz, CH_2Br), 3.63-3.48 (2H, m, $CH_2CH_2CH_2$).

^{13}C -NMR: δ 168.24 (C=O), 134.06 (C-H phthalimide), 132.02 (C-C phthalimide), 123.33, 122.93 (C-H phthalimide), 36.73, 31.87, 29.77 (CH_2).

MS $[M]^+$: calculated for $C_{11}H_{10}BrNO_2$: 266.9895 amu; found $[M]^+$ 266.9884 amu.

2-[3-(3,6,7,10,11-Pentakishexyloxytriphenylen-2-yloxy)propyl]isoindole-1,3-dione, 9

2-(3-Bromopropyl)isoindoline-1,3-dione (5.00 g, 18 mmol) **8** and 3,6,7,10,11-pentakis(hexyl-oxy)triphenylen-2-ol **3a** (5.70 g, 7.70 mmol) and 3.00 g K_2CO_3 in 2-butanone (50 ml) were stirred at reflux for 21 h. Afterwards the solvent was evaporated under vacuum, 100 ml water was added and the crude product extracted with dichloromethane (3 x 50 ml). The organic layer was washed with brine and afterwards dried over anhydrous sodium sulfate. The solvent was evaporated under *vacuum* and the product recrystallized from acetonitrile, when 7.00 g (7.50 mmol, 97 %) of **9** was obtained. M.p. 88 °C.

1H -NMR: δ 7.92-7.68 (10H, m, ArH), 4.31-4.17 (12H, m, OCH_2), 4.02 (2H, t, J = 6.00 Hz, CH_2N), 2.35-1.25 (m, 42H, CH_2), 0.95 (15H, m, CH_3).

^{13}C -NMR: δ 166.53 (C=O), 147.39-146.63 (ArC-O triphenylene), 132.08 (C-H phthalimide), 130.35 (C-C phthalimide), 122.35-121.55 (ArC-C triphenylene), 121.33 (C-H phthalimide), 107.15-105.19 (ArC-H triphenylene), 67.91-67.68 ($OCH_2(CH_2)_4$), 66.02 ($OCH_2CH_2CH_2N$), 33.67 ($NCH_2CH_2CH_2O$), 29.84-20.81 ($OCH_2(CH_2)_4CH_3$), 12.20 (CH_3).

MS $[M]^+$: calculated for $C_{59}H_{81}NO_8$: 931.5962 amu; found $[M]^+$ 931.5973 amu.

2-Hydroxy-6,7,10,11-tetrakis(hexyloxy)-3-(butyloxy)triphenylene, 3b

A mixture of 1.20 g (7.20 mmol) of **1b** and 5.30 g (9.74 mmol) of **2** was dissolved in 20 ml freshly distilled dichloromethane. Under anhydrous conditions, 5.00 g of $FeCl_3$ was then

carefully added. The reaction mixture was stirred, under nitrogen, for 30 minutes at room temperature. The triphenylene compound crystallized after addition of 150 ml cold methanol. The reaction mixture was further cooled to -35 °C and the precipitate filtered off. The crystals were washed several times with cold methanol. The crude product was purified by column chromatography over silica gel eluting with dichloromethane / petroleum ether 40-60, in a (1:1) ratio. After recrystallization from acetonitrile, 1.30 g (1.80 mmol, 25 %) of **3b** as white crystals, was obtained. M.p. 103 °C.

¹H-NMR: δ 7.89-7.71 (6H, m, ArH), 5.82 (1H, s, OH), 4.23 (2H, t, J = 6.00 Hz, OCH₂), 4.18-4.11 (8H, m, OCH₂), 1.91-1.82 (10H, m, OCH₂CH₂), 1.57-1.28 (26H, m, CH₂), 1.01 (3H, t, J = 6.00 Hz, CH₃), 0.89 (12H, bt, J = 7.14 Hz, CH₃).

¹³C-NMR: δ 149.18-148.78, 145.84-145.28 (ArC-O), 123.96-122.98 (ArC-C), 106.67-104.35 (ArC-H), 69.97-68.79 (OCH₂), 31.69-19.36 (CH₂), 14.05, 13.92 (CH₃).

MS [M]⁺: calculated for C₄₆H₆₈O₆: 716.5016 amu; found [M]⁺ 716.5007 amu.

2-Hydroxy-6,7,10,11-tetrakishexyloxy-3-(2-methylbutoxy)triphenylene, 3c

A mixture of **1c** (1.20 g, 6.67 mmol) and **2** (4.99 g, 9.02 mmol) was dissolved in 20 ml freshly distilled dichloromethane. Under anhydrous conditions, 7.00 g of FeCl₃ was then carefully added. The reaction mixture was stirred, under nitrogen, for 30 minutes at room temperature. The triphenylene compound crystallized after addition of 150 ml cold methanol. The mixture was further cooled to -35 °C and the precipitate filtered off. The crystals were washed several times with cold methanol. The crude product was purified by column chromatography over silica gel eluting with dichloromethane / petroleum ether 40-60, in a (1:1) ratio. After recrystallization from acetonitrile, 1.30 g (1.78 mmol, 27 %) of **3c** was obtained. M. p. 94 °C.

¹H-NMR: δ 7.98-7.78 (6H, m, ArH), 5.90 (1H, s, OH), 4.25 (8H, t, J = 6.00 Hz, OCH₂), 4.20-4.10 (2H, m, OCH₂CH), 2.10-1.91 (1H, m, CH chiral), 1.74-1.27 (34H, m, CH₂), 1.16 (3H, d, J = 6.00 Hz, CH₃CH), 1.06 (3H, t, J = 6.00 Hz, CH₂CH₃), 0.95 (12H, bt, J = 6.00 Hz, CH₃).

¹³C-NMR: δ 149.19-145.29 (ArC-O), 123.77-122.99 (ArC-C), 107.82-104.33 (ArC-H), 73.79 (OCH₂CH), 70.05-69.16 (OCH₂CH₂), 34.83 (CH chiral), 31.69-22.66 (CH₂), 16.78 (CHCH₃), 14.05 (CH₃), 11.45 (CHCH₂CH₃).

MS [M]⁺: calculated for C₄₇H₇₀O₆: 730.5172 amu; found [M]⁺ 730.5165 amu.

2-(4-Bromobutyloxy)-6,7,10,11-tetrakishexyloxy-3-(butyloxy)triphenylene, 4b

A mixture of **3b** (1.30 g, 1.80 mmol), 1.90 g of 1,4-dibromobutane (8.70 mmol) and 2.00 g of K_2CO_3 was dissolved in 60 ml of 2-butanone. The mixture was refluxed for 20 h. After cooling the reaction mixture to room temperature, 50 ml of dichloromethane was added and K_2CO_3 removed by filtration. Afterwards the filtrate was *vacuum* dried and then recrystallized from acetonitrile, when 1.30 g (1.60 mmol, 90 %) of **4b**, as white crystals, was obtained. Cr - 56 °C - Col_h - 70 °C - I.

¹H NMR: δ 7.86-7.85 (6H, asymmetric singlet, ArH), 4.31-4.23 (12H, m, OCH₂), 3.62 (2H, t, J = 6.00 Hz, CH₂Br), 2.22-2.11 (4H, m, CH₂CH₂CH₂Br), 2.01-1.91 (10H, m, CH₂), 1.67-1.37 (26H, m, CH₂), 1.07 (3H, t, J = 7.53 Hz, CH₃), 0.95 (12H, bt, J = 6.96 Hz, CH₃).

¹³C NMR: δ 149.10-148.56 (ArC-O), 123.91-123.48 (ArC-C), 107.63-106.92 (ArC-H), 69.79-69.74 (OCH₂), 69.15 (OCH₂), 68.81 (OCH₂), 33.70 (CH₂Br), 31.69-19.43 (CH₂), 14.05-13.99 (CH₃).

MS [M]⁺: calculated for C₅₀H₇₅BrO₆: 850.4747 amu; found [M]⁺ 850.4729 amu.

2-(4-Bromobutyloxy)-6,7,10,11-tetrakisheptyloxy-3-(2-methylbutoxy)triphenylene, 4c

A mixture of 1.10 g (1.50 mmol) of **3c**, 1.62 g (7.50 mmol) of 1,4-dibromobutane and 2.00 g of K_2CO_3 was dissolved in 60 ml of 2-butanone. The mixture was refluxed for 20 h. After cooling the reaction to room temperature, 50 ml of dichloromethane was added and K_2CO_3 separated by filtration. Afterwards the filtrate was *vacuum* dried and then recrystallized from acetonitrile, when 0.76 g (0.88 mmol, 59 %) of **4c** was obtained. Cr - 51 °C - Col_h - 70 °C - I.

¹H NMR: δ 7.86-7.83 (6H, m, ArH), 4.31-4.23 (10H, m, OCH₂), 4.11-4.03 (2H, m, OCH₂CH), 3.61 (2H, t, J = 6.00 Hz, CH₂Br), 2.23-1.36 (39H, m, CH₂ + chiral CH), 1.16-1.14 (3H, d, J = 6.60 Hz, CH₃CH), 1.05 (3H, t, J = 7.53 Hz, CH₃CH₂CH), 0.95 (12H, t, J = 7.14 Hz, CH₃).

¹³C NMR: δ 149.20-148.60 (ArC-O), 123.92-123.41 (ArC-C), 107.69-106.79 (ArC-H), 74.24 (OCH₂CH) 69.90-68.78 (OCH₂CH₂), 34.99 (CH chiral), 33.71 (CH₂Br), 31.69-22.66 (CH₂), 16.80 (CH₃CH), 14.05 (CH₃), 11.50 (CH₃CH₂CH).

MS [M]⁺: calculated for C₅₁H₇₇BrO₆: 864.4904 amu; found [M]⁺ 864.4891 amu.

2-(5-Bromopentyloxy)-3,6,7,10,11-pentakisheptyloxytriphenylene, 4d

A mixture of 2.38 g (3.19 mmol) of 2-hydroxy-3,6,7,10,11-pentakisheptyloxytriphenylene **3a**, 2.50 g of 1,5-dibromopentane (10.9 mmol) and 5.00 g of K_2CO_3 was refluxed in 2-butanone, under nitrogen, for 24 h. After filtration of the salts and removal of the solvent, the product

was recrystallized from acetonitrile, when 2.22 g (2.48 mmol; 78 %) of **4d** was obtained, as colorless crystals. M. p. 69 °C.

¹H-NMR: δ 7.86 (6H, s, ArH), 4.45-4.24 (12H, m, OCH₂), 3.44 (2H, t, J = 6.80 Hz, CH₂Br), 2.08-1.28 (46H, m, CH₂), 0.96 (15H, t, J = 6.80 Hz, CH₃).

¹³C-NMR: δ 148.91 (ArC-O), 123.53 (ArC-C), 107.21 (ArC-H), 69.63 (OCH₂), 40.68 (CH₂Br), 31.90-22.65 (CH₂), 14.12-14.05 (CH₃).

MS [M]⁺: calculated for C₅₃H₈₁BrO₆: 892.5217 amu; found: [M]⁺ 892.5204 amu.

2-(6-Bromohexyloxy)-3,6,7,10,11-pentakishexyloxytriphenylene, 4e

A mixture of 1.77 g (2.37 mmol) of 2-hydroxy-3,6,7,10,11-pentakishexyloxytriphenylene **3a**, 5.70 g of 1,6-dibromohexane (23 mmol) and 5.00 g of Cs₂CO₃ was refluxed in acetonitrile, under nitrogen, for 5 h. After filtration of the salts and removal of the solvent, the product was recrystallized from acetonitrile, when 1.52 g (1.67 mmol; 71 %) of **4e** was obtained, as colorless crystals. M. p. 62 °C.

¹H-NMR: δ 7.85 (6H, s, ArH), 4.25 (12H, t, J = 6.00 Hz, OCH₂), 3.47 (2H, t, J = 6.00 Hz, CH₂Br), 2.19-1.91 (12H, m, CH₂CH₂O), 1.75-1.09 (36H, m, CH₂), 0.93 (15H, bt, J = 6.00 Hz, CH₃).

¹³C-NMR: δ 149.01 (ArC-O), 123.59 (ArC-C), 107.40 (ArC-H), 69.73 (OCH₂), 33.76 (CH₂Br), 32.74-22.66 (CH₂), 14.05 (CH₃).

MS [M]⁺: calculated for C₅₄H₈₃BrO₆: 906.5373 amu; found: [M]⁺ 906.5388 amu.

2-(4-Azidobutyloxy)-6,7,10,11-tetrakishexyloxy-3-(butyloxy)triphenylene, 5b

A mixture of 1.30 g (1.80 mmol) of **4b** and 0.51 g (7.90 mmol) of sodium azide was refluxed in 50 ml ethanol for 10 h. After adding dichloromethane, the excess of sodium azide was filtrated off and the crude product was purified by column chromatography over silica gel eluting with dichloromethane / petroleum ether 40/60, in a (2:1) ratio. After recrystallization from acetonitrile, 0.74 g (0.91 mmol, 58 %) of **5b**, as white crystals, was obtained. Cr - 60 °C - Col_h - 84 °C - I.

¹H NMR: δ 7.77 (6H, s, ArH), 4.21-4.14 (12H, m, OCH₂), 3.38 (2H, t, J = 6.00 Hz, CH₂N₃), 1.93-1.82 (14H, m, CH₂), 1.46-1.32 (26H, m, CH₂), 0.98 (3H, t, J = 6.00 Hz, CH₃), 0.89-0.84 (12H, m, CH₃).

¹³C NMR: δ 149.10-148.65 (ArC-O), 123.90-123.48 (ArC-C), 107.61-106.93 (ArC-H), 69.79-69.14 (OCH₂), 69.08 (OCH₂), 51.31 (CH₂N₃), 31.69-19.41 (CH₂), 14.05-13.97 (CH₃).

MS $[M]^{+\bullet}$: calculated for $C_{50}H_{75}N_3O_6$: 813.5656 amu; found $[M]^{+\bullet}$ 813.5643 amu.

2-(4-Azidobutyloxy)-6,7,10,11-tetrakishexyloxy-3-(2-methylbutoxy)triphenylene, 5c

A mixture of 0.76 g (0.88 mmol) of **4c** and 0.29 g (4.40 mmol) of sodium azide yielded 0.70 g (0.85 mmol, 97 %) of **5c**. Cr - 46 °C - Col_h - 64 °C - I.

¹H NMR: δ 7.86-7.84 (6H, m, ArH), 4.30-4.23 (10H, m, OCH₂CH₂), 4.12, 4.03 (2H, 2 x dd, J = 6.00 Hz, J = 3.00 Hz, OCH₂CH), 3.47 (2H, t, J = 6.60 Hz, CH₂N₃), 2.05-1.91 (7H, m, 3 x CH₂ + CH chiral), 1.63-1.36 (32H, m, CH₂), 1.15 (3H, d, J = 6.00 Hz, CH₃CH), 1.05 (3H, t, J = 6.00 Hz, CH₃CH₂CH), 0.98-0.93 (12H, m, CH₃).

¹³C NMR: δ 149.20-148.60 (ArC-O), 123.78-123.40 (ArC-C), 107.67-106.79 (ArC-H), 74.22 (OCH₂CH), 69.90-69.07 (OCH₂CH₂), 51.31 (CH₂N₃), 34.98 (CH chiral), 31.69-22.66 (CH₂), 16.80 (CH₃CH), 14.05 (CH₃), 11.48 (CH₃CH₂CH).

MS $[M]^{+\bullet}$: calculated for $C_{51}H_{77}N_3O_6$: 827.5812 amu; found $[M]^{+\bullet}$ 827.5808 amu.

2-(5-Azidopentyloxy)-3,6,7,10,11-pentakishexyloxytriphenylene, 5d

A mixture of 1.94 g (2.17 mmol) of **4d** and 1.64 g (25 mmol) of sodium azide in ethanol was refluxed for 10 h. After the reaction was complete the solvent was evaporated. After addition of 20 ml of water, the reaction mixture was extracted with 2 x 20 ml of CH₂Cl₂; the organic layer was dried over anhydrous sodium sulfate and the solvent was evaporated under *vacuum*. After recrystallization from acetonitrile, 1.96 g (2.29 mmol; 95 %) of compound **5d**, as white crystals, was obtained. M. p. 63°C.

¹H-NMR: δ 7.86 (6H, s, ArH), 4.26 (12H, t, J = 6.40 Hz, OCH₂), 3.38 (2H, t, J = 6.40 Hz, CH₂N₃), 2.13-1.28 (46H, m, CH₂), 0.96 (15H, t, J = 6.80 Hz, CH₃).

¹³C-NMR: δ 149.00 (ArC-O), 123.56 (ArC-C), 107.39 (ArC-H), 69.74 (OCH₂), 51.42 (CH₂N₃), 31.69-22.66 (CH₂), 14.05 (CH₃).

MS $[M]^{+\bullet}$: calculated for $C_{53}H_{81}N_3O_6$: 855.6125 amu; found $[M]^{+\bullet}$ 855.6119 amu.

2-(6-Azidohexyloxy)-3,6,7,10,11-pentakishexyloxytriphenylene, 5e

A solution of 1.52 g (1.67 mmol) of **4e** and 1.23 g (19.0 mmol) of sodium azide in ethanol was refluxed for 15 h. After the reaction was complete the solvent was evaporated. After addition of 20 ml of water the reaction mixture was extracted with 2 x 20 ml of CH₂Cl₂; the organic layer was dried on anhydrous sodium sulfate and the solvent was evaporated under

vacuum. After recrystallization from acetonitrile, a quantitatively amount of compound **5e**, as white crystals, was obtained. M. p. 57 °C.

¹H-NMR : δ 7.85 (6H, s, ArH), 4.25 (12H, t, J = 6.00 Hz, OCH₂), 3.33 (2H, t, J = 6.96 Hz, CH₂N₃), 2.00-1.91 (12H, m, OCH₂CH₂), 1.68-1.41 (36H, m, CH₂), 0.95 (15H, bt, J = 6.96 Hz, CH₃).

¹³C-NMR: δ 149.04-148.85 (ArC-O), 123.73-123.59 (ArC-C), 107.40-107.26 (ArC-H), 69.73-69.48 (OCH₂), 51.41 (CH₂N₃), 31.69-22.66 (CH₂), 14.05 (CH₃).

MS [M]⁺: calculated for C₅₄H₈₃N₃O₆: 869.6282 amu; found [M]⁺ 869.6289 amu.

3-(3,6,7,10,11-Pentakis-hexyloxy-triphenylen-2-yloxy)propan-1-amine, 6a

A stirred mixture of 2-(3-(3,6,7,10,11-pentakis-hexyloxy-triphenylen-2-yloxy)propyl)-isoindoline-1,3-dione **9** (7.00 g, 7.50 mmol) and hydrazine monohydrate (1.90 g, 38 mmol) was refluxed in 40 ml ethanol. A white precipitate was rapidly produced. This was later decomposed with high excess of hydrochloric acid at refluxing temperature. The new formed precipitate was then removed by warm filtration. The filtrate was cooled down to room temperature and the solvent evaporated. The residue was re-dissolved in dichloromethane and a new precipitate was obtained. This was separated by filtration and the filtrate was once again concentrated under *vacuum*. The crude product was purified by recrystallization from acetonitrile to give 3-(3,6,7,10,11-pentakis-hexyloxy-triphenylen-2-yloxy)propan-1-amine **6a** (4.80 g, 6.00 mmol, 80 %).

¹H-NMR: δ 7.85-7.78 (6H, m, ArH), 4.43 (2H, t, J = 6.00 Hz, OCH₂CH₂CH₂NH₂), 4.24 (10H, t, J = 6.00 Hz, OCH₂(CH₂)₄CH₃), 3.74 (2H, t, J = 6.00 Hz, CH₂NH₂), 3.40 (2H, bs, NH₂), 2.35 (2H, m, OCH₂CH₂CH₂NH₂), 2.29-1.27 (40H, m, OCH₂(CH₂)₄CH₃), 0.98-0.85 (15H, m, CH₃).

¹³C-NMR: δ 149.51-147.36 (ArC-O), 125.81-123.44 (ArC-C), 107.82-105.81 (ArC-H), 70.15-68.81 (OCH₂), 59.44 (NCH₂CH₂CH₂O), 31.83-22.78 (OCH₂(CH₂)₄CH₃), 14.11 (CH₃).

MS [M]⁺: calculated for C₅₁H₇₉NO₆: 801.5907 amu; found [M]⁺ 801.5897 amu.

4-[6,7,10,11-Tetrakis-hexyloxy-3-(butyloxy)-triphenylen-2-yloxy]butylamine, 6b

A mixture of 0.74 g (0.91 mmol) of **5b** and 0.35 g (9.10 mmol) LiAlH₄ yielded 0.67 g of **6b** (0.85 mmol, 93 %). No further purification was required for the next reaction step.

MS [M]⁺: calculated for C₅₀H₇₇NO₆: 787.5751 amu; found [M]⁺ 787.5737 amu.

4-[6,7,10,11-Tetrakis-hexyloxy-3-(2-methylbutoxy)-triphenylen-2-yloxy]butylamine, 6c

0.70 g (0.85 mmol) of **5c** was reduced with 0.59 g (15 mmol) LiAlH₄ in dry THF under nitrogen, at room temperature within 2 h. The excess of LiAlH₄ was destroyed by adding a solution of 1M NaOH and additional Na₂SO₄ • 10H₂O. The salts were filtered off and the crude product concentrated under *vacuum*. No further purification was required for the next reaction step.

MS [M]⁺: calculated for C₅₁H₇₉NO₆: 801.5907 amu; found [M]⁺ 801.5898 amu.

The amino-terminated triphenylene derivatives **6d-e** have been successfully synthesized by reduction of **5d-e** derivatives with LiAlH₄ in THF.

6d: **MS** [M]⁺: calculated for C₅₃H₈₃NO₆: 829.6220 amu; found [M]⁺ 829.6193 amu;

6e: **MS** [M]⁺: calculated for C₅₄H₈₅NO₆: 843.6377 amu; found [M]⁺ 843.6323 amu.

N,N',N''-Tris(2-propyloxy-3,6,7,10,11-pentakis-hexyloxy-triphenylene)-benzene-1,3,5-tricarboxamide, 7a

A mixture of 1.50 g (1.87 mmol) of amine-terminated triphenylene **6a** and 0.80 g triethylamine was dissolved in 20 ml freshly distilled dichloromethane and stirred under nitrogen, for 10 minutes, at room temperature. To this another solution of 1,3,5-benzenetricarboxylic acid chloride (0.16 g, 0.60 mmol) in 5.00 ml dichloromethane was drop wise added. After 24 h the reaction mixture was *vacuum* dried and the crude product was purified by column chromatography, using silica gel, eluting with dichloromethane / methanol (gradual increase from 0.5 up to 1 %). The product was afterwards precipitated from acetonitrile, when 70 mg (0.03 mmol, 4.50 %) of **7a**, as white powder, was obtained.

¹H NMR: δ 8.56 (3H, s, benzene C-H), 7.82-7.77 (12H, m, C-H triphenylene), 7.55 (3H, bt, J = 5.46 Hz, NH), 7.45 (6H, d, J = 5.24 Hz, C-H triphenylene), 4.26-4.19 (18H, m, OCH₂), 4.10 (6H, t, J = 6.00 Hz, OCH₂), 4.04 (6H, bt, J = 6.00 Hz, OCH₂), 3.90 (6H, t, J = 6.00 Hz, OCH₂), 3.82 (6H, q, J = 6.00 Hz, CH₂NH), 2.14-1.14 (126H, m, CH₂), 0.98-0.88 (36H, m, CH₃), 0.80 (9H, t, J = 7.17 Hz, CH₃).

¹³C NMR: δ 165.82 (C=O), 149.12-148.21 (ArC-O triphenylene), 135.68 (ArC-C=O benzene), 128.72 (ArC-H benzene), 123.75-123.21 (ArC-C triphenylene), 107.11-106.23 (ArC-H triphenylene), 69.74-68.75 (OCH₂), 38.75 (CH₂NH), 31.74-22.50 (CH₂), 14.05-13.95 (CH₃). ¹H - ¹H COSY and HETCOR (indicated also in the Results and Discussions part of this manuscript) NMR measurements also confirm the structure of compound **7a**.

MS: MALDI-TOF-MS $[M+H]^+$: calculated for $C_{162}H_{238}N_3O_{21}$: 2561.76 amu; found $[M+H]^+$ 2562.10 amu.

N,N',N''-Tris(2-butyloxy-6,7,10,11-tetrakis-hexyloxy-3-(butyloxy)-triphenylene)-benzene-1,3,5-tricarboxamide, 7b

A similar procedure as above described was used for the synthesis of **7b**. For this reaction, argon was used as anhydrous conditions instead of nitrogen. A mixture of 0.67 g (0.85 mmol) of **6b** and 0.07 g (0.26 mmol) of 1,3,5-benzenetricarboxylic acid chloride was reacted, when 117 mg (0.05 mmol, 18 %) of **7b**, as a white powder, was obtained.

1H NMR: δ 8.46 (3H, s, C-H benzene), 7.82-7.67 (18H, m, C-H triphenylene), 7.07 (3H, t, $J = 5.46$ Hz, NH), 4.25-4.05 (36H, m, OCH_2), 3.57 (6H, bq, $J = 5.46$ Hz, CH_2NH), 1.96-1.41 (120H, m, CH_2), 0.97-0.90 (45H, m, CH_3).

^{13}C NMR: δ 165.75 (C=O), 149.12-148.16 (ArC-O triphenylene), 135.58 (ArC-C=O benzene), 128.19 (ArC-H benzene) 123.74-123.43 (ArC-C triphenylene), 107.42-106.93 (ArC-H triphenylene), 69.82-68.91 (OCH_2), 55.01 (CH_2NH), 31.72-19.26 (CH_2), 14.05-13.88 (CH_3). $^1H - ^1H$ COSY and HETCOR NMR measurements also confirm the structure of compound **7b**.

MS: MALDI-TOF-MS $[M+H]^+$: calculated for $C_{159}H_{232}N_3O_{21}$: 2519.71 amu; found $[M+H]^+$ 2519.94 amu.

N,N',N''-Tris(2-butyloxy-6,7,10,11-tetrakis-hexyloxy-3-(2-methylbutoxy)-triphenylene)-benzene-1,3,5-tricarboxamide, 7c

A mixture of 0.72 g (0.90 mmol) of amine-terminated triphenylene **6c** and 0.50 g triethylamine was dissolved in 20 ml freshly distilled dichloromethane and stirred under nitrogen, for 10 minutes, at room temperature. To this another solution of 1,3,5-benzenetricarboxylic acid chloride (64.0 mg, 0.24 mmol) in 5.00 ml dichloromethane was added. After 24 h the reaction mixture was *vacuum* dried and the crude product was purified by column chromatography, using silica gel, eluting with dichloromethane / methanol (gradual increase from 0.5 up to 1 %). The product was afterwards precipitated from acetonitrile, when 0.28 g (0.11 mmol, 46 %) of **7c**, as white powder, was obtained.

1H NMR (400 MHz): δ 8.40 (3H, s, C-H benzene), 7.83-7.74 (18H, m, C-H triphenylene), 6.90 (3H, t, $J = 5.60$ Hz, NH), 4.26-3.96 (30H, m, OCH_2), 3.97 (6H, dd, $J = 6.80$ Hz, 3 x OCH_2CH), 3.58 (6H, q, $J = 6.00$ Hz, 3 x CH_2NH), 1.97-1.28 (117H, m, CH chiral + CH_2), 1.05 (9H, d, $J = 6.80$ Hz, 3 x CH_3CH), 0.97-0.93 (45H, m, CH_3).

¹³C NMR (100 MHz): δ 165.72 (C=O), 149.13-148.30 (ArC-O triphenylene), 135.49 (ArC-C=O benzene), 128.00 (ArC-H benzene), 123.74-123.36 (ArC-C triphenylene), 107.56-106.46 (ArC-H triphenylene), 74.12 (OCH₂CH), 69.87-69.18 (OCH₂CH₂), 39.85 (CH₂NH), 34.71 (CH chiral), 31.71-22.66 (CH₂), 16.78 (CH₃CH), 14.05 (CH₃CH₂CH₂), 11.44 (CH₃CH₂CH). ¹H - ¹H COSY and HETCOR NMR measurements also confirm the structure of compound **7c**.

MS: MALDI-TOF-MS [M+H]⁺: calculated for C₁₆₂H₂₃₈N₃O₂₁: 2561.76 amu; found [M+H]⁺ 2561.28 amu.

N,N',N''-Tris(2-pentyloxy-3,6,7,10,11-pentakis-hexyloxy-triphenylene)-benzene-1,3,5 tricarboxamide, 7d

A mixture of 0.80 g (0.96 mmol) of amine-terminated triphenylene **6d** and 2.50 g pyridine was dissolved in 10 ml benzene and stirred under nitrogen, for 10 minutes, at room temperature. To this, another solution of 1,3,5-benzenetricarboxylic acid chloride (114 mg, 0.43 mmol) in benzene, was then slowly added. After 24 h the reaction mixture was poured over ice-water mixture and concentrated HCl solution was added in order to bring the pyridine, under its salt form, in the water layer. The organic layer was concentrated under *vacuum* and dried on Na₂SO₄ · 10H₂O. The crude product was then purified by column chromatography, using silica gel, eluting with dichloromethane / methanol (gradual increase from 0.5 up to 1 %). The product was afterwards precipitated from acetonitrile, when 0.35 g (0.13 mmol, 31 %) of **7d**, as white powder, was obtained.

¹H NMR (400 MHz): δ 8.41 (3H, s, C-H benzene), 7.84-7.83 (18H, m, C-H triphenylene), 6.80 (3H, t, J = 5.20 Hz, NH), 4.23-4.19 (36H, m, OCH₂), 3.51-3.47 (6H, q, J = 6.40 Hz, 3 x CH₂NH), 2.02-1.27 (138H, m, CH₂), 0.96-0.89 (45H, m, CH₃).

¹³C NMR (100 MHz): δ 167.92 (C=O), 151.31-150.93 (ArC-O triphenylene), 137.56 (ArC-C=O benzene), 130.28 (ArC-H benzene), 125.97-125.81 (ArC-C triphenylene), 109.64-109.32 (ArC-H triphenylene), 72.04-71.75 (OCH₂), 42.52 (CH₂NH), 33.96-24.92 (CH₂), 16.32 (CH₃). ¹H - ¹H COSY and HETCOR NMR measurements also confirm the structure of compound **7d**.

MS: MALDI-TOF-MS [M]⁺: calculated for C₁₆₈H₂₄₉N₃O₂₁: 2644.85 amu; found [M]⁺ 2644.18 amu.

N,N',N''-Tris(2,3,6,7,10,11-hexakis-hexyloxy-triphenylene)-benzene-1,3,5 tricarboxamide, 7e

A mixture of 1.01 g (1.19 mmol) of amine-terminated triphenylene **6e** and 2.00 g pyridine was dissolved in 10 ml benzene and stirred under nitrogen, for 10 minutes, at room temperature. To this, another solution of 1,3,5-benzenetricarboxylic acid chloride (133 mg, 0.50 mmol) in benzene, was then slowly added. After 24 h the reaction mixture was poured over ice-water mixture and concentrated HCl solution was added in order to bring the pyridine, under its salt form, in the water layer. The organic layer was concentrated under *vacuum* and dried on Na₂SO₄ · 10H₂O. The crude product was then purified by column chromatography, using silica gel, eluting with dichloromethane / methanol (gradual increase from 0.5 up to 1 %). The product was afterward precipitated from acetonitrile, when 0.25 g (0.93 x 10⁻¹ mmol, 19 %) of **7e**, as white powder, was obtained.

¹H NMR: δ 8.34 (3H, s, C-H benzene), 7.85 (18H, s, C-H triphenylene), 6.45 (3H, t, J = 5.64 Hz, NH), 4.24 (36H, t, J = 6.00 Hz, OCH₂), 3.49 (6H, q, J = 6.00 Hz, 3 x CH₂NH), 2.00-1.90 (36H, m, OCH₂CH₂), 1.70-1.40 (108H, m, CH₂), 0.97-0.90 (45H, m, 15 x CH₃).

¹³C NMR: δ 165.60 (C=O), 149.02-148.85 (ArC-O triphenylene), 135.26 (ArC-C=O benzene), 127.87 (ArC-H benzene), 123.68-123.59 (ArC-C triphenylene), 107.36-107.26 (ArC-H triphenylene), 69.72-69.49 (OCH₂), 40.24 (CH₂NH), 31.69-22.66 (CH₂), 14.05 (CH₃). ¹H - ¹H COSY and HETCOR NMR measurements also confirm the structure of compound **7e**.

MS: MALDI-TOF-MS [M+3H]⁺: calculated for C₁₇₁H₂₅₈N₃O₂₁: 2689.92 amu; found [M+3H]⁺ 2689.54 amu.

5.5 Acknowledgements

The author would like to thank Mr. Barend van Lagen for help with the NMR measurements, Dr. Maarten A. Posthumus for the exact mass determinations, Mr. Adrie Westphal from the Biochemistry Laboratory (WUR) for help with CD measurements and Mr. Edwin Bakx from the Food Chemistry Laboratory (WUR) for help with the Maldi-Tof determinations.

5.6 References

¹ Kato, T.; Mizoshita, N.; Kishimoto, K. *Angew. Chem. Int. Ed.* **2006**, *45*, 38-68.

² An exception from this rule is found by: Barberá, J.; Rakitin, O. A.; Ros, B.; Torroba, T. *Angew. Chem. Int. Ed.* **1998**, *37*, 296-299.

³ Watson, M. D.; Fechtenkötter, A.; Müllen, K. *Chem. Rev.* **2001**, *101*, 1267-1300.

- ⁴ (a) Wu, J.; Watson, M. D.; Zhang, L.; Wang, Z.; Müllen, K. *J. Am. Chem. Soc.* **2004**, *126*, 177-186. (b) Kastler, M.; Schmidt, J.; Pisula, W.; Sebastiani, D.; Müllen, K. *J. Am. Chem. Soc.* **2006**, *128*, 9526-9534.
- ⁵ (a) Adam, D.; Schuhmacher, P.; Simmerer, J.; Haussling, L.; Siemensmeyer, K.; Etzbach, K. H.; Ringsdorf, H.; Haarer, D. *Nature* **1994**, *371*, 141-143. (b) Kumar, S. *Chem. Soc. Rev.* **2006**, *35*, 83-109.
- ⁶ (a) van de Craats, A. M.; Warman, J. M.; Müllen, K.; Geerts, Y.; Brand, J. D.; Haarer, D. *Adv. Mater.* **1998**, *10*, 36-38. (b) Wang, Z.; Watson, M. D.; Wu, J.; Müllen, K. *Chem. Commun.* **2004**, 336-337. (c) Watson, M. D.; Debije, M. G.; Warman, J. M.; Müllen, K. *J. Am. Chem. Soc.* **2004**, *126*, 766-771. (d) Pisula, W.; Menon, A.; Stepputat, M.; Lieberwirth, I.; Kolb, U.; Tracz, A.; Sirringhaus, H.; Pakula, T.; Müllen, K. *Adv. Mater.* **2005**, *17*, 684-689.
- ⁷ (a) van de Craats, A. M.; Warman, J. M.; Fechtenkötter, A.; Brand, J. D.; Harbison, M. A.; Müllen, K. *Adv. Mater.* **1999**, *11*, 1469-1472. (b) Meijer, E. W.; Schenning, A. *Nature* **2002**, *419*, 353-354. (c) Cornil, J.; Lemaure, V.; Calbert, J. P.; Brédas, J. L. *Adv. Mater.* **2002**, *14*, 726-729.
- ⁸ Lemaure, V.; da Silva Filho, D. A.; Coropceanu, V.; Lehmann, M.; Geerts, Y.; Piris, J.; Debije, M. G.; van de Craats, A. M.; Senthilkumar, K.; Siebbeles, L. D. A.; Warman, J. M.; Brédas, J. L.; Cornil, J. *J. Am. Chem. Soc.* **2004**, *126*, 3271-3279.
- ⁹ (a) Boden, N.; Bushby, R. J.; Clements, J.; Movaghar, B. *J. Mater. Chem.* **1999**, *9*, 2081-2086. (b) Barberá, J.; Garcés, A. C.; Jayaraman, N.; Omenat, A.; Serrano, J. L.; Stoddart, J. F. *Adv. Mater.* **2001**, *13*, 175-180. (c) Kawata, K. *The Chemical Record* **2002**, *2*, 59-80.
- ¹⁰ (a) Nelson, J. *Science* **2001**, *293*, 1059-1060. (b) Schmidt-Mende, L.; Fechtenkötter, A.; Müllen, K.; Moons, E.; Friend, R. H.; MacKenzie, J. D. *Science* **2001**, *293*, 1119-1122. (c) Schmidtke, J.; Friend, R. H.; Kastler, M.; Müllen, K. *J. Chem. Phys.* **2006**, *124*, 174704.
- ¹¹ (a) Lüssem, G.; Wendorff, J. H. *Polym. Adv. Technol.* **1998**, *9*, 443-460. (b) Bacher, A.; Erdelen, C. H.; Paulus, W.; Ringsdorf, H.; Schmidt, H. W.; Schuhmacher, P. *Macromolecules* **1999**, *32*, 4551-4557.
- ¹² (a) Katsuhara, M.; Aoyagi, I.; Nakajima, H.; Mori, T.; Kambayashi, T.; Ofuji, M.; Takanishi, Y.; Ishikawa, K.; Takezoe, H.; Hosono, H. *Synth. Met.* **2005**, *149*, 219-223. (b) Pisula, W.; Menon, A.; Stepputat, M.; Lieberwirth, I.; Kolb, U.; Tracz, A.; Sirringhaus, H.; Pakula, A.; Müllen, K. *Adv. Mater.* **2005**, *17*, 684-689.

- ¹³ Warman, J. M.; Piris, J.; Pisula, W.; Kastler, M.; Wasserfallen, D.; Müllen, K. *J. Am. Chem. Soc.* **2005**, *127*, 14257-14262.
- ¹⁴ Itaka, K.; Yamashiro, M.; Yamaguchi, J.; Haemori, M.; Yaginuma, S.; Matsumoto, Y.; Kondo, M.; Koinuma, H. *Adv. Mater.* **2006**, *18*, 1713-1716.
- ¹⁵ Lehmann, M.; Kestemont, G.; Aspe, R. G.; Buess-Herman, C.; Koch, M. H. J.; Debije, M. G.; Piris, J.; de Haas, M. P.; Warman, J. M.; Watson, M. D.; Lemaur, V.; Cornil, J.; Geerts, Y. H.; Gearba, R.; Ivanov, D. A. *Chem. Eur. J.* **2005**, *11*, 3349-3362.
- ¹⁶ Foster, E. J.; Jones, R. B.; Lavigueur, C.; Williams, V. E. *J. Am. Chem. Soc.* **2006**, *128*, 8569-8574.
- ¹⁷ Grimsdale, A. C.; Müllen, K. *Angew. Chem. Int. Ed.* **2005**, *44*, 5592-5629.
- ¹⁸ Cornil, J.; Beljonne, D.; Calbert, J. P.; Brédas, J. L. *Adv. Mater.* **2001**, *13*, 1053-1065.
- ¹⁹ (a) Brienne, M. J.; Gabard, J.; Lehn, J. M.; Stibor, J. *Chem. Commun.* **1989**, 1868-1870. (b) Hirschberg, J. H. K. K.; Brunsveld, L.; Ramzi, A.; Vekemans, J. A. J. M.; Sijbesma, R. P.; Meijer, E. W. *Nature*, **2000**, *407*, 167-170. (c) Sautter, A.; Thalacker, C.; Würther, F. *Angew. Chem. Int. Ed.* **2001**, *113*, 4557-4560.
- ²⁰ (a) Gearba, R. I.; Lehmann, M.; Levin, J.; Ivanov, D. A.; Koch, M. H. J.; Barberá, J.; Debije, M. G.; Piris, J.; Geerts, Y. H. *Adv. Mater.* **2003**, *15*, 1614-1618. (b) Wasserfallen, D.; Fischbach, I.; Chebotareva, N.; Kastler, M.; Pisula, W.; Jäckel, F.; Watson, M. D.; Schnell, I.; Rabe, J. P.; Spiess, H. W.; Müllen, K. *Adv. Funct. Mater.* **2005**, *15*, 1585-1594. (c) Wan, W.; Monobe, H.; Sugino, T.; Tanaka, Y.; Shimizu, Y. *Mol. Cryst. Liq. Cryst.* **2001**, *364*, 597-603.
- ²¹ (a) Bushey, M. L.; Hwang, A.; Stephens, P. W.; Nuckolls, C. *J. Am. Chem. Soc.* **2001**, *123*, 8157-8158. (b) van Gorp, J. J.; Vekemans, J. A. J. M.; Meijer, E. W. *J. Am. Chem. Soc.* **2002**, *124*, 14759-14769. (c) Bushey, M. L.; Hwang, A.; Stephens, P. W.; Nuckolls, C. *Angew. Chem. Int. Ed.* **2002**, *41*, 2828-2831. (d) Bushey, M. L.; Nguyen, T. Q.; Nuckolls, C. *J. Am. Chem. Soc.* **2003**, *125*, 8264-8269. (e) Zhang, W.; Horoszewski, D.; Decatur, J.; Nuckolls, C. *J. Am. Chem. Soc.* **2003**, *125*, 4870-4873. (f) Wilson, A. J.; van Gestel, J.; Sijbesma, R. P.; Meijer, E. W. *Chem. Commun.* **2006**, DOI: 10.1039/b610051a.
- ²² Paraschiv, I.; Giesbers, M.; van Lagen, B.; Grozema, F. C.; Abellon, R. D.; Siebbeles, L. D. A.; Marcelis, A. T. M.; Zuilhof, H.; Sudhölter, E. J. R. *Chem. Mater.* **2006**, *18*, 968-974.
- ²³ Lemaur, V.; da Silva Filho, D. A.; Coropceanu, V.; Lehmann, M.; Geerts, Y.; Piris, J.; Debije, M. G.; van de Craats, A. M.; Senthilkumar, K.; Siebbeles, L. D. A.; Warman, J. M.; Brédas, J. L.; Cornil, J. *J. Am. Chem. Soc.* **2004**, *126*, 3271-3279.
- ²⁴ Warman, J. M.; van de Craats, A. M. *Mol. Cryst. Liq. Cryst.* **2003**, *396*, 41-72.

- ²⁵ (a) Kraft, A.; Reichert, A.; Kleppinger, R. *Chem. Commun.* **2000**, 1015-1016. (b) Lau, K.; Foster, J.; Williams, V. *Chem. Commun.* **2003**, 2172-2173. (c) Dierking, I. *Textures of Liquid Crystals* **2003**, Wiley-VCH. (d) Grelet, E.; Bock, H. *Europhys. Lett.* **2006**, *73*, 712-718.
- ²⁶ Zhao, K. Q.; Gao, C. Y.; Hu, P.; Wang, B. Q.; Li, Q. *Acta Chimica Sinica*, **2006**, *64*, 1051-1062.
- ²⁷ Ladd, M.; Palmer, R. *Structure Determination by X-ray Crystallography* **2003**, Fourth Edition, Kluwer Academic / Plenum Publishers.
- ²⁸ Kettner, A.; Wendorff, J. H. *Liq. Cryst.* **1999**, *26*, 483-487.
- ²⁹ (a) Simmerer, J.; Glusen, B.; Paulus, W.; Kettner, A.; Schuhmacher, P.; Adam, D.; Eitzbach, K. H.; Siemensmeyer, K.; Wendorff, J. H.; Ringsdorf, H.; Haarer, D. *Adv. Mater.* **1996**, *8*, 815-819; (b) Glusen, B.; Heitz, W.; Kettner, A.; Wendorff, J. H. *Liq. Cryst.* **1996**, *20*, 627-633. (c) Glusen, B.; Kettner, A.; Wendorff, J. H. *Mol. Cryst. Liq. Cryst.* **1997**, *303*, 115-120.
- ³⁰ Gray, G. W.; Winsor, P. A. *Liq. Cryst. & Plastic Crystals* **1974**, Ellis Horwood: Chichester, vol. I.
- ³¹ Wasserfallen, D.; Kastler, M.; Pisula, W.; Hofer, W. A.; Fogel, Y.; Wang, Z.; Müllen, K. *J. Am. Chem. Soc.* **2006**, *128*, 1334-1339.
- ³² Pisula, W. "Control of the Long-Range Self-Organization of Polycyclic Aromatic Hydrocarbons for Devices Applications", *Ph. D. Thesis* **2005**, Mainz University, Germany.
- ³³ (a) Skrovanek, D. J.; Howe, S. E.; Painter, P. C.; Coleman, M. M. *Macromolecules*, **1985**, *18*, 1676-1683. (b) Setoguchi, Y.; Monobe, H.; Wan, W.; Terasawa, N.; Kiyohara, K.; Nakamura, N.; Shimizu, Y. *Thin Solid Films*, **2003**, *438-439*, 407-413. (c) Xue, C.; Jin, S.; Weng, X.; Ge, J. J.; Shen, Z.; Shen, H.; Graham, M. J.; Jeong, K. U.; Huang, H.; Zhang, D.; Guo, M.; Harris, F. W.; Cheng, S. Z. D.; Li, C. Y.; Zhu, L. *Chem. Mater.* **2004**, *16*, 1014-1025.
- ³⁴ Günzler, H.; Gremlich, H. U. "IR Spectroscopy – An Introduction", **2002**, Wiley-VCH, 225-226.
- ³⁵ (a) Brunsveld, L.; Vekemans, J. A. J. M.; Hirschberg, J. H. K. K.; Sijbesma, R. P.; Meijer, E. W. *PNAS* **2002**, *99*, 4977-4982. (b) Kamikawa, Y.; Nishii, M.; Kato, T. *Chem. Eur. J.* **2004**, *10*, 5942-5951.
- ³⁶ (a) Warman, J. M.; Gellinck, G. H.; de Haas, M. P. *J. Phys.: Condens. Matter.* **2002**, *14*, 9935-9954. (b) Watson, M. D.; Debije, M. G.; Warman, J. M.; Müllen, K. *J. Am. Chem. Soc.* **2004**, *126*, 766-771. (c) Warman, J. M.; de Haas, M. P.; Dicker, G.; Grozema, F. C.; Piris, J.; Debije, M. G. *Chem. Mater.* **2004**, *16*, 4600-4609.

³⁷ Pisula, W.; Kastler, M.; Wasserfallen, D.; Mondeshki, M.; Piris, J.; Schnell, I.; Müllen, K.
Chem. Mater. **2006**, *18*, 3634-3640.

Appendix

Polarized Optical Microphotographs

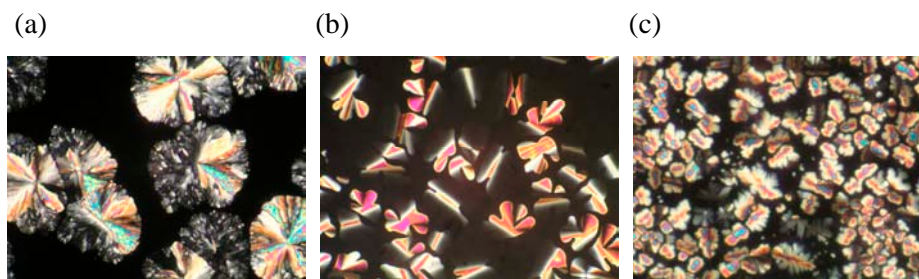


Figure 1. Polarized optical microphotographs of **2-3T1** at 64 °C (a), **2-3T2** at 63 °C (b) and **2-4T1** at 57 °C (c) (Chapter 2 – page 29).

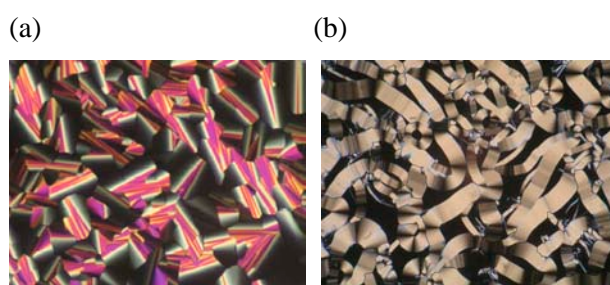


Figure 2. Polarized optical microphotographs of **4-2** at 78 °C (a) (Chapter 3 – page 56) and of **1** at 196 °C (b) (Chapter 4 – page 77).

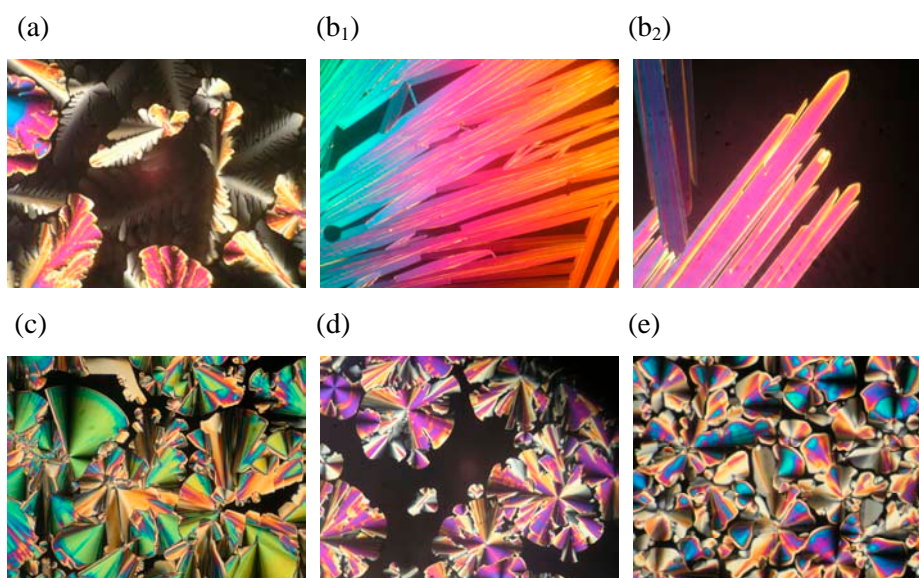


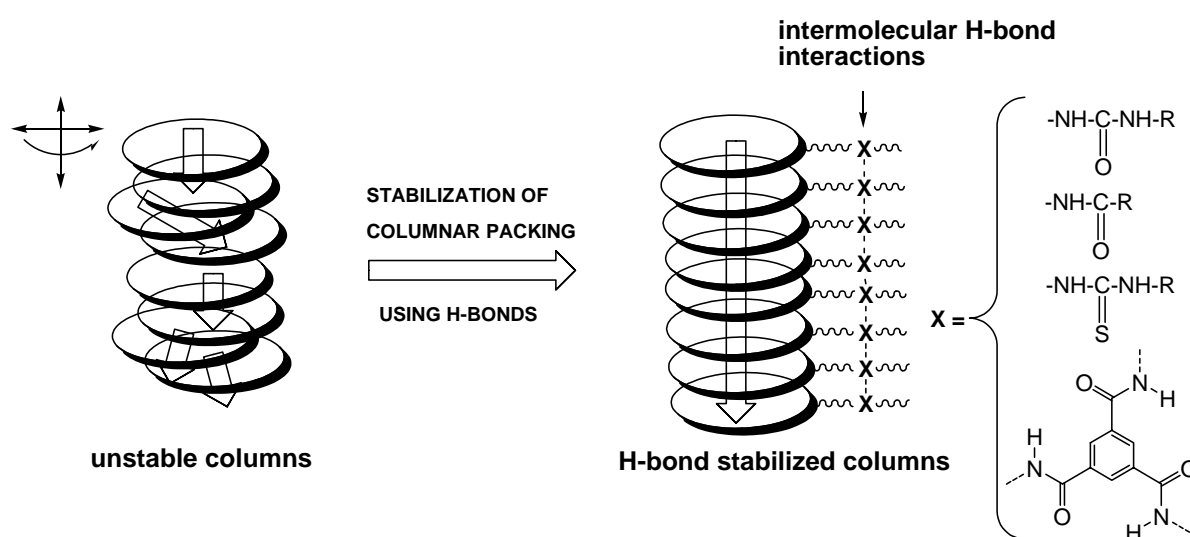
Figure 3. Polarized optical microphotographs of **7a** at 169 °C (a), **7b** at 193 °C (b₁ and b₂), **7c** at 172 °C (c), **7d** at 187 °C (d) and **7e** at 177 °C (e) (Chapter 5 – page 97).

Summary

Since 1977, more than 2300 publications on discotic (disk-like) liquid crystalline materials have appeared. Discotic liquid crystals, which usually consist of polyaromatic molecules surrounded by long peripheral alkyl tails, can form liquid crystalline mesophases in a wide temperature range. Within these mesophases, the molecules self-assemble in large columnar stacks *via* π -stacking interactions between the aromatic cores. These assemblies can provide an efficient charge transport pathway, as indicated by their informal designation as “*molecular-wires*”. As a result, they nowadays attract significant interest for optoelectronic applications. Several possible applications where discotic liquid crystals could be used are field effect transistors (FETs), light emitting diodes (LEDs) and photovoltaic solar cells.

In all the discotic materials described so far, the molecules inside the columns, can still rotate around the columnar axis, slide out of the columns or oscillate within the columnar stack. This represents a limitation of their applicability as “*molecular-wires*”. Therefore, in this research, an additional stabilization of columnar discotic mesophases was envisaged in order to increase their organization, without the frequently concomitant loss of processability that would result from extensions of the aromatic core.

The research described in this thesis focuses on the stabilization of columnar mesophases by highly tunable (i.e. controlled) H-bonding interactions, without enlarging the aromatic cores and thus maintaining their processability. This approach is depicted in Scheme 1.



Scheme 1. Representation of the use of H-bond stabilization of columnar discotic liquid crystals.

Summary

Functional H-bonding groups, such as urea, amide, thiourea or 1,3,5-benzenetrisamide, have been used in this work, in order to create a H-bonding network parallel to the columnar axis, alongside the existing π - π stacking interactions between the disk-like molecules.

In *Chapter 1* an overview of the different types of liquid crystalline phases is presented, with emphasis on the organization of columnar discotic mesophases. Since this work focuses on the hydrogen bond stabilization of the triphenylene-based discotic liquid crystals, the most important synthetic approaches towards these materials are discussed. Several of these methods were applied to prepare the materials investigated in Chapters 2 to 5. Besides the *synthetic* aspect, several characterization techniques, which are normally used to investigate the properties of the liquid crystal materials, are shortly discussed.

Chapter 2 deals with the synthesis and thermotropic properties of a series of hexaalkoxytriphenylenes that contain one amide, urea or thiourea group in one of their alkoxy tails, as H-bond forming group. The biphenyl route turns out to be the best with respect to yields and versatility, as compared to other methods. The optical polarization microscopy, differential scanning calorimetry and X-ray studies show that the intermolecular hydrogen bonding has a negative influence on the formation and stability of the columnar liquid crystalline phases: The stronger the hydrogen bonding, the more the liquid crystallinity is suppressed. This is probably due to disturbance of the π - π stacking of the triphenylene disks and a lower flexibility of the alkyl tails. So far, the urea and amide containing triphenylene derivatives do not exhibit liquid crystalline properties, probably because an H-bond stabilization of the crystalline state is obtained. However, several thiourea derivatives show columnar hexagonal (Col_h) mesophases, because in these compounds the π - π interactions are more important than the relatively weak thiourea hydrogen bonding.

Because in the columnar mesophases the motions of the aromatic core and the alkyl tails are strongly correlated, the length of the alkyl chains, which surround the disk-like aromatic cores, is an important factor that determines the stability of the columns. Since in the previous chapter long substituents carrying an urea, amide or thiourea group have been used, a complementary study, with focus on the synthesis and phase behavior of unsymmetrically substituted hexaalkoxytriphenylenes, is described in *Chapter 3*. In this study, one of the hexyloxy chains in hexahexyloxytriphenylene (HAT6) is replaced by either a shorter or longer chain. In the series $\text{HAT}-(\text{OC}_6\text{H}_{13})_5-(\text{OC}_n\text{H}_{2n+1})$, with n ranging from 2 to 18, the compounds with $n \geq 13$ are not liquid crystalline anymore. For all compounds with $n \leq 12$, Col_h phases are found. Furthermore, X-ray investigations show that the intercolumnar

distance gradually increases from 20.19 Å to 22.03 Å, with increasing n , while a small odd-even effect on the increase of the intercolumn distance with n is observed. This odd-even effect is also found in the change of ΔH of isotropization with n . The interdisk distance remains constant (3.6 Å).

Since the stabilization of the columnar mesophase by H-bonding interactions still remains an unsolved issue, *Chapter 4* describes a 1,3,5-benzenetrisamide with three pendant hexaalkoxytriphenylene groups, as a new approach for the intermolecular H-bond-stabilization of columnar discotic liquid crystalline materials. This compound forms a columnar hexagonal plastic (Col_{hp}) discotic phase with a clearing point at 208 °C. Surprisingly, the material does not crystallize on cooling from the isotropic phase, even after annealing for a few days at room temperature, but goes into a glassy state due to the enforced H-bonding network formed between the benzenetrisamide units. Modeling studies show that the central 1,3,5-benzenetrisamide cores are rotated 60° with respect to each other, which makes the adjacent triphenylene moieties to stack with a small 15° rotation. This small rotation observed between the adjacent triphenylene units plays a key role, since for such a rotation ~85 % of the maximum charge transfer integral is achieved. This result is correlated to the very high charge carrier mobility of 0.12 cm² V⁻¹ s⁻¹ at 180 °C, found for this particular compound. This value is the second highest ever reported for liquid crystalline triphenylene systems. This is a first proof for the intermolecular H-bonding stabilization of the columnar organization of triphenylene moieties, without losing the ease of processing provided by the liquid crystalline phase.

Since the modeling discussed in the previous chapter suggests that the conformation of the butyl spacer, which is used for that particular compound, dictates the π - π overlap of the triphenylene units within the liquid crystal phase, a new series of 1,3,5-benzenetrisamide derivatives with three hexaalkoxytriphenylene pendant groups is prepared and their properties discussed in *Chapter 5*. In this case, the length of the spacer, as well as the size of the *ortho*-substituent at the triphenylene core is varied. Taking into account these modifications, all these materials show liquid crystalline behavior with high isotropization points (170-200 °C). Different columnar hexagonal phases have been identified going from a columnar hexagonal plastic (Col_{hp}) phase, when using a butyl spacer, with a shorter butyl *ortho*-substituent of the triphenylene core, to a columnar hexagonal disordered (Col_{hd}) phase, when a pentyl spacer is used and a hexyl *ortho*-substituent is present on the triphenylene groups. A chiral 1,3,5-benzenetrisamide was shown to form columnar stacks with a single helical organization, both

Summary

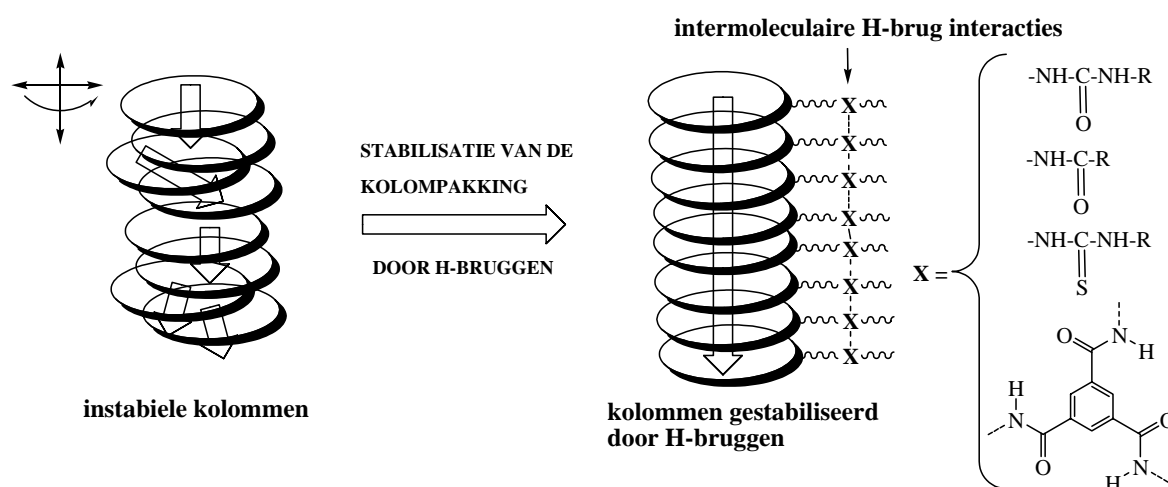
in an apolar solvent and in a film, as found by circular dichroism studies. By using pulse-radiolysis time-resolved microwave conductivity, charge carrier mobilities as high as $0.25 \text{ cm}^2 \text{ V}^{-1} \text{ s}^{-1}$ are found for the liquid crystalline phase (Col_h) of this chiral derivative. This mobility is twice the highest value ever reported for triphenylene-based liquid crystalline materials, approaching mobilities found for hexabenzocoronene-based liquid crystals, with a much larger aromatic core. This is a substantial improvement regarding the stabilization of disk-like molecules within their liquid crystal phase, without expanding the aromatic cores, but by tuning the H-bonding and the length of the spacer.

Samenvatting

Sinds 1977 zijn er meer dan 2300 publicaties over discotische of schijfvormige vloeibaar kristallijne materialen verschenen. Discotische moleculen, die meestal bestaan uit polyaromatische kernen omgeven door lange perifere alkylstaarten, kunnen vloeibaar kristallijn mesofasengedrag vertonen in een breed temperatuurtraject. In deze mesofasen zijn de moleculen gerangschikt in lange kolommen door π - π interacties tussen de aromatische kernen. Door deze ordening kan er een efficiënt ladingstransport door de kolommen plaatsvinden, waardoor ze ook wel informeel “moleculaire stroomdraden” worden genoemd. Dit is één van de redenen waardoor er tegenwoordig grote interesse is in opto-elektronische toepassingen van deze moleculen. Enkele van deze mogelijke toepassingen, waarbij discotische vloeibare kristallen gebruikt worden, zijn veldeffekt transistors, licht-emitterende diodes en fofovoltaïsche zonnecellen.

In alle discotische materialen die tot nu toe beschreven zijn kunnen de moleculen in de kolommen nog steeds kunnen roteren rond de kolom-as, uit de kolom kunnen schuiven of oscilleren in de kolomrangschikking. Dit beperkt hun toepasbaarheid als “moleculaire stroomdraden” zeer. Daarom is in dit onderzoek getracht om een additionele stabilisatie van de kolomfasen te introduceren, zonder de verwerkbaarheid te verminderen zoals vaak optreedt bij vergroting van de aromatische kernen.

Het onderzoek beschreven in dit proefschrift is gericht op de stabilisatie van kolomfasen door tot in detail controleerbare waterstofbruginteracties, zonder vergroting van de aromatische kern en dus met behoud van verwerkbaarheid. Deze benadering is weergegeven in Schema 1.



Schema 1. Weergave van het gebruik van waterstofbrugstabilisatie van kolomvormende schijfvormige vloeibare kristallen.

Samenvatting

In dit project zijn functionele waterstofbrugvormende groepen gebruikt, zoals urea, amide, thiourea, of 1,3,5-benzeentrisamide om waterstofgebrugde netwerken te creëren parallel aan de kolom-as langs de bestaande π - π interacties tussen de schijfvormige moleculen.

In *Hoofdstuk 1* wordt een overzicht van verschillende typen vloeibaar kristallijne fasen gegeven, met nadruk op de organisatie van kolomfasen van schijfvormige moleculen. Vanwege de focus op waterstofbrugstabilisatie van trifenyleen-bevattende schijfvormige vloeibare kristallen, zijn de meeste belangrijke syntheseroutes voor deze materialen beschreven. Enkele methoden, die zijn toegepast bij de bereiding van de materialen, beschreven in Hoofdstukken 2 tot en met 5 zijn onderzocht. Naast het synthetische aspect worden verscheidene karakterisatietechnieken, die gebruikt worden om de eigenschappen van vloeibaar kristallijne materialen te onderzoeken, kort besproken.

In *Hoofdstuk 2* worden de synthese en de thermotrope eigenschappen van enkele series van hexaalkoxytrifenylenen behandeld, die een amide, urea of thiourea groep in één van hun alkylstaarten als waterstofbrugvormende groep bevatten. Ten opzichte van andere methoden blijkt de bifenyl route het beste te werken, met betrekking tot opbrengst en veelzijdigheid. Studies met optische polarisatiemicroscop, differential scanning calorimetry en X-ray laten zien dat de intermoleculaire waterstofbrugvorming een negatieve invloed heeft op de vorming en stabilisatie van de kolomnaire vloeibaar kristallijne fasen. Hoe sterker de waterstofbruggen, hoe meer de vloeibaar kristallijne mesofase is onderdrukt. Dit komt waarschijnlijk door de verstoring van de π - π interacties in de trifenyleen schijven en de verminderde bewegingsmogelijkheden van de alkylstaarten. Tot dusverre vertonen de urea en amide bevattende trifenyleenderivaten geen vloeibaar kristallijne eigenschappen, doordat er waarschijnlijk een waterstofbrugstabilisatie in de kristallijne toestand plaatsvindt. Echter, verscheidene thioureaderivaten vertonen hexagonale (Col_h) mesofasen, omdat in deze stoffen de π - π interacties belangrijker zijn dan de relatieve zwakke thiourea waterstofbruggen.

Door de sterke correlatie tussen de bewegingen van de aromatische kernen en de alkylstaarten, is de lengte van de perifere alkylketens een belangrijke factor in de stabiliteit van de kolomfasen. Omdat de in Hoofdstuk 2 genoemde verbindingen lange substituenten met een urea, amide of thiourea groep bevatten, zijn de synthese en het fasengedrag van een serie niet-symmetrisch gesubstitueerde hexaalkoxytrifenyleen onderzocht in *Hoofdstuk 3*. In deze studie is één van de hexyloxyketens in hexahexyloxytrifenyleen (HAT6) vervangen door een kortere of een langere keten. In de serie HAT-(OC₆H₁₃)₅-(OC_nH_{2n+1}), met n variërend van 2 tot 18 zijn de stoffen met $n \geq 13$ niet meer vloeibaar kristallijn. Voor alle stoffen met $n \leq 12$

zijn Col_h fasen waargenomen. Bovendien tonen X-ray studies aan dat de interkolomnaire afstanden toenemen van 20.19 Å naar 22.03 Å bij een toenemende n , terwijl er klein even-oddeven effect wordt waargenomen op de toenemende kolom-kolomafstand. Dit effect wordt ook gevonden bij de verandering van de ΔH van isotropisatie met n . De afstanden tussen de schijven blijft constant (3.6 Å) bij toenemende n .

Een andere benadering om de kolomfasen te stabiliseren door vorming van intermoleculaire waterstofbruginteracties, wordt in *Hoofdstuk 4* beschreven. Een 1,3,5-benzeentrisamideverbinding met drie daaraan bevestigde hexaalkoxytrifenyleen groepen is onderzocht. Dit materiaal vormt een kolomnaire hexagonale plastic (Col_{hp}) fase met een isotropisatietemperatuur van 208 °C. Opmerkelijk is dat dit materiaal niet uitkristalliseert na afkoeling uit de isotrope fase, ook niet na enkele dagen bewaren op kamertemperatuur. Het materiaal gaat over in een glastoestand door het gevormde waterstofbrugnetwerk tussen de benzeentrisamide eenheden. Modelstudies tonen aan dat de centrale 1,3,5-benzeentrisamide kernen 60° zijn geroteerd ten opzichte van elkaar, wat het mogelijk maakt de aangrenzende trifenyleen eenheden te rangschikken in kolommen met een kleine rotatie van 15° ten opzichte van elkaar. Deze kleine rotatie tussen de aangrenzende trifenyleen eenheden speelt mogelijk een belangrijke rol, omdat daardoor ~ 85 % van de maximale ladingsoverdrachts-integraal wordt bereikt. Dit resultaat is mogelijk direct gecorreleerd aan de zeer hoge ladingsdragermobiliteit van 0.12 cm² V⁻¹ s⁻¹ bij 180 °C, die voor deze specifieke stof is gevonden. Deze waarde is de op twee na hoogste ooit gerapporteerd voor vloeibaar kristallijne trifenyleensystemen. Dit is het eerste bewijs voor de intermoleculaire waterstofbrugstabilisatie van de kolomnaire organisatie van trifenyleen bevattende moleculen, zonder verlies van de vloeibare kristallijne fase.

Omdat het model zoals bediscussieerd in het voorgaande hoofdstuk suggereert dat de conformatie van het butyl tussenstuk, dat gebruikt wordt in deze specifieke stof, de π - π overlap van de triphenyleen eenheden in de vloeibaar kristallijne fase dicteert, zijn er nieuwe series van 1,3,5-benzeentrisamide derivaten met drie hexaalkoxytrifenyleen zijgroepen gesynthetiseerd en zijn hun eigenschappen bestudeerd zoals beschreven in *Hoofdstuk 5*. In dit geval is de lengte van het tussenstuk en de grootte van de *ortho*-substituent op de trifenyleen schijf gevarieerd. Al deze materialen vertonen vloeibaar kristallijn gedrag met hoge isotropisatiepunten (170-200 °C). Verschillende hexagonale kolomnaire fasen zijn geïdentificeerd; van hexagonale plastic kolomfasen (Col_{hp}), bij gebruik van een butyl spacer met een korte butyl *ortho*-substituent op de trifenyleen schijf tot een hexagonaal verstoorde

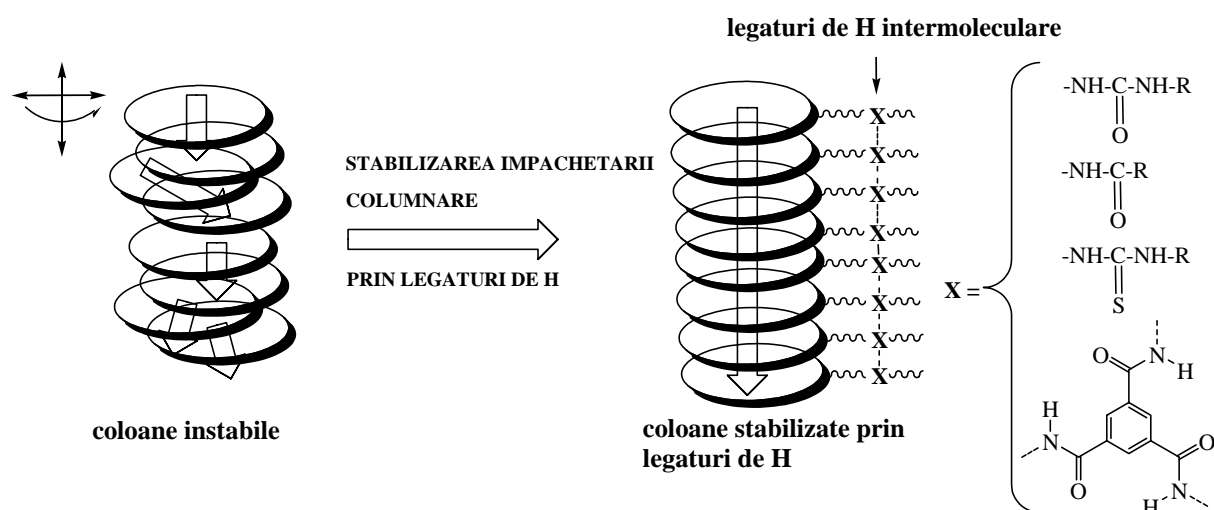
Samenvatting

kolomfase (Col_{hd}) bij gebruik van een pentyl spacer en een hexyl *ortho*-substituent op de trifenyleengroep. Er is aangetoond dat een chiraal 1,3,5-benzeentrisamide een kolomnaire rangschikking vertoont met een enkele spiraalvormige organisatie, zowel in een apolair oplosmiddel als in een film zoals is waargenomen met circulair dichroïsme studies. Met behulp van een studie van de puls-radiolyse geïnduceerde tijdsopgeloste microgolf geleidbaarheid werd een ladingsoverdrachtsmobiliteit bepaald van $0.25 \text{ cm}^2 \text{ V}^{-1} \text{ s}^{-1}$ voor de vloeibaar kristallijne fase (Col_{h}) van dit chirale derivaat. Deze mobiliteit is zelfs tweemaal de hoogste tot nu toe gerapporteerde waarde voor trifenyleen- bevattende vloeibaar kristallijne materialen. Deze waarden zijn vergelijkbaar met waarden gevonden voor hexabenzocoroneen-bevattende vloeibare kristallen met een veel grotere aromatische kern. Dit is een aanzienlijke verbetering ten opzichte van de stabilisatie van schijfvormige moleculen in hun vloeibaar kristallijne fase zonder vergroting van het aromatische gedeelte, door het inbouwen van waterstofbruggen en variatie in de lengte van de spacers.

Rezumat

Un număr de peste 2300 de articole științifice au fost publicate începând cu 1977, cu privire la moleculele în formă de disc (discotice), prezentând proprietăți de cristal lichid. În principiu, cristalele lichide discotice, sunt constituite din molecule poli-aromatice substituie cu lungi lanțuri alchilice. Datorită acestor substituenți, aceste molecule au abilitatea de a forma mezofaze pe un domeniu larg de temperatură. În aceste mezofaze, moleculele pot să se autoasambleze sub formă columnară de înălțimi apreciabile. Această organizare are la bază interacțiunile dintre orbitalii π , ce aparțin nucleelor aromatice adiacente, dispuse paralel. Aceste coloane pot juca rolul unor conductori eficienți ale sarcinilor electrice, așa cum sugerează denumirea lor formală: “cabluri-moleculare”. Ca rezultat al acestei abilități, aceste sisteme indică, în prezent, un mare punct de atracție, pentru aplicațiile din industria optico-electronică. Câteva dintre posibilele aplicații în acest domeniu, unde cristalele lichide discotice ar putea fi folosite sunt tranzistorii, diodele luminescente și celulele solare fotovoltaice.

În toate materialele discotice descrise până în prezent, aceste molecule au abilitatea de a se roti în jurul axei columnare, de a efectua mișcări de translație în afara coloanei sau să oscileze în interiorul coloanei. Toate aceste fluctuații nedorite micșorează utilitatea practică a acestor materiale discotice în scopul folosirii lor drept “cabluri-moleculare”. Din acest motiv, a fost preconizată o stabilizare adițională a moleculelor discotice în interiorul mezofazei, în vederea creșterii gradului de ordonare, fără pierderea concomitentă a procesabilității (ex. scăderea solubilității), fenomen ce ar apărea în cazul extinderii nucleelor aromatice.



Schema 1. Reprezentarea rolului legăturilor de hidrogen în vederea stabilizării cristalelor lichide discotice columnare.

Rezumat

Cercetarea descrisă în această teză este concentrată pe stabilizarea mezofazelor columnare prin intermediul legăturilor de H, introduse controlat, fără extinderea nucleelor aromatice și fără a afecta procesabilitatea materialului sintetizat. Acest concept este descris în Schema 1. Diferite „motive” funcționale, ca cele întâlnite de exemplu în uree, amide substituie, tiouree și 1,3,5-benzotrisamide, toate capabile să formeze legături de hidrogen, au fost folosite în vederea „proiectării” unei rețele de legături de H, paralelă cu axa columnară, în „sfera a doua de coordonare” a deja existentei împachetări π - π dintre nucleele aromatice.

Capitolul 1, cuprinde o prezentare generală a tipurilor de faze întâlnite în cristalele lichide, insistându-se în special asupra organizării mezofazelor columnare discotice. Deoarece, subiectul prezentei teze este focalizat pe stabilizarea cristalelor lichide discotice ce pornesc de la trifenilen, în Capitolul 1 se prezintă cele mai importante căi de sinteză pentru aceste materiale în urma studiului exhaustiv al literaturii de specialitate. O parte dintre acestea au fost utilizate în sinteza materialelor prezentate în Capitolele 2-5. Tot în Capitolul 1 se face o trecere succintă în revistă a diferitelor tehnici de caracterizare și investigare a proprietăților materialelor ce prezintă caracter de cristal lichid.

În *Capitolul 2* sunt prezentate sinteza și proprietățile termotropice a unei serii de hexaalchiloxitriphenileni substituiți cu lanțuri alchilice, în care unul din lanțuri conține inserat un „motiv” de tip amidic, ureic sau tioureic, toate capabile să angajeze legături de H de intensități diferite. În ceea ce privește randamentul și versalitatea metodelor folosite, cea mai eficientă este metoda bifenil. Pentru acești compuși, studiile de microscopie optică în lumină polarizată, calorimetrie diferențială (DSC) și raze X arată că legăturile intermoleculare de H influențează în mod negativ formarea și stabilitatea fazelor columnare de cristal lichid. Cu cât legăturile de H sunt mai puternice, cu atât intervalul de temperatură, în care proprietatea de cristal lichid se manifestă, este mai mic. Acest efect este datorat probabil, perturbării interacțiunilor π - π de instivuire a discurilor de trifenilen și reducerii flexibilității lanțurilor alchilice. Derivații de trifenilen, ce conțin grupări amidice sau de tip uree substituită, nu prezintă proprietăți de cristal lichid, probabil, datorită stabilizării puternice prin legături de H a fazei cristaline. Cu toate acestea, o parte din derivații de trifenilen cu grupări tioureice formează mezofaze columnare hexagonale (Col_h). În acest caz, interacțiunile π - π de instivuire dintre nucleele aromatice devin mult mai importante în raport cu legăturile de H, relativ slabe, existente între grupările amino și tiocarbonil ce se angajează între unitățile de tiouree substituită, din lanțurile paralele.

Ținând cont de faptul că în fazele columnare mișcările nucleelor aromatice sunt puternic corelate cu mișcările lanțurilor alchilice, lungimea acestor lanțuri, care de fapt înconjoară discurile aromatice, joacă un rol determinant în ceea ce privește stabilitatea organizării columnare. Deoarece în capitolul anterior au fost prezentate rezultatele obținute la folosirea substituenților cu lanțuri alchilice foarte lungi ce conțin grupări amidice, ureice sau tioureice, în *Capitolul 3* este prezentat un studiu complementar asupra sintezei și proprietăților termotropice a unei serii de derivați de hexaalchiloxitriifenilen, asimetric substituiți. În acest studiu, unul dintre lanțurile substituente din hexaalchiloxitriifenilen (**HAT6**) este înlocuit cu un lanț alchilic mai lung sau mai scurt decât radicalul hexil. În seria HAT-(OC₆H₁₃)₅-(OC_nH_{2n+1}), cu n între 2 și 18, compușii cu $n \geq 13$ nu indică proprietăți de cristal lichid. Pentru ceilalți compuși în care $n \leq 12$ a fost pusă în evidență o mezofază columnară hexagonală (Col_h). În plus, studiile de raze X arată că distanța intercolumnară crește gradual de la 20.19 Å până la 22.03 Å, o dată cu creșterea lui n . În ceea ce privește această creștere graduală, se poate observa un mic efect par-impair. Acest efect se regăsește și în cazul variației entalpiei de izotropizare, ΔH , ca funcție de n . Distanța între discurile aromatice rămâne constantă, cu un pas de 3.6 Å.

Deoarece stabilizarea mezofazei columnare prin legături de H a rămas o problemă nerezolvată, în *Capitolul 4* se descrie, drept soluție pentru stabilizarea prin legături de H intermoleculare a mezofazei columnare discotice, un nou compus și anume o 1,3,5-benzentrisamidă cu trei grupări de hexaalchiloxitriifenilen. Acest compus prezintă o mezofază plastică hexagonală columnară discotică, a cărei punct de izotropizare este 208 °C. Surprinzător, acest material nu cristalizează la răcirea din faza izotropă, chiar și după menținerea la temperatura camerei timp de câteva zile, dar trece într-o fază sticloasă datorită formării unei rețele de legături de H puternice între grupările amidice ale unităților de 1,3,5-benzentrisamidă. Studii computaționale de modelare moleculară sugerează că, partea centrală a moleculei și anume unitățile de 1,3,5-benzentrisamidă sunt rotite cu 60° una față de cealaltă, ceea ce induce o rotație cu numai 15° a unităților adiacente de trifenilen, organizate columnar. Această mică rotație, observată între unitățile adiacente de trifenilen joacă un rol cheie. La acest unghi de rotație este atins aproximativ 85 % din maximul integralei de transfer de sarcină. Acest rezultat s-a corelat foarte bine cu o creștere spectaculoasă a mobilității purtătorilor de sarcină, determinată experimental pentru acest compus ($0.12 \text{ cm}^2 \text{ V}^{-1} \text{ s}^{-1}$, la 180 °C). Această valoare neobișnuit de mare este a doua ca mărime raportată vreodată pentru cristalele lichide pe bază de trifenilen. Această corelație constituie un argument ferm al ideii

Rezumat

stabilizării prin legături de H intermoleculare a organizării columnare a derivaților de trifenilen fără pierderea ușurinței de procesare oferită de faza de cristal lichid.

Rezultatele modelărilor, discutate în capitolul anterior, sugerează că, aranjamentul conformațional al lanțului butilic (ca distanțier) controlează împachetarea π - π a unităților de trifenilen în interiorul fazei de cristal lichid. Pornind de la această constatare, au fost sintetizați o nouă serie de derivați ai 1,3,5-benzentrisamidei substituiți cu trei grupări de hexaalchiloxitriphenilen. Rezultatele obținute în urma sintezelor efectuate precum și proprietățile acestor compuși sunt discutate în *Capitolul 5*. În acest caz, pe lângă lungimea distanțierului, a fost modificată și mărimea substituentului din poziția *orto* a nucleului trifenilenic. Aceste modificări structurale au condus la o serie de compuși, care au în totalitate, comportament de cristal lichid cu temperaturi ridicate de izotropizare (170-200 °C). În seria de compuși nou sintetizați, au fost identificate diferite faze hexagonale columnare: o fază plastică hexagonală columnară discotică (Col_{hp}) pentru compusul ce conține un distanțier butilic, având substituentul butil în poziția *orto* la nucleul trifenilenic și o fază hexagonală dezordonată (Col_{hd}) pentru compusul ce conține un distanțier pentilic, având substituentul hexil în poziția *orto* a nucleului trifenilenic.

Studiile de dicroism circular efectuate asupra unui derivat chiral al 1,3,5-benzentrisamidei atât în soluție cât și în peliculă, au arătat o împachetare columnară cu o singură orientare a helixului. În faza de cristal lichid, a acestui compus chiral (Col_h), mobilitatea purtătorilor de sarcină în urma determinărilor de conductivitate, are valoarea apropiată de $0.25 \text{ cm}^2 \text{ V}^{-1} \text{ s}^{-1}$ la 150 °C.

Această valoare este de două ori mai mare decât cea mai mare valoare raportată vreodată în literatura de specialitate pentru materialele cu comportament de cristal lichid pe bază de trifenilen, valoare care se apropie de cea a cristalelor lichide construite pe bază de hexabenzocoronan, caracterizate printr-un nucleu aromatic mult mai mare.

Aceasta este o îmbunătățire substanțială în ceea ce privește stabilizarea fazei de cristal lichid a moleculelor discotice, fără extinderea nucleului aromatic, ci doar prin exploatarea cu precizie a legăturilor de H intermoleculare și exploatarea aranjamentului conformațional privilegiat al unui distanțier.

Curriculum Vitae

Ioan Paraschiv was born on August 4th 1976 in Roman, Romania. After attending the primary school, he went to the secondary school at “Roman-Vodă” Lyceum, where he obtained his baccalaureate diploma in 1995. Later, in the same year, he began his undergraduate studies at the Faculty of Chemistry of the “Al. I. Cuza” University of Iași, Romania. He specialized in Physical Chemistry, under the supervision of Prof. Dr. A. Onu. He obtained the Bachelor of Science (B.Sc.) degree (*cum laude*) in 1999, with the graduation thesis entitled: “*Glass transition of polymers: significance and determination methods*”.

Starting from autumn 1999, he has been working part-time, for one year, at “Petru-Poni” Institute of Macromolecular Chemistry in Iași, in the Polymer Physics and Structure Department, under the supervision of Dr. Virgil Bărboiu. Meanwhile, he followed the M.Sc. courses in the Structure and Reactivity Section, of the Faculty of Chemistry, at the same university in Iași. With the M.Sc. thesis, entitled “*Starch / clay nano-composites: a new biodegradable and "green" material for bio-plastic applications*”, prepared under the supervision of Prof. Dr. A. Onu, he obtained the M.Sc. degree in 2001. The experimental work for his M.Sc. thesis was done in the Laboratory of Polymer Technology, under the supervision of Prof. Dr. P. J. Lemstra, at the Technical University Eindhoven (TU/e). Also at TU/e, he worked for a period of seven months on an *experimental study of 3D mixing* of viscous fluids, under the supervision of Prof. Dr. H. E. H. Meijer at the Materials Technology Institute.

In January 2002, he joined the Laboratory of Organic Chemistry, at Wageningen University. After six months as a research-fellow, he was appointed as a PhD-student from 1st of July 2002, on an NWO research project on the H-bond stabilization of columnar discotic liquid crystals (project number 700.50.003). The results obtained during these last four years are presented in this thesis and a number of publications.

Since January 2007 he has been working as a Junior Project Leader - Life Sciences Group at Avantium Technologies B.V. in Amsterdam.

List of Publications

Paraschiv, I.; Giesbers, M.; van Lagen, B.; Grozema, F. C.; Abellon, R. D.; Siebbeles, L. D. A.; Marcelis, A. T. M.; Zuilhof, H.; Sudhölter, E. J. R., H-Bond-Stabilized Triphenylene-Based Columnar Discotic Liquid Crystals, *Chem. Mater.* **2006**, *18*, 968-974.

Paraschiv, I.; Delforterie, P.; Giesbers, M.; Posthumus, M. A.; Marcelis, A. T. M.; Zuilhof, H.; Sudhölter, E. J. R., Asymmetry in Liquid Crystalline Hexaalkoxy Triphenylene Discotics, *Liq. Cryst.* **2005**, *32*, 977-983.

Yildirim, Z.; Wübbenhorst, M.; Mendes, E.; Picken, S. J.; Paraschiv, I.; Marcelis, A. T. M.; Zuilhof, H.; Sudhölter, E. J. R., Multiple Glass Transitions in the Plastic Crystal Phase of Triphenylene Derivatives, *J. Non-Cryst. Solids* **2005**, *351*, 2622-2628.

Yildirim, Z.; Mendes, E.; Paraschiv, I.; Zuilhof, H.; de Vos, W. M.; Marcelis, A. T. M.; Sudhölter, E. J. R.; Picken, S. J., Binary Phase Diagram of Triphenylene Derivatives: The Role of Hydrogen Bonds, *Mol. Cryst. Liq. Cryst.* **2005**, *439*, 2103-2109.

Catanescu, O.; Paraschiv, I.; Sava, I.; Simionescu, Cr. I.; Hurduc, N.; Scutaru, D., Liquid crystalline polymers: 10: Synthesis and thermal behavior of some polyethers containing a hexamethylenic spacer, *Int. J. Polym. Mater.* **2004**, *53*, 33-43.

Vasile, C.; Cazacu, G.; Onu, A.; Paraschiv, I.; Agafitei, G., Influence of the Polyethyleneglycol (PEG) Content on the Properties of the Ethyleneglycolterephthalate / Polyethyleneglycol Terephthalate Copolymers, *Int. J. Polym. Mater.* **2003**, *52*, 573-585.

Gaina, V.; Gaina, C.; Paraschiv, I., Thermal behavior and cured products of bis(4-maleimidodiphenyl)methane, bis(isomaleimidodiphenyl)methane and 4,4'-diaminodiphenyl methane mixtures, *J. Appl. Polym. Sci.* **2003**, *89*, 3547-3556.

Filip, D.; Simionescu, Cr. I.; Macocinschi, D.; Paraschiv, I., Miscibility of liquid crystal / polymer blends, *J. Thermal Anal. Cal.* **2001**, *65*, 821-827.

List of Publications

Catanescu, O.; Hurduc, N.; Scutaru, D.; Sava, I.; Paraschiv, I.; Alazaroaie, S., Liquid crystalline polymers. 12 Thermal behavior of some aromatic polyethers containing azobenzene and biphenyl moieties, *Rev. Roum. Chimie*, **2000**, *45*, 709-715.

Manuscripts in Preparation

Paraschiv, I.; Tomkinson, A.; Giesbers, M.; Posthumus, M. A.; Marcelis, A. T. M.; Zuilhof, H.; Sudhölter, E. J. R., Amide, Urea and Thiourea-Triphenylene Derivatives: Synthesis and Mesomorphic Properties - manuscript in preparation.

Paraschiv, I.; de Lange, K.; Yildirim, Z.; Mendes, E.; Picken S. J.; Grozema, F. C.; Giesbers, M.; Posthumus, M. A.; Marcelis, A. T. M.; Zuilhof, H.; Sudhölter, E. J. R., High Charge Carrier Mobility in H-Bond Stabilized 1,3,5-Benzenetrisamide Triphenylene Derivatives - manuscript in preparation.

Paraschiv, I.; Yildirim, Z.; Mendes, E.; Picken S. J.; Grozema, F. C.; Giesbers, M.; Marcelis, A. T. M.; Zuilhof, H.; Sudhölter, E. J. R., H-Bond Stabilization in N,N'-Dibutyloxy Benzenedicarboxamide Triphenylene Derivatives - manuscript in preparation.

Kruglova, O.; Mulder, F. M.; Picken, S. J.; Stride, J. A.; Paraschiv, I.; Zuilhof, H.; Kearly, G. J., A New Approach to Dispersive Kinetics: Experiment and Theory – submitted to *J. Chem. Phys.*

Yildirim, Z.; Grozema, F. C.; Mendes, E.; Abellon, R. D.; Wübbenhorst, M.; Siebbeles, L. D. A.; Picken, S. J.; Paraschiv, I.; Marcelis, A. T. M.; Zuilhof, H.; Sudhölter, E. J. R., Effect of Minor Structural Changes in a Homologous Series of Triphenylene Derivatives: Crystalline Phase - manuscript in preparation.

Yildirim, Z.; Grozema, F. C.; Mendes, E.; Abellon, R. D.; Siebbeles, L. D. A.; Picken, S. J.; Paraschiv, I.; Marcelis, A. T. M.; Zuilhof, H.; Sudhölter, E. J. R., Structural Changes and Their Effects on Physical Properties of Triphenylene Derivatives: Effects on Col Mesophase - manuscript in preparation.

Yildirim, Z.; Kotlewski, A.; Mendes, E.; Norder, B.; Picken, S. J.; Paraschiv, I.; Marcelis, A. T. M.; Zuilhof, H.; Sudhölter, E. J. R., A New Supramolecular Discotic Phase in Triphenylene Derivatives - manuscript in preparation.

Dankwoord

Looking back, after my Ph.D. research period, I honestly can say “*I worked very hard to get my degree!*” but also “*I had great fun!*” Throughout the last years my life slowly but surely changed, often without me perceiving it. As a result I became if not a personality, then at least a different person. Many people will exclaim: “*That’s normal, it happens to every Ph.D. student!*”. One thing I am extremely sure about: I’ve changed more than I expected, but most of these changes will definitely help me in the near future, not only as a scientist but also outside of my working area.

I wanted to say this before I begin to thank several people in the Laboratory of Organic Chemistry and also my fellow-workers outside the laboratory, for their time and patience while dealing with my *character*.

First of all, I want to thank Professor Ernst J. R. Sudhölter, my promoter, who reserved enough time and patience to show me that there always exists a second solution for a complex situation. I learned that going to extremes does not solve problems, but generates additional ones, which ultimately give you more headaches than you might have anticipated. I very much appreciate his scientific suggestions and most of all, that my opinions were also heard and taken into account.

Additionally, I would like to thank my co-promoters, Dr. Han Zuilhof and Dr. Ton Marcelis, for their infinite patience and dedicated time for my project. Many thanks also for taking care of the smallest details while correcting my papers and for indicating your scientific point of view with regard to my initial writings. I will always recall the trust I had from you two, from the beginning of my project. I thank you both, Han and Ton, for your didactical supervision, but most of all for the freedom I had working in the laboratory and supervising my students.

Regarding the persons involved directly in my project, I would like to thank Zeynep Yildirim (Delft University of Technology) for the collaboration, which resulted in several publications. I would like also to thank Professor Stephen J. Picken for the fruitful scientific observations and remarks on my manuscript. I appreciate the interest he showed for “*our discotics project*”, and for the periodical meetings we had in Wageningen and Delft, which provided me with useful information about the physical chemistry of discotic liquid crystals.

Dankwoord

Many thanks for the people from Opto-electronic Materials Section at TU Delft for their suggestions and help with the TRMC measurements: Professor L. D. A. Siebbeles, Dr. Ferdinand C. Grozema and Dr. R. D. Abelen.

I would like also to thank Professor G. J. Kearley and Olga Kruglova from IRI (Interfaculty Rector Institute) in Delft, for their remarks and scientific suggestions I received during our meetings.

The results presented in my thesis would not have been possible without the help I received regarding the synthesis of discotic liquid crystals. I would like to thank Wiebe M. de Vos, Paul Delforterie, Alistair Tomkinson, Puck Moll, Cristina Şişu, Kim de Lange, for their help and interest in the research they have performed, together with me, during different periods of time.

As I said in the beginning of my "*Dankwoord*", I had a great time while working at the Laboratory of Organic Chemistry, and that would not have been possible without my special colleagues and friends: Ganesan, Kishore, Ruud, Tina & Remko, Louis, Michael, Feng, Qiao-yu, Dawei, Floor, Frédérique, Cindy, Gregor, Annemarie, Ahmed, Agnes, Giedrius, Milena & Michel, Maud, Luc, Jurjen, Rosalie, Suzanne, Aliaksei, Bin, Bart, Jacob, Marloes, Melle, Loes and TuHa. We had a lot of fun together at *Loburg*, and later on at *Café Meijer*, having nice drinks. I enjoyed every labtrip organized throughout the years, and the AIO-excursions abroad. "*Hé Guys!*" ..., it has been a great time in Switzerland (2003) and in USA, California (2005).

My thanks also go to Dr. Marcel Giesbers for his help with X-ray analysis, Beb van Veldhuizen and Barend van Lagen for their help with NMR measurements, Elbert van der Klift for the elemental analysis, Dr. Maarten A. Posthumus for the determinations of exact masses, Adrie Westphal from Biochemistry Department for his help with CD spectroscopy measurements, Edwin Bakx from Food Chemistry Department for the help with Maldi-tof investigations.

Arie Koudijs, I thank you for the pleasant time I had in the lab, and also for the help you gave me regarding the Dutch language.

Without the Romanian support I would not have been able to go on with my work for all these years. Romanians are all over the world now, but one thing they always miss: their country

and their customs. My thanks go also to Dana Ionescu, Vanessa Maria, Oxana and Liviu Prodan, Manfred George Denzin, Gabi Preda, Eugen and Cristina Șișu, Marilena Cernat, Cozmina Vrabie & Rob Joosten, Ovidiu Danci, Mihai Gras, Ciprian Popovici, Anda Nicoleta and Gabi Istudor, and Olivia Radu, for making me feel a little bit closer to Romania. *Vă mulțumesc din inimă pentru timpul petrecut împreună și pentru zâmbetul fiecăruia dintre voi.*

I would like to thank Henk J. W. Berkel for his support, friendship, help and suggestions I received over the last few years, which made it easier for me to better understand the customs of Dutch society. *Dank je Henk!*

I need to acknowledge the support I got from my parents, my mother Irina (♣) and my father Victor, my brother Victor, my sister-in-law Gabi and my little niece Maria. I thank you all for the patience and trust you had in me. *Să vă dea Domnul zile cu sănătate să puteți avea grijă de Maria.*

One thing gives me a lot of joy and happiness in every moment and that's because with the help of God I managed during all these years to bring my family over here from time to time and show them various places in The Netherlands.

ioan.

OVERVIEW OF COMPLETED TRAINING ACTIVITIES

Discipline specific activities

Courses

Winter School on Organic Reactivity (WISOR), Bressanone, Italy, January 6th - 13th, **2003**

Interpretation of Crystal Structure Determinations, NWO Course, Utrecht University, The Netherlands, **2004**

Ischia Advanced School in Organic Chemistry (IASOC), Ischia, Italy, September 18th - 23rd, **2004**

Meetings

KNCV Meetings, "Liquid Crystals and Surfactants", Wageningen University, The Netherlands, **2002**

Ph.D. Study Trip, Organised by Organic Chemistry Laboratory, Switzerland, **2003**

KNCV Meetings, "Liquid Crystals and Surfactants", Technical University Eindhoven, The Netherlands, **2003**

NWO Meetings, "Structure and Reactivity Section", Lunteren, The Netherlands, **2003**

20th International Liquid Crystal Conference (ILCC), Ljubljana, Slovenia, July 4th – 9th, **2004**

NWO Meetings, "Structure and Reactivity Section", Lunteren, The Netherlands, October 25th - 27th, **2004**

KNCV Meetings, Liquid Crystals and Surfactants, Technical University Delft, The Netherlands, **2004**

33rd Topical Meeting on Liquid Crystals, Paderborn, Germany, March 16th – 18th, **2005**

NWO Meetings, "Structure and Reactivity Section", Lunteren, The Netherlands, October 17th - 19th, **2005**

Ph.D. Study Trip, Organised by Organic Chemistry Laboratory, California, USA, **2005**

NWO Meetings, "Structure and Reactivity Section", Lunteren, The Netherlands, October 23th -25th, **2006**

General courses

Dutch Language Course (4 levels out of 6), Language School, Wageningen University, The Netherlands, **2002 - 2004**

Scientific writing, Wageningen University, The Netherlands, **2003**

Organising and supervising M.Sc. thesis projects, Wageningen University, The Netherlands, **2004**

Career perspectives, Wageningen Graduate Schools, The Netherlands, **2005**

Optionals

Preparation PhD Research Proposal

Literature Study - Organic Chemistry Laboratory, Wageningen University, The Netherlands, **2002**

